Role of Checkpoint Kinase 1 in Malignant Melanoma

Joanne Louise Smith

Submitted in fulfilment of the requirements for the Degree of Doctor of Philosophy

The Beatson Institute for Cancer Research

College of Medical, Veterinary & Life Sciences

University of Glasgow

February, 2013

Abstract

Chk1 is a conserved protein kinase which is activated in response to multiple exogenous and endogenous genotoxic stresses. In response Chk1 mediates several cell cycle checkpoint responses which are important components of the cellular DNA damage response (DDR) pathway and as such are important in maintaining genome integrity throughout the cell cycle. The aim of this study was to investigate the potential role that Chk1 may play in the maintenance and progression of malignant melanoma using both *in vitro* and *in vivo* models; and to determine if Chk1 inhibition could be a viable therapeutic approach to malignant melanoma treatment.

Initially I investigated the importance of Chk1 in the cells of origin for melanoma; melanocytes. In this thesis I have examined the importance of Chk1 on melanoblast proliferation and survival during development. I demonstrated that targeted deletion of Chk1 in the melanoblasts of developing mice causes complete loss of these cells from the developing embryo. This manifests itself as complete lack of a pigmented coat in adult mice. Chk1 deleted melanoblasts exhibit DNA damage as marked by γH2AX.

To examine the role of Chk1 in melanoma maintenance and progression I utilized cell lines generated from a murine model of metastatic melanoma in allograft nude mouse experiments and investigated how the conditional genetic deletion of Chk1 in this model affects disease progression. Using this model I showed that complete loss of Chk1 during tumour development caused a profound reduction in the proliferation potential of melanoma tumour formation with a concurrent significant increase in survival time in these mice. In addition I also showed that hemizygous deletion of Chk1 during tumour development exerts a more modest but nevertheless measurable effect on melanoma tumour formation, however with no demonstrable effect on survival time.

To further understand how the loss of Chk1 leads to cell death and how this may be beneficial for the treatment of melanoma I utilised a specific allosteric inhibitor of Chk1 in human melanoma cell lines. I found that Chk1 inhibition led to collapse of replication forks in S-phase cells resulting in the generation of DNA damage specifically in S-phase cells, leading to a cell death signal characterised

by cleavage of PARP and Annexin V positivity. I also showed that Chk1 inhibition has significant toxicity *in vitro* in all metastatic melanoma cell lines; however there is a broad range of relative toxicities to Chk1 inhibition between cell lines. Further *in vivo* analysis also showed that Chk1 inhibition caused a measurable reduction in the tumour growth rate of subcutaneously injected metastatic melanoma cells in CD1 nude mice.

Overall the work presented here provides evidence that Chk1 is essential for both melanocyte and melanoma cell survival with the essential function of Chk1 being in S-phase of the cell cycle, and that Chk1 inhibition may be a viable therapeutic option for melanoma therapy.

Table of Contents

List of Tables

List of Figures

Acknowledgement

I would like to take this opportunity to express my appreciation to my supervisor Prof. David Gillespie for giving me the chance to study for this PhD, and for his help throughout my PhD. I would also like to thank my advisor Dr. Owen Sansom and Dr. Karen Blyth for their guidance and enthusiasm over the last four years.

Thanks to all members of R11 both past and present (Elizabeth, Max, Mary, Naihan, Conor, Lye-Mun, Silvana, Desireé and Eun-Yeung) for providing a positive and stimulating environment in which to work. Plus a special thanks to my Italian girls, Desireé and Silvana, without whom my PhD experience would have been far less colourful. In addition a thank you to all the support staff throughout the Beatson Institute, especially the Biological Services staff for their invaluable help.

A special thank you to my parents, Chris and Sylvia Hall, and my wonderful boyfriend, Martyn Dunlop, for their continued love and support throughout my PhD.

Finally I would like to thank Cancer Research UK for providing the funding for this PhD, without which it would not have been possible.

Author's Declaration

I declare that all of the work presented in this thesis was personally performed. I am the sole author of this thesis. No part of this work has been submitted for the consideration as part of any other degree or award.

Abbreviations

ACTH	Adrenocorticotropic hormone
A-T	Ataxia-telangiectasia
ATM	Ataxia-telangiectasia mutated protein
ATR	Ataxia-telangiectasia and Rad3-related protein
ATRIP	ATR-interacting protein
BrdU	5-bromo-2'-deoxyuridine
CDK	Cyclin-dependant kinase
Chk1	Checkpoint kinase 1
Chk2	Checkpoint kinase 2
DCT	Dopachrome tautomerase
DDR	DNA damage response
DNA	Deoxyribonucleic acid
DSB	Double strand break
DTIC	Dacarbazine
EDNRB	Endothelin-B receptor
EdU	5-ethynyl-2'-deoxyuridine
EMT	Epithelial-to-mesenchymal transition
ERK	Extracellular signal-related kinases
ET3	Endothelin-3
FACs	Fluorescence Activated Cell Sorting
HR	Homologous recombination
IHC	Immunohistochemistry
IR	Gamma ionising irradiation
LacZ	Beta-galactosidase gene
MAPK	Mitogen-activated protein kinases

MC1R	Melanocortin-1 receptor
Mitf	Microphthalmia-associated transcription factor
MRN	complex of Mre11:Rad50:Nbs1
MSH	Melanocyte stimulating hormone
mTOR	Mammalian target of rapamycin
NC	Neural crest
NER	Nucleotide excision repair
NF-κB	Nuclear factor kappa-light chain enhancer of activated B-cells
PARP	Poly (ADP-ribose) polymerase)
PCNA	Proliferating cell nuclear antigen
PI (3) K	Phosphatidylinositol 3-kinase
PIKKs	Phosphatidylinositol 3-kinase-related kinases
PTEN	Phosphatase and tensin homolog
p53BP1	p53 binding protein 1
Rb	Retinoblastoma protein
RPA	Replication protein A
RPE	Retinal pigment epithelium
RGP	Radial growth phase
SCF	Stem cell growth factor
siRNA	Short interfering RNA
SNP	Single nucleotide polymorphism
Sox10	SRY-related HMG-box 10 protein
ssDNA	Single stranded DNA
TPA	Phorbol 12-myristate 13-acetate
TMZ	Temozolomide
TSCs	Tumour stem cells
Tyr	Tyrosinase

TRP2   Tyrosinase-related protein 2

UV   Ultra-violet radiation

VGP   Vertical growth phase

Chapter 1: Introduction

1 Introduction

1.1 Cell cycle and Checkpoints

1.1.1 The Cell Cycle

The eukaryotic cell cycle is an evolutionarily conserved process, from unicellular organisms to complex multicellular organisms, that regulates cell division. The majority of cells in the human body are not actively cycling. These cells are either in a reversible withdrawal from cell cycling known as G0, which happens in response to high cell density or in the absence of growth factor stimulation (Tessema et al, 2004), or in a permanent withdrawal from cell cycling becoming either terminally differentiated or senescent. Differentiation is the normal process by which a less specialized cell develops or matures to become more distinct in form and function whereas senescence is a stress induced response.

The cell cycle consists of four sequential phases; G1-S-G2 and M. The most dynamic phases are S-phase, when DNA replication occurs, and M-phase, when the cells divide into two identical daughter cells. These are bridged by two gap phases that govern the readiness of cells to enter S and M-phases (Tessema et al, 2004). During G1, which follows mitosis, the cells are sensitive to both positive and negative cues from growth factor signalling networks. Progression through the cell cycle is mediated by the cyclin-dependant kinase (CDK) family of serine/threonine kinases and their regulatory partners' cyclins (Morgan, 1997; Nurse, 2000; Vermeulen et al, 2003). Active CDKs comprise a protein kinase subunit whose catalytic activity is dependent on association with a regulatory cyclin subunit. The abundance of different cyclins is regulated by protein synthesis and degradation in a cell cycle-dependant manner which regulates their association with CDKs to control different stages of cell division (Johnson & Walker, 1999; Sherr, 1996). The different combinations of cyclins and CDKs work together by phosphorylating downstream targets to alter their activity. CDK-cyclin complexes are negatively regulated by a complex network of proteins including phosphatases, the INK4 and CIP/KIP family of proteins and through proteolysis (Elledge, 1996; Lee M et al, 2001).

The cyclin D-CDK4/6 and cyclin E-CDK2 complexes drive G1 progression through the restriction point, which commits a cell to the cell cycle. Cyclin D is produced in response to extracellular growth signals and binds to CDK4/6, which in turn phosphorylates the retinoblastoma (Rb) protein (Winston and Pledger 1993). Hyper-phosphorylated Rb dissociates from E2F transcription factors allowing them to become active. Active E2F promotes transcription of genes including the S-phase cyclins (E and A) and enzymes required for DNA replication such as DNA polymerase. Cyclin E thus produced binds to CDK2, forming the cyclin E-CDK2 complex, which pushes the cell from G1 to S phase (Blomen & Boonstra, 2007; Schafer, 1998).

S-phase is initiated by the cyclin A-CDK2 complex which phosphorylates proteins of the pre-replication complexes. This phosphorylation serves two purposes, to activate each assembled pre-replication complex and to prevent new complexes from forming (Kelly & Brown, 2000; Nishitani & Lygerou, 2002). This ensures that every portion of the cells genome is replicated only once (Blow & Hodgson, 2002). The cyclin B-CDK1 complex regulates entry into mitosis. Activation of the cyclin B-CDK1 complex causes breakdown of the nuclear envelope and initiation of prophase (Nigg, 2001). Its subsequent deactivation causes the cell to exit mitosis. Passage through the cell cycle and transition from one phase to the next is tightly monitored by sensor mechanisms. These mechanisms are called checkpoints which act to maintain the correct order and integrity during cell division, and as such are critical in the maintenance of genome integrity (Elledge, 1996; Hartwell & Weinert, 1989; Nyberg et al, 2002).

1.1.2 Checkpoint function and control

Cells are constantly exposed to DNA damage arising from a variety of internal and external sources, and to replicative stress. To protect the integrity of their genomes cells have developed a variety of different repair mechanisms which are equipped to deal with specific lesions (Christmann et al, 2003; Sancar et al, 2004). These include non-homologous end joining and homologous recombination to deal with double stranded breaks and base excision repair to deal with single or short patches of nucleotide damage (Christmann et al, 2003; Morita et al, 2010). However in order for DNA repair to occur normal progression through the cell cycle needs to be temporarily suspended. This allows time for recognition of

the lesion, recruitment of various repair proteins and the repair process to proceed without error. Checkpoint proteins are central to this process, which act by either preventing entry into or halting progression at specific phases of the cell cycle (Sancar et al, 2004) (Figure 1.1). Key players in these checkpoint responses are the ATM-Chk2 and ATR-Chk1 pathways (Reinhardt & Yaffe, 2009; Smith et al, 2012). Activation of these pathways is crucial for the proper co-ordination of checkpoint and DNA repair processes. They also play key roles in initiating apoptosis or cellular senescence in the presence of extensive DNA damage which cannot be repaired.
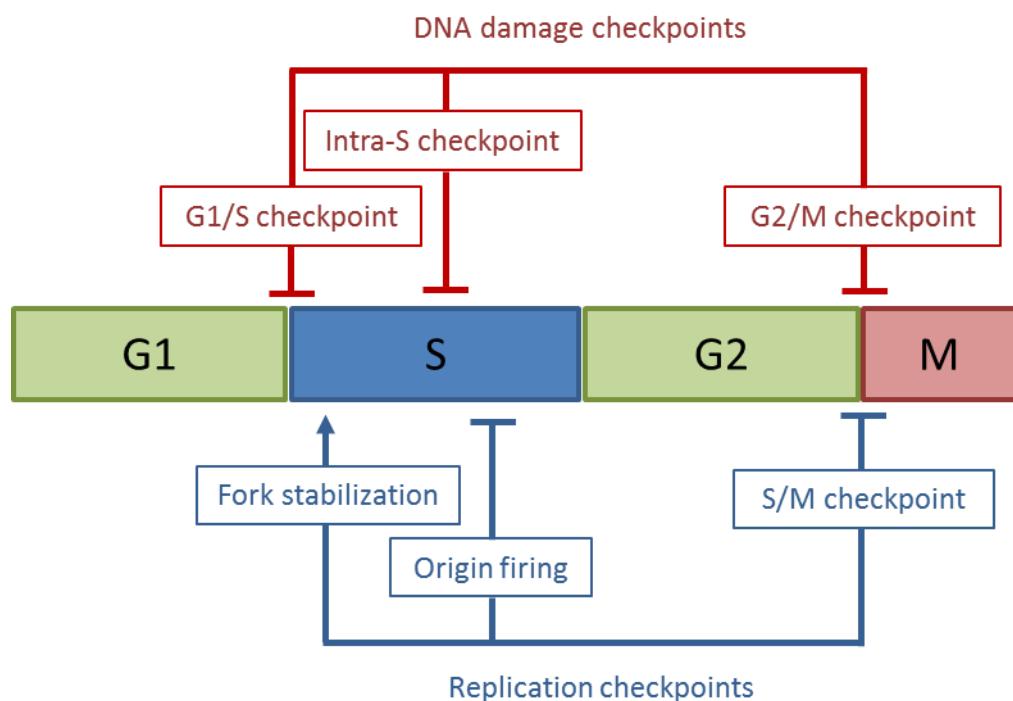
taken from Smith et al 2010

Figure 1.1: Multiple DNA damage and replication checkpoints in vertebrate cells.
DNA damage and DNA synthesis inhibition evoke multiple, mechanistically distinct, checkpoint responses in vertebrate cells that are controlled by the ATM/Chk2 and ATR/Chk1 pathways. In response to DNA damage cells can delay entry to S-phase (G1/S checkpoint), slow the replication of damaged DNA (Intra-S checkpoint) or prevent entry to mitosis while damage persists (G2/M checkpoint). When DNA synthesis is inhibited distinct checkpoint responses are triggered that serve to stabilise stalled replication forks, suppress the firing of latent replication, and delay the onset of mitosis until DNA replication is complete (S/M checkpoint).

1.1.2.1 DNA damage and G2/M checkpoint

When DNA damage is acquired during the G2-phase of the cell cycle, the G2/M checkpoint is activated in order to prevent entry of the damaged cell into mitosis. This is imposed by blocking activation of the mitotic cyclin B-CDK1 complex which is required for breakdown of the nuclear envelope and initiation of prophase. DNA damage triggers a rapid cascade of phosphorylation events involving the ATM/Chk2 pathway (upon IR induced DNA DSBs) or ATR/Chk1 pathway (upon UV induced tracts of ssDNA) kinases. Inhibition of the cyclin B-CDK1 complex is achieved through the addition of inhibitory phosphorylation on threonine 14 and tyrosine 15 (T14/Y15), which is imposed by the Wee1 kinase (Den Haese et al, 1995; Rowley et al, 1992). The Wee1 kinase is a direct target of the Chk1 kinase which phosphorylates and activates Wee1 in the presence of DNA damage (Lee J et al, 2001). Activation of the cyclin B-CDK1 complex is achieved through removal of the inhibitory phosphorylation (T14/Y15), which is accomplished by the CDC25 family phosphatases. Upon DNA damage these phosphatases are inhibited to prevent removal of the inhibitory phosphorylation. The CDC25A and CDC25C phosphatases are direct targets of Chk1 and Chk2. In response to DNA damage active Chk1 and Chk2 can phosphorylate CDC25A on serine 123 which primes it for ubiquitination and rapid degradation by the proteasome (Falck et al, 2002). Concurrently active Chk1 can also phosphorylate CDC25C on serine 216 which causes it to binds to 14-3-3 proteins, causing its subsequent exportation from the nucleus (Peng et al, 1997). Collectively these mechanisms prevent activation of the mitotic cyclin B-CDK1 complex resulting in cell cycle blockage in G2-phase. Other kinases such as p38 have also been implicated in carrying out this function (Astuti et al, 2009; Thornton & Rincon, 2009). Transcriptional programmes regulated by p53 and Brca1 can also contribute to sustaining G2/M checkpoint arrest (Kastan & Bartek, 2004).

1.1.2.2 DNA replication arrest and S/M checkpoint

When DNA synthesis is inhibited distinct checkpoint responses are triggered that serve to stabilize stalled replication forks, suppress the firing of latent replication origins, and to delay the onset of mitosis until DNA replication is complete. The ATR/Chk1 pathway plays a major role in all these responses. Upon inhibition of DNA synthesis, for example through nucleotide pool depletion

or by direct damage to the replicating DNA, long tracks of ssDNA are produced. These tracks of ssDNA recruit and activate ATR which subsequently activates Chk1 (Choi et al, 2010). As in the G2/M checkpoint, Chk1 prevents the entry of cells with incomplete DNA replication into mitosis by inhibition of the cyclin B-CDK1 complex. Chk1 had also been implicated in the maintenance of stalled replication forks and suppression of origin of firing (Broderick & Nasheuer 2009; Zachos et al, 2005). The CDC45 protein plays a central role in the regulation of both the initiation and elongation stages of DNA replication, and is thought to be the main target of the Chk1-depedent S/M checkpoint (Bailis et al, 2008; Liu et al, 2006). CDC45 interacts with the replication factors MCM5 and MCM7, which is required for DNA replication (Hardy, 1997). Chk1 activity negatively regulates the association of CDC45 and MCM7 at origins of replication via a CDC25A/CDK2-independent pathway, and as such suppresses origin of firing during DNA damage (Liu et al, 2006).

1.1.2.3 DNA damage and the G1/S checkpoint

When DNA damage is acquired during the G1-phase of the cell cycle, the G1/S checkpoint is activated in order to prevent the damaged cells from initiating DNA replication. This is imposed by blocking activation of the S-phase cyclin E-CDK2 complex which is required for the initiation of DNA replication by promoting CDC45 loading on chromatin, an attractant for DNA polymerase onto pre-replication complexes (Kneissl et al, 2003; Mimura & Takisawa, 1998). Blockage of the cyclin E-CDK2 complex is carried out by two mechanisms, which cause a rapid and sustained induction of the G1/S checkpoint respectively. DNA damage triggers a rapid cascade of phosphorylation events involving the ATM/Chk2 pathway (upon IR induced DNA DSBs) or ATR/Chk1 pathway (upon UV induced tracts of ssDNA) kinases. Inhibition of the cyclin E-CDK2 complex is achieved through the addition of inhibitory phosphorylation on threonine 14 and tyrosine 15 (T14/Y15). Activation of Chk1/Chk2 maintains this inhibition by phosphorylation of CDC25A phosphatase, which primes CDC25A for ubiquitination and rapid destruction by the proteasome (Falck et al, 2002). The absence of CDC25A phosphatase activity 'locks' the CDK2 kinase in its inactive form. Maintenance of the G1/S arrest after DNA damage requires new protein synthesis. As in the rapid response the ATM/ATR and Chk2/Chk1 kinases play a pivotal role through the phosphorylation and stabilisation of p53 (Maclaine &

Hupp, 2009; Shieh et al, 2000). Phosphorylation of p53 prevents its binding to MDM2, a specific inhibitor of p53 and a p53 ubiquitin ligase. This leads to accumulation of a stable and transcriptionally active p53 protein which results in the induction of the p21 protein, an inhibitor of CDKs (Mirza et al, 2003). When accumulated to a threshold level, p21 can bind to and inhibit all cyclin E–CDK2 complexes, and thereby secure the maintenance of the G1 arrest.

1.2 DNA damage response pathway

The DNA damage response (DDR) pathway consists of a highly complex collection of signal transduction processes which orchestrate together to allow the correct coordination and induction of DNA damage repair processes, cell cycle checkpoints and apoptosis/senescence. The DDR pathway is critical for the maintenance of genome integrity and as such plays a central role in the evolution of cancer. In fact inherited defects in DNA damage responses can predispose to cancer by enhancing the accumulation of oncogenic mutations. Key players' among the DDR are the ATM/Chk2 and ATR/Chk1 signalling pathways, which are evolutionary conserved.

1.2.1 The ATM/Chk2 pathway

The ATM/Chk2 pathway is primarily activated in response to radiation and genotoxins which cause DNA DSBs, with weak, if any, activation following agents that block DNA replication without inducing damage (Matsuoka et al, 2000). ATM is a large serine/threonine kinase that belongs to the family of Phosphatidylinositol 3-kinase-related kinases (PIKKs). ATM phosphorylates numerous protein substrates, key of which is the serine/threonine kinase Chk2. ATM is recruited to and activated primarily at DNA DSBs in conjunction with the Mre11: Rad50: Nbs1 (MRN) sensor complex (Lee & Paull, 2005; Suzuki et al, 1999) (Figure 1.2). The exact nature of the primary signal that triggers ATM activation following DNA DSBs remains unknown; however it does not appear to be limited to the immediate vicinity of the damage and may be linked to long-range alterations in chromatin structure (Bakkenist & Kastan, 2003). The relationship between MRN and ATM activation at DNA DSBs is exemplified by human disorders resulting from mutation in these genes. Hypomorphic mutations in the Nbs1 and Mre11 genes lead to the genetic instability disorders Nijmegen breakage

syndrome and Ataxia-like disease respectively. These clinically resemble ATM deficiency which causes the genetic disorder ataxia-telangiectasia (A-T) that is characterized by cerebellar degeneration, immunodeficiency, radiation sensitivity, chromosomal instability and cancer predisposition.

In undamaged cells ATM is thought to be kept in an inactive state by the formation of homo-dimers. In response to DNA DSBs these inactive homo-dimers are rapidly induced to auto-phosphorylate *in trans*. This results in dissociation of the homo-dimers to form monomers which are partially active (Bakkenist & Kastan, 2003). Although it is unclear how this auto-phosphorylation is induced it is not directly dependant on sites of DNA DSBs but more on a rapid change induced by DSBs which change some aspect of higher-order chromatin structure, and that this chromatin alteration initiates ATM activation (Bakkenist & Kastan, 2003). The first auto-phosphorylation site to be identified was serine 1981 (S1981). Modification of this residue has been shown to be tightly linked with activation of ATM under most circumstances (Bakkenist & Kastan, 2003). However this residue is not essential for ATM activation in mice (Pellegrini et al, 2006). Further studies have identified two additional auto-phosphorylation sites, S367 and S1893, which may contribute to ATM activation. ATM has also been shown to undergo acetylation which is mediated by the TIP60 acetyl-transferase. This modification may also play a role in the full activation of ATM (Lavin & Kozlov, 2007). Full activation of ATM monomers is induced by interactions with members of the MRN complex (Lee & Paull 2007; Uziel et al, 2003). This not only allows for full activation of ATM but also recruits ATM to sites of DNA DSBs where it can act locally on its substrates. Local substrates include the variant histone, H2AX, forming the DNA damage associated γ-H2AX histone mark (Fernandez-Capetillo et al, 2004), the Nbs1 member of the MRN complex, BRAC1 and CtIP which are important in initiating homologous recombination (HR) repair, MDC1, p53BP1 (Kastan & Lim, 2000; Lavin, 2008), the cohesin SMC1 (Kitagawa et al, 2004) and the downstream effector kinase Chk2 (Lukas et al, 2003). In addition, ATM acts on other substrates which do not necessarily concentrate at sites of damage. For example, ATM plays an important role in activating the p53 response to DNA damage both by phosphorylating p53 itself and its stability regulators, MDM2 and MDMX (Chen et al, 2005; Lavin & Kozlov, 2007) and there

is increasing evidence that ATM also has substrates and functions in the cytoplasm (Lavin, 2008).

ATM activates Chk2 by phosphorylation on a specific threonine (T) residue, T68. This residue is located within an N terminal serine/ threonine-glutamine (SQ/ TQ) rich motif (Ahn et al, 2000). Once phosphorylated, the SQ/ TQ motif of one Chk2 molecule is recognized by the phosphopeptide-binding Fork-head associated (FHA) domain of another, leading to transient homo-dimerization, intermolecular activation loop auto-phosphorylation, and full activation (Ahn et al, 2002; Cai et al, 2009; Oliver et al, 2006).Once activated, Chk2 is thought to dissociate from sites of damage and disperse as a monomer throughout the nucleus to act on multiple substrates involved in cell cycle progression, apoptosis, and gene transcription. (Lukas et al, 2003). Known substrates of Chk2 include the p53 tumour suppressor protein (Chehab et al, 2000; Shieh et al, 2000) and its regulator MDMX (Chen et al, 2005), CDC25 family phosphatases (Blasina et al, 1999; Chaturvedi et al, 1999; Matsuoka et al, 1998), the BRCA1 tumour suppressor (Lee J et al, 2000) and transcription factors such as FOXM1 (Tan et al, 2007) and E2F1 (Stevens et al, 2003).

1.2.2 The ATR/Chk1 pathway

The ATR/Chk1 pathway is activated most strongly when DNA replication is impeded, for example as a result of nucleotide depletion or replication blocking DNA damage lesions such as those inflicted by ultraviolet (UV) light (Abraham, 2001). ATR, like ATM, is a large serine/threonine kinase that belongs to the family of PIKKs. ATR phosphorylates numerous protein substrates, key of which is the serine/threonine kinase Chk1. ATR is recruited to and activated at tracts of single-stranded DNA (ssDNA) in association with its partner protein ATRIP, which interacts directly with ssDNA in complex with Replication Protein A (RPA) (Figure 1.2). Tracts of ssDNA can be generated by several mechanisms. Firstly when replication is blocked, DNA polymerases become uncoupled from the replicative helicase (Byun et al, 2005) causing the generation of tracts of ssDNA through unwinding of the DNA double helix. These structures can also be generated through the action of nucleotide excision repair (NER) or at dysfunctional telomeres. Finally they can also be generated at sites of DNA DSBs as a result of nucleolytic strand resection. Conversely, replication of damaged DNA can result

in DSBs when leading-strand DNA polymerases encounter single strand nicks or abasic sites. As a result, the ATM/Chk2 and ATR/Chk1 pathways are frequently activated simultaneously in cells exposed to diverse genotoxic stresses, including ionizing radiation and cytotoxic chemotherapy agents. Upon generation these tracts of ssDNA rapidly become coated with the trimeric ssDNA-binding protein complex, RPA, which interacts with ATRIP through the 70kD RPA1 subunit (Zou & Elledge, 2003).

Like ATM, there is evidence that ATR activation involves auto-phosphorylation. Upon DNA damage the ATR-ATRIP complex is recruited to RPA-coated tracts of ssDNA, where ATR is induced to auto-phosphorylate *in trans* on a single site, T1989 (Liu et al, 2011). This phosphorylation is crucial for full activation of ATR, and is dependent on RPA, ATRIP and ATR kinase activity, but not on the ATR mediator TopBP1 (Liu et al, 2011). In addition, efficient ATR activation and downstream phosphorylation of Chk1 depends on the actions of two mediator proteins, TopBP1 and Claspin. TopBP1, which is recruited to ssDNA-RPA via the PCNA-like Rad9: Rad1: Hus1 checkpoint clamp (Delacroix et al, 2007), contains a domain that stimulates ATR activity, although exactly how this occurs is unclear (Kumagai et al, 2006; Mordes et al, 2008). Claspin, which associates with active replication forks (Lee J et al, 2003), is phosphorylated in an ATR-dependant manner within a short repeated motif. Phosphorylated Claspin then binds to and recruits Chk1 (Jeong et al, 2003) to ssDNA-RPA complexes, bringing it into close proximity with active ATR (Kumagai & Dunphy, 2003) and enabling ATR to phosphorylate Chk1 directly. Recently studies have revealed a requirement for two additional mediators, Timeless and Tipin (Timeless-interacting protein); both for normal replication and for ATR-Chk1 activation in response to replication stress (Kondratov & Antoch, 2007). Timeless binds to both ATR and Chk1 whereas Tipin can interact with Claspin (Kemp et al, 2010). Recent data indicate that like ATRIP, Tipin binds to a specific subunit of the RPA complex (although RPA2 rather than RPA1) and is required for stable association of both Timeless and Claspin with tracts of ssDNA-RPA (Kemp et al, 2010). In addition to checkpoint activation, Timeless and Tipin also seem to be required for replication fork stabilization and restart (Errico et al, 2007). As with ATM, ATR is also thought to act on many other substrates in addition to Chk1, including

BRCA1, mini-chromosome maintenance (MCM) proteins, and components of the RPA complex (Cimprich & Cortez, 2008).

ATR phosphorylates Chk1 directly at multiple S/T-Q sites within the C-terminal regulatory domain, most notably at S317 and S345. Phosphorylation of these sites, and in particular S345, is essential for Chk1 biological activity, although exactly how these modifications regulate Chk1 catalytic remains poorly understood (Niida et al, 2007; Walker et al, 2009). ATR-mediated phosphorylation is reported to stimulate Chk1 kinase activity by relieving inhibition by the C-terminal regulatory domain (Oe et al, 2001; Walker et al, 2009); however it may also promote release of Chk1 from chromatin (Smits et al, 2006). Chk1 also undergoes auto-phosphorylation during activation (Kumagai et al, 2004), however this does not occur within the activation loop (Chen et al, 2000), and the exact target sites and functional consequences of this modification have not yet been fully established. Once activated, Chk1 is thought to dissociate from Claspin to act on both nuclear and cytoplasmic substrates (Lukas et al, 2003). Known substrates of Chk1 include CDC25A (Falck et al, 2002), CDC25C (Blasina et al, 1999), and Wee1 (Lee J et al, 2001), which are important regulators of cell cycle transitions. Chk1-mediated phosphorylation inhibits the activity of both CDC25A and CDC25C under conditions of genotoxic stress, although by different mechanisms; phosphorylation of CDC25A targets the protein for degradation (Falck et al, 2002), whilst phosphorylated CDC25C is sequestered in an inactive form through association with 14-3-3 proteins (Peng et al, 1997). Wee1 kinase activity, by contrast, is stimulated by Chk1 mediated phosphorylation (Lee J et al, 2001). Chk1 is also thought to modulate recombination by phosphorylating Rad51 (Sorensen et al, 2005) and BRCA2 (Bahassi et al, 2008), and to mediate DNA damage-induced repression of gene transcription through phosphorylation of histone H3 (Shimada et al, 2008). Although predominantly nuclear, a proportion of active Chk1 also localizes at the centrosome, where it is thought to control the timing of activation of the mitotic cyclin B-CDK1 complex, and thus the onset of mitosis, both after damage and during unperturbed cell cycles (Kramer et al, 2004). In contrast to ATM and Chk2, ATR and Chk1 are thought to be active at low levels even during unperturbed cell cycles, particularly during S-phase

(Syljuasen et al, 2005), potentially explaining why they are essential in many cell types.
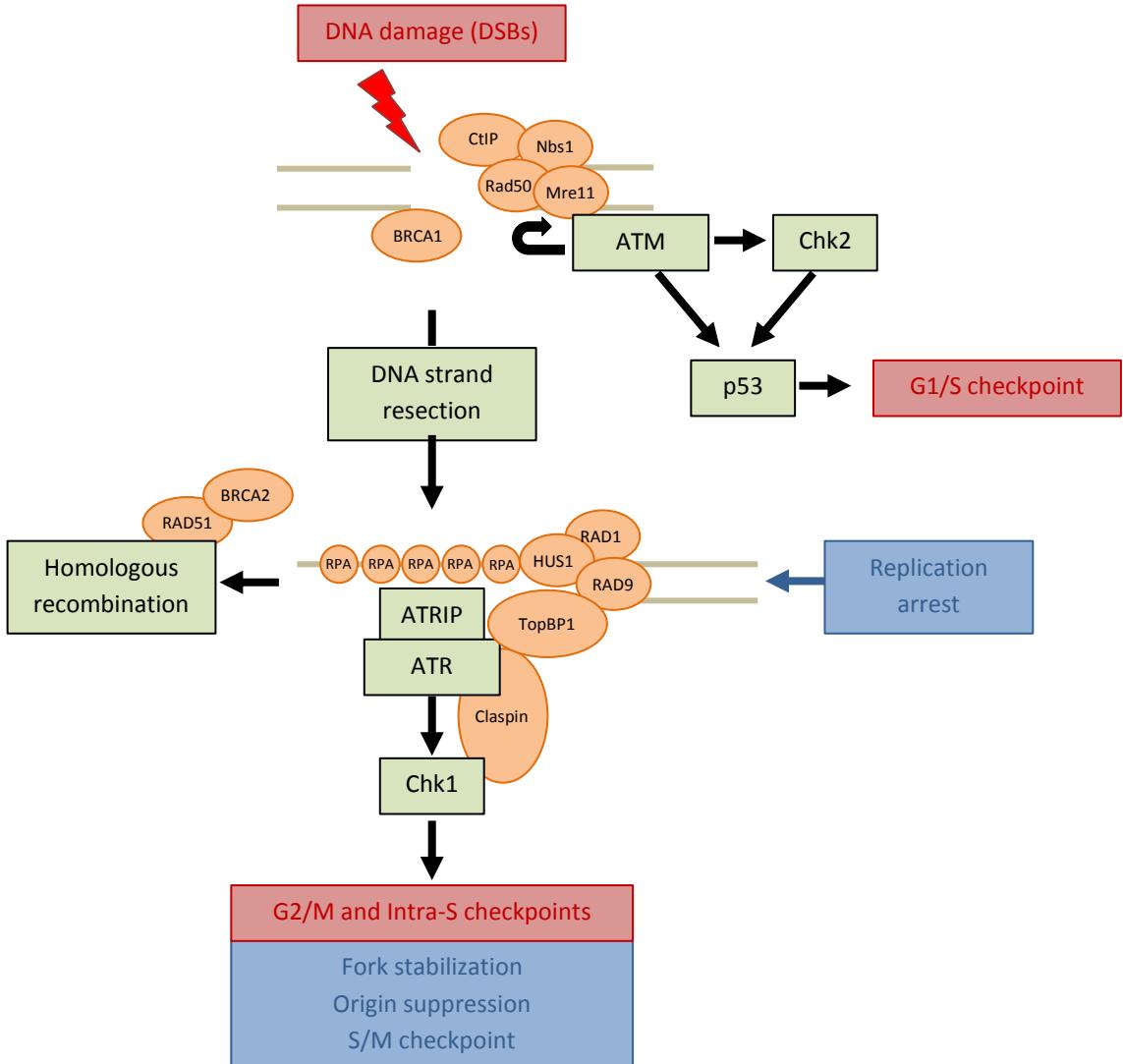
Figure 1.2: Activation of the ATM/Chk2 and ATR/Chk1 pathways. ATM and ATR are activated in response to DNA DSBs and ssDNA respectively, although ATR can also be activated in response to DNA DSBs by ATM-dependent strand resection. In response to DSBs ATM, in conjunction with the MRN complex, CtIP and BRCA1, stimulates nucleolytic strand resection to generate tracts of ssDNA. These tracts of ssDNA act as platforms for the recruitment of ATR-ATRIP leading to Chk1 activation and also initiating HRR.

1.3 Checkpoint pathway alterations in cancer

Genomic instability occurs in most human cancers, and the importance of maintaining the integrity of our genomes is highlighted by both inherited and sporadic loss-of-function mutations which occur in DNA damage response genes, resulting in human cancer predisposition syndromes and cancer. Examples of both have been seen to affect the ATM/Chk2 pathway, whereas mutations in the ATR/Chk1 pathway are rarer.

Homozygous germline loss-of-function mutations affecting ATM cause the human disease syndrome Ataxia telangiectasia (A-T), characterised by immunodeficiency, neurodegeneration, hypersensitivity to radiation and spontaneous predisposition to cancer (Shiloh & Kastan, 2001). As with A-T humans, ATM knockout mice are predisposed to lymphomas and are sensitive to radiation (Xu et al, 1996). Interestingly although A-T is a recessive condition individuals which are heterozygous for ATM mutations also show an increased incidence of cancer, which may be related to medical and occupational exposure to radiation (Briani et al, 2006; Swift et al, 1991). Furthermore cells taken from heterozygous individuals show sensitivity to radiation *in vitro* that is intermediate between those seen from A-T patients and normal individuals (Swift et al, 1991). Somatic mutations affecting ATM have also been documented in sporadic lymphoid malignancies and lung adenocarcinomas (Ding et al, 2008; Gumy-Pause et al, 2004). The importance of DNA damage signalling is further emphasised by mutations in members of the MRN complex, which is important in sensing damage and activating ATM. Hypomorphic mutations affecting the Nbs1 and Mre11 genes give rise to the human conditions Nijmegen breakage syndrome and Ataxia-like disorder respectively, which both share clinical similarities with A-T (Stewart et al, 1999; Varon et al, 1998). Similarly mice with hypmorphic mutations of Nbs1 and Rad50 also show predisposition to cancer (Bender et al, 2002; Kang et al, 2002; Williams et al, 2002).

Mutations in downstream targets of ATM; including the important effector kinase Chk2, BRCA1 and p53 also show functional significance in cancer development. Studies have established that individuals who are heterozygous for mutations in Chk2 suffer from a statistically significant increase in the incidence of breast, prostate and other cancers (Antoni et al, 2007). However tumours that arise in

these Chk2 heterozygous individuals do not consistently lose the remaining allele of Chk2, indicating that Chk2 is not functioning as a classical tumour suppressor protein (Antoni et al, 2007). Interestingly Chk2 knockout mice develop normally and are not prone to spontaneously cancer development (Takai et al, 2002). However they are more sensitive to chemical-induced skin carcinogenesis showing both an increase in tumour burden and tumour growth rate (Hirao et al, 2002). Humans that are heterozygous for the BRCA1 and BRCA2 genes show an increased incidence of breast and ovarian cancers (O'Donovan & Livingston, 2010). Tumourigenesis in these individuals is attributed to functional inactivation of the remaining allele of BRCA1/2 (Collins et al, 1995; Neuhausen & Marshall, 1994). The functional consequence of this is loss of HR-mediated DNA repair in these cells. This is demonstrated by tumours that arise in susceptible individuals which show deficiency for HR repair, whereas the normal surrounding tissue remains proficient in HR (Turner et al, 2005). Inherited mutations in p53 cause the human condition Li-Fraumeni syndrome, which is characterised by multi-organ cancer predisposition including sarcomas and cancers of the breast, brain and adrenal glands (Birch, 1994). Mice that are knockout for p53 develop normally however they are predisposed to a wide variety of cancers, primarily lymphomas and sarcomas, by 6 months of age (Donehower et al, 1992).

Homozygous germline hypomorphic mutations affecting ATR cause the human disease Seckel Syndrome, characterised by a wide range of symptoms including growth retardation and microcephaly. Interestingly these individuals do not show an increased incidence of cancer (Kerzendorfer & O'Driscoll, 2009). In mouse models of Seckel syndrome degenerative and premature ageing-like phenotypes are observed, demonstrating that ATR is critically important in normal development, stem cell survival and tissue homeostasis. Similarly to humans with Seckel syndrome, these mice do not show predisposition to cancer (Murga et al, 2009; Ruzankina et al, 2007). Consistent with this somatic mutations affecting ATR are not widely found in cancers (Heikkinen et al, 2005), with the exception of rare sporadic stomach and endothelial tumours with microsatellite instability (Menoyo et al, 2001; Vassileva et al, 2002; Zighelboim et al, 2009). This shows that in general loss of ATR function does not perturb genomic stability in such a way as to promote carcinogenesis.

Germline mutations in Chk1 have thus far not been implicated in any human disease and somatic mutations affecting Chk1 in human cancers is very rare, with rare exceptions in tumours displaying microsatellite instability (Bertoni et al, 1999; Menoyo et al, 2001). This may be explained by the observation that Chk1 knockout in mice is embryonic lethal (Liu et al, 2000). However the development of a conditional Chk1 knockout mouse model, whereby Chk1 can be deleted in a tissue specific manner has enabled the study of Chk1 during carcinogenesis. Studies have shown that homozygous loss of Chk1 is deleterious for tumour formation including in mammary tumour formation on both a p53 null background (Fishler et al, 2010) and a WNT-1 transgene model (Liu et al, 2000), and in chemical-induced skin carcinogenesis (Tho et al, 2012). These data suggest that Chk1 is essential for tumour cell survival. Interestingly studies have also shown that while complete loss of Chk1 function is detrimental to tumour formation heterozygous loss of Chk1 can promote tumourigenesis. In mammary tumour formation on both a p53 null background and a WNT-1 transgene model heterozygous deletion of Chk1 enhanced tumour formation (Fishler et al, 2010; Liu et al, 2000), whereas in chemical-induced skin carcinogenesis Chk1 heterozygous deletion increased the progression of benign papilloma to malignant carcinoma (Tho et al, 2012). These data show that Chk1 hemizygousity, at least in some systems, can promote tumourigenesis.

The functional consequences on cell survival and cancer development induced by alterations in the ATM/Chk2 and ATR/Chk1 pathways are very different. While impairment or complete loss of function of the ATM/Chk2 pathway is compatible with cell survival, it comes at the cost of cancer predisposition. This is a result, at least in part, of loss of genome stability resulting in more rapid accumulation of oncogenic mutations. In contrast impairment or complete loss of function of the ATR/Chk1 pathway appears incompatible with cell survival in most cell types, presumable because it controls aspects of DNA replication that are essential for cell proliferation and survival, and which lead to cell death if dysfunctional.

1.3.1 DNA damage signalling as a barrier to tumourigenesis

Maintenance of genomic integrity is fundamental to continued life, and which is maintained by the DDR pathway. This is a complex cellular network of dynamic and mutually co-ordinated transduction pathways which elicit DNA repair, cell cycle arrest, senescence and cell death. As a consequence of this important role the DDR pathway has emerged as a powerful anti-cancer barrier which blocks malignant progression (Halazonetis et al, 2008). The initial observation for this phenomenon came from clinical specimens of human breast and lung carcinomas harvested before the patients had received any treatment. These samples displayed constitutively activated DNA damage checkpoint signalling as determined by phosphorylation of Chk2 at T68 (DiTullio et al, 2002). This was further emphasised by studies which showed that in contrast to normal human tissue, tumour specimens from various tissues often showed constitutive activation of DNA damage signalling as demonstrated by the presence of activated phosphorylated forms of ATM, Chk2, p53 and γH2AX and 53BP1 foci (Bartkova et al, 2005; Gorgoulis et al, 2005). Interestingly the observed DDR pathway activation was at its peak level in early stage tumours with attenuation in later malignant stages. Furthermore it was noted that in these early pre-invasive lesions DDR pathway activation preceded the occurrence of mutations or loss of expression of DDR pathway components such as ATM, Chk2 and p53 (Bartkova et al, 2005; Gorgoulis et al, 2005). On the basis of these results it was postulated that the DDR machinery serves as an inducible barrier to constrain tumour development in its early stages. This is achieved by inducing cellular senescence or cell death. It was also postulated that this may exert a selective pressure for specific mutations which could over-ride this effect such as p53. These earlier observations were subsequently supported by further studies. *In vitro* cell culture models driven by ras, mos, cdc6, cyclin E and Stat5 oncogenes and *in vivo* mouse model experiments with ras-driven mouse epithelial tumours have demonstrated that activated oncogenes evoke a robust DDR pathway activation leading to the establishment of cellular senescence in diverse cell types including primary fibroblasts, lymphocytes and epithelial cells (Bartkova et al, 2006; Di Micco et al, 2006; Mallette et al, 2007; Mallette & Ferbeyre, 2007). Experimental blockage of oncogene-induced DNA damage signalling through siRNA mediated knockdown of targets such as ATM resulted in escape from

senescence and increase in DNA synthesis. This observation was equal in degree to that achieved by knockdown of p53 (Bartkova et al, 2006; Di Micco et al, 2006).

Accumulating evidence suggests that replicative stress may be the underlying trigger of oncogene-induced DDR pathway activation and senescence. It has been shown that in cells exposed to oncogenic stimuli the ATR/ATRIP module engages with RPA coated tracts of ssDNA, resulting in both S-phase and G2-phase arrest (Bartkova et al, 2005; Gorgoulis et al, 2005). Other studies have also documented co-localisation of oncogene-evoked DDR foci with replication foci, as marked by the presence of proliferating cell nuclear antigen (PCNA) in S-phase cells (Bartkova et al, 2006). DNA combing, a technique used to produce an array of uniformly stretched DNA that is then highly suitable for nucleic acid hybridization studies, has shown that oncogenes induce aberrant replication forks coupled with premature termination. Such replication forks are unstable and can collapse leading to DNA breakage (Branzei & Foiani, 2005). The exact mechanism by which oncogenes induce replicative stress remains unclear; however deregulation of CDK activity is a potential candidate. Tightly coordinated activation and deactivation of CDK- cyclin complexes is essential for the proper transitioning of the cell cycle including initiation of DNA synthesis. The action of many oncogenes and tumour suppressor genes is to ultimately deregulate CDK activity thus amplification of CDK activity as a result of oncogenic signalling could lead to aberrant DNA replication and thus DNA damage (Blow & Gillespie, 2008). An example of this is Ras-oncogenes which affect CDK activity by up-regulating cyclin D1 and down-regulating p27, a CDK inhibitor (Takuwa, 2001).

Cellular senescence has been shown to critically dependant on two powerful tumour suppressor pathways; the p53 and pRb/p16^{Ink4a} pathways. Escape from oncogene-induced replicative stress resulting in cellular senescence had mainly been attributed to mutations in one or both of these pathways (Beausejour et al, 2003). The importance of this in tumour progression is highlighted by the fact that in humans a significant proportion of cancers harbour mutations in the p53 and pRb pathways. Inactivation of either p53 or p16 has been shown to prevent Ras-induced arrest in mouse cells *in vitro* (Kamijo et al, 1997; Serrano et al,

1997). More recently an *in vivo* model of prostate cancer shows p53-dependant growth arrest induced by PTEN inactivation, which is reversed upon loss of p53 resulting in aggressive invasive cancer (Chen et al, 2005).

1.3.2 Checkpoint suppression as a therapeutic target

Although drugs which target pathways important in tumour development, such as Imatinib, a bcr-abl inhibitor in chronic myeloid leukaemia, and Vemurafenib, a B-Raf inhibitor in melanoma (Hauschild et al, 2012) are starting to be used in the clinic, the main treatment for most cancers still focuses on radiation and genotoxic chemotherapy. These agents cause massive amounts of DNA damage, and as such will be potent activators of the DDR pathway. As a result in recent years much interest has been focused on the cellular DDR and whether it can be manipulated for therapy; including proteins involved in both DNA repair such as DNA-PK, BRCA1 and PARP and DNA damage checkpoint proteins such as ATM, ATR, Chk2 and Chk1 (Ljungman, 2009). The ATR/Chk1 pathway in particular is an attractive target as unlike ATM and Chk2 which are frequently mutated in both familial and sporadic cancer, ATR and Chk1 are very rarely mutated. In addition the ATR/Chk1 pathway has been shown to be essential for both S-phase and G2-phase cell cycle arrest following replicative stress and DNA damage, whereas the ATM/Chk2 pathway appears to be less crucial.

A large proportion of cancers are thought to have an inactivated p53 pathway (Zhou & Bartek, 2004), plus a significant proportion have been shown to have defects in the ATM/Chk2 pathway (Bartkova et al, 2005; Bartkova et al, 2006; Gorgoulis et al, 2005). As a consequence many cancer cells will be deficient for the G1/S checkpoint, which hampers the tumour cells ability to arrest in response to genotoxic stress. Thus it has been postulated that such G1/S checkpoint-deficient cancer cells become more reliant on Chk1 in order to respond to DNA damage than the surrounding normal tissue (Dai & Grant, 2010; Zhou & Bartek, 2004). Therefore the initial strategy for Chk1 inhibition focused on preferentially sensitizing tumour cells to DNA damaging agents in combination therapy.

Inhibition of Chk1 using either siRNA depletion or the selective chemical inhibitor, UCN-01, has been shown to potentiate cell killing by a wide range of

genotoxic agents, including IR, alkylating agents, nucleoside analogues, cisplatin, and topoisomerase inhibitors (Carrassa et al, 2004; Cho et al, 2005; Ganzinelli et al, 2008; Hirose et al, 2001; Karnitz et al, 2005; Koniaras et al, 2001; Wang et al, 1996; Yu et al, 2002). In many, although not all, of these studies Chk1 inhibition resulted in a greater degree of sensitization in tumour cells that were deficient for p53 than in their proficient counterparts, consistent with the idea that loss of G1 arrest indeed creates a therapeutic index. More selective inhibitors of Chk1, such as AZD7762, PF-00477736, XL844 and SCH 900766, have been developed which all showed promising preclinical activities in combination with a wide range of DNA damaging agents including IR, gemcitabine and camptothecin in both *in vitro* and *in vivo* analysis (Ashwell et al, 2008; Dai & Grant, 2010). These studies showed evidence for amplified levels of damage, mitotic catastrophe with damaged or incompletely replicated DNA, and increased levels of apoptosis (Carrassa et al, 2004; Cho et al, 2005; Ganzinelli et al, 2008; Hirose et al, 2001; Karnitz et al, 2005; Koniaras et al, 2001; Wang et al, 1996; Yu et al, 2002). However more recent studies have also shown that Chk1 inhibitors may have potential as single agents in some cancer types (Brooks et al, 2012; Davies et al, 2011a; Ferrao et al, 2012), and in combination with other inhibitors which target important cell cycle proteins such as Wee1 (Aarts et al, 2012; Carrassa et al, 2012; Davies et al, 2011b). In single agent studies Chk1 inhibition was more selective in both myc-driven cancer cells and those which displayed high levels of replicative stress, and was associated with collapse of DNA replication forks and increased levels of apoptosis.

Together these studies demonstrate that Chk1 is a valuable target in the treatment of cancer whose pharmacological inhibition can both potentiate tumour cell killing by a wide range of genotoxic agents and exhibit potency as a single agent. Much remains to be understood about the mechanisms involved in chemo-sensitization however; Chk1 inhibition can clearly both amplify the extent of damage inflicted by a given agent and promote the formation of more lethal lesions, for example by triggering stalled replication fork collapse to form DSBs. In addition, evidence suggests that damage escalation as a result of Chk1 inhibition can enhance tumour cell killing both by conventional routes, for

example by increasing apoptosis, but also by triggering novel mechanisms such as premature entry to mitosis with un-replicated DNA.

1.4 Melanocytes

Melanocytes are a specialised cell type which resides predominantly in the skin, where they are found in the basal layer of the epidermis in humans and in the hair follicles of animals with hair. However they can also be found in the eye, inner ear, meninges, bones and heart. Melanocytes comprise only 5-10% of the cells present in the basal layer of the epidermis; however despite this they are phenotypically prominent. The principle function of melanocytes is their ability to produce the pigment melanin, contained within membrane-bound organelles termed melanosomes, which are exported to the surrounding keratinocytes in the skin or to newly synthesised hair. Melanin is important in providing photo-protection from UV-induced DNA damage and thermoregulation to cells in the skin, the bodies' main barrier to the external environment.

1.4.1 Early embryonic development

Melanocytes develop from neural-crest (NC) precursor cells during embryogenesis. NC-cells are pluripotent cells that arise from the dorsal-most point of the neural tube between the surface ectoderm and the neural plate (Erickson & Reedy, 1998). In addition to melanocytes they also give rise to sensory neurons, glial cells, osteocytes, chrondocytes and craniofacial tissue (Le Douarin et al, 2004). The development of NC-cells (NCC) into mature melanocytes has been well studied showing that they first develop into bi-potential glial-melanocytes lineage progenitors before becoming un-pigmented precursors called melanoblasts and finally maturing into differentiated melanocytes (Dupin et al, 2000) (Figure 1.3). Development of a mouse model whereby the LacZ reporter gene is expressed from the melanocyte specific promoter, Trp2, has enabled dissection of the migratory path taken by the melanocytes during embryogenesis (Mackenzie et al, 1997). In mice, melanoblasts differentiate at embryonic day 8.5 (E8.5) migrating along the dorsolateral pathway and eventually diving ventrally through the dermis. By E14.5 they exit from the underlying dermis and populate the epidermis and developing hair follicle (Mackenzie et al, 1997). Numerous signalling pathways

and transcription factors tightly regulate melanocyte migration and differentiation during embryogenesis (White & Zon, 2008). These proteins and pathways provide and integrate spatial and temporal signals to create the proper environment for normal development. Defects in these pathways cause hypopigmentation arising from lack of melanocyte cells.

1.4.1.1 Mitf

The importance of the Microphthalmia-associated transcription factor (Mitf) in melanocyte development is highlighted by the human diseases Tietz syndrome and Waardenburg Type IIa syndrome; both characterised by deafness and reduced pigmentation. Mitf belongs to the myc-related family of basic helix-loop-helix leucine zipper (bHLH-Zip) transcription factors (Moore, 1995; Steingrimsson et al, 2004). Like other bHLH-Zip factors it binds to the canonical E box sequence (CA[T/C]GTG) (Steingrimsson et al, 2004). Mitf regulates the melanocyte lineage, at least in part, through the transcriptional activation of genes related to pigment cell function including DCT, Tyrosinase, Tyrp1, c-Kit, AIM1 and MC1r (Aoki & Moro, 2002; Du & Fisher, 2002; Tsujimura et al, 1996; Yasumoto et al, 1995). These genes play central roles in melanin production, and as such mutations in these genes in mice have been found to be associated with lack of pigmentation due to defects in melanin synthesis rather than an absence of viable melanocytes (Guyonneau et al, 2004). However Mitf mutant mice and zebrafish have been shown to be completely devoid of both embryonic and adult melanocytes suggesting that Mitf plays an important role in melanocyte survival as well as pigmentation (Hodgkinson et al, 1993; Lister et al, 1999). Studies have shown that Mitf mutant mice lack melanoblasts at early stages prior to their migration from the neural tube (Hornyak et al, 2001). This apparent apoptotic cell death of melanoblasts is due, at least in part, to disruption in the expression of Bcl-2, an anti-apoptotic protein. Mitf has been shown to be a direct transcriptional activator of Bcl-2 expression, and therefore promotes cell survival by up-regulation of Bcl-2 (McGill et al, 2002). The importance of this is demonstrated by the observation that overexpression of Bcl-2 is able to rescue the apoptotic phenotype seen in Mitf mutant melanocytes (McGill et al, 2002).

1.4.1.2 c-Kit

c-Kit is a receptor tyrosine kinase that is expressed on the surface of early embryonic melanoblasts during development. c-Kit is activated by its ligand SCF, which leads to activation of the Ras/MAPK pathway. One consequence of this is to induce post-translational modification of Mitf (Hemesath et al, 1998; Wu et al, 2000) indicating its role in differentiation. Melanocyte migration and localisation during embryogenesis is strongly correlated with SCF expression. In the absence of functional c-Kit or SCF melanoblasts remain fixed laterally to the dorsolateral neural tube with no migration beyond this point, and ultimately disappear (Wehrle-Haller & Weston, 1995). Analysis of humans, mice and zebrafish bearing mutations in either c-Kit or its ligand SCF demonstrate its importance in the survival, proliferation and migration of melanoblasts during development (Jordan & Jackson, 2000; Mackenzie et al, 1997; Wehrle-Haller & Weston, 2003). The human disease piebaldism, which is characterised by white de-pigmented areas of skin, is caused by a heterozygous mutation in c-Kit (Giebel & Spritz, 1991; Spritz, 1994). Mouse models whereby either c-Kit or SCF harbour mutations exhibit varying degrees if pigmentation defects associated with a reduced number of melanocytes (Brannan et al, 1991; Geissler et al, 1988). In sparse mutant zebrafish, which corresponds to c-Kit, melanoblasts are formed normally but they subsequently die by 11 days post-fertilisation, revealing a role in melanoblast survival (Parichy et al, 1999). These melanoblasts also show a defect in migration, with a greater degree located closer to the site of origin than in wild-type animals (Parichy et al, 1999).

1.4.1.3 Wnt

The first evidence that Wnt signalling was important in melanocyte development came from the Wnt1/Wnt3a knockout mice which have almost no detectable melanocytes (Ikeya et al, 1997). Studies in zebrafish suggest that Wnt/ß-catenin signalling controls the fate decision of bi-potential glial-melanocyte stem cells; overexpression of ß-catenin lead to increased numbers of melanocytes but with a reciprocal reduction in neuron and glial cells whereas inhibition of ß-catenin signalling caused NCC to adopt a neural rather than pigment cell fate (Dorsky et al, 1998). In culture studies of mouse cells showed that directed gene transfer of Wnt1 and ß-catenin into NC-precursor cells caused an increase in the both the

number of differentiated melanocytes and their pigmentation levels (Dunn et al, 2000). Further studies have shown that this occurs in an endothelin-dependant manner, but with two distinct mechanisms for Wnt1 and Wnt3a (Dunn et al, 2005). Wnt3a or ß-catenin overexpression causes an increase in melanocyte numbers by biasing the fate of NCC towards the melanocyte lineage, whereas overexpression of Wnt1 does not alter the fate of NCC but instead acts through paracrine signalling on melanoblast precursors to increase the number that become melanocytes (Dunn et al, 2005). Interestingly in the mouse, conditional deletion of ß-catenin in pre-migratory NCC prevents the generation of both melanocytes and sensory neurons (Hari et al, 2002), showing that Wnt/ß-catenin signalling *in vivo* controls both sensory and melanocyte lineage formation. This has been shown to be due to two sequential waves of Wnt/ß-catenin signalling; ß-catenin activation in pre-migratory NCC promotes the formation of sensory neurons at the expanse of all other cell lineages, however ß-catenin activation in later migratory NCC promotes the formation of melanocytes while other lineages are suppressed (Hari et al, 2012). Wnt1/Wnt3a triggers the canonical ß-catenin pathway, resulting in ß-catenin-induced transcription at TCF/LEF promoter/enhancer elements. Wnt signalling is thought to drive the differentiation of the melanocyte lineage, as least in part, through its direct transcriptional up-regulation of Mitf (Takeda et al, 2000). Mitf in turn has been shown to interact with LEF1, where they act synergistically to increase the transcription of melanocyte specific-target promoters (Schepsky et al, 2006; Yasumoto et al, 2002).

1.4.1.4 Snail/Slug and Sox10

Snail and Slug are zinc-finger transcription factors that bind to E-box motifs and which have been associated with the human diseases piebaldism (Tachibana et al, 2003) and Waardenburg Type IIa syndrome (Sanchez-Martin et al, 2003). Mice with Slug mutations display a phenotype similar to piebaldism with depigmentation of the ventral trunk, tail and feet, and white forelock (Perez-Losada et al, 2002). The earliest known response to signals that induce NCC during embryogenesis is the expression of Snail/Slug transcription factors (LaBonne & Bronner-Fraser, 1999). Before migration of NCC from the neural plate can occur they must undergo an epithelial-to-mesenchymal transition (EMT) in which down-regulation of cell adhesion molecules such as E-cadherin

allows for movement to occur (Acloque et al, 2009; Kalluri & Weinburg, 2009). The Snail and Slug family of transcription factors have been shown to be important in this process by direct transcriptional repression of E-cadherin (Cano et al, 2000). In fact, onset of Snail transcription coincides with migration of NCC from the neural plate. In Xenopus repression of Slug leads to reduced expression of both Slug and Snail in late stage embryos, which is associated with the inhibition of NCC migration and the reduction or loss of many NCC derivatives (Carl et al, 1999; LaBonne & Bronner-Fraser, 2000). This phenotype is rescued by overexpression of either Slug or Snail that leads to an excess of melanocytes (Carl et al, 1999; LaBonne & Bronner-Fraser, 2000). Snail/Slug expression is important at two distinct phases where it contributes to both cell fate and migration. Inhibition at early stages of embryogenesis prevents formation of NC precursor cells, whereas inhibition at later stages interferes with NCC migration (LaBonne & Bronner-Fraser, 2000).

Sox10 is a transcription factor that belongs to the SOX (SRY-related HMG-box) family of transcription factors, which are involved in the development and normal physiology of numerous tissues, including melanocytes (Harris et al, 2010). Mutations in Sox10 are associated with the human disease Waardenburg Type IV, a combination of both Waardenburg syndrome and Hirschsprung disease (Bondurand et al, 2007). Mice which express a dominant negative Sox10 are a model for Waardenburg Type IV (Herbarth et al, 1998; Southard-Smith et al, 1998). These mice exhibit an increased number of apoptotic cells in the NCC migratory pathway early in development with an almost complete loss of NCC at later stages (Hou et al, 2006; Pottorf et al, 2001; Southard-Smith et al, 1998). Sox10 has been shown to play a key role in the transcriptional control of Mitf (Lang & Epstein, 2003; Lee M et al, 2000; Potterf et al, 2000; Verastegui et al, 2000), and as such has the ability to regulate a number of genes related to pigment cell function including DCT, Tyrosinase and Tyrp1 (Jiao et al, 2004; Murisier et al, 2007). These genes play central roles in melanin production. Consistent with this primary NCC cultures generated from Sox10 mutant mice have an absence of Mitf expression (Hou et al, 2006). However, although Sox10 is thought to act primarily through the regulation of Mitf, overexpression of Mitf was not able to induce the expression of Tyrosinase or to rescue pigmentation in

the absence of Sox10 (Hou et al, 2006), therefore demonstrating that Sox10 also acts independently of Mitf.

1.4.1.5 Endothelins

The initial observation that endothelin signalling was important in melanocyte development came from the endothelin-B receptor (EDNRB) and endothelin-3 (ET3) knockout mice which both have almost a complete lack of pigmentation (Baynash et al, 1994; Hosoda et al, 1994). EDNRB is a G-protein coupled receptor which is activated by binding of its ligand ET3. Upon activation EDNRB signals to numerous pathways inducing activation of PKC, MAPK, Raf1, p90 ribosomal S6 kinase, CREB and cAMP protein kinase (Bohm et al, 1995; Imokawa et al, 1996; Imokawa et al, 1997; Sato-Jin et al, 2008). EDNRB signalling has also been shown to regulate the melanocyte specific transcription factor Mitf at both the transcriptional and translational level (Sato-Jin et al, 2008). EDNRB/ET3 signalling plays various roles in melanocyte development including promoting the survival, proliferation, differentiation and migration of committed melanocyte precursors (Saldana-Caboverde & Kos, 2010). Animal studies have shown that EDNRB signalling is only critically required from E10 to E12.5 in mice in order to develop a normal pigmentation pattern, with loss at this time leading to complete loss of melanocytes from adult mice (Lee H et al, 2003; Shin et al, 1999). In this model it was shown that the phenotype caused by loss of EDNRB could be rescued by activating EDNRB as late as E10, therefore indicating that endothelin signalling is not necessary for the initial specification of mammalian NCC but rather for the dispersal and survival of melanoblasts (Shin et al, 1999).
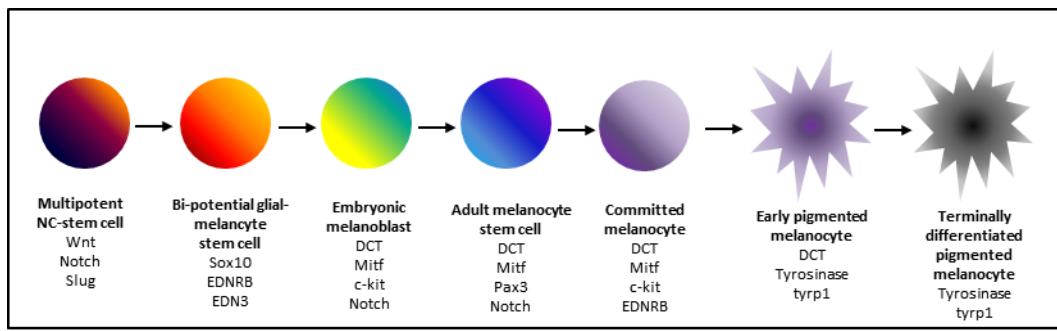
taken from White & Zon 2008

Figure 1.3: Neural-Crest differentiation. Stages of differentiation from a neural-crest precursor cell to a fully differentiated melanised melanocyte, with the important pathways for each stage

1.4.2 Adult melanocytes

The skin is one of the most regenerative organs known in both human and animal biology. On any given day millions of new epidermal skin cells and hair are generated, both of which are pigmented in an identical fashion to their predecessors by melanocytes. During the final stages of development melanocytes are correctly localised to the base of newly formed hair follicles and to niches in the basal layer of the epidermis, where they will be able to exert their functions during the lifespan of the organism. In the hair follicle the new developing hair shaft becomes pigmented due to the transfer of melanin from melanocytes located in the bulb of the hair follicle. In the skin melanocytes transfer melanin to the surrounding keratinocytes forming the basis of skin pigmentation. In mice the skin is often (although not exclusively) non-pigmented.

1.4.2.1 Melanocyte function and pigmentation

The most obvious function of melanocytes is the manufacture and distribution of pigment, melanin, which is packaged into specialised organelles called melanosomes and transferred to the surrounding keratinocytes in the skin and newly formed hair in hair follicles. While most melanocytes are found in the skin and hair of organisms it can also been found in the RPE and iris of the eye, the inner ear where they are essential for hearing and in certain parts of the central nervous system. While pigmentation in nature performs a wide range of purposes in humans it acts primarily to protect the skin from UV-induced DNA damage (Abdel-Malek et al, 2010). This is achieved by melanin which forms a

cup over the nuclei of keratinocytes thereby creating a physical barrier to protect the cellular DNA (Meredith & Sarna, 2006). This cup of melanin also acts as a 'sink' for reactive oxygen species. There are two types of melanin, red/yellow pheomelanin and brown/black eumelanin (Westerhof et al, 1987), the ratio of which determines the skin phenotype of individuals including both the colour and tanning ability of the skin (Fitzpatrick, 1988). Differences in pigmentation between individuals arise not from differences in the number of melanocytes, which remains relatively constant, but rather from variations in the number, size, composition and distribution of melanosomes. Melanosomes are lysosomal-related organelles that contain acid-dependant hydrolyses and lysosome-associated membrane proteins (Schiaffino, 2010). Melanosomes originate from endosome precursors which go through a four stage maturation process; stage II are non-pigmented, stage III are partially pigmented immature organelles and stage IV are fully melanised mature melanosomes (Marks & Seabra, 2001). Important proteins for this process include the enzymes Tyrosinase, Tyrp1 and DCT, as well as the structural protein Pmel17, the main constituent of the internal matrix of the organelles (Berson et al, 2003), the membrane transporters P, MATP/SLC45A2 and SLC24A5 (Lamason et al, 2005; Newton et al, 2001); and the G protein-coupled receptor OA1. The master regulator of pigmentation is the Mitf, which is evolutionary conserved, and is responsible for expression of the essential enzymes required for melanin synthesis including Tyrosinase, a copper-dependant rate-limiting enzyme, Tyrp1 and DCT (Goding, 2000). Other important factors for the regulation of pigmentation include keratinocyte-derived factors such as SCF and α-MSH which signal through the c-Kit and MC1R cell membrane receptor respectively to induce activation of Mitf.

The basal pigmentation capabilities of melanocytes per individual are mostly genetically determined. For example a single nucleotide polymorphism (SNP), that leads to the substitution of a conserved amino acid within the SLC24A5 gene accounts for almost 100% of skin colour differences between Europeans and Africans (Lamason et al, 2005), whereas SNPs within the MC1R gene, of which at least 30 allelic variants exist, are the main cause of differences in skin colour within the European community (Rana et al, 1999; Rees, 2003; Sturm et al, 2003). Despite this melanocytes in the skin do also possess the ability to adapt

their pigmentation capabilities in response to a number of extracellular and external environmental stimuli. One of the main stimuli is UV radiation which induces a tanning response mediated through the MC1R protein (Garcia-Borron et al, 2005). The MC1R gene encodes a G-protein coupled receptor that is responsive to both α-MSH and ACTH while being antagonised by Agouti (Chhajlani & Wikberg, 1992; Cone et al, 1993; Furumura et al, 1996). Activation of MC1R stimulates the cAMP pathway, whereby adenylyl cyclase is activated leading to accumulation of cAMP which in turn activates PKA and CREB. Active CREB enhances the transcription of Mitf which ultimately leads to up-regulation of the machinery necessary for melanin synthesis and melanosome biogenesis. The importance of MC1R and its regulators is emphasised by the consequences of mutations in these genes. Inactivating mutations in the *Agouti* gene are responsible for the black fur of C57Bl/6 mice whereas SNPs in the human *Agouti* gene have been associated with dark hair and brown eyes (Kanetsky et al, 2002). Mutations in MC1R, R151C, R160W and D294H, which result in the inability of MC1R to bind its ligand or to activate adenylyl cyclase, are all associated with red hair, pale skin and freckling (Healy et al, 2001; Ringholm et al, 2004). UV radiation induces the tanning response through activation of p53 in keratinocytes (Cui et al, 2007; Liu et al, 2010). Induced p53 binds to the promoter of POMC driving its transcription. POMC is the precursor for both α-MSH and ACTH which are subsequently secreted by UV-induced keratinocytes; α-MSH and ACTH then bind to MC1R on neighbouring melanocytes triggering the Mitf-dependant induction of pigmentation (Cui et al, 2007; Liu et al, 2010; Song et al, 2009). DNA damage induced by UV radiation such as thymidine dimers are thought to be important in the initial activation of p53. Studies have shown that topical administration of small DNA fragments such as thymidine dimers induce tyrosinase up-regulation and increase pigmentation (Eller et al, 1994).

1.4.2.2 Melanocyte stem cells in adult skin

Fully differentiated melanocytes exist in the basal layer of the epidermis and in the bulb of the hair follicle. However there also exist a population of melanocyte stem cells in the adult that are located in the bulge region of the hair follicle just below the sebaceous gland along with the multi-potent epidermal stem cells which give rise to the keratinocytes (Moore & Lemischka, 2006) (Figure 1.4). These melanocyte stem cells are responsible for restoring the

pool of differentiated melanocytes and maintaining pigmentation throughout the lifespan of the organism. The features that define a stem cell population include slow cycling, self-renewal, immaturity, and ability to generate progeny when appropriately stimulated (Nishimura et al, 2005). Analysis of the DCT-LacZ transgenic mouse model has helped to elucidate the location of the melanocyte stem cell population (Nisihimura et al, 2002). Inhibition of c-Kit postnatally in these mice results in lack of hair pigmentation; however subsequent hair cycles showed re-colouration of the hair presumably by a Kit-independent population of melanocytes. These were traced to a DCT+ population of melanocytes located in the bulge area of the hair follicle (Nishmura et al, 2002). Analysis of DCT+ melanocytes located in the bulge region showed that they had a significantly different transcription profile compared to the DCT+ melanocytes located in the bulb region. These cells expressed DCT and Pax3 but were virtually negative for markers of mature melanocytes such as Tyrosinase, Tyrp1, Mitf and MC1R (Osawa et al, 2005). The importance of the melanocyte stem cell population in adults for continued pigmentation is highlighted by animal models whereby genetic alterations in Bcl2 and Mitf cause a loss of DCT+ melanocyte cells located in the bulge region which is rapidly preceded by premature greying of the hair (Nishimura et al, 2005; Veis et al, 1993).
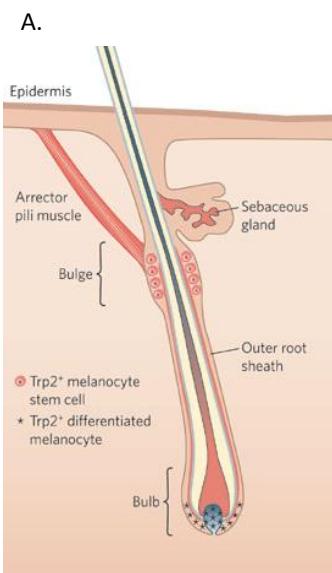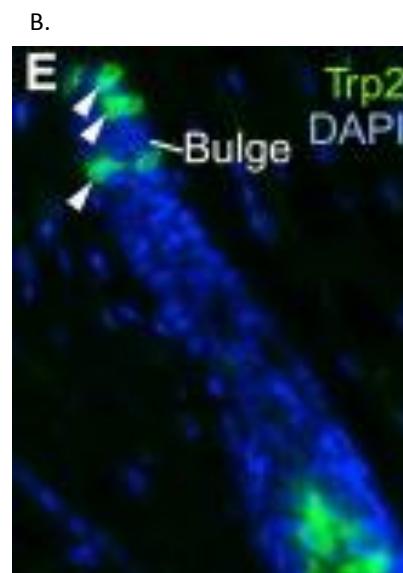
Figure 1.4: Melanocyte populations within the hair follicle. (A) Cartoon representation of a hair follicle, showing melanocyte stem cells located in the bulge area and differentiated melanocytes at the base of the hair follicle in the bulb region. (B) Immunofluorescent microscopy showing the two populations of Trp2+ melanocytes cells in the bulge and bulb regions of the hair follicle.

1.5 Melanoma

Melanoma is an aggressive type of skin cancer whose cell of origin is the melanocyte. Melanoma is the 19th most common cancer worldwide, however in certain countries that are predominantly occupied by white Caucasians the incidence rate is much higher, for example in Australia melanoma is the 3rd most common type of cancer in both sexes (Ferlay et al, 2010). Alarmingly the incidence rate for melanoma has increased more rapidly over the past 30 years than for any of the other top ten cancers in both the UK and USA (Cancer Research UK; Howlader et al, 2012; Jemal et al, 2010). Although melanoma only accounts for a fraction of skin cancer cases, 5-10%, it is the most dangerous form, accounting for >80% of deaths from skin cancer. When melanoma is diagnosed early it can be cured by surgical resection, however once the condition becomes metastatic it is largely refractory to existing treatments with a median survival rate of 6 months and a 5 year survival rate of only 15% (Siegel et al, 2012).

1.5.1 Genetics of melanoma

The genetic alterations associated with the malignant transformation of melanocytes to melanoma are well established (Chin, 2003). The MAPK signalling pathway is important in the regulation of cellular proliferation and survival of melanocytes and as such is mutated causing hyper-activation in up to 90% of human melanomas (Cohen et al, 2002). The MAPK pathway is activated downstream of numerous receptor tyrosine kinases and G-protein coupled receptor (Wellbrock et al, 2004). In melanocytes this pathway is specifically activated in response to growth factors including SCF, FGF and HGF. The most common mutations of this pathway are found in B-Raf and N-Ras, and which are generally mutually exclusive owing to the fact that N-Ras is considered to act directly upstream of B-Raf and therefore the mutations are considered to be functionally equivalent. Mutations in B-Raf are seen in as many as 60% of human melanoma samples and cell lines (Davies et al, 2002), with the most common mutation being a valine to glutamic acid substitution at position 600, V600E. Activating point mutations in N-Ras have been seen in as many as 56% of congenital nevi, 33% of primary melanomas and 26% of metastatic samples (Demunter et al, 2001), with the most common mutation being a glutamine to

leucine substitution at position 61, Q61L. Both B-Raf and N-Ras mutations persist from early nevi to malignant disease, suggesting that MAPK signalling is important throughout melanoma development with particular emphasis on tumour maintenance. Mutant B-Raf (V600E) has been shown to be approximately 480-fold more active than wild-type (Wan et al, 2004), resulting in constitutive ERK signalling that provides essential functions for the growth and maintenance of tumour growth (Gray-Schopfer et al, 2005). In addition to activation of ERK signalling, mutant B-Raf and N-Ras have been shown to activate other pathways important in tumour maintenance and progression. Mutant B-Raf is able to activate NF-κB, a known anti-apoptotic factor (Ikenoue et al, 2004) thus promoting cell survival. B-Raf has also been shown to regulate cell migration, with mutant B-Raf cells having increased levels of actin stress fibres (Pritchard et al, 2004), as well as up-regulation of MMP-2, which degrades the extracellular matrix, and ß-integrin (Sumimoto et al, 2004). Mutant B-Raf also contributes towards angiogenesis by stimulating VEGF (Sharma et al, 2005), an important factor in promoting tumour growth by allowing the delivery of essential nutrients and oxygen to the tumour mass. More recently ERK signalling has also been implicated in altering the expression of Mitf, the master regulator of melanocyte function (Wellbrock et al, 2008; Primot et al, 2010).

Although alterations in MAPK signalling represents the major oncogenic signal in melanoma the phosphoinositide-3-OH kinase (PI(3)K) pathway also plays a significant role. Mutations in PI(3)K occur in 3% of metastatic melanoma (Omholt et al, 2006) with overexpression of the downstream effector kinase PKB (also known as Akt) seen in up to 60% of melanomas (Stahl et al, 2004). The main inhibitor of the PI(3)K pathway is the lipid phosphatase PTEN, which is lost in 5-20% of late stage melanomas (Wu et al, 2003) and in 30-40% of established melanoma cell lines (Guldberg et al, 1997; Teng et al, 1997). The PI(3)K pathway is activated in response to stimuli from receptor tyrosine kinases, and is important in regulating cell survival, proliferation, growth (Increase in cellular mass) and motility (Shaw & Cantley, 2006). The importance of this pathway is highlighted by three-dimensional *in vitro* melanoma cultures whereby both MAPK and PI(3)K signalling must be inhibited in order to suppress cell proliferation (Smalley et al, 2006). Finally another important pathway associated with melanoma tumour cell growth is Mitf, which has been shown to be expressed in

most human melanomas with its target genes being diagnostic markers of the disease (Levy et al, 2006). Furthermore continued expression of Mitf is essential for melanoma cell proliferation and survival (Levy et al, 2006), with loss of expression leading to cell cycle arrest and apoptosis. However high levels of expression promote cell cycle arrest and differentiation with a reduction of proliferation seen even in the presence of oncogenic B-Raf (Wellbrock & Marais, 2005), therefore melanoma cell must maintain intermediate levels of Mitf expression in order to favour proliferation. In culture B-Raf and Mitf have been shown to co-operate thereby promoting immortalisation of primary melanocytes (Garraway et al, 2005).

Many of the aforementioned oncogenes associated with melanoma are known to induce senescence, a barrier to tumourigenesis that is important in suppressing melanoma progression *in vivo*. In fact mutant B-Raf and N-Ras are frequently found in benign nevi, yet most nevi remain indolent for decades and only rarely progress to melanoma (Bauer et al, 2007; Pollock et al, 2003; Poynter et al, 2006). This shows that both B-Raf and N-Ras mutations alone are not sufficient to promote malignant transformation, but that they more likely contribute to malignant melanoma only in conjunction with other mutations. The main gene implicated in oncogene-induced senescence in melanoma is the CDKN2A locus, which encodes two protein; p16^{Ink4a} and p14Arf (humans) or p19Arf (mice) (Sharpless & Chin, 2003), that play key roles in the CDK4/6-pRB and ARF-p53 pathways respectively. The importance of the CDKN2A locus is emphasised by the fact that loss of this locus is the most common mutation seen in familial melanoma (Hussussian et al, 1994). Furthermore p16^{Ink4a} defects are found in dysplastic nevi but not benign nevi (Papp et al, 2003), with p16^{Ink4a} loss also being seen in 15-28% of primary sporadic melanomas and almost all established melanoma cell lines (Fujimoto et al, 1999; Walker et al, 1998). Mutations in CDK4, the target of p16^{Ink4a}, are also frequently seen in both sporadic and familial melanoma (Sharpless & Chin, 2003; Zuo et al, 1996). Notably mutant B-Raf cannot transform human melanocytes in culture even when they are immortalised by TERT expression (Garraway et al, 2005); however mutant B-Raf is able to transform p16^{Inka}-deficient mouse melanocytes (Wellbrock et al, 2004). This is further emphasised by mouse models of melanoma whereby p16^{Ink4a} deficiency is required for N-Ras induced melanoma (Chin et al, 1999).

Collectively these underpin the importance of mutations affecting the CDK4-pRB pathway in overcoming senescence and driving malignant progression.

1.5.2 Development and progression

There are currently two models of melanoma development, one of which holds that melanoma originates from benign nevi whilst a second holds that it originates from isolated cutaneous melanocytes in normal skin. Only 25% of melanomas are associated with pre-existing nevi. These nevi have mutations in either B-Raf or N-Ras, with melanoma progression being dependant on acquirement of a secondary mutation (Bevona et al, 2003). The remaining 75% of melanomas arise in otherwise normal skin in the absence of pre-existing nevi (Bevona et al, 2003). This model is based on the idea that a melanocyte precursor cell in the skin, possibly a melanocyte stem cell, accumulates a number of mutations which drive malignancy. However, regardless of whether development starts from a nevus or directly from a cutaneous melanocyte, melanomas typically go through several defined stages of growth. Firstly cells proliferate in a radial-like fashion with contained of the cellular mass within the epidermis, this is termed the radial-growth phase (RGP). These lesions can then progress to a vertical-growth phase (VGP) characterised by cells breaking through the basement membrane and invading into the dermis, with distinct nodules or nests of cells. VGP cells have metastatic potential, from this point invading both the blood and lymphatic system leading first to local metastasis and eventually distant metastasis (Figure 1.5) (Clark et al, 1984; Cummins et al, 2006; Miller & Mihm, 2006). However not all melanomas pass through each of these individual stages. Both RGP and VGP can develop directly from single melanocytes or nevi, and both can progress directly to metastatic melanoma (Cummins et al, 2006; Miller & Mihm, 2006).

The cell of origin for melanoma is debatable; with arguments for both epidermal melanocytes and melanocyte stem cells. The nevus model for melanoma development supports the idea of the cell of origin being epidermal. This is supported by studies which reveal that melanocytes in culture can be transformed by the expression of oncogenes allowing them to acquire a malignant phenotype and invasive properties (Chudnovsky et al, 2005). Furthermore the tyrosinase promoter, which is not expressed in melanocyte

stem cells (Osawa et al, 2005), has been shown to induce melanoma when driving oncogenic proteins SV40E (Kelsall & Mintz, 1998) and N-Ras (Wong & Chin, 2000). Thus it is possible to generate melanoma from a cell expressing melanocyte proteins which are normally associated with fully differentiated melanocytes. However the extent to which these melanocytes are differentiated and their degree of plasticity is not fully understood. Conversely, the cell of origin has also been postulated to be a melanocyte stem cell located in the bulge region of the hair follicle, especially in the case of melanomas which develop in the absence of pre-existing nevi. This has already been shown in other skin tumour models whereby expression of an activated oncogene from a stem-cell specific promoter drives squamous cell carcinoma (Lapouge et al, 2011; White et al, 2011). However regardless of the origin of melanoma it is clear that a subpopulation of tumour stem cells (TSCs) exist in melanoma. Studies on metastatic melanoma cell lines have revealed that the cultures are heterogeneous even when derived from a single cell clone (Grichnick et al, 2006). The different cell populations within such cultures have distinct properties; the small cell phenotype which proliferate slowly but have the ability to expand the culture, and the large cell phenotype, which gives rise to melanised cells that appear to be terminally differentiated and are eventually lost from the culture (Grichnick et al, 2006). Other groups have also seen TSCs in melanoma cell cultures. These TSCs could be induced to differentiate into melanocytes, adipocytes, osteocytes and chondrocytes lineages (Fang et al, 2005). Markers of these cells have been shown to be CD133, CD166 and nestin (Frank et al, 2005; Klein et al, 2007; Monzani et al, 2007), with cells isolated for these markers more tumorigenic in animal models (Fang et al, 2005; Monzani et al, 2007).
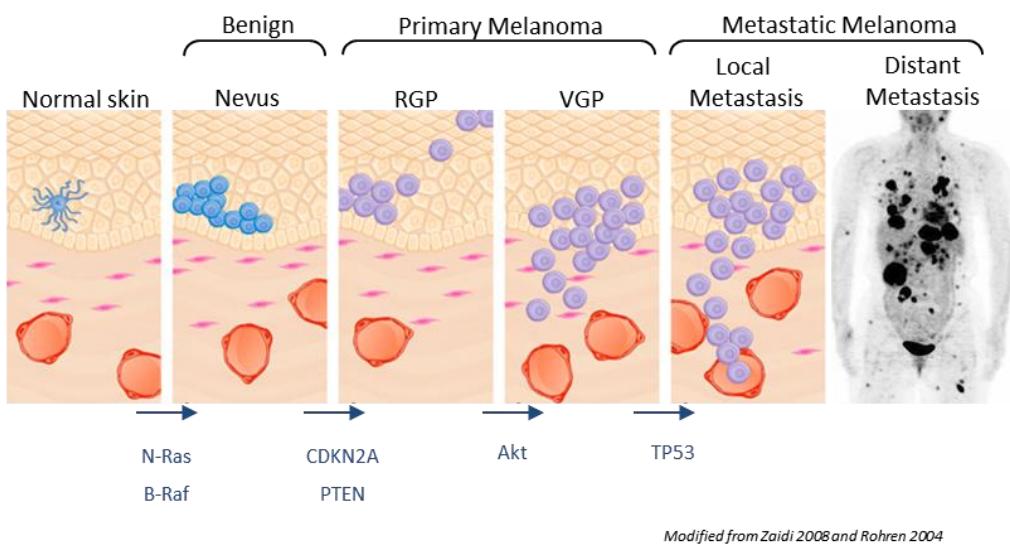
Modified from Zaidi 2008 and Rohren 2004

Figure 1.5: Molecular modelling of melanoma initiation and progression. This illustration depicts human melanoma progression and molecular alterations that can occur at different stages. Aberrant proliferation of normal melanocytes results in the formation of benign or dysplastic nevi. Radial growth phase (RGP) melanoma exhibits the ability to grow intra-epidermally, followed by invasion of the dermis in the vertical growth phase (VGP), and culminating with metastasis. Note that only about 25% of melanomas are known to arise from nevi, and progression can occur without going through all the stages depicted.

1.5.3 Treatment

Metastatic melanoma is an extremely aggressive disease that is largely refractory to current therapies including genotoxic agents, radiotherapy and immunotherapy. This is thought to be because of two reasons; firstly, the cell of origin for melanoma, melanocytes, originates from highly motile precursor cells, and secondly, melanocytes can absorb UV radiation and survive considerable genotoxic stress. This is demonstrated by the low levels of spontaneous apoptosis seen in melanoma tissue samples compared to other cancers, and by the relative resistance to drug-induced apoptosis seen in melanoma cells in culture (Soengas & Lowe, 2003). Recently melanocytes have been shown to possess higher levels of oxidative DNA damage than normal human skin fibroblasts (NHSFs), however despite this they also showed a reduced capability to repair this damage compared to NHSFs, suggesting a higher mutation frequency in melanocytes which could contribute towards malignant transformation (Wang et al, 2010).

The only standard chemotherapeutic agents currently approved for the treatment of metastatic melanoma are interferon-α, high dose interleukin-2 and dacarbazine. However all show low response rates with little improvement on

patient survival times (Comis, 1976; Petrella et al, 2007; Tarhini et al, 2012). Given this novel therapies which target specific alterations associated with melanoma and to which melanoma cells are considered to be 'addicted' have recently started to emerge for the treatment of at least a subset of metastatic melanoma patients (Eggermont & Robert, 2011). As discussed previously one of the most altered pathways in melanoma is the MAPK signalling pathway, which is hyper-activated in up to 90% of melanomas by mutations in either N-Ras or B-Raf (Cohen et al, 2002). Both mutations in N-Ras and B-Raf persist from early nevi to malignant disease, and are essential for tumour growth and maintenance. As such knockdown of either N-Ras or B-Raf by siRNA has been shown to inhibit cell growth, invasion, and to induce apoptosis (Eskandarpour et al, 2005; Sumimoto et al, 2004). N-Ras is a small G-protein that is active when bound to GTP, and is therefore a less 'druggable' target than B-Raf which is a serine/threonine protein kinase. Despite this, Ras inhibitors have been generated; the farnesyl transferase inhibitor R115777 (tipifarnib) was shown to have anti-tumour effects in both human cell cultures and *in vivo* model of melanoma (End et al, 2001). However R115777 never reached clinical trials as a single-agent but has been trialled in combination with the multi-kinase inhibitor sorafenib, but this combination therapy did not show any significant improvement over sorafenib only treatment (Margolin et al, 2012). While some non-selective kinase inhibitors such as sorafenib and Raf265 have showed some efficacy as single agents in both pre-clinical and clinical-phase trials neither has progressed successfully to patients (Maki et al, 2009; Panka et al, 2006; Su et al, 2012). The first selective B-Raf inhibitors to be developed were vemurafenib and dabrafenib. Both have shown very impressive single agent activity against melanoma in clinical trials (Chapman 2011 and Hauschild 2012), however both have also shown a significant appearance of squamous cell carcinomas in treated patients, with up to 18% affected (Chapman et al, 2011; Hauschild et al, 2012). Unfortunately, despite the initial reduction in metastatic tumour growth all patients became resistant to B-Raf inhibitor treatment, which has attributed to reactivation of the MAPK pathway and enhanced tumour growth through c-Raf (Hatzivassiliou et al, 2010; Heidorn et al, 2010; Johannessen et al, 2010; Nazarian et al, 2010; Robert et al, 2011). This has led to the conclusion that combination therapy with MEK inhibitors may be preferable, as all isoforms of both Ras and Raf signal through MEK. Phase I and II trials of combined treatment

with dabrafenib and trametinib (a selective MEK inhibitor) have shown increased progression free survival with a slight but statistically non-significant reduction in the appearance of squamous cell carcinoma (Flaherty et al, 2012).

Other targets which are being investigated as possible treatments for melanoma include inhibitors of the PI(3)K pathway, both of PI(3)K itself and its downstream effectors Akt and mTOR (Lopez-Fauqued et al, 2010). Interestingly treatment with a dual PI(3)K/mTOR inhibitor promoted *in vivo* tumour growth and survival of sorafenib treated melanoma cells (Lopez-Fauqued et al, 2010). A phase I trial with sorafenib and an mTOR inhibitor showed significant toxicity and failed to achieve any clinical response (Davies et al, 2012). Other targets involve inhibitors of the CDK-pRb pathway, such as CDK inhibitors, which has shown to be important in malignant progression (Caporali et al, 2012; Jalili et al, 2012). Finally a new immunotherapy is emerging for the treatment of melanoma, with the use of Ipilimumab, a monoclonal antibody that blocks cytotoxic T-lymphocyte-associated antigen-4 (CTLA-4), a negative regulator of T-cells (Hodi et al, 2012; Robert et al, 2011). Ipilimumab single agent therapy has recently been approved by the FDA for the treatment of late stage melanoma.

1.5.4 Murine models of melanoma

Owing to our better understanding of the genetics involved in driving the initiation and progression of human melanoma, more sophisticated models of melanoma in mice have been developed, which mimic the human condition more closely than ever before (Damsky & Bosenberg, 2010). Technical advances in mouse modelling techniques, especially inducible lox-Cre based recombination technology, has also played a key role in the development of these novel and useful models.

1.5.4.1 B-Raf

Activating point mutations in B-Raf are known to be important in driving melanoma, with up to 60% of human melanoma samples and cell lines containing mutant B-Raf (Davies et al, 2002). However B-Raf mutations are also common in benign nevi (Pollock et al, 2003; Poynter et al, 2006), and malignant transformation is dependent on other secondary mutations. This is demonstrated

by the observation that mutant B-Raf alone cannot transform human melanocytes in culture. There have been several mouse models of melanoma developed which use B-Raf (V600E) as the driving mutation (Dankort et al, 2009; Dhomen et al, 2009; Goel et al, 2009). All these models express B-Raf(V600E) in a melanocyte specific manner, resulting in skin hyperpigmentation and development of benign melanocytic nevi which express markers of senescence (Dhomen et al, 2009; Goel et al, 2009), and which in most cases failed to progress to melanoma. In the Dankort model all mice developed benign melanocytic nevi within 21-28 days after induction of B-Raf expression, however none of these progressed to melanoma over a 15-20 month period. In comparison two other models showed development of melanoma with B-Raf expression alone (Dhomen et al, 2009; Goel et al, 2009). In the Dhomen model 64% of mice developed malignant primary melanomas within 12 months, whereas the Goel model had only 10% penetrance of melanoma which occurred in mice that expressed the highest levels of B-Raf mRNA. Combination of B-Raf with loss of a tumour suppressor gene; including PTEN, CDKN2A and p53, increased penetrance of melanoma and decreased latency in all models. PTEN loss resulted in 100% penetrance of melanoma with a short latency of 25-50 days (Dankart et al, 2009), p16^{Ink4a} loss resulted in 80% penetrance with a median latency of 7 months (Dhomen et al, 2009), CDKN2A loss resulted in 11-38% penetrance with a latency of 185 days and p53 loss resulted in 6-53% penetrance with a median latency of 107 days (Goel et al, 2009). However, only PTEN loss in combination with mutant B-Raf resulted in consistent metastatic disease, with metastatic growths seen in 100% of the lymph nodes and lungs (Dankart et al, 2009). Both CDKN2A and p53 loss also showed some metastasis to the lymph nodes and lungs, but this was only seen in a small subset of mice (Goel et al, 2009). This demonstrates that loss of PTEN appears to be more effective at inducing metastatic spread, which is consistent with other models of melanoma where oncogenesis is driven by the H-Ras oncogene in combination with PTEN loss (Nogueira et al, 2010). It is interesting to note that in the p16^{Ink4a} model, mice still developed nevi prior to malignant conversion (Dhomen et al, 2009), while the nevi from B-Raf alone mice were histologically similar to both blue and epithelioid blue nevi in humans (Dhomen et al, 2009).

1.5.4.2 N-Ras

Activating point mutations in N-Ras are also frequently seen in melanoma, with as many as 56% of congenital nevi, 33% of primary melanoma and 26% of metastatic samples expressing mutant N-Ras (Demunter et al, 2001). As with B-Raf, N-Ras is also frequently seen in benign nevi (Bauer et al, 2007; Poynter et al, 2006) with malignant progression being dependent on the acquisition of additional mutations. There have been several mouse models of melanoma developed that use N-Ras(Q61K) as the driving mutation (Ackermann et al, 2005; Delmas et al, 2007; Ferguson et al, 2010; VanBrocklin et al, 2010). Most of these models express N-Ras(Q61K) in a melanocyte specific manner (Ackermann et al, 2005; Delmas et al, 2007; Ferguson et al, 2010), with one model using a retrovirus containg N-Ras linked to Cre recombinase injected into mice (VanBrocklin et al, 2010). Melanocyte specific expression of mutant N-Ras caused hyperpigmentation of the skin (Ackermann et al, 2005; Delmas et al, 2007). In most of the models expression of N-Ras alone did not promote the formation of melanoma (Ferguson et al, 2010; VanBrocklin et al, 2010), with the exception of the Ackermann model were N-Ras alone caused melanoma with a penetrance of 29% and median latency of 12 months. This difference may be due to different strain backgrounds, as the Ackermann mice are C57Bl/6 whereas others are FVB (Ferguson et al, 2010; VanBrocklin et al, 2010). Combination of N-Ras with loss of a tumour suppressor gene, including p53 and CDKN2A, activation of CDK4 or stabilisation of ß-catenin, increased penetrance and decreased latency of melanoma. Both activating mutation of CDK4 (R24C) and loss of p53 resulted in 100% penetrance with a median latency of 210 and 160 days respectively (Ferguson et al, 2010). Interestingly mutation of CDK4 was associated with the formation of benign nevi prior to malignant conversion whereas p53 loss was not (Ferguson et al, 2010). Stabilisation of ß-catenin resulted in a penetrance of 85% with a median latency of 28 weeks (Delmas et al, 2007) whereas loss of CDKN2A resulted in 94% penetrance of melanoma by 6 months of age (Ackermann et al, 2005). It is of note that CDKN2A loss was also associated with a high metastatic potential with 64% of tumour bearing mice having metastasis to the lymph nodes and 36% having metastasis to either the liver or lungs (Ackermann et al, 2005). Unlike the other models whereby the mice are genetically altered to express N-Ras, the VanBrocklin model uses a retrovirus expressing N-Ras in combination

with Cre recombinase. This is used for injection into mice which express a CDKN2A conditional allele driven from a melanocyte specific promoter, thereby allowing for loss of CDKN2A only in melanocytes infected with the virus. In this context no tumours arose from mice injected with N-Ras and Cre alone, while 63% of mice bearing the CDKN2A allele injected with N-Ras and Cre developed a tumour at the site of injection with a mean latency of 47 days (VanBrocklin et al, 2010). It is of interest that VanBrocklin and colleagues also developed a retrovirus expressing a mutant K-Ras and Cre, however upon injection in combination with CDKN2A no tumours formed, demonstrating that mutant K-Ras does not induce melanoma.

1.6 Project Aims

Melanoma is an extremely aggressive type of skin cancer, which is largely refractory to standard therapies including genotoxins, radiotherapy and immunotherapy. Many of these agents will induce massive amounts of DNA damage and as such will strongly activate the DNA damage response network. Large components of this network are the DNA damage checkpoints which function to prevent cell cycling in the presence of DNA damage and DNA replicative stress. The ATR/Chk1 pathway is a key player in several of these checkpoints and is maintained in most cell types.

The main aims of this thesis were to further understand the role that ATR/Chk1 signalling may play in the initiation, maintenance and progression of melanoma using both *in vitro* and *in vivo* models, and to elucidate if targeting the Chk1 kinase is a suitable therapeutic strategy for the treatment of melanoma.

Chapter 2: Materials & Methods

2 Materials & Methods

2.1 Materials

2.1.1 General Reagents and Buffers

<u>Fisher Scientific</u>

Hydrochloric acid (HCl), Dimethyl sulfoxide (DMSO), Sodium dodecyl sulphate (SDS), Ammonium persulphate (APS), Isopropanol, Magnesium chloride, Sodium deoxycholate, Potassium chloride, EDTA, Glycerol, Sodium pyrophosphate

<u>Melford Laboratories Ltd</u>

Tris Base Ultrapure, Tris Hydrochloride Ultrapure, Agarose

<u>Sigma Aldrich</u>

Butanol, Methanol

<u>VWR</u>

Ethanol

2.1.1.1 Buffers

Buffer	Composition
PBS	170mM NaCl, 3.3mM KCl, 1.8mM Na_2HPO_4, 10.6mM H_2PO_4
1x Semi Dry Blotting Buffer	48mM Tris-Cl pH9.2, 39mM Glycine, 1.3mM SDS-20% Methanol added just prior to use
10 x Tris Buffered Saline Tween (TBS-T)	200mM Tris-Cl pH7.6, 1.37M Sodium Chloride, 1% Tween 20
1 x SDS-PAGE Running Buffer	250mM Tris-Hcl, 1.92M Glycine, 0.01% SDS
50 x TAE Buffer	2M Tris Acetate, 50mM EDTA

2.1.2 Animal Biology

Amresco

1M Calcium chloride (sterile)

Axon Medchem

CHIR-124

Invitrogen (Gibco)

Collagenase type I and IV, HBSS, Dissociation Buffer, Geneticin (G418)

Leica Biosystems

10% Neutral buffered formalin

Melford Laboratories Ltd

5-bromo-4-chloro-3-indolyl-ß-D-galactopyranoside (X-Gal)

Roche

DNase

Science Services Ltd

16% Paraformaldehyde

Sigma Aldrich

Gluteraldehyde, Formaldehyde solution, Ferricyanide, Ferrocyanide, Phorbol 12-myristate 13-acetate (TPA), 4-hydoxytamoxifen (4-OHT), Tamoxifen, Corn oil, Sunflower oil, Dacarbazine (DTIC)

2.1.3 Molecular Biology

2.1.3.1 DNA

<u>Fermentas</u>

6x DNA loading dye, O'GeneRuler 100bp, O'GeneRuler 1kb, O'GeneRuler 1kb Plus

<u>Invitrogen</u>

Platinum® Pfx DNA polymerase, 10mM dNTP Mix

<u>Qiagen Ltd</u>

Qiaquick Gel Extraction kit, Qiaquick PCR purification kit, Qiagen QIAamp DNA Mini Kit

<u>Quanta Biosciences</u>

PerfeCTa® SYBR® Green FastMix

<u>Roche</u>

Expand High Fidelity PCR kit

<u>Sigma Aldrich</u>

Ethidium Bromide

2.1.3.2 Protein

<u>Calciochem</u>

NP-40

<u>Fermentas</u>

High Range, Spectra™ Multicolor Broad Range Protein Ladder

GE Healthcare Life Sciences

Full Range Rainbow Molecular Weight Markers, Amersham ECL™ Western Blotting Detection Reagents

Invitrogen (Gibco)

1M HEPES, NuPAGE LDS Sample Buffer

Marvel

Non-fat milk powder

React Scientific

Supported Nitrocellulose Membrane (30cm × 3 m) 0.45µm pore size

Severn Biotech

30% acrylamide solution (37.5:1), 40% acrylamide solution (125:1)

Sigma Aldrich

Tween 20, Benzamidine, Aprotinin, Leupeptin, Okadaic acid, EGTA, Sodium orthovanate, Sodium fluoride, ß-glycerophosphate, Dithiothreitol, Triton-X-100, DTT, PMSF, Ponceau S solution, TEMED, BSA

Thermo Fisher Scientific

Bradford Assay Reagent, SuperSignal* West Femto Chemiluminescent Substrate

2.1.4 Cell Biology

2.1.4.1 Tissue Culture

Fisher Scientific

Mr Frosty cell freezing container

Invitrogen (Gibco)

DMEM (high glucose, with pyruvate, no glutamine), DMEM: F12 (1:1), RPMI 1640, 200mM, Glutamine, 2.5% Trypsin, OptiMEM, Lipofectamine 2000, Alamar Blue

PAA

Foetal Bovine serum (FBS)

Sigma Aldrich

Penicillin G, Streptomycin, Aphidicolin, Etoposide, Nocodazole, Temozolomide (TMZ)

2.1.4.2 Flow Cytometry

Biolegend

Annexin V binding buffer

Invitrogen

Click-iT® EdU Imaging kit

Qiagen Ltd

RNase A 100mg/ml

Sigma Aldrich

Propidium Iodide (PI), Bromo-deoxyuridine (BrdU)

2.1.4.3 Microscopy

Dako

DAB Envision+® kit, Hydrogen peroxidase blocking reagent

<u>Sigma Aldrich</u>

Citrate Buffer pH6, DPX Mountant, Normal goat serum, Normal donkey serum

<u>Vector Labs</u>

Vectashield containing Dapi

2.2 Methods

2.2.1 Generation of *In vivo* models

2.2.1.1 Mice for Chapter 3: Chk1 requirement in embryonic development of murine melanocytes

To examine the effect of Chk1 deletion on the survival and proliferation of neural-crest derived melanoblasts in utero *Chk1 fl/fl* mice were crossed with *Tyr-Cre* mice and *DCT-LacZ* mice to yield *Chk1 fl/+, Tyr-Cre+, DCT-LacZ+* mice. These were then inter-crossed to produce pregnant females whose litters would contain *Chk1 fl/fl, Chk1 fl/+ and Chk1 +/+* in the ratio of 1:2:1 respectively. These litters were harvested from the pregnant mother at appropriate days (E10.5 and E13.5). *Chk1 fl/fl, Tyr-Cre+, DCT-LacZ+* embryos were the experimental mice with *Chk1 fl//+, Tyr-Cre+, DCT-LacZ+ and Chk1+/+, Tyr-Cre+, DCT-LacZ+* embryos as controls. The *Chk1* flox mice were made by Stephen Elledges's group at the Harvard Medical School, Boston (Liu et al, 2000). A *chk1* flox targeting vector was used which contained exon 2 of Chk1 flanked by LoxP sites. Exon 2 of Chk1 contains the translational initiation sequence and ATP-binding site of the kinase. The *Tyr-Cre* mice were made by Lionel Larue's group at the Institut Curie, Paris (Delmas 2003). The *DCT-LacZ* mice were made by Ian Jackson's group at the MRC Human Genetics Unit, Edinburgh (MacKenzie 1997).

2.2.1.2 Mice for Chapter 4: Chk1 requirement in melanoma initiation and progression *in vivo*

To examine the effect of Chk1 deletion on the initiation and progression of melanoma in mice *Chk1 fl/fl* mice were crossed with mice containing oncogenic N-Ras targeted to the melanocyte lineage (*Tyr-N-Ras^{Q61K}*) and heterozygous knockout of the *CDKN2A locus* (loss of one allele of p16 and p19) combined with expression of p16^{Ink4a} (which harbors a single point mutation to knockout p16 protein only leaving p19 intact); this genotypically leaves the mice heterozygous for p19 and homozygous knockout for p16. These mice were then crossed with mice expressing *Tyr-CreER^{T2}* in order to facilitate inducible knockout of Chk1 in the *Chk1 fl/fl* mice. Cre expression was induced systemically with IP injection of 4-OHT in mice at age 8 weeks. From birth mice were monitored at least once per week to note the presence of a primary tumor. From the time of the first appearance of a primary tumor animals were monitored multiple times a week

and weighed at least weekly. Tumor size was monitored using a skin caliper. Mice were monitored for signs of ruffling of coat, hunched appearance and loss of 20% body weight; if mice exhibited these symptoms they were culled using Schedule 1 methods. Equally if the primary tumor reached 1.5cm or became ulcerated the mice were culled using Schedule 1 methods. The Beermann melanoma mice expressing the *Tyr-N-Ras*^{Q61K}transgene on a CDKN2A deficient background were made by Friedrich Beermann's group at the ISREC, Switzerland (Ackermann 2005). The p16^{Ink4a} mice were made by Anton Berns's group at the Netherlands Cancer Institute, Amsterdam (Krimpenfort 2001). The *Tyr-CreER*^{T2} mice were made by Lionel Larue's group at the Institut Curie, Paris (Yajima 2006).

2.2.2 Breeding Strategy and Colony Maintenance

All mice were bred and maintained in the Beatson Institute for Cancer Research animal facility and in accordance with UK Home Office guidelines and regulations. All colonies were maintained on a mixed (minimum 75% C57Bl/6) genetic background. Animals were humanely culled using Schedule 1 techniques as stipulated in our project licence.

2.2.3 Animal Genotyping

For routine genotyping all animals were ear clipped at weaning and samples sent to Transnetyx genotyping service for analysis. Transnetyx analyses samples using real time PCR. For the genotyping of the Chk1 flox and wt alleles probes were designed which span the site of insertion for the first LoxP site before exon 2.

2.2.4 Harvesting of Embryos and β-Galactosidase Assay

Pregnant mice were sacrificed using Schedule 1 methods. Embryos were then harvested from the mother at appropriate days using aseptic techniques. The yolk sac was detached from the embryo and used for genotyping. Dissected embryos were put on ice in PBS until dissection was complete. Following dissection the PBS was aspirated off and cold fixative solution (0.25% Gluteraldehyde, Sigma) was added and incubated for 20-40mins at 4°C on a rocker (20mins for E9.5; 40mins for E14.5) followed by a wash in PBS for 15mins at 4°C. Aspirate PBS and add permeabilisation solution (2nM MgCl$_2$, 0.01% Na-

deoxycholate, 0.02% NP-40 in 100ml PBS), incubate for 30mins at room temperature (RT). Repeat with fresh permeabilisation solution for 2 further 15min incubations (PBS washes were substituted for E10.5 where permeabilisation is not necessary). Aspirate and add staining solution (0.8g Ferricyanide, 1.0g Ferrocyanide, 1ml 1M $MgCl_2$ in 500ml PBS, before staining add fresh 20ul NP-40, 1ml 1% Na-deoxycholate, 1ml 4% X-Gal in 100ml of staining solution) to the embryos. Incubate for 3-48hrs (depending on the size of the embryo) at RT on a rocker. Staining can also be done at 30^oC to shorten the staining period. After staining embryos were post-fixed in 4% paraformaldehyde for 2-4hrs at 4^oC and then rinsed in PBS overnight at 4^oC. Embryos were then stored in N-formalin at 4^oC. In some cases embryos were also embedded for sectioning however isopropanol should be substituted for xylene to prevent loss of staining.

2.2.5 Melanocyte Isolation from mice

All mice were sacrificed using Schedule 1 method. The backs of the mice were thoroughly shaved to remove most of the hair and cleaned with 70% ethanol before dissection. The back skin was then removed (approximately 2 cm2) and placed into a small petri dish containing ice-cold PBS for a few seconds. The skin was then cut up into pieces in a fresh petri dish containing 3ml of collagenase type I and 3ml of collagenase type IV (both at 5 mg/ml in PBS w/o Ca and Mg) and left to incubate at 37^oC, 5% CO_2 for 30-50mins. After incubation the epidermis was detached (keep) from the dermis (discard) with forceps (if this was difficult the pieces were just cut further). The content was transferred to a 15ml tube with 10ml Wash Buffer (1 x HBSS (10ml of 10x), 1mM $CaCl_2$ (100µl 1M), 0.005% DNase (5 ml 1mg/ml)) and spun at 1100rpm for 5mins at RT. The pellet was re-suspended in 2ml Dissociation Buffer (Gibco) and placed in a small petri dish for incubation at 37C, 5% CO_2 for 10mins. The content was then put through an 18g needle and then a 20g needle in order to further break up the tissue. The content was transferred to a 15ml tube with 10ml Wash Buffer and allowed to settle for 10mins. After 10mins the top layer consisting of grease and fur was removed and the remaining content was spun at 1100rpm for 5mins at RT. The pellet was re-suspended in PBS and the cells were counted. Cells were placed into a 6-well plate and put into a 37^oC, 5% CO_2 incubator, in DMEM: Ham F12 (1:1) media supplemented with 10% FBS, 200nM TPA, 2mM Glutamine, 50U/ml

penicillin G and 50µg/ml Streptomycin. About 2 days after first putting the cells into culture, add G418 at 50 µg/ml and leave in the media for 3 days, then replace with fresh media for 4 days and repeat this cycle. This should selectively reduce the growth of fibroblasts. Use PBS-EDTA to carefully remove dying fibroblasts by adding a few mls and swilling around the plate for a few minutes. When the plate becomes confluent, trypsinise as normal, spin and re-suspend cells and use a very low dilution for the first few splits (i.e. just 1:2 or 1:3). Establishment of a pure population of melanocytes typically takes about 8 weeks.

2.2.6 Preparation and administration of substances into mice

2.2.6.1 4-hydoxytamoxifen (4-OHT)

4-OHT for IP injection into mice was prepared by dissolving 5mg of 4-OHT (Sigma H7904 active Z-isomer >98%) in 500µl 100% ethanol. This was subsequently diluted further in 4500µl of autoclaved sunflower oil (Sigma) to make a 1mg/ml solution. Mice received 100µl of this solution per day for 8 consecutive days, totalling 40mg/kg of 4-OHT.

2.2.6.2 Tamoxifen

Tamoxifen for IP injection into CD1 nude mice was prepared by dissolving 1g of tamoxifen (Sigma T5648) in 10ml 100% ethanol. This was subsequently diluted further in 40ml of corn oil (Sigma) to make a 20mg/ml solution. Mice received 100ul of this solution per day for 8 consecutive days followed by 3x weekly treatments until endpoint reached.

2.2.6.3 CHIR-124

CHIR-124 for oral gavage into CD1 nude mice was prepared by dissolving 25mg of CHIR-124 (Axon Medchem 1636) in DMSO to make a 40mg/ml solution. This was subsequently diluted further in PBS to make a 0.4mg/ml solution. Mice received 100ul of this solution twice daily for 6 consecutive days, totalling 20mg/kg.

2.2.6.4 Dacarbazine (DTIC)

DTIC for IP injection into CD1 nude mice was prepared by dissolving 1g of DTIC (Sigma D2390) into DMSO to make an 80mg/ml solution. This was subsequently diluted further in corn oil (Sigma) to make a 0.8mg/ml solution. Mice received 100ul of this solution twice daily for 3 consecutive days, totalling 20mg/kg.

2.2.6.5 Cell suspension for allografts and xenografts

Cells for subcutaneous and tail vein injection into CD1 nude mice were grown in the appropriate antibiotic free growth medium to ~70% confluency. Cells were trypsinised and counted using the Casy cell counter. Each mouse received the appropriate amount of cells in a volume of 100µl. The required amounts of cells were spun down for 5mins, the pellet washed in PBS and re-spun. The pellet was re-suspended in PBS for injection into the mice.

2.2.7 Tissue fixation

Tissue samples were harvested using aseptic techniques and fixed in 10% formaldehyde in PBS for 24 hours. They were paraffin embedded and tissue sections cut and fixed onto slides by the Histology Service at the Beatson Institute. Staining with Hematoxylin & Eosin (H&E), which marks the nucleus, cytoplasm and connective tissue in sections, was also carried out by Histology Service.

2.2.8 Immunohistochemistry

All immunohistochemistry (IHC) was performed on standard paraffin embedded sections of tissue fixed in 10% formaldehyde in PBS for 24hrs before processing. All sections were de-waxed in xylene (3x washes of 5mins each) before being rehydrated through decreasing concentrations of ethanol to distilled water (2x washes of 5mins each in 100% ethanol, 1x wash of 10mins in 95% ethanol and 1x wash of 10mins in 70% ethanol). Slides were then washed in excess dH_2O (5mins) followed by 1x wash in PBS (5mins). Antigen retrieval was performed in citrate buffer (pH 6) by the water bath method (detailed below). Following antibody incubation (see below) and visualisation using DAB (3, 3'-diaminobenzidine) chromogen (except DCT which was visualised using a fluorescent method), slides

were counterstained with haematoxylin (1min) and Scots tap water (1-5mins), prior to being dehydrated in increasing concentrations of ethanol (1x 70% ethanol 5mins, 1x 95% ethanol 5mins, 1x 100% ethanol 5mins) washed in xylene (15mins) and mounted with DPX mountant (Sigma).

2.2.8.1 Water bath antigen retrieval

300ml of 10mM Citrate antigen retrieval buffer was put into a plastic slide chamber placed in a cold water bath and then heated to 99.9^{o}C, prior to immersion of the slides. Slides were then place in the pre-heated solution for 20 minutes. The slides were then removed from the water bath still immersed in the buffer and allowed to cool till the temperature fell below 35°C.

2.2.8.2 γH2AX

Following antigen retrieval slides were washed in excess dH$_2$0 and then endogenous peroxidase activity was blocked by incubating the slides in 3% hydrogen peroxide for 10 minutes. After endogenous peroxidase blocking, slides were blocked in 10% normal goat serum (NGS) for 30 minutes. Primary mouse anti-γH2AX antibody (Millipore, 1:100 in 10% NGS) was applied overnight at 4°C. After washing 3xPBS the secondary anti-mouse Envision +system (Dako) was used for 1hour at RT. After washing positivity was visualized using DAB for 10mins at RT and slides mounted as described in 2.2.8

2.2.8.3 DCT (Tryp2)

Following antigen retrieval slides were washed in excess dH$_2$0 and then blocked in 10% normal donkey serum (NDS) for 30 minutes. Primary goat anti-DCT (TRP2) antibody (Santa Cruz, 1:100 in 10% NDS) was applied overnight at 4°C. After washing 3xPBS the fluorescent secondary Alexa 555 anti-goat (Invitrogen, 1:500 in 10% NDS) was used for 1hour at RT in the dark. After washing slides were mounted in Vectashield containing DAPI.

2.2.9 DNA Preparation and PCR Genotyping

Animal tissue and cells were genotyped by both PCR and rt-PCR analysis. DNA extraction was carried out using the Qiagen QIAamp DNA Mini Kit. Briefly animal

tissue was prepared in tissue lysis buffer ATL + proteinase K and incubated at 56°C for 3hrs (tumour samples) to overnight (tail tips). Cultured cell pellets were re-suspended in 200μl PBS then prepared in lysis buffer AL + proteinase K and incubated at 56°C for 10mins. DNA was precipitated in ethanol, bound to a QIAamp mini spin column, washed and eluted into 200μl distilled water. DNA concentration was determined using a NanoVue spectrophotometer from GE Healthcare.

2.2.9.1 PCR

Standard PCR was carried out using either Platinum® Pfx (Invitrogen) or Expand High Fidelity (Roche) PCR kits. The PCR reactions were assembled in thin walled domed capped PCR tubes and typically consisted of 50-100ng of genomic DNA, 1.5 ×PCR Buffer, 300μM each dNTP, 0.3μM forward and reverse primers and 1U of polymerase in a final volume of 50μl.

Genotyping for the presence of the Chk1 flox and wild-type alleles using primer pair Chk1 581 (forward) and 1004 (reverse) was carried out using the Platinum® Pfx DNA polymerase kit. The PCR protocol consisted of initial denaturation at 94°C for 2 minute, followed by 35 cycles of 94°C for 15 sec, annealing at 55°C for 30 sec followed by 68°C for 30 sec. The PCR product was then cooled to 4°C until use.

Primers;

Chk1 581 forward: 5' AGGACAAACGTGGAAACAGG 3'

Chk1 1004 reverse: 5' TCCCTCCAAACCTTCAACAG 3'

Genotyping for the presence of Tyr-Cre on the X-chromosome of female mice using the primer pairs LL1433:LL1441 for X^{wt} and LL1403:LL1326 for X^{tg} was carried out using the Expand High Fidelity PCR kit. The PCR protocol for primer pair LL1433:LL1441 consisted of initial denaturation at 94°C for 2 minute, followed by 35 cycles of 94°C for 20 sec, annealing at 60°C for 30 sec followed by 72°C for 60 sec. A final extension of 10 minutes at 72°C was carried out and the PCR product was then cooled to 4°C until use. The PCR protocol for primer pair

LL1403:LL1326 consisted of initial denaturation at 94°C for 2 minute, followed by 35 cycles of 94°C for 20 sec, annealing at 64°C for 30 sec followed by 72°C for 50 sec. A final extension of 10 minutes at 72°C was carried out and the PCR product was then cooled to 4°C until use.

Primers;

LL1433: 5' TTCTGTTTGTGAATACCTGCAA 3'

LL1441: 5' TTGAGGGACTTCTGGATATTGTAAG 3'

LL1403: 5' GCCAGGACCAAGAAGTGAGA 3'

LL1326: 5' CAGCAGACACCAAGGAAACA 3'

2.2.9.2 RT-PCR

RT-PCR for recombination of the Chk1 flox and wild-type alleles was carried out using the PerfeCTa® SYBR® Green FastMix® (Quanta Biosciences). The PCR reactions were assembled in white walled 96 well qPCR plates. PCR reactions were carried out using 1ng, 4ng and 16ng of DNA per reaction. Reaction mixes consisted of template DNA, 2x reaction cocktail mix and 0.2µM forward and reverse primers in a final volume of 10µl. The PCR protocol consisted of initial denaturation at 95°C for 15 minute, followed by 40 cycles of 95°C for 20 sec, annealing at 60°C for 20 sec followed by 72°C for 20 sec. A final extension of 5 minutes at 72°C was carried out followed by melt curve analysis whereby the reaction is heated from 65°C to 95°C in 0.5°C increments for 5 sec each.

Primers;

Chk1 821 forward: 5' CTGGGATTTGGTGCAAACTT 3'

Chk1 1004 reverse: 5' TCCCTCCAAACCTTCAACAG 3'

Arbp 652 forward: 5' CATCTGAGACCTGCCAGTCA 3'

Arbp 858 reverse: 5' TAGAGAGGTCGGGGGGATCTT 3'

2.2.9.3 Agarose gel electrophoresis

Agarose gel electrophoresis was used for the routine analysis of DNA from PCR. 0.8% -2% agarose gels in 1×TAE buffer was boiled in the microwave, allowed to cool and poured into the casting tray. Prior to pouring Ethidium Bromide (final concentration 1µg/ml) was added to visualise the DNA. The DNA was mixed with 6×DNA loading dye (Fermentas) and loaded into the gel along with DNA ladder for size estimation (O'GeneRuler 100bp, O'GeneRuler 1kb and O'GeneRuler 1kb Plus, Fermentas). The gel was typically run at between 8-10V/cm and the DNA visualised using a transilluminator or the Syngene Genius Bio imaging system with GeneSnap Software.

2.2.9.4 DNA Sequencing

DNA sequencing was carried out by the Molecular Technology Service at the Beatson Institute. DNA sequencing is carried out using the BigDye® Terminator v3.1 Cycle Sequencing Kit from Applied Biosystems, routinely using approximately 500ng of plasmid DNA as template and 20ng of sequencing primer. The resulting sequencing reactions are analysed using an Applied Biosystems 3130xl (16 capillary) sequencer. The data was analysed using CLC Genomics Workbench 5. Prior to sequencing the DNA was 'cleaned up' using the following Qiagen kits following manufacturer's instructions.

Qiaquick Gel Extraction kit (Qiagen) – for routine purification of DNA from agarose gels.

Qiaquick PCR purification kit (Qiagen) – for routine clean-up of PCR products.

2.2.10   Tissue culture

2.2.10.1   Culturing Human Melanoma cell lines

Human melanoma cell lines Sk-Mel-2, Sk-Mel-5, Sk-Mel-28, Sk-Mel-37 and Sk-Mel-39 were cultured in DMEM: F-12 (1:1) supplemented with 10% FBS, 2mM Glutamine, 50U/ml penicillin G and 50µg/ml Streptomycin. The cells were grown in a humidified incubator at 37oC. Cells were passaged by trypsinising and diluting 1:10-1:20 into fresh media every 4-5 days to maintain the cells in

exponential growth phase. Human melanoma cell lines A375MM, Sk-Mel-103 and Sk-Mel-147 were cultured in DMEM supplemented with 10% FBS, 2mM Glutamine, 50U/ml penicillin G and 50μg/ml Streptomycin. The cells were grown in a humidified incubator at 37oC. Cells were passaged by trypsinising and diluting 1:10-1:20 into fresh media every 4-5 days to maintain the cells in exponential growth phase. Human melanoma cell lines WM35, WM793 and MRI-H-221 were cultured in RPM1 supplemented with 10% FBS, 2mM Glutamine, 50U/ml penicillin G and 50μg/ml Streptomycin. The cells were grown in a humidified incubator at 37oC. Cells were passaged by trypsinising and diluting 1:5-1:10 into fresh media every 4-5 days to maintain the cells in exponential growth phase. All Sk-Mel cell lines were kindly donated by the Sloan Kettering Memorial Centre New York and are from metastatic melanoma patients. MRI-H-221 was provided by ICC and is from a metastatic phase melanoma that has been shown to be haplo-insufficient for Chk1 (Papp 2007). WM35 and WM793 were kindly donated by the Wister Institute Philadelphia, WM35 is from a radial growth phase melanoma and WM793 is from a vertical growth phase melanoma. A375MM was provided by ATCC and is a highly metastatic variant of the A375 cell line.

2.2.10.2   Culturing Mouse derived melanocytes

Mouse melanocyte cell lines were derived from mice maintained in the Beatson animal facility (see 2.5) with the following genotypes: Chk1 fl/fl, Tyr-N-Ras+, $p16^{Ink4a-/-}$, Arf+/-, Tyr-CreER^{T2}; Chk1 fl/+, Tyr-N-Ras+, $p16^{Ink4a-/-}$, Arf+/-, Tyr-CreER^{T2}; Chk1 +/+, Tyr-N-Ras+, $p16^{Ink4a-/-}$, Arf+/-, Tyr-CreER^{T2}. They were all cultured in DMEM: F-12 (1:1) supplemented with 10% FBS, 200nM TPA, 2mM Glutamine, 50U/ml penicillin G and 50μg/ml Streptomycin. The cells were grown in a humidified incubator at 37°C. Cells were passaged by trypsinising and diluting 1:3-1:5 into fresh media every 4-5 days to maintain the cells in exponential growth phase. The cells express and secrete melanin which colours the medium brown.

2.2.10.3   Passaging Adherent Cells

Once the cells had reached confluence an aliquot of the cells was transferred to a new flask to allow continued growth of the culture. The media was first aspirated from the cells and they were then washed with 10mls of pre-warmed

PBS. 1ml of pre-warmed 1% trypsin in PBS was added to the flask (the volume of trypsin depends on the size of the flask/dish, 1ml is sufficient for a T75 flask) and the trypsin solution was distributed evenly over the surface of the flask/dish. The flask was then returned to the incubator and monitored until the cells had detached form the plate. Once detached, 10mls of fresh pre-warmed media was added to the cells to inactivate the trypsin. An aliquot of this cell suspension was then added to a flask containing fresh media. The cells were then returned to the incubator to allow re-attachment of the cells.

2.2.10.4   Cryogenetic Preservation of Cell lines

For long term storage of cells, log phase healthy cells were trypsinised if necessary and then re-suspended in 90% FBS/10% DMSO and divided into 1ml aliquots in 1.5ml cryovials. Initial freezing was carried out in a Mr Frosty container (containing isopropanol) at $-70^{o}C$ to give a cooling rate of $1^{o}C$/minute. Once a temperature of $-70^{o}C$ was reached the cells were transferred to storage in liquid nitrogen vapour phase tanks at $-180^{o}C$. To revive the cells the vials were retrieved and were quickly warmed up to $37^{o}C$ by placing in a container of warm water. Once thawed the cells were added to pre-warmed media. The following day the cells were passaged or the media was changed depending on the confluence of the cells.

2.2.10.5   Counting of Cells

Cells were counted using the automated Casy® Cell Counter and Analyser System (Innovatis). The appropriate dilution of cells following trypsinisation was automatically counted by the machine set to exclude debris from the calculation. This also allows for easy determination of the viability of the culture. For growth curve analysis measurements were taken in triplicate.

2.2.10.6   Transient transfection using Lipofectamine® 2000

Lipofectamine® 2000 (Invitrogen) was used in order to introduce plasmid DNA into cells following the manufacturer's instructions. Briefly the cells were set up the day before transfection to be 70-80% confluent. The cells were set up in antibiotic free medium. Separately an appropriate amount of plasmid and Lipofectamine® 2000 was diluted in OptiMEM®. For plasmid transfections the

ratio of Lipofectamine® 2000 to plasmid was typically 2.5µl:1µg. Following a 5 minute incubation the diluted Lipofectamine® 2000 and plasmid was mixed and complexes were allowed to form for 20 minutes. The lipid – plasmid complexes were then applied to the cells and the dish rocked gently to ensure even coverage of the cells with the complexes. Cells were returned to the incubator and harvested at the appropriate time to check for expression.

2.2.10.7   Irradiating cells

As a method of inducing DNA damage cells were treated with γ-IR. Cells were irradiated with γ-IR using an Alcyon II Cobalt-60 Teletherapy Unit. Dose rates varied from 2-10 Gymin-1. Cells were irradiated directly in the media in the culture flask. Control cells were brought to the Co-60 source but were not exposed to the ionising radiation.

2.2.11   Flow Cytometry

2.2.11.1   Fixing Cells

Cells were treated as required and pelleted at 250×g for 5 minutes in 15ml polystyrene tubes. The resulting pellet was then re-suspended in 200µl of ice cold PBS. While vortexing, 2mls of ice cold 70% Ethanol was added drop wise to fix the cells. This minimises the formation of clumps and ensures uniform fixing of the cells. Fixed cells were stored at 4^oC overnight or at -20^oC for a couple of hours to several weeks before further analysis.

2.2.11.2   DNA content

Cells were fixed as described and stored at -20^oC for at least 30 minutes. The cells were pelleted and re-suspended in 1ml of PBS containing 10µg/ml Propidium Iodide and 250µg/ml RNase A. The cells were stored in the dark for 30 minutes before analysis on the flow cytometer.

2.2.11.3   S-phase

To monitor DNA replication, cells were tested for their ability to incorporate either the synthetic thymidine analogue 5-bromo-2'-deoxyuridine (BrdU) or 5-ethynyl-2'-deoxyuridine (EdU) into their DNA. Cells were treated as required and

then before being harvested 25µM BrdU or EdU was added for the appropriate time to the culture. Cells were then fixed as above and stored until use.

For BrdU analysis the cells were centrifuged at 250×g and the ethanol was removed. The cells were re-suspended in 1ml of PBS and then 1ml of 4M HCl was added. The samples were incubated at RT for 15 minutes. The HCl treatment denatures the DNA and exposes the BrdU epitopes that are recognised by the anti-BrdU antibody. The cells were then washed once with PBS and once with PBT (0.5% BSA, 0.1% Tween 20 in PBS). The resulting pellet was re-suspended in 200µl of PBT containing a 1:100 dilution of the anti-BrdU antibody (Dako for BrdU only analysis, Abcam for EdU/BrdU analysis) and incubated at RT for 30 minutes. The cells were then washed with 1ml of PBT and re-suspended in 200µl of PBT containing a 1:100 dilution of the FITC conjugated anti-mouse antibody (for BrdU only analysis) or the Alexa 647 conjugated anti-sheep antibody (for EdU/BrdU analysis). The cells were incubated for 30 minutes in the dark and then washed with 1ml of PBT. The cell pellet was then re-suspended in 1ml of PBS containing 10µg/ml Propidium Iodide and 250µg/ml RNase A. The cells were stored in the dark for 30 minutes before analysis on the flow cytometer. Data was collected on a FACS Calibur flow cytometer and the data analysed using WinMDI software.

For EdU analysis the cells were centrifuged at 250×g and the ethanol was removed. The cells were then washed once with PBS and once with PBT (0.5% BSA, 0.1% Tween 20 in PBS). The resulting pellet was re-suspended in EdU reaction buffer (Click-iT reaction buffer, $CuSO_4$, Alexa Fluor 488 azide and 10x reaction buffer additive, Invitrogen) and incubated at RT for 30 minutes in the dark. The cells were then washed with 1ml of PBT and then either re-suspended in 1ml of PBS containing 10µg/ml Propidium Iodide and 250µg/ml RNase A or stained for BrdU (see above). The cells were stored in the dark for 30 minutes before analysis on the flow cytometer. Data was collected on a FACS Calibur flow cytometer and the data analysed using WinMDI software.

2.2.11.4   Mitosis

The number of mitotic cells was estimated by counting the number of cells that were positive for the mitosis specific marker, pS10 Histone H3, by flow

cytometry. Cells were treated as required, then fixed as above and stored until use. The cells were centrifuged at 250×g and the ethanol was removed. The cells were then re-suspended in 1ml of PBS containing 0.25% Triton-X-100 and incubated on ice for 15 minutes. The cells were then pelleted and re-suspended in 100μl of PBT (0.5% BSA, 0.1% Tween 20 in PBS) containing a 1:50 dilution of the anti-pS10 H3 antibody followed by 90 minute incubation at RT. The cells were washed once with PBT and then re-suspended in 100μl of PBT containing a 1:100 dilution of the FITC conjugated anti-rabbit antibody. The cells were incubated for 30 minutes in the dark and then washed with 1ml of PBS. The cell pellet was then re-suspended in 1ml of PBS containing 10μg/ml Propidium Iodide and 250μg/ml RNase A. The cells were stored in the dark for 30 minutes before analysis on the flow cytometer. Data was collected on a FACS Calibur flow cytometer and the data analysed using WinMDI software.

2.2.11.5   Apoptosis

To monitor induction of apoptosis cells were tested for their Annexin V and Propidium Iodide staining. Cells were treated as required and then collected fresh by centrifugation at 250×g without fixing. The cells were then washed once with PBS and re-suspended in 50μl Annexin V binding buffer (BioLegend) containing 2.5μl FITC conjugated Annexin V. Cells were incubated for 15 minutes at RT in the dark. After the incubation period 250μl of Annexin V binding buffer containing 3μl of 1mg/ml Propidium Iodide was added. The cells were mixed gently, kept on ice and analysed as soon as possible on the flow cytometer. Data was collected on a FACS Calibur flow cytometer and the data analysed using WinMDI software.

2.2.12   Protein Extraction

Cells were treated or not as appropriate, pelleted at 250×g, then washed once with ice cold PBS. Unless cells were lysed immediately they were snap frozen on dry ice and stored at -70°C until use. Cell pellets were lysed in whole cell extract buffer (400mM Potassium Chloride, 20mM HEPES, 5mM EDTA, 10mM EGTA, 1mM DTT, 0.4% Triton-X-100, 10% Glycerol, 5μg/ml Leupeptin, 285μM PMSF, 1mM Benzamidine, 5μg/ml Aprotinin, 5mM Sodium Fluoride, 50ng/ml Okadaic Acid, 1mM Sodium Orthovanadate, 10mM β-glycerophosphate, 5mM

Sodium pyrophosphate) then incubated on ice for 20-30 minutes. The samples were then spun at 16,100 x g in a refrigerated microfuge for 15 minutes to pellet the cellular debris. The cleared lysate was then transferred to a fresh tube and an aliquot removed for quantitation. The remainder was snap frozen on dry ice and stored at -70°C until use.

2.2.12.1   Protein Quantitation: Bradford Assay

The Bradford Assay relies on the blue colour generated when Coomassie Brilliant Blue reagent binds to protein side chains. A standard curve of BSA was generated in a 1:10 dilution of the corresponding lysis buffer at the following concentrations: 2000µg/ml, 1000µg/ml, 750µg/ml, 500µg/ml, 250µg/ml, 125µg/ml and 63µg/ml. The protein samples of unknown concentration were diluted 1:10 in dH2O. 10µl of each standard and 10µl of the diluted samples were placed in a cuvette. 1ml of working Bradford Assay reagent (50% Bradford Assay reagent: 50% dH2O) was then added to each cuvette. The absorbance at 595nm of the standards and samples were then read using a Biophotometer. The concentration of protein in the unknown samples was determined by comparison with the standard curve.

2.2.13   SDS-PAGE and Western Blotting

SDS-PAGE was carried out in order to separate proteins so they could be analysed further by Western Blotting or to directly analyse protein by staining the gel. The mini vertical gel system from Atto was used. To cast the resolving gel a solution containing 6-15% acrylamide (acrylamide:bisacrylamide 37.5:1),375mM Tris-HCl pH 8.8 and 0.1% SDS was made. To polymerise the gel ammonium persulphate and TEMED was added to a final concentration of 0.1% and 0.08% respectively. The gel mix was placed in the gel casting apparatus and over-laid with water-saturated butanol. Once set the stacking buffer (5% acrylamide (acrylamide:bisacrylamide 37.5:1), 125mM Tris-HCl pH 6.8, 0.1% SDS, 0.1% ammonium persulphate and 0.1% TEMED) was layered on top and the combs were inserted to allow the loading of samples. Once set the gel apparatus was correctly assembled and 1 × SDS-PAGE Running Buffer was added to the upper and lower chambers of the tank. Samples to be analysed were added to 1x NuPAGE sample buffer (Invitrogen) and were boiled for 5 minutes to denature

the proteins. The samples were centrifuged briefly to remove debris and the samples were then loaded into the wells. Molecular weight markers were also run to estimate the size of the proteins to be analysed. The gels were then run at 180V at constant voltage until the dye front had just entered the running buffer. Western Blotting was carried out using the semi-dry blotting technique. Once the SDS-PAGE was run it was placed on top of 5 sheets of 3MM paper pre-soaked in dry blot buffer and cut to the size of the gel. On top of this was placed the nitrocellulose membrane and then 5 more sheets of soaked 3MM paper. Air bubbles were removed by gently rolling with a marker pen. The 'sandwich' was placed on the transfer apparatus such that the gel was closest to the negative electrode. The proteins were transferred as standard at 20V, 200mA, 8W for 1hour 20 minutes. Ponceau S stain (Applichem) was used to ensure even transfer of the proteins onto the membrane. Then the membrane was blocked in blocking buffer (5% Marvel (non-fat dried milk powder) solution in 1 × TBS-T) for 1 hour at RT with gentle agitation. The membrane was then incubated with the appropriate primary antibody. (See Table for the dilution of antibody used and what blocking buffer was used) The membrane was then washed three times for 10 minutes each with 1 × TBS-T with gentle agitation. The membrane was then incubated with the secondary antibody coupled to horseradish peroxidase for 1hour at RT. The appropriate secondary antibodies were diluted 1:5000 in blocking buffer. After this incubation the membrane was washed as before and the bound secondary antibody was detected using Enhanced Chemiluminescence and X-ray film. The film was developed in a Kodak X-Omat 3000RA automatic film processor.

2.2.14   Microscopy

2.2.14.1   Fluorescence

After plating on glass coverslips Human melanoma cells were treated as required and then before being harvested 25µM EdU was added for 1hr. The cells were then fixed with 4% paraformaldehyde for 15 minutes at RT, washed in PBS + 3% BSA and then permeabilised with 0.5% triton X-100 for 20 minutes at RT. Following fixation the cells were then washed twice with PBS + 3% BSA. The resulting pellet was re-suspended in EdU reaction buffer (Click-iT reaction buffer, $CuSO_4$, Alexa Fluor 488 azide and 10x reaction buffer additive,

Invitrogen) and incubated at RT for 30 minutes in the dark. The cells were then washed twice with 1ml of PBS + 3% BSA and then blocked with 3% BSA in PBS for 10-30 minutes. Fixed cells were probed with anti-γH2AX antibody (Millipore) diluted 1:100 in PBS + 3% BSA for 1hr at RT. Following washing the cells were stained with Alexa 555 conjugated anti-rabbit antibody (Invitrogen) diluted 1:500 in PBS + 3% BSA for 40 minutes at RT in the dark. Samples were then washed and mounted with Vectashield mounting medium containing DAPI (Vector labs). Fluorescent microscopic images were acquired with a 60x oil immersion lens on a Nikon A1R laser scanning confocal microscope.

2.2.14.2   Alamar Blue Cytotoxicity Assay

The cytotoxicity of the Chk1 inhibitor CHIR-124 and the chemotherapeutic agent's dacarbazine (DTIC) and temozolomide (TMZ) on human melanoma cell lines was measured using the fluorimetric indicator, Alamar Blue (Invitrogen), which detects cellular metabolic activity. The greater the level of metabolic activity, or corresponding cell viability, the more reduction of the Alamar Blue dye from a blue non-fluorescent product to a red-fluorescent product. Cells were plated in 96 well plate format at 2000-3500 cells per well in 100µl of media. Cells were treated as required and then incubated for 72 hrs at 37°C. After incubation 10µl Alamar Blue was added to the cells and incubated for a further 4hrs at 37°C. Absorbance was read at 570nm and 600nm using spectrophometer. Alamar Blue data was calculated as the percent difference in reduction between treated cells and control cells, which were calculated using the molar coefficients for both the oxidised and reduced forms of alarm blue at both 570nm and 600nm (see manufacturer's instructions for details). The percent reduction is directly proportional to the percent cell viability. Dose response curves were plotted in GraphPad Prism and EC50 values were calculated using a non-linear regression with variable slope analysis.

2.2.15 List of primary antibodies

Antigen (Ab Type)	Supplier	Dilution and incubation conditions
Chk1 (Mouse monoclonal)	Santa Cruz (G-4) Cat No: sc-8408	WB- 1:1000 in 5% Marvel in TBS-T overnight at 4°C/ RT 3hrs
Actin (Mouse monoclonal)	Sigma (AC-40) Cat No: A4700	WB- 1:1000 in 5% Marvel in TBS-T overnight at 4°C/ RT 3hrs
pS345 Chk1 (Rabbit monoclonal)	Cell Signalling (133D3) Cat No: 2348	WB- 1:1000 in 5% BSA in TBS-T overnight at 4°C/ RT 3hrs
Chk2 (Goat polyclonal)	Santa Cruz (N-17) Cat No: sc-8812	WB- 1:1000 in 5% Marvel in TBS-T overnight at 4°C/ RT 3hrs
pT68 Chk2 (Rabbit monoclonal)	Cell Signalling (C13C1) Cat No: 2197	WB- 1:1000 in 5% BSA in TBS-T overnight at 4°C/ RT 3hrs
ATM (Rabbit polyclonal)	Santa Cruz (H-248) Cat No: sc-7230	WB- 1:1000 in 5% Marvel in TBS-T overnight at 4°C/ RT 3hrs
ATR (Goat polyclonal)	Santa Cruz (N-19) Cat No: sc-1887	WB- 1:1000 in 5% Marvel in TBS-T overnight at 4°C/ RT 3hrs
ATRIP (Rabbit polyclonal)	Santa Cruz (H-300) Cat No: sc-33790	WB- 1:1000 in 5% Marvel in TBS-T overnight at 4°C/ RT 3hrs
Mre11 (Mouse monoclonal)	Novus Biologicals (12D7): Cat No: NB100-473	WB- 1:1000 in 5% Marvel in TBS-T overnight at 4°C/ RT 3hrs
Nibrin (Nbs1) (Rabbit polyclonal)	Santa Cruz (H-300) Cat No: sc-11431	WB- 1:1000 in 5% Marvel in TBS-T overnight at 4°C/ RT 3hrs
Rad50 (Mouse monoclonal)	Abcam (13B3/2C6) Cat No: ab89	WB- 1:1000 in 5% Marvel in TBS-T overnight at 4°C/ RT 3hrs
Wee1 (Mouse monoclonal)	Santa Cruz (B-11) Cat No: sc-5285	WB- 1:1000 in 5% Marvel in TBS-T overnight at 4°C/ RT 3hrs
CDC25A (Mouse monoclonal)	Santa Cruz (F-6) Cat No: sc-7389	WB- 1:1000 in 5% Marvel in TBS-T overnight at 4°C/ RT 3hrs
pS216 CDC25C (Rabbit monoclonal)	Cell Signalling (63F9) Cat No: 4901	WB- 1:1000 in 5% BSA in TBS-T overnight at 4°C/ RT 3hrs
PARP (Rabbit polyclonal)	Cell Signalling Cat No: 9542	WB- 1:1000 in 5% Marvel in TBS-T overnight at 4°C/ RT 3hrs

Cdk1 (cdc2) (Rabbit polyclonal)	Cell Signalling Cat No: 9112	WB- 1:1000 in 5% Marvel in TBS-T overnight at 4°C/ RT 3hrs
pT15/Y15 Cdk1 (cdc2 p34) (Rabbit polyclonal)	Santa Cruz Cat No: sc-12340-R	WB- 1:1000 in 5% BSA in TBS-T overnight at 4°C/ RT 3hrs
α-tubulin (Mouse monoclonal)	Sigma Cat No: T9026	WB- 1:2000 in 5% Marvel in TBS-T overnight at 4°C/ RT 3hrs
BrdU (Mouse monoclonal)	Dako (CloneBu20a) Cat No: M0744	FACs- 1:100 in PBT for 30mins RT
BrdU (Sheep polyclonal)	Abcam Cat No: ab1893	FACs- 1:100 in PBT for 30mins RT
pS10 Histone H3 (Rabbit polyclonal)	Santa Cruz Cat No: sc-8656-R	FACs- 1:50 in PBT for 90mins RT
Annexin-V FITC conjugated	BioLegend Cat No: 640906	FACs- 1:20 in Annexin-V binding buffer for 15mins RT
EdU Alexa 488 conjugated	Invitrogen Cat No: C35002	FACs/IF- 7.5µl in 3ml EdU reaction buffer mix
γH2AX (Mouse monoclonal)	Millipore (Clone JBW301) Cat No: 05-636	IHC- 1:100 in 10% normal goat serum overnight at 4°C IF- 1:100 in PBS + 3% BSA for 1hr RT
DCT (TRP2) (Goat polyclonal)	Santa Cruz (D-18) Cat No: sc-10451	IHC(F)- 1:100 in 10% normal donkey serum overnight at 4°C

2.2.16   List of secondary antibodies

Antigen (Ab Type)	Supplier	Dilution and incubation conditions
Anti-Mouse HRP conjugated	Cell Signalling Cat No: 7076	WB- 1:3000 in 5% Marvel in TBS-T for 1hr RT
Anti-Rabbit HRP conjugated	Cell Signalling Cat No: 7074	WB- 1:3000 in 5% Marvel in TBS-T for 1hr RT
Anti-Goat HRP conjugated	Santa Cruz Cat No: sc-2020	WB- 1:5000 in 5% Marvel in TBS-T for 1hr RT
Anti-Mouse FITC conjugated	Jackson Immuno Research Cat No: 515-095-003	FACs: 1:100 in PBT for 30mins RT
Anti-Rabbit FITC conjugated	Jackson Immuno Research Cat No: 111-095-003	FACs: 1:100 in PBT for 30mins RT
Anti-Sheep Alexa 647 conjugated	Invitrogen Cat No: A21448	FACs: 1:100 in PBT for 30mins RT

Anti-Mouse Alexa 555 conjugated	Invitrogen Cat No: A21427	IF- 1:500 in PBS + 3% BSA for 40mins RT
Anti-Goat Alexa 555 conjugated	Invitrogen Cat No: A21432	IHC(F)- 1:500 in 10% normal donkey serum for 1hr RT
Anti-Mouse Envision+ system-HRP labelled	Dako Cat No: K4000	IHC- apply enough to cover specimen on slide for 1hr RT

Chapter 3: Chk1 requirement in embryonic development of melanocytes

3 Chk1 requirement in embryonic development of melanocytes

3.1 Introduction

Murine melanocytes originate from a highly migratory group of embryonic cells called the neural crest, which gives rise to many cell types including osteocytes, chondrocytes and sensory neurons and are therefore truly multi-potent (Erickson & Reedy, 1998). The development of neural crest cell into mature melanocytes has been well studied showing that neural crest cells first develop into a bi-potential glial-melanocyte lineage progenitor before becoming an un-pigmented precursor termed melanoblasts and finally maturing into a differentiated melanocyte (Dupin et al, 2000). Several genes have been identified to play crucial roles in melanocyte development including MITF (Lister et al, 1999; Hornyak et al, 2001), c-Kit (Wehrle-Haller & Weston 1995; Parcihy et al, 1999), WNT (Ikeya et al, 1997; Dorsky et al, 1998; Dunn et al, 2000), Snail/Slug, and Sox10 (Cano et al, 2000; Meulemans & Bronner-Fraser 2004). Melanocytes are the cell of origin for melanoma, an aggressive form of skin cancer and many of the genes involved in melanocyte development have also been implicated in the development of melanoma. Thus I examined the requirement of Chk1 in melanocyte development during embryogenesis.

3.2 Developmental deletion of Chk1 leads to loss of pigmentation in adult mice

Constitutive deletion of Chk1 is embryonic lethal (Liu et al, 2000) therefore in order to assess the consequences of Chk1 deletion in melanocytes I utilised a conditional knockout mouse model of Chk1 whereby exon 2 of the gene is flanked by LoxP sites (Figure 3.1). Upon recombination by Cre-recombinase exon 2, which contains the translation initiation codon is deleted resulting in loss of Chk1 protein expression (Liu et al, 2000; Lam et al, 2004). To specifically knockout Chk1 in the melanocyte lineage I utilised a mouse model expressing Cre-recombinase under the control of the Tyrosinase (Tyr) promoter which is melanocyte specific and actively expressed at later times (E10.5) during embryonic development (Delmas et al, 2003). All mice were maintained on a C57Bl/6 background in order to maintain a pigmented phenotype. The Tyr-Cre

transgene is located on the X-chromosome, therefore in order to avoid problems associated with X-inactivation only male mice were initially used for the analysis.
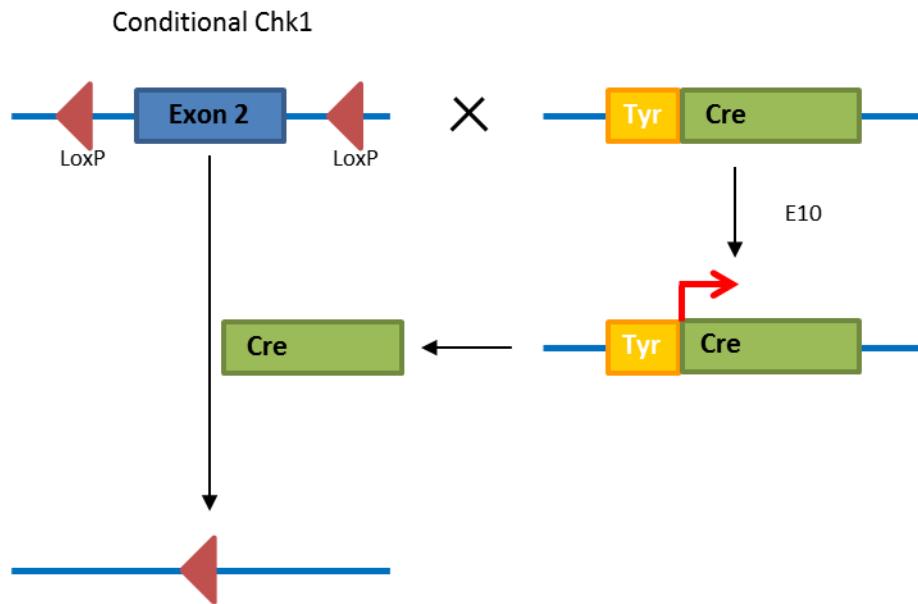
Figure 3.1: Conditional deletion of Chk1 in the melanocyte lineage. Conditional Chk1 flox mice, whereby Exon 2 (containing the translation initiation codon) of the Chk1 gene is flanked by LoxP sites, were crossed with mice expressing Cre-recombinase under the control of the Tyrosinase (Tyr) promoter allowing constitutive expression of Cre in the melanocyte lineage.

Upon Chk1 deletion in adult C57Bl/6 mice all detectable pigmentation of the coat is lost converting a black coated mouse as seen in Chk1 +/+: Tyr-Cre (Figure 3.2Ai) to a white coated mouse in Chk1 fl/fl: Tyr-Cre (Figure 3.2Aii). Mice which are wild-type for Chk1 in melanocytes are fully pigmented. This pigmentation is due to the presence of melanocyte cells which can be seen located at the base of their hair follicles (Figure 3.2Bi). These melanocytes are responsible for the synthesis of melanin which is transferred to the growing hair. However in Chk1 deleted mice all detectable pigmentation of the coat is lost. Analysis of their hair follicles shows that these melanocyte cells are absent from the base of their hair follicles (Figure 3.2Bii). This demonstrates that loss of Chk1 specifically in the melanocyte lineage leads to the loss of melanocyte cells from the skin, resulting in the loss of melanin production and ultimately pigmentation. The phenotype observed upon Chk1 deletion is distinct from that observed in FVB albino mice (Figure 3.2Aiii). FVB albino mice possess the classical albino

mutation (*c*) which affects the expression of the *tyrosinase* gene (Montoliu et al, 1996; Taketo et al 1991). Tyrosinase is the rate limiting enzyme in the melanin biosynthesis pathway. As such FVB albino mice retain melanocytes in their hair follicles (Figure 3.2Biii) but these cells lack expression of tyrosinase and thus melanin.

Although most pigment cells are NC-derived including melanocytes of the skin, hair follicle, iris and choroid, pigment cells of the retinal pigmented epithelium (RPE) located in the eye are derived from the optic cup (Zhao et al, 1997). The expression of tyrosinase has been shown to be differentially regulated in the two pigment cell lineages with a specific enhancer-promoter combination allowing for expression to be specifically targeted to the NC-derived melanocytes (Camacho-Hubner & Beermann, 2001). The 6.1kb Tyr promoter used here contains 2.5kb of the region immediately upstream of exon 1 and 3.6kb of a region located 15kb upstream of exon 1. These regions encompass the two important elements for differential expression; the 270bp promoter fragment and the hs enhancer (Camacho-Hubner & Beermann, 2001; Delmas et al, 2003), which restricts the expression of the promoter to melanocytes of neural-crest origin and not to the RPE which is derived from the optic cup. As such we can see that in Chk1 deleted adult C57Bl/6 mice although coat pigmentation is lost they still retain pigment in the eye (Figure 3.3ii). This is presumably due to the continued expression of Chk1 within the RPE of these mice, although loss of NC-derived melanocytes in the eye can still be seen (Figure 3.3v) in comparison to Chk1 +/+ mice which maintain this population of cells located posterior to the ciliary processes (Figure 3.3iv). This is in contrast to FVB albino mice which lack pigmentation in all structures of their eyes (Figure 3.3iii and vi). Collectively this data shows that Chk1 expression in melanocytes during embryogenesis from E10.5 is essential for the formation or survival of this cell type.
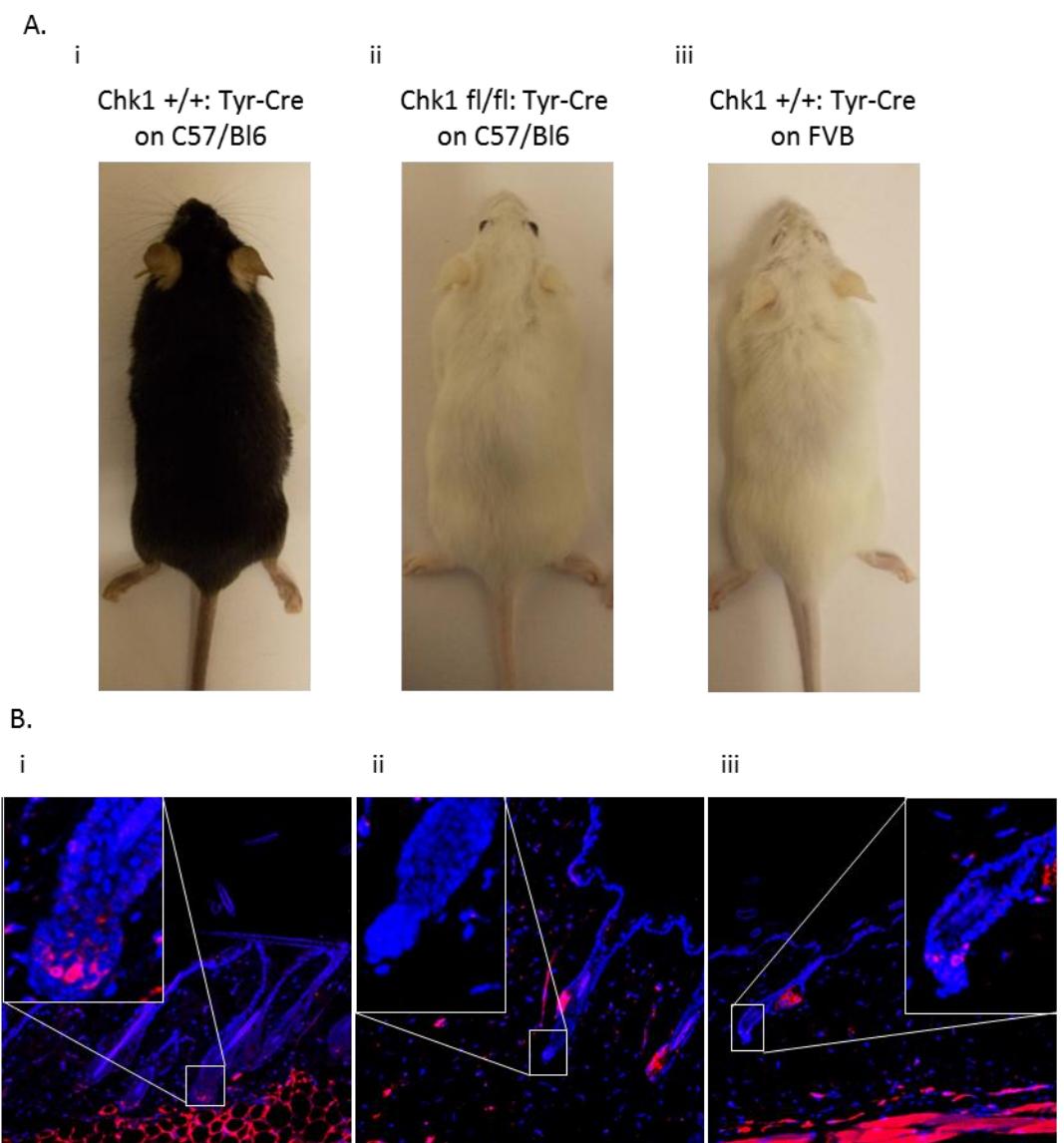
Figure 3.2: Loss of pigmentation in adult mice upon Chk1 deletion. (A) Images of adult mice showing a black coated (i), a white coated (ii) and albino (iii) with the genotypes Chk1 +/+: Tyr-Cre on C57Bl/6, Chk1 fl/fl: Tyr-Cre on C57Bl/6 and Chk1 +/+: Tyr-Cre on FVB respectively. (B) Immunofluorescence microscopy of paraffin-embedded skin sections. Antibodies against DCT (red), a melanocyte specific marker, were used. Inserts show individual hair follicles in skin sections. Positive labelling for DCT was seen in Chk1 +/+ on both C57Bl/6 (i) and FVB (iii) in the hair follicle bulb. Chk1 fl/fl (ii) on C57Bl/6 were devoid of DCT expressing cells in the hair follicles.
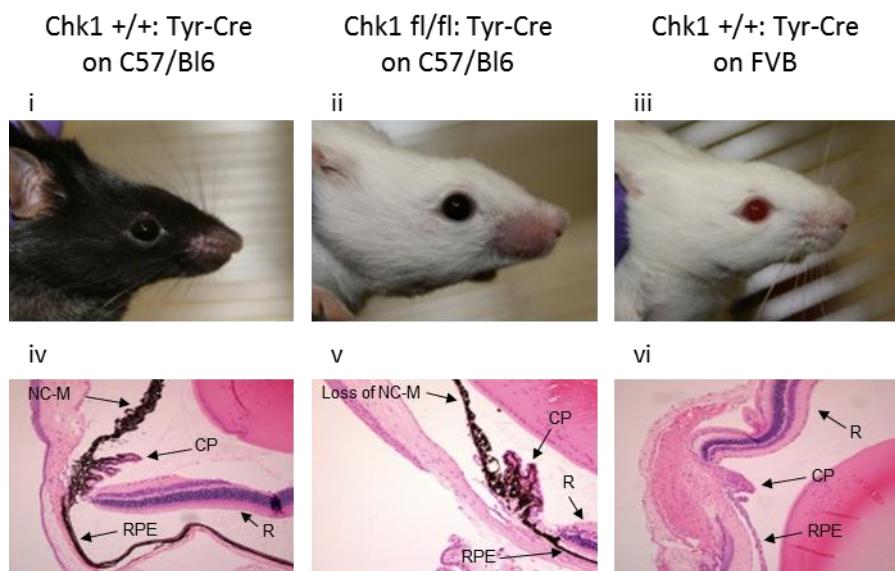
Figure 3.3: Loss of Neural Crest (NC)-derived melanocyte in the eye Chk1 fl/fl: Tyr-Cre mice.
(A) Images and corresponding H&E stained eye sections of adult mice. (ii and v) Chk1 fl/fl: Tyr-Cre on C57Bl/6 mice has black eyes due to the RPE (retinal pigment epithelium) but lack NC-derived melanocytes. (i and iv) Chk1 +/+: Tyr-Cre on C57Bl/6 mice has black eyes with NC-derived melanocytes present. (iii and vi) Albino mice have red non-pigmented eyes. H&E sections show ciliary processes (CP) and retina (R).

3.3 Developmental deletion of Chk1 leads to loss of melanocyte precursor cells during embryogenesis

The specific Tyr promoter used for the expression of Cre-recombinase becomes active at the early embryonic stage of E10.5, thus deletion of Chk1 is predicted to begin at this time during embryogenesis (Ferguson & Kidson 1997). In order to establish the time frame for melanocyte loss *in utero* I utilised a transgenic mouse model whereby the reporter gene *LacZ* is expressed in a melanocyte specific manner allowing visualisation of melanocytes by ß-galactosidase cleavage of X-Gal (Figure 3.4A and B). The transgene is a recombinant construct in which the *Escherichia coli ß-galactosidase* gene is driven by the mouse DCT promoter (Mackenzie et al, 1997). DCT is an enzyme involved in the biosynthesis of melanin and is first expressed in E9 melanoblasts and is still expressed later in adult melanocytes.
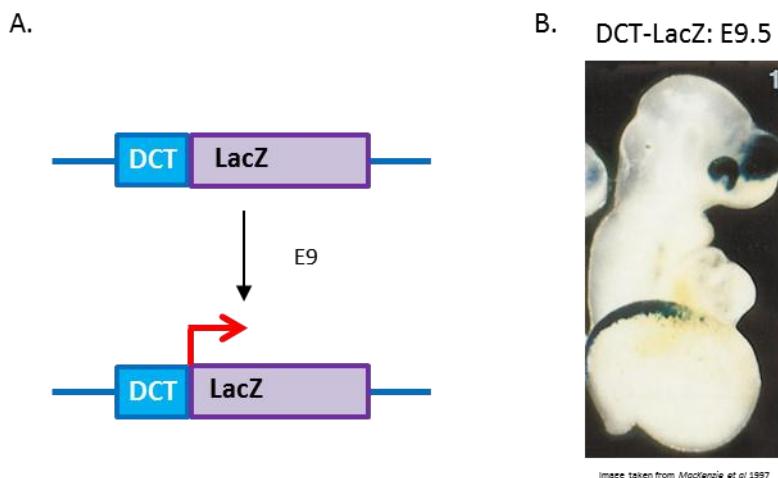
Figure 3.4: The LacZ reporter allele. (A) The *LacZ* transgene is under the control of the melanocyte specific DCT promoter which becomes expressed from embryonic day 9. (B) Image of wholemount β-galactosidase stained DCT-LacZ E9.5 embryo, taken from paper MacKenzie *et al* 1997.

To elucidate when Chk1 deletion is affecting melanocytes during embryogenesis whole-mount distribution of LacZ positive cells in Chk1 +/+: Tyr-Cre: DCT-LacZ and Chk1 fl/fl: Tyr-Cre: DCT-LacZ embryos at E10.5 through to E13.5 were compared (Figure 3.5). In early stage E10.5 (shortly after Cre-recombinase expression is activated) and E11.5 there was no obvious visual alteration in either the number or distribution pattern of melanocytes between Chk1 +/+ and Chk1 fl/fl embryos. In E10.5 embryos of both genotypes there is a high concentration of melanocytes in the brain, eye and neural tail tube with a smaller number visible in the head, shoulder, and dorsolateral trunk regions. In E11.5 embryos of both genotypes there are a greater number of melanocytes present in the head, shoulder and dorsolateral trunk regions than in E10.5; however the melanocytes are still concentrated in the brain, eye and neural tail tube. By E12.5 we can see that there is a visible reduction in the overall number of melanocytes in Chk1 fl/fl embryos compared to Chk1 +/+, but with no obvious effect on the distribution pattern and therefore presumably of the migratory potential. This reduction is particularly evident in the head, shoulder and dorsolateral trunk regions of the embryo. Strikingly by E13.5 we can see that all melanocytes are absent in Chk1 fl/fl embryos whereas Chk1 +/+ have a normal distribution of melanocytes with expansion throughout the whole embryo, uniformly across both dorsal and lateral surfaces of the trunk.
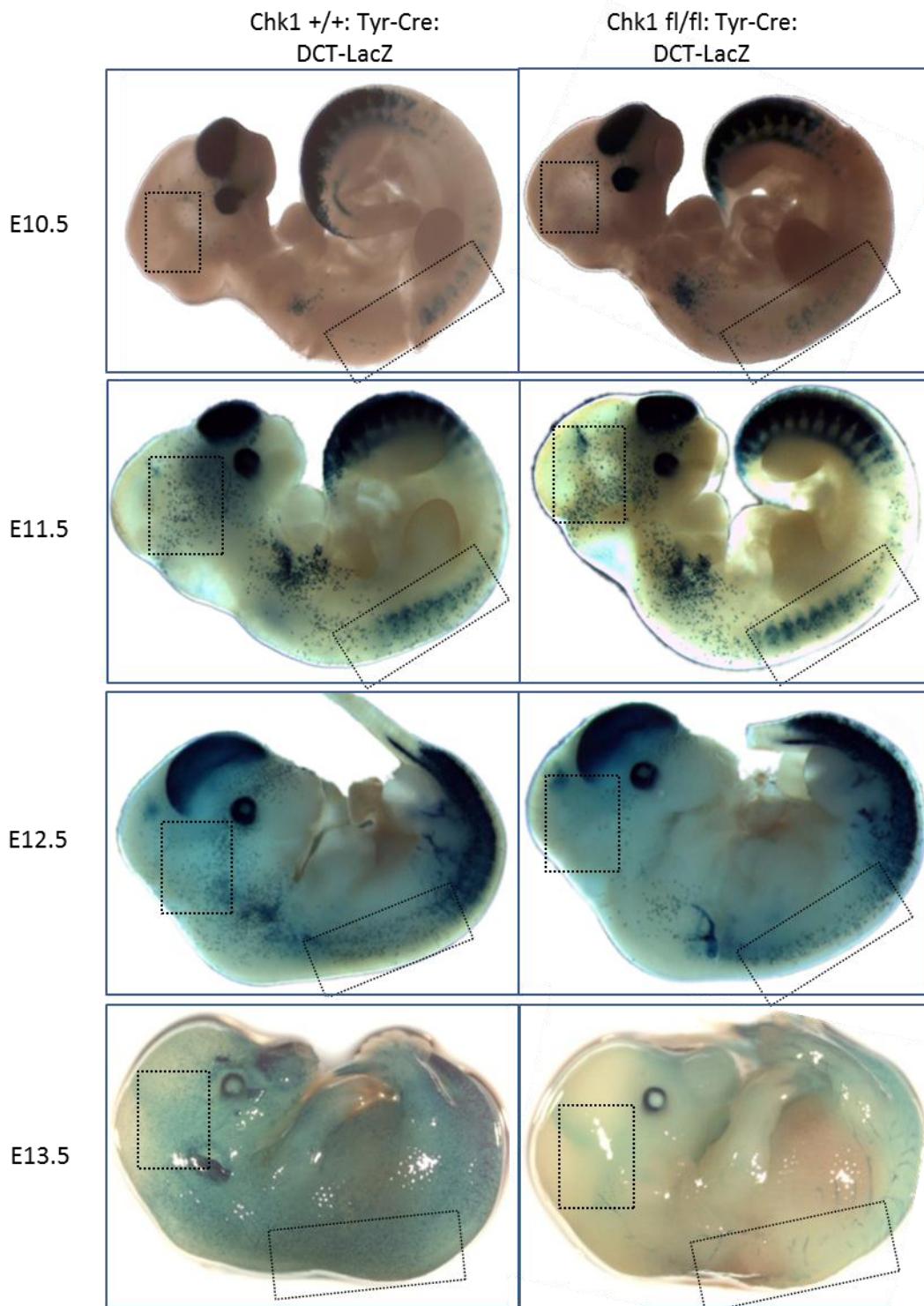
Figure 3.5: Loss of melanocytes between E12.5and E13.5 during embryogenesis upon Chk1 deletion. Images of Wholemount β-galactosidase stained embryos from E10.5 to E13.5 for Chk1 wildtype (Chk1 +/+: Tyr-Cre: DCT-LacZ) and Chk1 flox (Chk1 fl/fl: Tyr-Cre: DCT-LacZ) embryos.
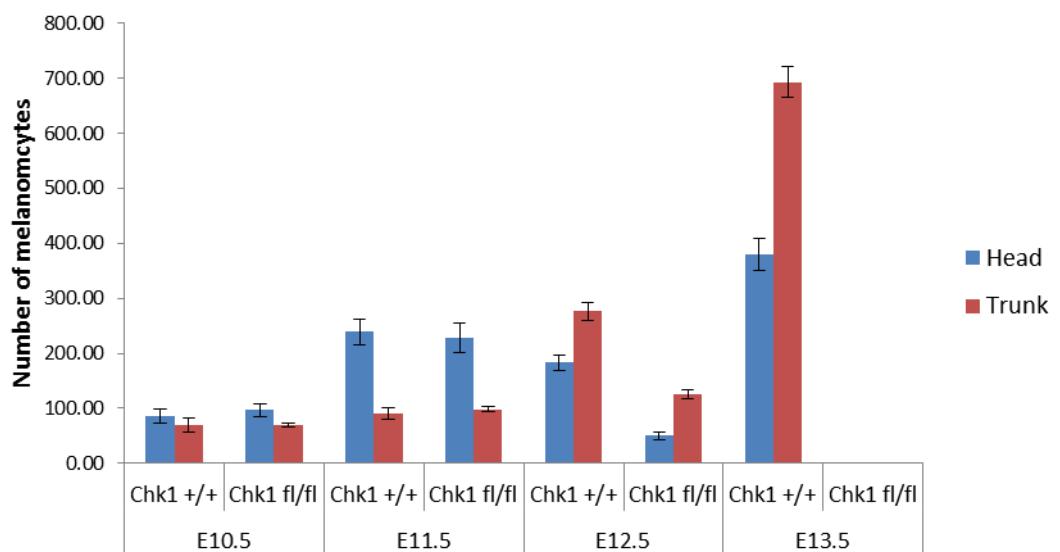
Figure 3.6: Graph of melanocyte numbers between E12.5 and E13.5 during embryogenesis upon Chk1 deletion. Graphical representation of the average number of melanocytes quantified in the regions represented in Figure 3.5.

Quantification of the number of melanocytes (Figure 3.6 and Table 3.1) in the head and dorsolateral trunk regions (as highlighted in Figure 3.5 and counted as one blue dot = one melanocyte) in E10.5 to E13.5 embryos confirmed that at early embryonic E10.5 (shortly after Cre-recombinase expression is activated) and E11.5 there is no significant difference between Chk1 deleted (Chk1 fl/fl) and Chk1 wild type (Chk1 +/+) embryos. However at later times in E12.5 embryos where there is a visible reduction in the number of melanocytes in the Chk1 deleted embryos there is statistically a very high significant difference in both the head (p=0.00018) and dorsolateral trunk (p=0.00017) regions between Chk1 fl/fl and Chk1 +/+ embryos. By E13.5 when all visible melanocytes have disappeared from the Chk1 deleted embryo, there is an even higher statistical significant difference in both the head (p=2.132E-7) and dorsolateral trunk (p=4.26E-9) regions between Chk1 fl/fl and Chk1 +/+ embryos. This data shows that although deletion of the *Chk1* gene presumably commences at E10.5 (when the Tyr promoter becomes active) no significant reduction in the number of melanocytes is seen until 48hrs later at E12.5. This may represent the timeframe for deletion of Chk1 to occur. In the model used it has been previously shown that Tyr-Cre is functional by E11.5, as shown by Cre-mediated expression of the *LacZ* reporter gene from the Rosa26 locus (Delmas et al, 2003; Soriano, 1999) whereby clear punctate staining was visible in E11.5 embryos. Thus Cre-mediated recombination of the *Chk1* gene should be complete by E11.5.

However in order for melanocytes to become functionally null for Chk1 any residual Chk1 protein present before recombination must be destroyed. The half-life of Chk1 in human cells has been shown to be fairly short; 3.4hrs in Hek293, 4.8hrs in A549 (Zhang et al, 2005) and 6h in Hela cells (Leung-Pineda et al, 2009) during unperturbed cycling with a reduction in the half-life seen in stressed cells. Therefore by late E11.5 melanocytes in Chk1 fl/fl embryos should express little or no Chk1. Within 24hrs of this, E12.5, the melanocyte number in both the head and dorsolateral trunk regions are significantly reduced (70% and 50% respectively) with complete loss by 48hrs, E13.5. This shows that loss of melanocytes after Chk1 deletion is remarkably rapid, demonstrating that Chk1 expression is highly essential for survival of melanocytes during embryogenesis.

		Head	p-value	Trunk	p-value
E10.5	Chk1 +/+	86.5 ± 12.5 (5)	0.62861	70 ± 13 (5)	0.97330
	Chk1 fl/fl	96.5 ± 12.5 (6)		69.5 ± 2.5 (6)	
E11.5	Chk1 +/+	228 ± 26.89 (9)	0.75978	98 ± 4.58 (9)	0.57980
	Chk1 fl/fl	239.67 ± 23.38 (7)		91 ± 10.69 (7)	
E12.5	Chk1 +/+	182.75 ± 14.53 (10)	0.00018[***]	276 ± 16.15 (10)	0.00017[***]
	Chk1 fl/fl	49.75 ± 7.36 (12)		124.75 ± 8.52 (12)	
E13.5	Chk1 +/+	380.5 ± 29.26 (11)	2.132E-7[***]	693.25 ± 27.69 (11)	4.26E-9[***]
	Chk1 fl/fl	0 (8)		0 (8)	

Table 3.1: Quantification of melanocytes in wholemount embryos. Shown are the average number of melanocytes quantified, standard deviation and number of samples in brackets. P-values are included with *** indicating highly significant values. The regions quantified are represented in Figure 5.

3.4 Hemizygous deletion of Chk1 during development marginally affects melanocyte number with no detriment to pigmentation

Although homozygous deletion of Chk1 in mice has been shown to be embryonic lethal (Liu et al, 2000), constitutively Chk1 hemizygous mice are viable. However tissue specific loss of one copy of Chk1 can result in cell cycle defects such as an increased number of S-phase cells, spontaneous DNA damage generation and premature mitotic entry (Lam et al, 2004). Recently a human Chk1 heterozygous cell line was generated using HCT116 cells. In this system Chk1 loss resulted in decreased proliferative potential accompanied by spontaneous cell death resulting in reduced cell survival (Wang et al, 2012). Therefore I analysed the effect of Chk1 heterozygosity on coat pigmentation in adult mice and melanocyte number in Chk1 fl/+ embryos whereby only one allele of Chk1 will be recombined upon Cre-recombinase treatment.

Comparison of Chk1+/+: Tyr-Cre and Chk1 fl/+: Tyr-Cre adult mice showed that loss of one copy of Chk1 had no visible effect on coat pigmentation (Figure 3.7Ai and ii respectively), with no subtle alterations such as loss of pigmentation at extremities. Wholemount distribution in E13.5 Chk1+/+: Tyr-Cre: DCT-LacZ and Chk1fl/+: Tyr-Cre: DCT-LacZ embryos (Figure 3.7Bi and ii respectively) showed that there was no obvious reduction in the overall melanocyte number or alterations in the pattern at this stage, whereas homozygous Chk1 deletion showed complete loss of melanocytes by E13.5. However careful quantification of the number of melanocytes in the head, dorsolateral trunk and abdominal regions (as highlighted in Figure 3.7B and counted as one blue dot= one melanocyte) revealed that there was a modest reduction in the number of melanocytes in all the areas analysed; 15%, 30% and 35% reduction in the dorsolateral trunk, head and abdominal regions respectively (Table 3.2). This difference is statistically significant in all regions; head p=0.0189, dorsolateral trunk p=0.006691 and abdomen p=0.000676. It is interesting to note that the statistical difference increases with distance of melanocytes from the original location in the brain and neural tube regions.
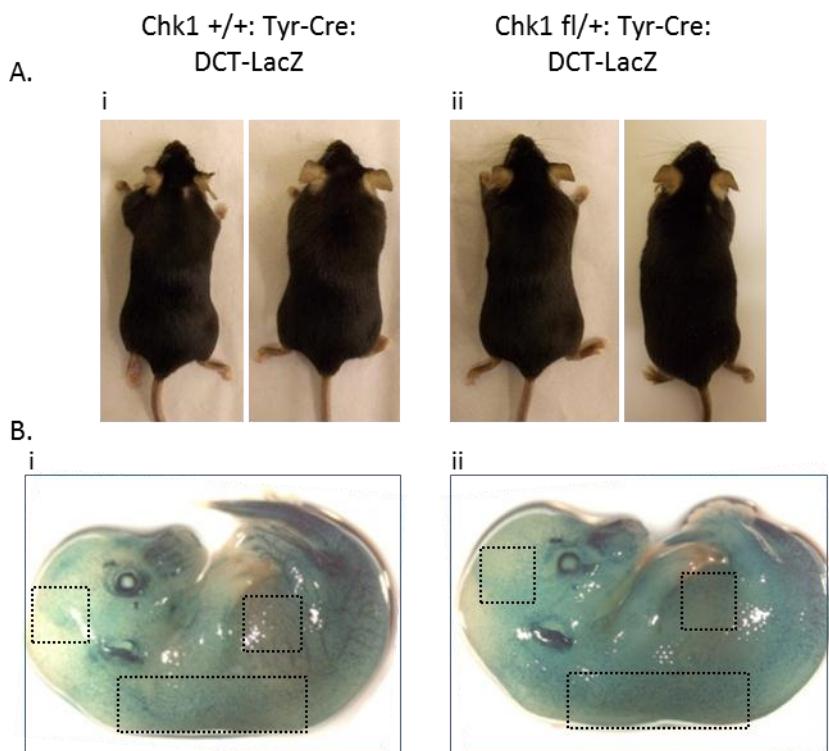
Figure 3.7: Chk1 hemizygousity in the melanocyte lineage. (A-B) Images of adult black coated mice and wholemount β-galactosidase stained E13.5 embryos of the genotypes Chk1 +/+: Tyr-Cre: DCT-LacZ (Ai and Bi) and Chk1 fl/+: Tyr-Cre: DCT-LacZ (Aii and Bii).

	Chk1 fl/+	Chk1 +/+	p-value
Head	276.5 ± 57.8 (13)	380 ± 29.2 (11)	0.01839[**]
Abdomen	264.5 ± 39.6 (13)	403.25 ± 17.2 (11)	0.000676[***]
Trunk	578.25 ± 49.5 (13)	693.25 ± 27.7 (11)	0.006691[***]

Table 3.2: Quantification of melanocytes in wholemount E13.5 embryos. Shown are the average number of melanocytes quantified, standard deviation and number of samples in brackets. P-values are included with ** indicating significant and *** indicating highly significant values. The regions quantified are represented in Figure 6.

3.5 Developmental deletion of Chk1 causes DNA damage in melanocyte precursor cells during embryogenesis

The previously used model for specific deletion of Chk1 in melanocytes during embryogenesis showed that Chk1 loss initiated at E10.5 caused rapid loss of all melanocyte cells within the embryo, with complete loss established by E13.5 (Figure 3.5) resulting in white non-pigmented adult mice (Figure 3.2Aii). In order to elucidate what is happening in the melanocytes upon Chk1 loss I analysed paraffin embedded sections of X-gal stained Chk1fl/fl: Tyr-Cre: DCT-LacZ and Chk1+/+: Tyr-Cre: DCT-LacZ E11.5 embryos. E11.5 embryos were used to establish any early phenotypes associated with Chk1 loss which could account for the loss of melanocytes from the embryo. At this embryonic stage melanocyte cells should be null for Chk1 but with no reduction seen in the melanocyte cell number, however within 24hrs a significant number of melanocytes (50-70%) are lost.

Immunohistochemistry (IHC) analysis showed that in the Chk1fl/fl: Tyr-Cre: DCT-LacZ embryo where Chk1 is deleted, melanocytes which are stained blue owing to the expression of LacZ are strongly positive for γH2AX, a marker of DNA damage (Figure 3.8A, red stars). However in the Chk1+/+: Tyr-Cre: DCT-LacZ embryo there was no positivity for γH2AX in melanocytes (Figure 3.8B), however there was γH2AX positive staining in other cell populations. This data suggests that upon deletion of Chk1 in melanocytes DNA damage is spontaneously generated, which suggests a possible mechanism for induction of cell death.

Previous studies have shown similar phenotypes in mammary cells, whereby specific deletion of Chk1 in proliferating mammary cells caused cell lethality by apoptosis as assessed by positivity for terminal transferase-based TUNEL assay(Lam et al, 2004). Heterozygous deletion of Chk1 in this model showed an increase in spontaneous DNA damage. In most cell types Chk1 loss appears to be lethal however in DT40 avian cells Chk1 loss does not affect viability however these cells show a reduction in their growth rate which is in part attributed to an increase in the levels of spontaneous apoptosis (Zachos et al, 2003). The role of DNA damage in the induction of apoptosis is well established (Norbury & Zhivotovsky, 2004) and is a key factor in maintaining genome integrity.
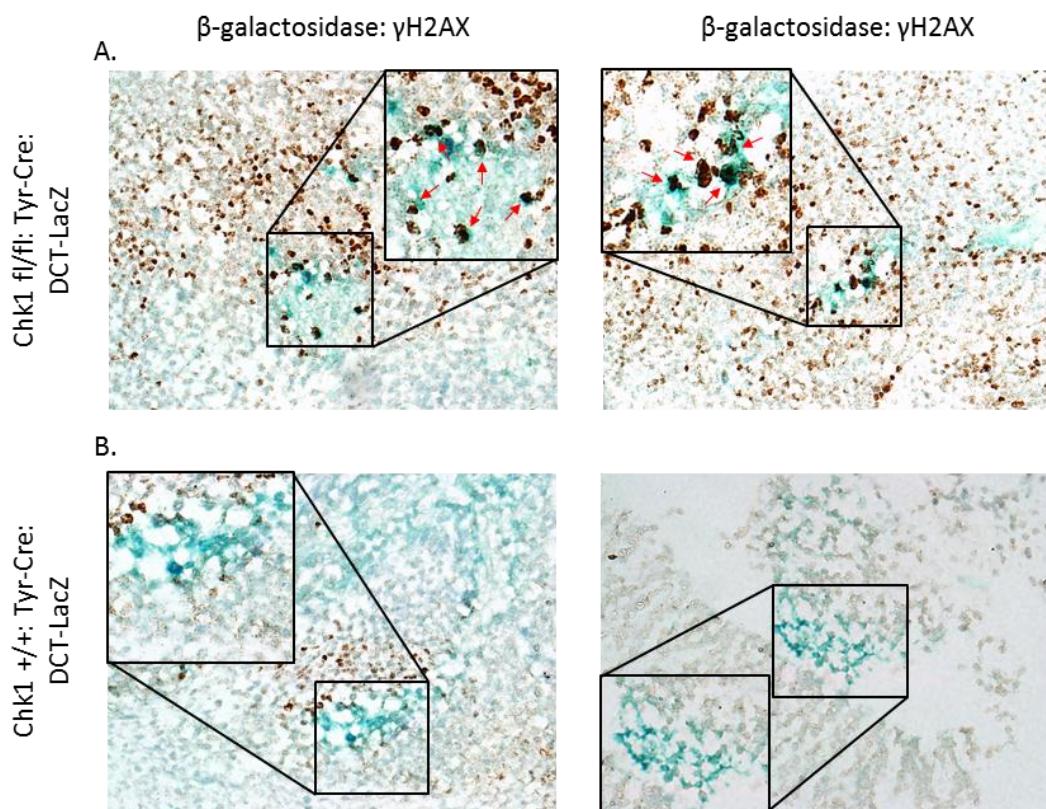
Figure 3.8: DNA damage in Chk1 deleted embryos. (A-B) Immunohistochemistry (IHC) analysis of paraffin-embedded E11.5 embryos with the genotypes Chk1 fl/fl: Tyr-Cre: DCT-LacZ (A) and Chk1 +/+: Tyr-Cre: DCT-LacZ (B). Sections were stained for β-galactosidase (blue) to visualise melanocytes and then labelled with γH2AX (brown). In Chk1 deleted embryos melanocytes are positive for γH2AX (A, red arrows).

3.6 Developmental deletion of Chk1 in female mice shows variation in coat pigmentation

The *Tyr-Cre* transgene in the model mouse used for the analysis of Chk1 deletion is located on the X-chromosome (Delmas et al, 2003). The sex chromosomes X and Y determine the sex in mammals with XY denoting a male and XX denoting a female. Therefore while all male progeny, which were used for the above analysis, are either positive, denoted as $X^{Tyr-Cre}Y$ or negative, donated as $X^{wt}Y$ for expression of Tyr-Cre; female progeny have the potential to be either homozygous positive, denoted as $X^{Tyr-Cre}X^{Tyr-Cre}$ or hemizygous positive, denoted as $X^{Tyr-Cre}X^{wt}$ for expression of Tyr-Cre. In order to compensate for gene dosage females undergo inactivation of one of their X-chromosomes in each cell of the body during early embryogenesis at about the 50-cell stage when the inner cell mass (which will form the embryo) differentiates from the primitive trophoblast (which will form the placenta) (Okamoto et al, 2004). This X-inactivation is random and can affect both the maternal and paternal derived X-chromosome; therefore female progeny of the hemizygous state have the potential to lose expression of Tyr-Cre in at least a sub-population of cells.

In female progeny, which were previously genotyped by Transnetyx to be Chk1fl/fl: Tyr-Cre without any discrimination between homozygosity and hemizygosity for Tyr-Cre expression three distinct coat pigmentation phenotypes were observed. Some females were uniformly white in coat colour (Figure 3.9Ai) although they retained pigmentation in the eye. This phenotype was observed in all male progeny of the genotype Chk1fl/fl: Tyr-Cre. However there were also females which had a fully pigmented black coat (Figure 3.9Aii) with no observable difference from females with the genotype Chk1+/+: Tyr-Cre. In addition there were females which had a patchy/mosaic coat phenotype whereby the coat was mostly white in colour but with small areas of grey colouring (Figure 3.9Aiii). These patches of pigmentation were always localised around the head and hind areas (Figure 3.9Bi and ii respectively) of the animals. It is of potential interest to note that these areas are where the majority of melanocytes originate from in early embryos as can be seen in E9.5 embryos were strong blue staining (representing melanocytes) can be seen in the brain and neural tail tube (Figure 3.4B).

In order to determine if this phenotype could be due to selective inactivation of the X-chromosome carrying the *Tyr-Cre* transgene a PCR reaction was carried out which had been shown to be able to distinguish between homozygosity and heterozygosity of the $X^{Tyr-Cre}$ gene in this model (Colombo et al, 2007). The *Tyr-Cre* gene is inserted at a specific location within the X-chromosome which has been mapped. The PCR is able to precisely distinguish the genotype by using primer pairs which exist either within the transgene or in the X-chromosome either side of the insertion site (Figure 3.10A). In a wild-type X-chromosome (X^{wt}) an 1172bp product is generated using the specific primers LL1433 and LL1441, whereas in a transgenic X-chromosome ($X^{Tyr-Cre}$) a 364bp product is generated using specific primers LL1403 and LL1326. Presence of both bands represents a heterozygous ($X^{Tyr-Cre}X^{wt)}$ female and presence of only the smaller band represents a homozygous ($X^{Tyr-Cre}X^{Tyr-Cre}$) female. PCR analysis showed that all black coated females were heterozygous for the *Tyr-Cre* transgene, whereas all white and patchy coated females were homozygous for the *Tyr-Cre* transgene (Figure 3.10B).

A.

B.
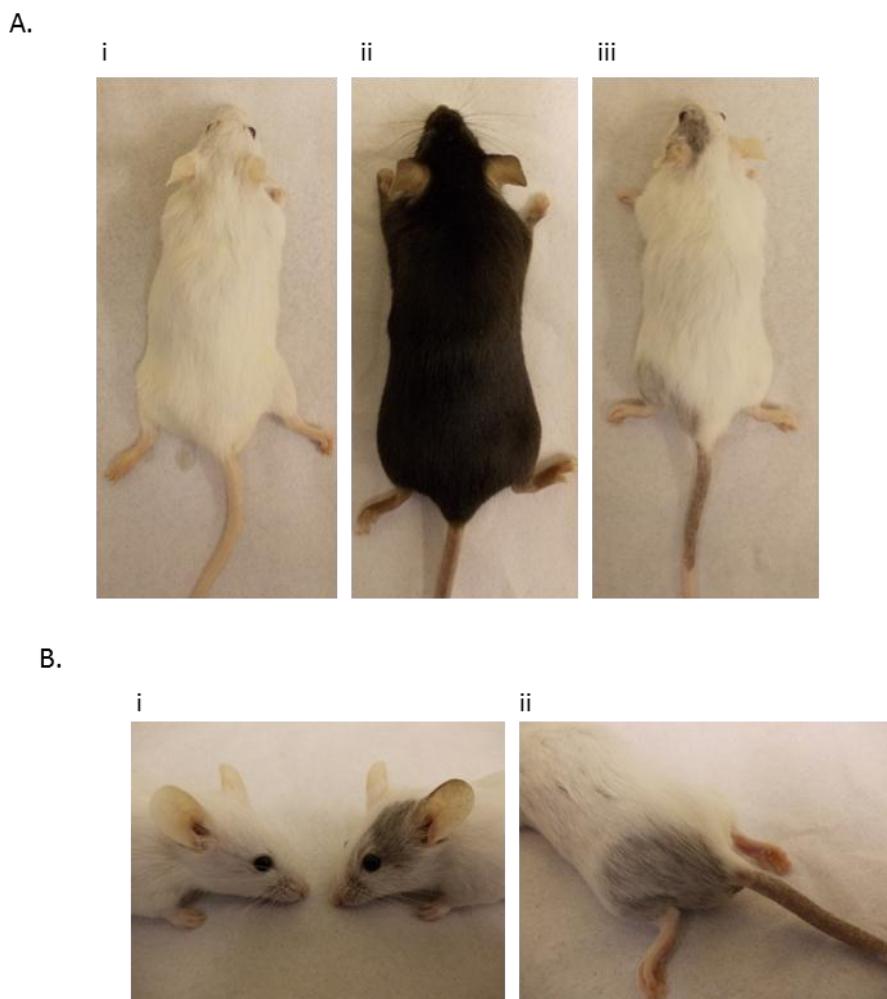
Figure 3.9: Variations in coat pigmentation in Tyr-Cre positive females. (A) Images of female mice with the genotype Chk1 fl/fl: Tyr-Cre as assessed by transnetyx showing various coat phenotypes including white (i), black (ii) and patchy (iii). (B) Images of the patches of pigmentation seen in female mice with the above genotype as seen on the face (i) and hind (ii) regions of the animal.

This data show that in heterozygous females up to 50% of the melanocytes express Tyr-Cre and therefore undergo recombination of the *Chk1* gene during embryogenesis have a fully pigmented coat. This suggests that a potential loss of 50% of the number of melanocytes, due to Chk1 loss, during embryogenesis has little or no impact on the coat pigmentation phenotype compared to controls. This is consistent with previous data showing that Chk1 fl/+: Tyr-Cre: DCT-LacZ male embryos, where up to 35% of melanocytes are lost in some regions of the embryo (Table 3.2), were still fully pigmented with a black coat as adults (Figure 3.7Aii). This suggests that an excess of melanocytes are present during embryogenesis and only a percentage of these are needed for a normal coat colour phenotype or that there is compensation through increased proliferation. However there is also the possibility that the X-chromosome carrying the *Tyr-Cre*

transgene is selectively inactivated during X-inactivation essentially making the females wild-type. In context of the white and patchy coated females this data shows that in homozygous females 100% of the melanocytes should express the *Tyr-Cre* transgene during embryogenesis, no matter which X-chromosome is inactivated and therefore recombination and loss of the *Chk1* gene should occur in all melanocytes. In some females this results in complete loss of coat pigmentation (as seen in the males) however in some females this can result in retention of at least a small number of viable melanocytes giving rise to patches of pigmentation. This phenotype could arise due to loss of recombination efficiency in a small sub-set of cells, potentially by either inactivation of the expressed Cre-recombinase protein or loss of Cre-recombinase expression due to silencing of the Tyr promoter. However this phenomenon was only seen in the female mice with a frequency of 50% in Chk1 fl/fl: Tyr-Cre homozygous females and did not occur in the male mice. As any potential mechanism should also occur in the male mice this suggests that there must be a female-dependant mechanism in place for loss of Tyr-Cre expression in a sub-set of melanocyte cells.
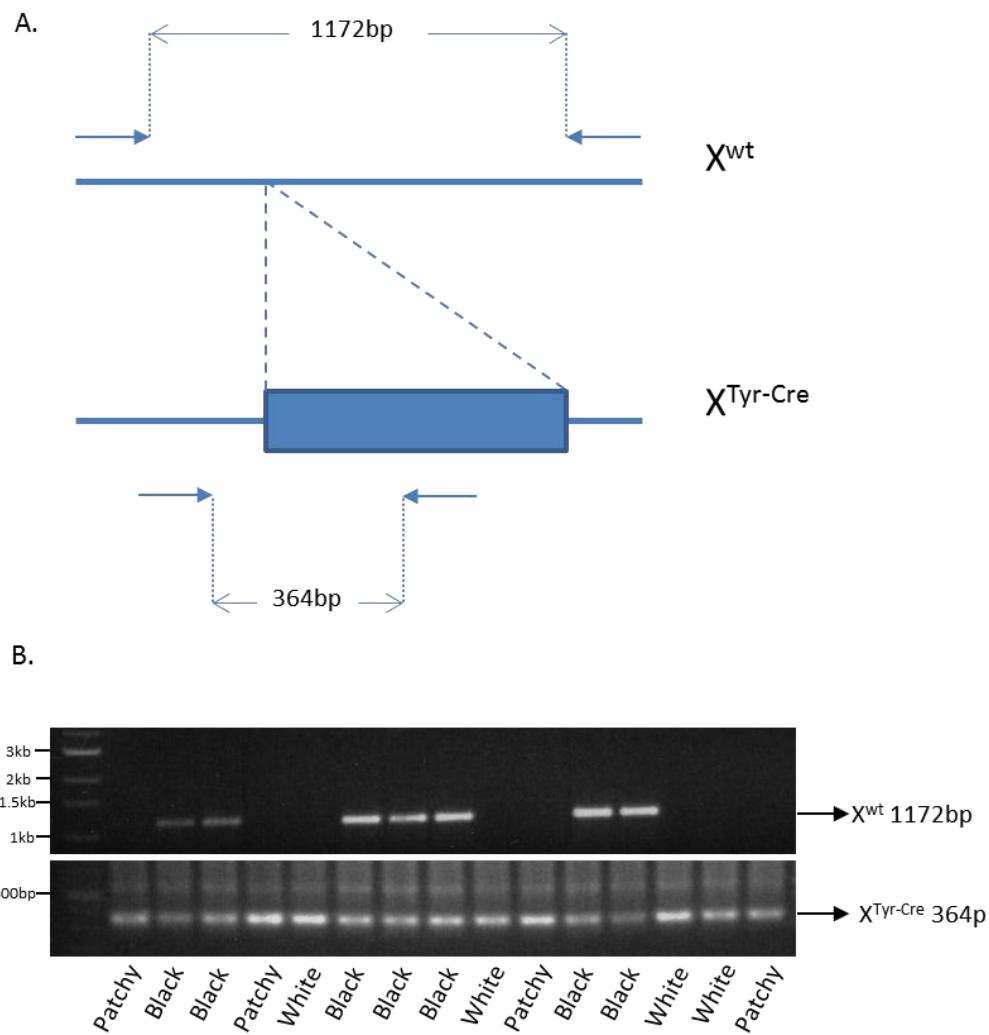
Figure 3.10: Genotyping of Tyr-Cre positive females by PCR. (A) Scheme of PCR amplification corresponding to a hemizygous female ($X^{wt}/X^{Tyr-Cre}$). The line corresponds to genomic DNA with the blue box representing the inserted Tyr-Cre transgene in the X-chromosome. PCR products of sizes 1172bp and 364bp screen for the presence of the X^{wt} and $X^{Tyr-Cre}$ respectively. (B) PCR analysis of DNA from female mice with the genotype Chk1 fl/fl: Tyr-Cre as assessed by transnetyx. Analysed according to coat pigmentation phenotype (patchy, white or black) as seen in figure 3.9.

3.7 Discussion

The main aim if this chapter was to establish the requirement of Chk1 for the continued proliferation and survival of melanocyte precursor cells during embryogenesis. This could be of significance as many of the genes involved in melanocyte development have also been implicated in the development of melanoma, an aggressive and fatal form of skin cancer that originates from melanocytes. Chk1 has been shown to be important in the survival of many cell types including mammary tissue (Lam et al, 2004), T-cells (Zaugg et al, 2007) and the small intestine (Greenow et al, 2009), with constitutive Chk1 loss being embryonic lethal at the early blastocyst stage (E3) in mice (Liu et al, 2000). This

indicates that Chk1 is essential for cell survival even in the absence of exogenous DNA damage. Chk1 has also been shown to be important in tumour development. Chk1 deficiency inhibited the formation of mammary tumours in a p53 null background in mice; however hemizygousity for Chk1 in combination with p53 induced mammary tumour formation (Fishler et al, 2010). Chk1 loss inhibited the formation of chemical-induced skin tumours with Chk1 hemizygousity having no effect on benign tumour formation but increasing the propensity for the conversion to carcinoma (Tho et al, 2012).

Using a conditional Chk1 knockout mouse model (Liu et al, 2000) in combination with a melanocyte specific constitutively expressed Cre-recombinase (Delmas et al, 2003) I was able to show that Chk1 expression is essential for the continued survival of melanocytes during embryogenesis with loss of Chk1 resulting in adult mice which lack any pigmentation despite being on a C57Bl/6 strain background (Figure 3.2). Loss of Chk1, which happens at around E11.5 with Cre-recombinase expression turned on at 10.5, results in rapid loss of melanocyte cells from the embryo with complete absence of melanocytes seen by E13.5 (Figure 3.5). Mathematical modelling of melanocyte development has shown that the total number of melanocyte cell in an E11.5 embryo is 393.77±142.37 and in an E13.5 embryo is 2873.86±419.51 (Aylaj et al, 2011). This constitutes a >700% increase in cell number over 48hrs, which represents extremely rapid proliferation of cells. Chk1 deletion was shown to cause spontaneous DNA damage (Figure 3.8), which suggests a possible mechanism for inducing cell death. Collectively this data shows that Chk1 loss is severely detrimental to melanocyte cells. The severity is possibly due to the rapid proliferation rate of these cells, as Chk1 is important during unperturbed cell cycle where it functions during S-phase in both the initiation of replication and stability of replication forks (Feijoo et al, 2001; Paulsen & Cimprich, 2007; Petermann et al, 2006; Petermann et al, 2010). The data is also consistent with other data that has shown Chk1 loss causes cell death by apoptosis (Liu et al, 2000; Lam et al, 2004).

However Chk1 hemizygosity in the melanocyte lineage was well tolerated with only a small but significant decrease in cell number observed and no obvious defect in the pigmentation phenotype of the adult mice (Figure 3.7). This is consistent with studies that have shown constitutive Chk1 hemizygous mice are

developmentally normal, fertile and lack an overt phenotype (Liu et al, 2000). Despite this, partial loss of Chk1 function has been shown to affect cell survival and tissue homeostasis *in vivo*. Chk1 hemizygosity induced specifically in the mammary tissue resulted in an increased proportion of S-phase cells, spontaneous DNA damage and premature entry to mitosis (Lam et al, 2004). Chk1 hemizygosity induced in the T-cell lineage led to developmental perturbation and cell loss (Zaugg et al, 2007). However Chk1 hemizygosity did not result in an obvious phenotype in the small intestine (Greenow et al, 2009). These data combined show that the consequences of partial loss of Chk1 functions for cell proliferation and survival seem to vary according to cell and tissue type.

Chapter 4: Chk1 requirement in melanoma initiation and progression *in vivo*

4 Chk1 requirement in melanoma initiation and progression *in vivo*

4.1 Introduction

Melanoma is the most aggressive type of skin cancer which predominantly affects Caucasians of north-western European descent. It is the 19th most common cancer worldwide with the most affected area being Australia, where it represents the 3rd most common type of cancer in both sexes (Ferlay et al, 2010). In the UK and USA melanoma is the 5th and 6th most common cancer respectively (Cancer Research UK; American Cancer Society). Unlike other types of cancer incidence rates for melanoma have increased over the past 30 years. In both the UK and USA incidence rates have increased more rapidly than any of the other ten most common cancers (Cancer Research UK; Howlader et al, 2012; Jemal et al, 2010). Although melanoma only accounts for 5-10% of skin cancer cases it is the cause of >80% of deaths from skin cancer with the 5 year survival of metastatic melanoma being only 15% (Siegel et al, 2012).

The cells of origin for melanoma are the pigment-producing melanocytes. The genetic alterations associated with the malignant transformation of melanocytes are well established (Chin et al, 2003). The MAPK signalling cascade is frequently mutated, with activating B-Raf mutations seen in as many as 60% of human melanoma samples and cell lines (Davies et al, 2002). Activating point mutations in N-Ras have been seen in as many as 56% of congenital nevi, 33% of primary melanomas and 26% of metastatic samples (Demunter et al, 2001). Mutations in B-Raf and N-Ras are mutually exclusive owing to the fact that N-Ras is directly upstream of B-Raf and therefore mutations in the two proteins act on the same pathway. The most common mutations seen in familial melanoma are loss of the tumour suppressor locus CDKN2A (also known as the INK4A locus) (Hussussian et al, 1994) which encodes for two proteins; p16^{Ink4a} and p14Arf (human) or p19Arf (mouse), and mutation of CDK4 (Zuo et al, 1996). This implicates the importance of both the p16^{Ink4a}- CDK4- RB and ARF-p53 pathways in the development of melanoma. In fact p16^{Ink4a} loss is also seen in 15-28% of primary sporadic melanoma samples and in almost all established melanoma cell lines (Fujimoto et al, 1999; Walker et al, 1998). PTEN loss is also common in melanoma,

occurring in 5-15% of uncultured melanoma specimens and metastasis as well as in 30-40% of established melanoma cell lines (Guldberg et al, 1997; Teng et al, 1997).

4.2 Mouse model of melanoma: N-Ras and CDKN2A

The melanoma model developed by Friedrich Beermann's group (Ackermann et al, 2005) expresses an oncogenic form of human N-Ras with a point mutation in codon 61 (Q61K) from the melanocyte specific Tyrosinase promoter. This allows specific expression of the oncogene in the melanocyte lineage only. These mice were crossed onto a CDKN2A deficient background which has loss of both p16^{Ink4a} and p19Arf (Serrano et al, 1996) (Figure 4.1A). In hereditary melanoma with germ line p16^{Ink4a} mutations, 95% of patients have oncogenic N-Ras^{Q61K} (Eskandarpour et al, 2003) therefore this model closely mimics the genetics of the human condition. These mice exhibit hyper-pigmented skin, as most evident in the ears and paws and develop melanoma in the dermis and/or epidermis with a high incidence (>90%) and short latency (6 months), with frequent metastasis to the lymph nodes, liver and lungs (Ackermann et al, 2005). However upon experimental handling these mice also developed lymphoma with extremely high penetrance and were therefore not viable as a melanoma model in our hands; this is perhaps not surprising as the CDKN2A deficient mice alone have been shown to develop sarcomas and lymphomas with a high penetrance (69%) and short latency (29 weeks) (Serrano et al, 1996). Upon DMBA/UVB induced carcinogenesis tumourigenesis is increased to 90% penetrance with an average latency of 9 weeks in these mice (Serrano et al, 1996). Lymphoma development is thought to be a result of loss of p19Arf as genetic disruption of Arf alone has been shown to predispose mice to tumourigenesis (Kamijo et al, 1997) whereas disruption of p16^{Ink4a} alone did not show a significant predisposition to spontaneous tumour formation (Krimpenfort et al, 2001).

In order to circumvent the development of lymphoma the Beermann melanoma mice were crossed with mice developed by Anton Berns's group that are deficient for p16^{Ink4a} but retain one copy of Arf (Figure 4.1A). These mice have been shown to develop a wide spectrum of tumours including melanoma with an average latency of 12 months (Krimpenfort et al, 2001; Sharpless et al, 2001). In combination these mice are hyper pigmented (Figure 4.1Bi-ii, black arrow),

develop melanoma (Figure 4.1Biii-iv, white arrows) with an average tumour onset of 8 months and have metastasis to the lymph nodes and lung (Figure 4.1Bv-vi, red arrow).
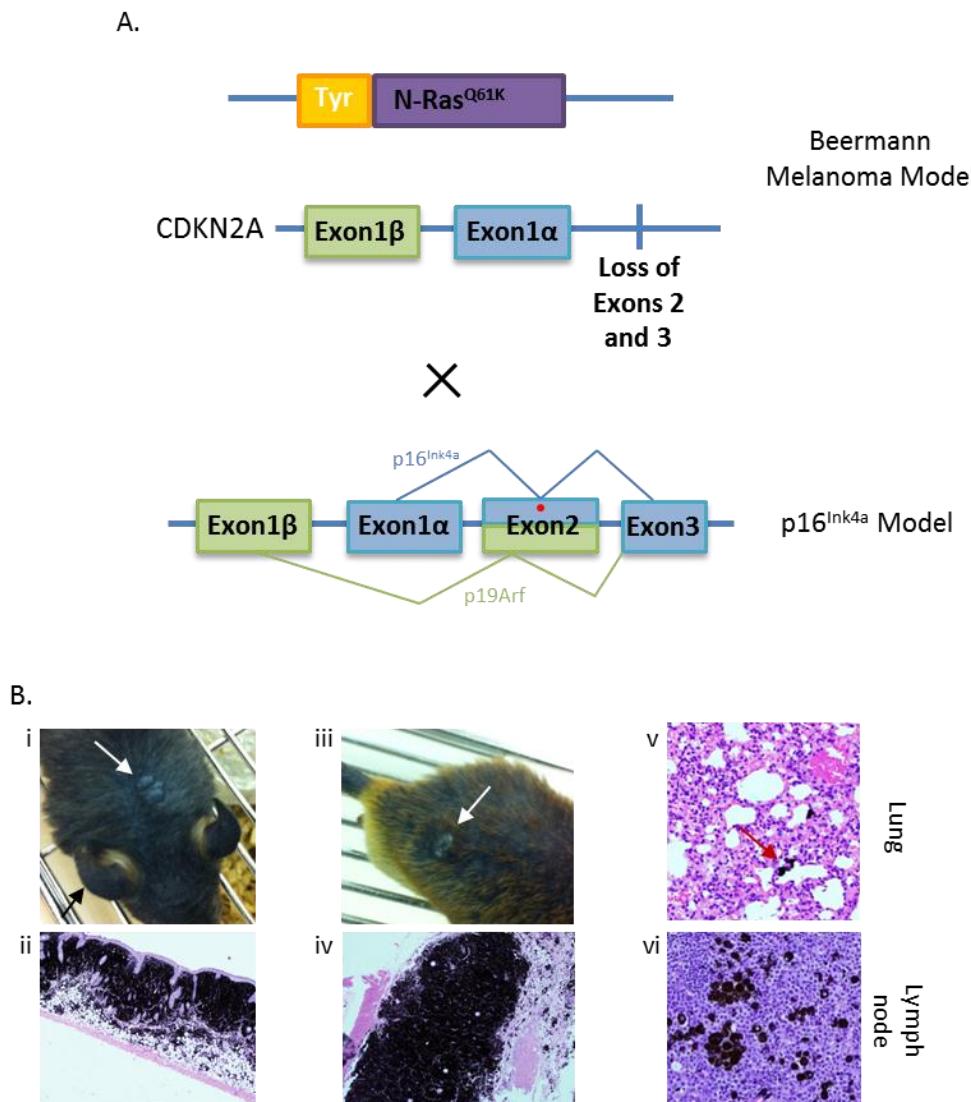
Figure 4.1: Mouse model of melanoma: N-Ras and CDKN2A. A) Beerman melanoma with expression of oncogenic N-Ras from the melanocyte specific Tyrosinase promoter in combination with loss of the CDKN2A locus crossed with the p16^{Ink4a} model with a point mutation in Exon 2 which affects the splicing of p16^{Ink4a} but not p19Arf. (B) Pictures and H&E sections of model mice with hyper-pigmented skin (i-ii), melanomas (i and iii white arrow, iv) and metastasis to the lung (v red arrow) and lymph nodes (vi).

4.3 Loss of Chk1 on tumour formation in nude mice

In order to analyse the role of Chk1 in melanoma development the aforementioned melanoma mice bearing the p16^{Ink4a}-deficient allele were crossed with a conditional knockout mouse model of Chk1 (as previously described in Chapter 3:2) in combination with a melanocyte specific inducible Cre-recombinase in which a Cre-recombinase: estrogen receptor fusion transgene is under the control of the tyrosinase promoter (Tyr-CreER^{T2}) (Figure 4.2). This allows for spatially and temporally controlled activation of Cre-recombinase upon addition of 4-hydroxytamoxifen (4-OHT) (Yajima et al, 2006), and thus selective partial or complete deletion of Chk1 in melanocytes.
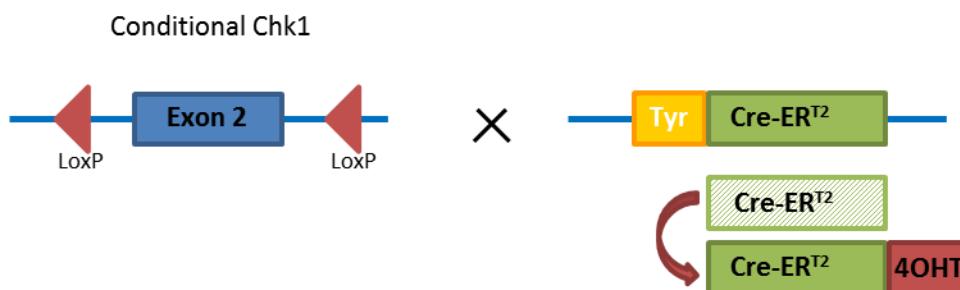
Figure 4.2: Inducible deletion of Chk1 in the melanocyte lineage. Conditional Chk1 flox mice, whereby Exon 2 (containing the translation initiation site) of the Chk1 gene is flanked by LoxP sites, were crossed with mice expressing Cre-recombinase: estrogen receptor fusion transgene under the control of the Tyrosinase (Tyr) promoter allowing spatially and temporally controlled activation of Cre, and thus deletion of Chk1 in the melanocyte lineage.

4.3.1 Melanocyte cell line generation and characterisation

In order to further analyse the effects of Chk1 deletion on tumourigenesis melanocyte cell lines were generated from the aforementioned mouse model, which were subsequently used in allograft experiments in CD1 nudes. Melanocyte cell lines were established from the back skin of adult mice (>6 weeks old) and selected for *in vitro* growth (Figure 4.3, see Materials and methods 2.2.5 for full protocol). Establishment of viable cell lines takes about 8 weeks. Cell lines with the genotypes Chk1 fl/fl, Chk1 fl/+ and Chk1 +/+ were established.

The Chk1 flox allele has the addition of two LoxP sites either side of exon 2 in the intervening introns that constitute a 78bp insert at each site. By using a primer pair that spans the first LoxP site (Forward 581: Reverse 1004) we can distinguish between the Chk1 flox allele, 501bp, and the Chk1 wild type allele,

423bp (Figure 4.4A). Screening by PCR showed that in both the Chk1 fl/fl and Chk1 fl/+ cell lines addition of 4-OHT [1µM] for five consecutive days resulted in very efficient loss of the Chk1 flox alleles (Figure 4.4B). This is further confirmed by WB analysis whereby in Chk1 fl/fl cells addition of 4-OHT [1µM] leads to rapid and complete loss of Chk1 protein within 5 days (Figure 4.5A). Chk1 loss is accompanied by cleavage of PARP, a marker of apoptosis. PARP is a nuclear protein that participates in DNA damage detection and repair, however during apoptosis the protein is cleaved by caspase-3 and caspase-7 (Duriez et al, 1997; Germain et al, 1999). This cleavage efficiently stops the ability of PARP to participate in DNA repair and contributes to the cell fate of apoptosis. Interestingly in Chk1 fl/+ cells addition of 4-OHT [1µM] also leads to significant loss of Chk1 protein within 5days of treatment, greater than a 50% reduction as expected (Figure 4.5B). Chk1 loss is also accompanied by cleavage of PARP as in the Chk1 fl/fl cell line. This effect is specific as addition of ethanol, the vehicle for 4-OHT, in both Chk1 fl/fl and Chk1 fl/+ cells had no effect on Chk1 protein levels or cleavage of PARP. Furthermore addition of 4-OHT in Chk1 +/+ cells also had no effect on Chk1 protein levels or cleavage of PARP (Figure 4.5C).
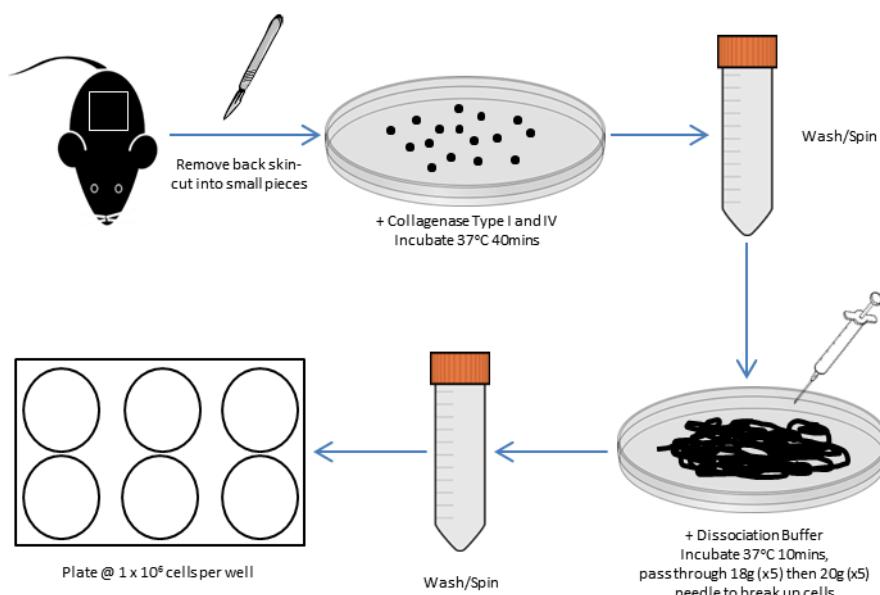
Figure 4.3: Establishment of melanocyte cell lines. Melanocyte cell lines were generated from the excised back skin of transgenic melanoma mice expressing the conditional Chk1 flox allele and Tyr-CreER^{T2}.

A.

Chk1

Intron   Intron

Exon1   Exon2   Exon3

AGTATTTTCTG**GGATCC**TGCATTTTACA
BamHI site

Forward primer (581)
Forward primer (821)
Reverse primer (1004)

78bp insert

ATAACTTCGTATAGCATACATTATACGAAGTTAT

LoxP sequence

B.

Untreated
+4OHT 5days
+EtOH 5days
Untreated
+4OHT 5days
+EtOH 5days
Untreated
+4OHT 5days

Flox allele: 501bp
WT allele: 423bp

Chk1 fl/+   Chk1 fl/fl   Chk1 +/+
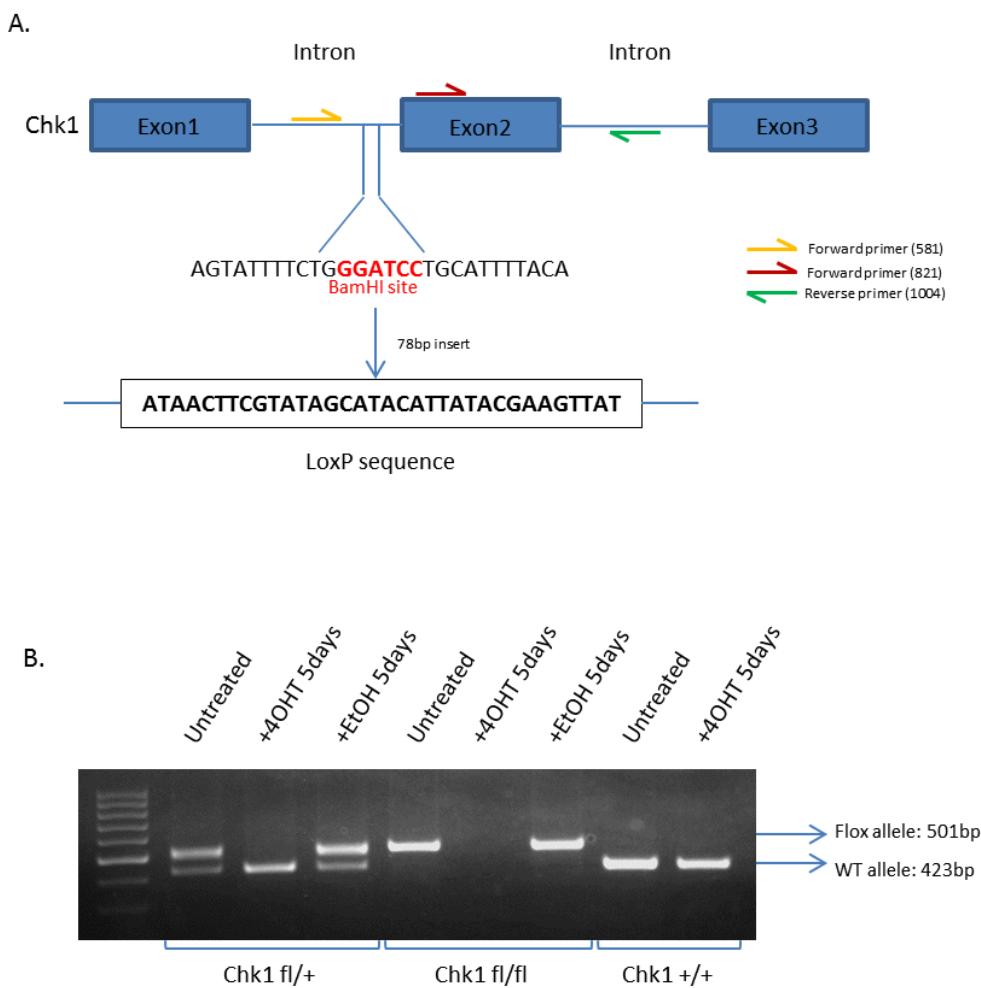
Figure 4.4: Screening of the Chk1 flox allele by PCR. (A) Scheme of PCR amplification. The line corresponds to genomic DNA with the blue boxes representing exons of the Chk1 gene. The Chk1 flox allele contains a 78bp LoxP site inserted in the intron between exon 1 and 2. Primer pair Forward 581: Reverse 1004 generates PCR products of sizes 501bp and 423bp which screen for the presence of the Chk1 flox and Chk1 wt allele respectively. (B) PCR analysis of DNA from melanocyte cells of the genotypes Chk1 fl/fl, Chk1 fl/+ and Chk1 +/+ treated with [1µM] 4OHT or ethanol for 5 consecutive days.
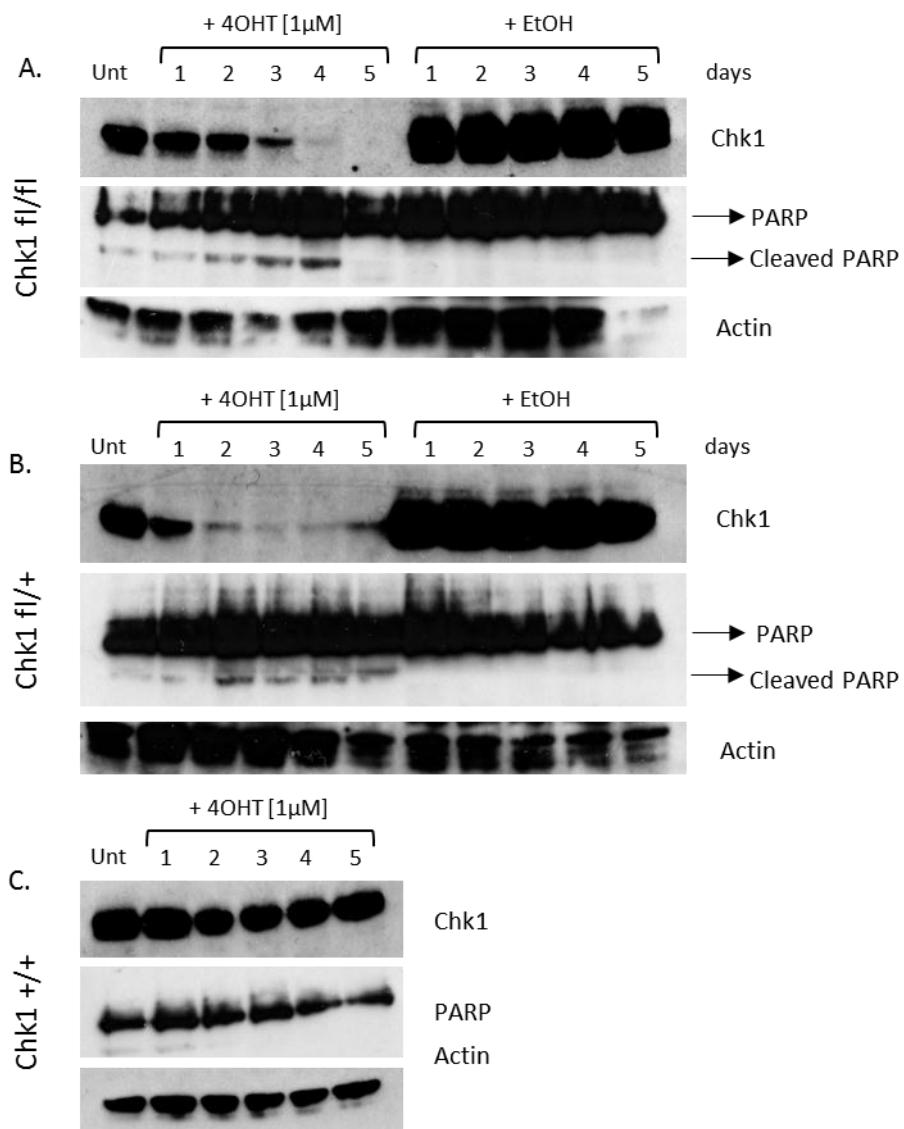
Figure 4.5: Inducible Chk1 deletion *in vitro*. Western blot analysis of the levels of Chk1 and cleavage of PARP from melanocyte cells of the genotypes Chk1 fl/fl, Chk1 fl/+ and Chk1 +/+ treated with [1µM] 4OHT or ethanol for 5 consecutive days. Antibodies against Chk1 and PARP were used. An equal quantity of protein was loaded as determined by Bradford Assay and confirmed by antibody against actin.

4.3.2 Homozygous deletion of Chk1 leads to decreased tumour growth

In order to assess the effect of complete Chk1 loss on melanoma tumour formation *in vivo* Chk1 fl/fl melanocyte cells were grown in culture until they were in a logarithmic phase of growth (70-80% confluent). Cells were then harvested and injected subcutaneously to the lower right flank of 6 week old female CD1 nudes at a concentration of 1×10^5 cells per mouse. One week after

injection 20 mice were randomised into the following treatment groups: vehicle alone (10 mice) or daily dosing of tamoxifen at 2mg/ml for 8 consecutive days (10 mice) followed by 3x weekly dosing until endpoint reached (Figure 4.6).
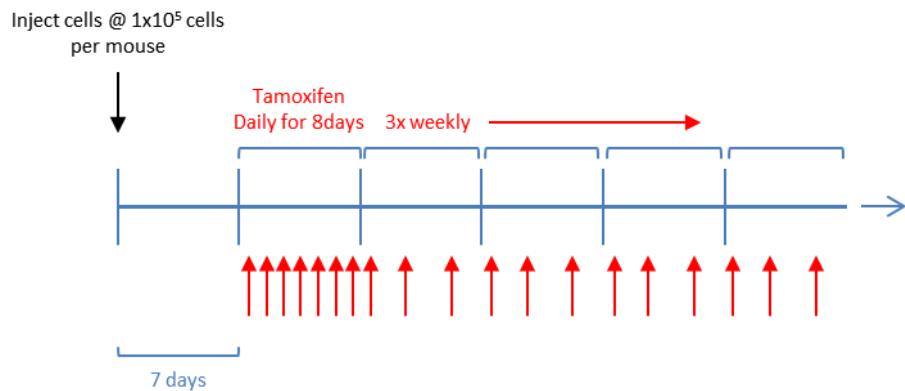
Figure 4.6: Treatment protocol for analysis of Chk1 loss in CD1 nude mice. Melanocyte cell lines of the genotypes Chk1 fl/fl and Chk1 fl/+ were injected into the lower right flank or tail vein of CD1 nude mice at 1x10^5 cells per mice. Seven days later mice were randomised into the treatment group's vehicle alone or daily dosing of tamoxifen at 2mg/ml for 8 consecutive days followed by 3x weekly dosing until endpoint reached.

PCR analysis of final tumour samples using primer pair, Forward 581: Reverse 1004, showed that in all tamoxifen treated animals the Chk1 flox alleles were lost or significantly reduced. This results in final tumours which have either lost or have a significant reduction in their Chk1 expression, in contrast to all vehicle treated tumours which retained expression of the Chk1 flox alleles (Figure 4.7A). It should be noted that in some of the samples there is a band corresponding to the Chk1 wt allele, this is most likely due to contamination from stromal tissue which is derived from the nude mice. This was further confirmed by real time PCR analysis using primer pair, Forward 821: Reverse 1004, whereby the average recombination efficiency of the Chk1 gene in tamoxifen treated animals were 69%, as compared to a control gene (Arbp), with the maximum being 80%. Whereas in vehicle treated animals the average recombination efficiency was negative compared to the control gene essentially meaning there was no recombination (Figure 4.7B). This data shows that the Cre-LoxP recombination system is working fairly efficiently in the Chk1 fl/fl cell line allografts *in vivo*. Complete efficiency would be represented by a 100% recombination rate; therefore the system is either not completely functional or there has been some

repopulation of the tumours by Chk1 proficient cells which have escaped
recombination.

A.

B.
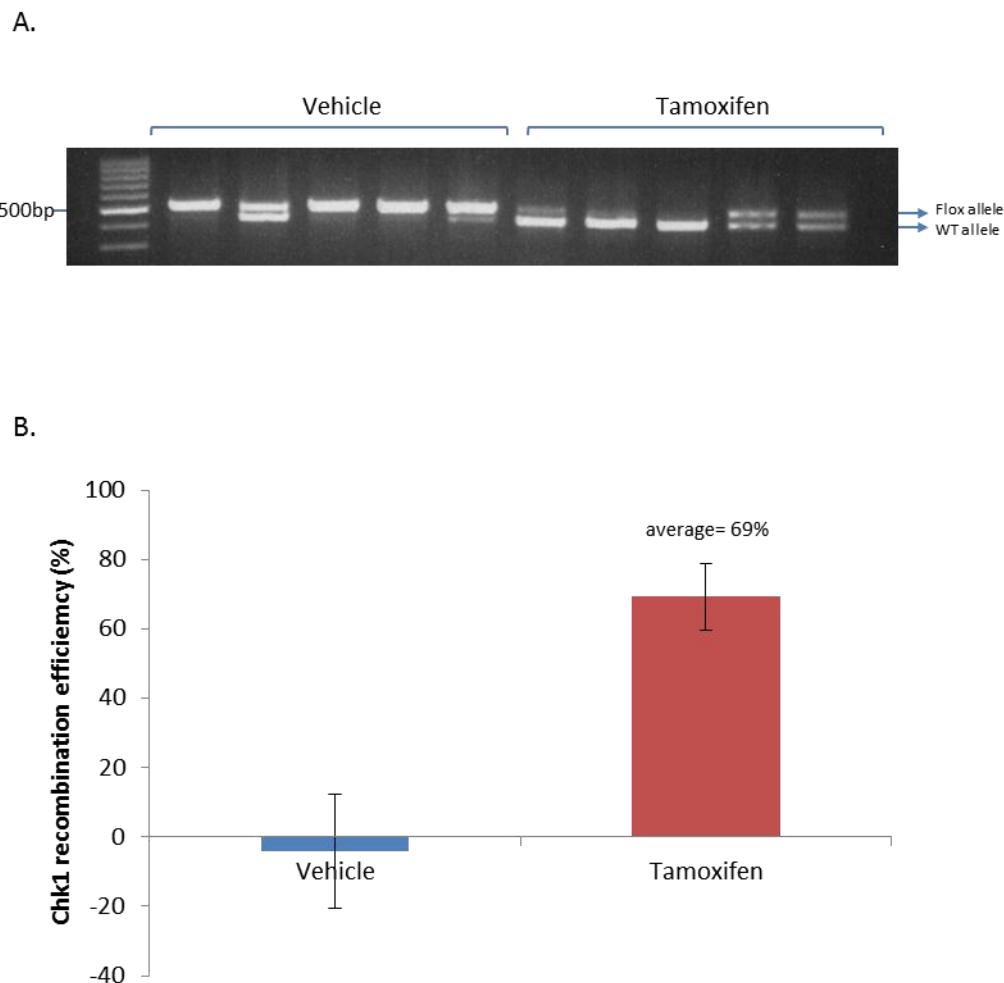
Figure 4.7: Screening for Chk1 deletion by PCR in final Chk1 fl/fl tumours of CD1 nudes. (A)
PCR analysis of DNA from final tumour samples of CD1 nudes injected with melanocyte cells of the
genotypes Chk1 fl/fl treated with tamoxifen or vehicle as outlined in figure 4.6. Chk1 flox allele is
lost or reduced in final tumours of all tamoxifen treated animals. (B) Real-time PCR analysis of
DNA from final tumour samples of CD1 nudes injected with melanocyte cells of the genotypes
Chk1 fl/fl treated with tamoxifen or vehicle as outlined in figure 4.6.

Analysis of the rate of tumour growth, as assessed by the increase in tumour
volume over time as compared to the initial tumour volume (taken at 7 days post
injection), showed that there is a very significant decrease in the tumour growth
rate in the tamoxifen treated cohort compared to vehicle treated (Figure 4.8A).
The reduction first becomes evident 31 days after the start of treatment. At
time-points, 36, 38, 41 and 43 days after treatment there is a statistical
significant reduction in the growth rate; p=0.039662, 0.015396, 0.032583 and

0.024268 respectively. 45 days after treatment this reduction in the growth rate becomes even more highly statistically significant; p=0.007695. Beyond this time point the tumour growth rate in tamoxifen treated animals does not increase much further, whereas in vehicle treated the growth rate increases exponentially. This reduction in tumour growth rate is paralleled by an increase in the survival time of the tamoxifen treated animals. Analysis by Kaplan Mier of the survival time in the tamoxifen and vehicle cohorts (Figure 4.8B) showed that there was a statistically significant increase in the survival potential of tamoxifen treated animals over vehicle (p=0.00174). The longest surviving vehicle treated animal was 52 days whereas the tamoxifen treated animal was 88 days.

This data demonstrates that Chk1 loss has a very significant effect on melanoma tumour formation in allograft models of melanoma development with a concurrent impact on survival. Chk1 has been shown to be important in tumour development in other models of cancer. Chk1 deficiency inhibits the formation of mammary tumours in a p53 null background in mice (Fishler et al, 2010) and inhibits the formation of chemical-induced skin tumours (Tho et al, 2012).
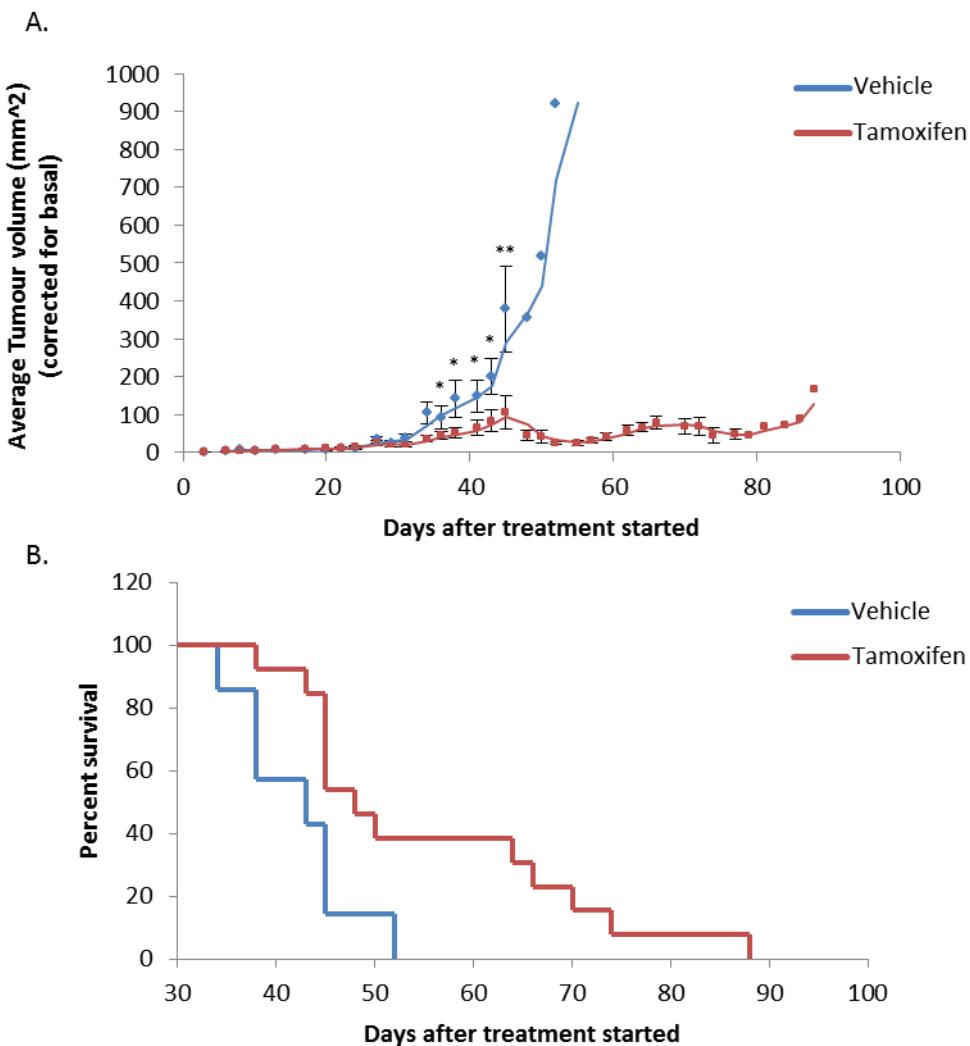
Figure 4.8: Effect of homozygous deletion of Chk1 on tumour formation and survival. (A) Analysis of the rate of tumour growth, as assessed by the increase in tumour volume over time as compared to the initial tumour volume in vehicle and tamoxifen treated cohorts. Statistically significant difference (*) as assessed by Student T-test at days 36, 38, 41, 43 and 45; p=0.039662, 0.015396, 0.032583, 0.024268 and 0.00769536 respectively. (B) Analysis of the survival time in vehicle and tamoxifen treated cohorts. Statistically significant difference as assessed by Kaplan Mier (Log rank test), p=0.0174; n=7 vehicle n=13 tamoxifen.

4.3.3 Effect of heterozygous deletion of Chk1 on tumour formation and metastatic potential

In order to assess the effect of loss of one copy of Chk1 on melanoma tumour formation *in vivo* Chk1 fl/+ transformed melanocyte cells were assessed as described above (2.3.2) for homozygous deletion of Chk1. PCR analysis of final tumour samples using primer pair, Forward 581: Reverse 1004, showed that in all ten tamoxifen treated animals the Chk1 flox allele was lost thereby resulting in final tumours being genetically hemizygous (Chk1 +/-) for Chk1 expression, in contrast to all ten vehicle treated tumours which retained expression of the

Chk1 flox allele (Figure 4.9A). This was further confirmed by real time PCR analysis using primer pair, Forward 821: Reverse 1004, whereby the average recombination efficiency of the Chk1 gene in tamoxifen treated animals was 43% as compared to a control gene (Arbp) whereas in vehicle treated animals the average recombination efficiency was negative compared to the control gene essentially meaning there was no recombination (Figure 4.9B). This data shows that the Cre-LoxP recombination system is working efficiently in the Chk1 fl/+ cell line allografts *in vivo*.
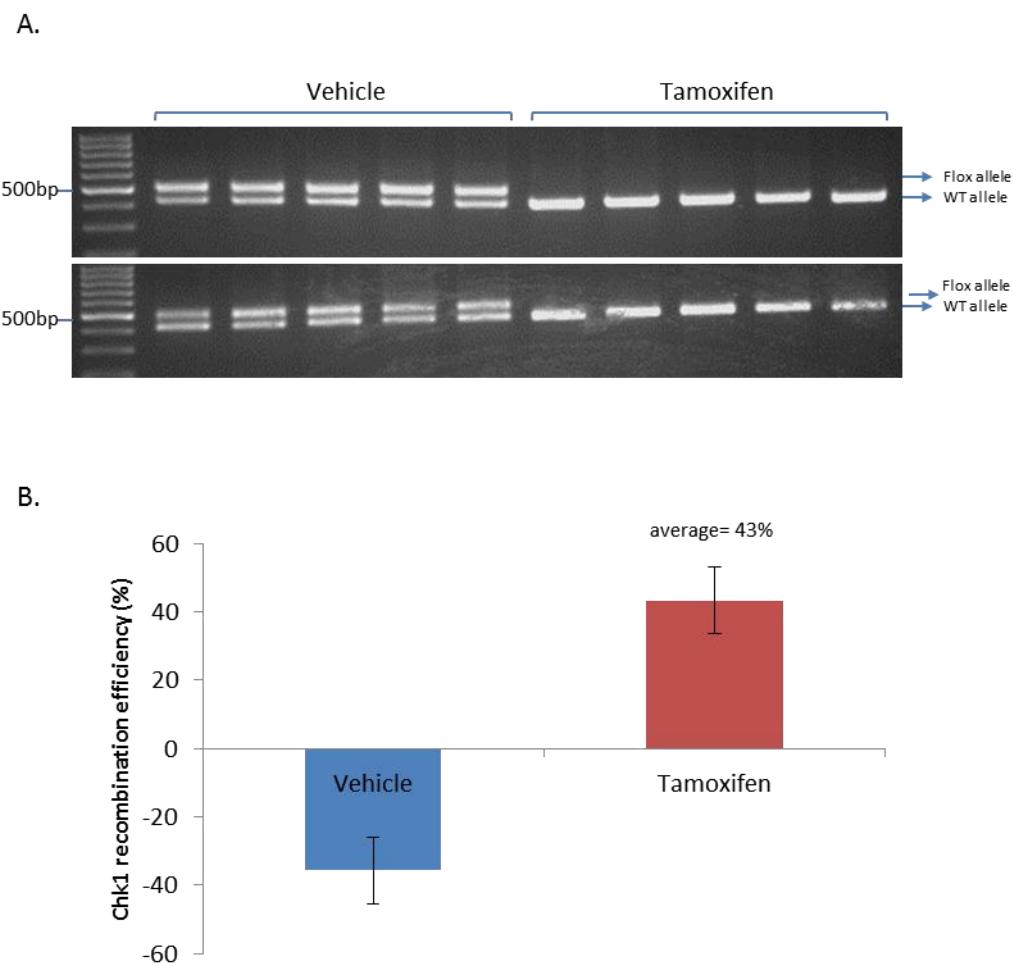

Figure 4.9: Screening for Chk1 deletion by PCR in final Chk1 fl/+ tumours of CD1 nudes. (A) PCR analysis of DNA from final tumour samples of CD1 nudes injected with melanocyte cells of the genotypes Chk1 fl/+ treated with tamoxifen or vehicle as outlined in figure 4.6. Chk1 flox allele is lost in final tumours of all tamoxifen treated animals. (B) Real-time PCR analysis of DNA from final tumour samples of CD1 nudes injected with melanocyte cells of the genotypes Chk1 fl/+ treated with tamoxifen or vehicle as outlined in Figure 4.6
.

Analysis of the rate of tumour growth, as assessed by the increase in tumour volume over time as compared to the initial tumour volume (taken at 7 days post injection), showed that there is an initial decrease in the tumour growth rate in

the tamoxifen treated cohort compared to vehicle treated however this reduction is not maintained indefinitely (Figure 4.10A). The reduction first becomes evident 14 days after the start of treatment. At time-points, 14 and 16 days after treatment there is a statistical significant reduction in the growth rate; p=0.017889 and 0.01645 respectively. At later time-points 18, 21, 23 and 25 days after treatment this reduction in the growth rate becomes highly statistically significant; p=0.002596, 0.007564, 0.001698 and 0.003952 respectively. However at later time-points, 27, 30 and 32 days after treatment there is no longer a statistical significant difference in growth rate, p=0.203279, 0.094093 and 0.48061 respectively with the curves converging.

This data shows that loss of one copy of Chk1 initially decreases the rate of tumour growth/proliferation *in vivo,* however ultimately this reduction in growth rate is reversed and does not prevent the tumours from reaching endpoint. This may represent an ability of the tumour cells to adapt to the loss of one copy of Chk1. Despite a high ulceration rate (5 out of 10 in vehicle cohort and 4 out of 10 in tamoxifen cohort) the remaining animals in each group were all able to reach the designated tumour size endpoint of 15mm. This is further emphasised by Kaplan Mier analysis of survival in the tamoxifen and vehicle cohorts (Figure 4.10Bi). Analysis of endpoint only animals showed that there was no statistically significant difference in the survival of tamoxifen treated animals over vehicle (p=0.6920) at any time-point, despite the initial reduction in the tumour growth rate. However this may be not be an accurate representation of the data as the average initial tumour volume at the commencement of treatment was 3 times larger in the tamoxifen treated cohort ($31.01mm^2$) than that of the vehicle treated cohort ($10.69mm^2$), due to inaccurate randomization of the animals prior to treatment . Analysis of the survival of animals whose initial tumour volume was between the ranges of $5mm^2$ to $20mm^2$ (Figure 4.10Bii) shows that there is an initial increase in the percentage of survival of tamoxifen treated animals between days 23-30 but that overall there is no statistically significant difference in the survival potential of tamoxifen treated animals over vehicle (p=0.4643) with the curves converging at 32 days post treatment. This data is consistent with the tumour growth analysis. Collectively these data show that the loss of one copy of Chk1 initially causes a decrease in the proliferation potential of melanocyte tumour cells; however this is a relatively transient

effect with the cells potentially able to adapt to the loss so that there is no longer an effect on tumour growth and ultimately no survival benefit. This adaptation is not a consequence of re-population of the tumour by cells which may have escaped Chk1 recombination as final tumour samples showed consistent loss of the Chk1 flox allele by PCR screening (Figure 4.9A).
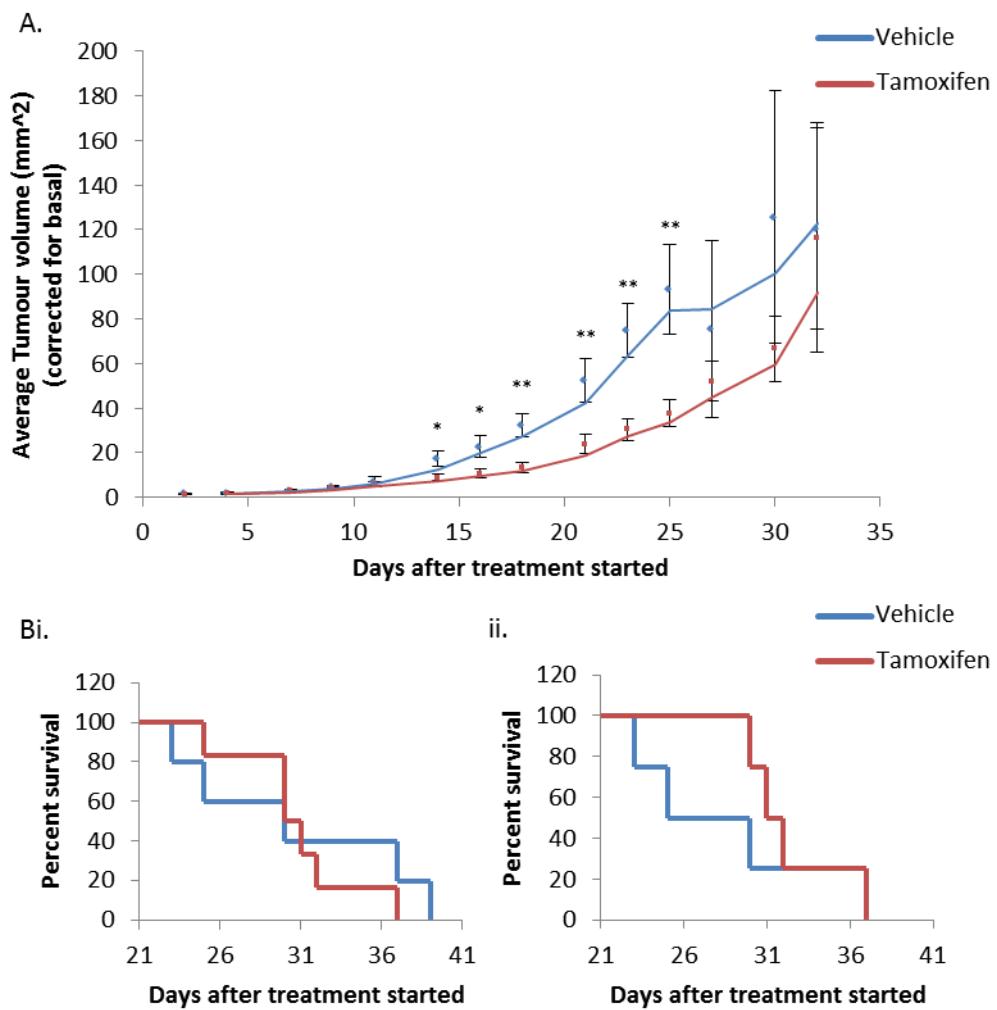
Figure 4.10: Effect of heterozygous deletion of Chk1 on tumour formation and survival. (A) Analysis of the rate of tumour growth, as assessed by the increase in tumour volume over time as compared to the initial tumour volume in vehicle and tamoxifen treated cohorts. Statistically significant difference (*) as assessed by Student T-test at days 14, 16, 18, 21, 23 and 25; p=0.017889, 0.01645, 0.002596, 0.007564, 0.001698 and 0.003952 respectively. (B) Analysis of the survival time in vehicle and tamoxifen treated cohorts of all animals which reached endpoint (i, n=5 vehicle n=6 tamoxifen) and animals whose initial tumour volume was between the ranges of 5mm^2 to 20mm^2 (ii, n=4 both) neither are significantly different.

The previous data shows that Chk1 heterozygosity has a transient effect on tumour growth *in vivo*. None of the subcutaneously grown tumours in either the vehicle or tamoxifen treated cohorts showed any metastasis. This result is probably a consequence of the fast nature of the CD1 nude mouse model and not necessarily an indication that Chk1 heterozygosity affects metastatic potential itself. In order to further assess the effect of loss of one copy of Chk1 on metastatic potential of melanoma cells *in vivo* Chk1 fl/+ transformed melanocyte cells were grown in culture until they were in a logarithmic phase of growth (70-80% confluent). Cells were then harvested and injected into the tail vein of 6 week old female CD1 nudes at a concentration of 1×10^5 cells per mouse. Mice were randomised and treated as previously described in 2.3.2. Analysis of the survival potential by Kaplan Mier (Figure 4.11A) showed that tamoxifen treated animals had a statistically significant increase in their survival time as compared to vehicle treated, p=0.0167. The longest surviving animal from the vehicle cohort was 24 days post treatment whereas in the tamoxifen cohort the longest surviving was 35 days post treatment. Endpoint was assessed by difficulty breathing, hunched appearance and/or >20% weight loss.
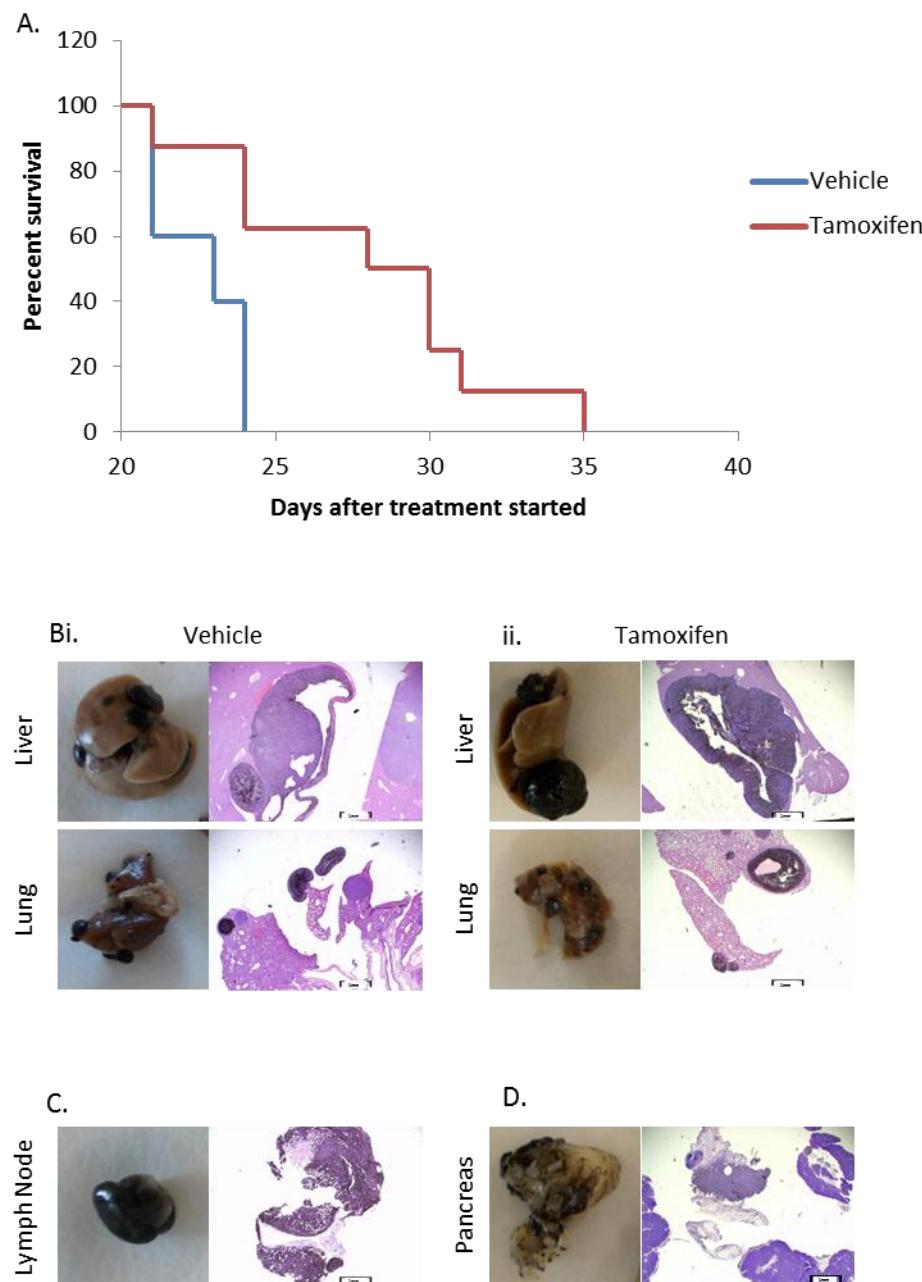
Figure 4.11: Effect of heterozygous deletion of Chk1 on metastasis formation and survival.
(A) Analysis of the survival time in vehicle and tamoxifen treated cohorts of all animals which reached endpoint (i, n=5 vehicle n=8 tamoxifen), p=0.0167. (B) Pictures and H&E sections of metastases to the liver and lungs of vehicle (i) and tamoxifen (ii) treated animals. (C-D) Pictures and H&E sections of metastases to the lymph nodes and pancreas.

At endpoint all mice in both cohorts had numerous metastases to both the lungs and liver (Figure 4.11Bi-ii). Metastasis was also seen in the pancreas of one tamoxifen treated mouse and in the lymph nodes of one vehicle treated mouse (Figure 4.11D and C respectively). Analysis of the final metastases size, burden and frequency in the liver of endpoint mice showed that there was no statistically significant difference between the vehicle cohort and tamoxifen cohort in any of the analysis (Figure 4.12A, B and C respectively). However, it is

interesting to note that the median values for metastases size and burden in the liver are significantly higher in the vehicle cohort as compared to the tamoxifen cohort; metastatic burden 162mm^2 and 73mm^2 respectively, metastases size 23mm^2 and 6mm^2 respectively. Analysis of the final size and burden in the lungs of endpoint mice also showed that there was no statistically significant difference between the vehicle cohort and tamoxifen cohort in either analysis (Figure 4.13A and B respectively). These data show that despite the increase in the survival time for the tamoxifen treated mice both cohorts are able to reach the specified endpoint with the same metastatic potential realised at endpoint. Therefore loss of one copy of Chk1 may delay but not completely suppress metastatic growth. Collectively these data show that the loss of one copy of Chk1 has a detrimental effect on the proliferation and/or survival potential of metastatic growths as demonstrated by the increase in survival time of the tamoxifen treated cohort. However this is only a transient effect with the cells able to adapt to the loss so that the final metastatic potential is the same in tamoxifen treated and vehicle treated animals.

This data demonstrates that Chk1 hemizygousity has a slight effect on melanoma tumour formation in allograft models of melanoma development. The role of Chk1 hemizygousity in tumourigenesis is controversial with evidence to suggest that Chk1 hemizygousity could promote tumourigenesis by increasing genetic instability. In mammary tumour formation Chk1 hemizygousity in combination with p53 has been shown to induce tumour formation (Fishler et al, 2010). However in studies on chemical-induced carcinogenesis of the skin Chk1 hemizygousity was shown to have no effect on benign tumour formation but increased the propensity for the conversion to carcinoma (Tho et al, 2012). Chk1 hemizygous mice are viable. However loss of one copy of Chk1 does infer cell cycle defects such as an increased number of S-phase cells, spontaneous DNA damage generation and early mitotic entry, all phenotypes which could contribute to tumourigenesis (Lam et al, 2004).
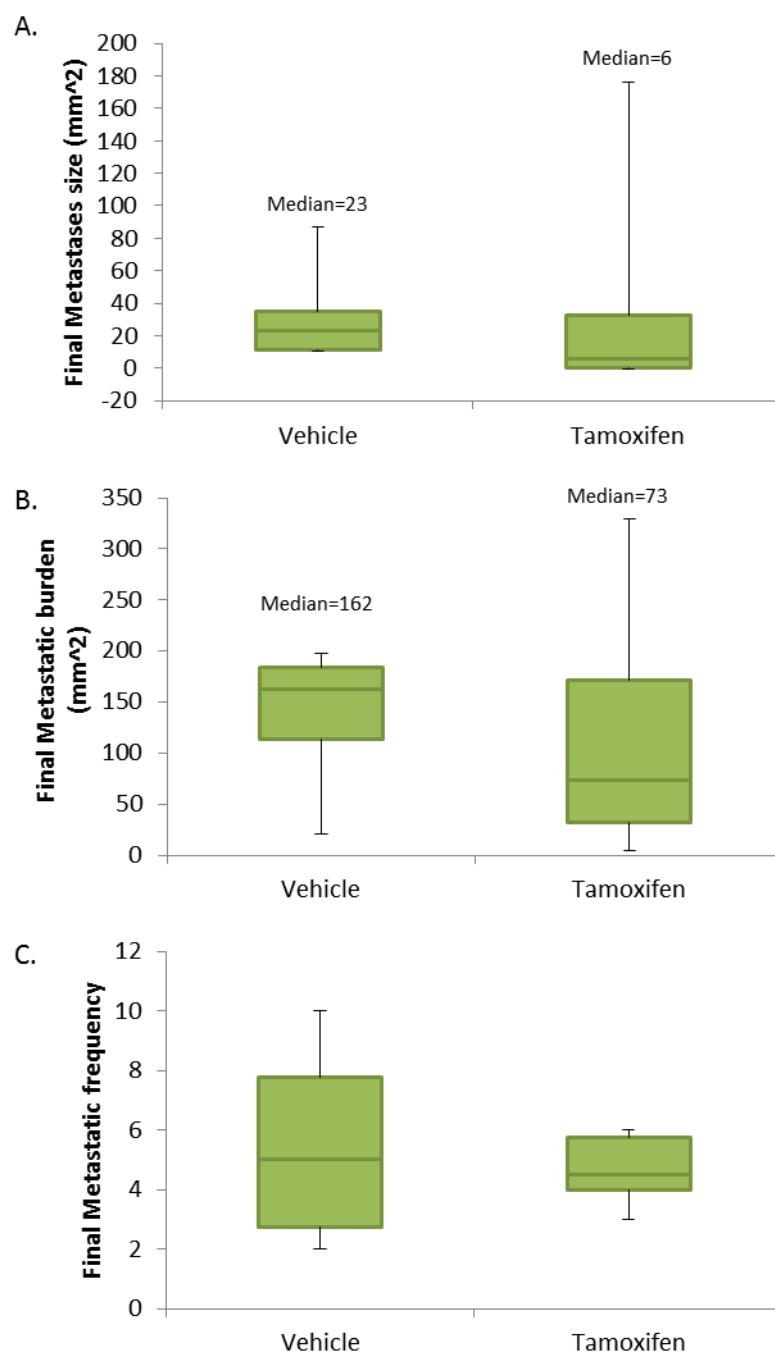
Figure 4.12: Effect of heterozygous deletion of Chk1 on metastatic burden in liver. (A) Analysis of the size of individual metastases in the liver of vehicle and tamoxifen treated animals. (B) Analysis of the final metastatic burden per animal in the liver of vehicle and tamoxifen treated animals. (C) Analysis of the number of metastases per animal in the liver of vehicle and tamoxifen treated animals. No statistically significant difference with any analysis
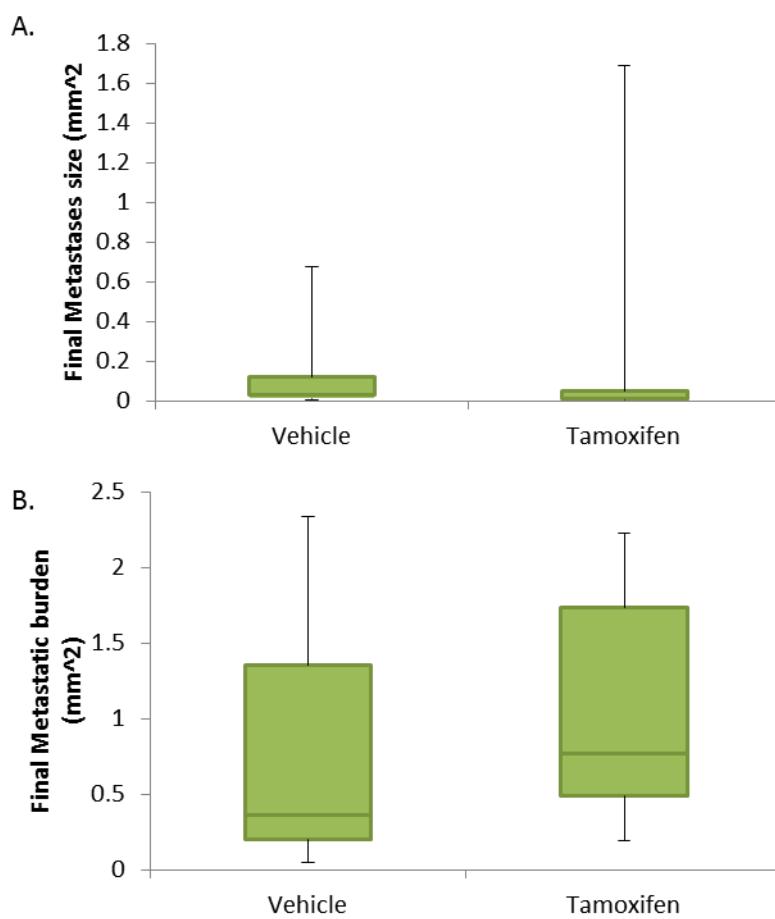
Figure 4.13: Effect of heterozygous deletion of Chk1 on metastatic burden in lungs. (A) Analysis of the size of individual metastases in the liver of vehicle and tamoxifen treated animals. (B) Analysis of the final metastatic burden per animal in the liver of vehicle and tamoxifen treated animals. No statistically significant difference with either analysis.

4.4 Discussion

The aim of this chapter was to understand the role that Chk1 may play in the initiation, progression and maintenance of melanoma *in vivo*. This could be significant as melanoma is an extremely aggressive form of skin cancer which accounts for >80% of deaths from skin cancer. Melanomas display high levels of chromosomal instability (Bauer & Bastian, 2006) and large numbers of nuclear foci positive for γH2AX, a marker of DNA strand breaks (Gorgoulis et al, 2005; Warters et al, 2005). Activation of the DNA damage pathway has been observed in dysplastic nevi and in human skin xenografts (Gorgoulis et al, 2005). Chk1 is a key component of the DNA damage signalling pathway and is rarely mutated in cancer. Thus Chk1 activation is probably high in at least the earliest stages of melanoma development.

The role that ATR-Chk1 activation plays in malignant transformation and progression is not fully understood, with evidence for roles in both tumour progression and suppression. Studies have shown that the DNA damage response pathway is induced by active oncogenes and acts as a barrier to the progression of cancer beyond its early stages (Bartek et al, 2007). The ATR/Chk1 signalling module has been shown to be activated in an acute manner in response to activated oncogenes including Ras, Mos, Cdc6, Cyclin E, E2F1 and Stat5 *in vitro* and in Ras-driven mouse epithelial tumours *in vivo*, whereby it leads to the prevention of cancer progression by cellular senescence (Bartkova et al, 2005; Bartkova et al, 2006; Di Micco et al, 2006; Mallette et al, 2007). Thus active ATR/Chk1 signalling is suppressing malignant progression and is therefore protective.

Other studies have shown that the ATR/Chk1 signalling module has a gatekeeping function which is essential to restrain oncogene-induced replicative stress and therefore for tumour maintenance (Campaner & Amati, 2012). In fact in myc-driven tumours it has been shown that Chk1 transcript and protein levels are indirectly induced and that these cells are sensitised to chemical inhibition of Chk1 which triggers a potent apoptotic response (Hoglund et al, 2011; Ferrao et al, 2012; Murga et al, 2011). In Ras-transformed cells ATR/Chk1 signalling is essential for limiting genomic instability; with siRNA knockdown of ATR causing increases in chromatid breaks, sister chromatid exchanges and γH2AX levels. In contrast to the synthetic lethal effects of ATR knockdown, haplo-insufficiency for ATR in combination with K-Ras elevated the incidence of lung adenocarcinoma, spindle cell sarcoma and thymic lymphomas *in vivo* (Gilad et al, 2010; Schoppy et al, 2012). Recently two point mutations in Chk1 have been identified that render Chk1 constitutively active. Expression of these mutant forms of Chk1 inhibits cancer cell proliferation (Wang et al, 2012).

By using a genetically manipulated mouse model of melanoma which mimics the human condition in combination with a conditional knockout model of Chk1 I was able to show that complete loss of Chk1 causes a profound reduction in the proliferation potential of melanoma tumour formation in *in vivo* models of melanoma development with a concurrent increase in the survival time of these mice (Figure 4.8). This data shows that Chk1 is essential for the maintenance and progression of melanoma *in vivo*. This result is similar to previous studies

which have also shown that loss of Chk1 inhibits tumour formation in both mammary tumour models on a p53 null background (Fishler et al, 2010) and chemically-induced skin tumour models (Tho et al, 2012). I was also able to show that while complete Chk1 loss has a pronounced negative effect on melanoma tumour formation hemizygousity for Chk1 also exerts a more modest but nevertheless measureable effect on melanoma tumour formation and survival *in vivo* (Figure 4.10). In addition Chk1 hemizygousity does appear to have a detrimental effect on the proliferation and/or survival potential of melanoma metastatic growths as demonstrated by the increase in survival time (Figure 4.11). However the final metastatic potential in the liver and lungs is not permanently suppressed but only delayed (Figure 4.12 and 4.13 respectively). This data shows that reduction in Chk1 levels modestly effects the primary tumour formation of melanoma *in vivo*, and also has a negative effect on the proliferation and/or survival of metastatic growths.

This is in contrast to previous data from my lab which showed that in chemical-induced skin carcinogenesis Chk1 hemizygousity had no effect on benign tumour formation but promoted benign-malignant conversion (Tho et al, 2012). However the role of Chk1 hemizygousity in tumourigenesis is controversial and seems to be tissue specific. In mammary tumour formation Chk1 hemizygousity in combination with p53 loss has been shown to induce tumour formation (Fisher 2010). Chk1 hemizygous cells have been shown to have spontaneous DNA damage (Lam et al, 2004) and to increase the conversions of benign skin papilloma to carcinoma *in vivo* (Tho et al, 2012). These data indicate that Chk1 hemizygous cells are more genetically unstable than Chk1 proficient cells. This may put a high selective pressure, potentially through increased levels of cell death or replicative failure, on metastatic growths which could account for the delay seen in the metastatic growth of melanoma cells *in vivo*.

Chapter 5: DNA damage signalling in human melanoma cell lines

5 DNA damage signalling in human melanoma cell lines

5.1 Introduction

In order to prevent the accumulation of mutations during cell division cells have developed complex mechanisms, known as the DNA damage responses. Key among these mechanisms is cell cycle checkpoints which are activated in response to DNA damaging agents and replication stress. They function by delaying cell cycle progression thus allowing cells to repair DNA damage or deal with replication problems. Consequently they are important in maintaining genome stability and defects in these pathways have been implicated in genetic instability and malignant progression (Rai et al, 2007; Smith et al, 2011). Key players in activation of the DNA damage checkpoint responses are the protein kinases Chk1 and Chk2 which are activated by the upstream protein kinases ATR and ATM respectively in response to a variety of DNA damaging agents including IR, UV, ROS and many chemical genotoxins (Bartek & Lucas, 2003; Sancar et al, 2004). Although Chk2 has been shown to be mutated in many cancers (Hangaishi et al, 2002; Ingvarsson et al, 2002; Papp et al, 2007; Wu et al, 2001) Chk1 expression and function is consistently conserved in cancer cells. Therefore I examined the proficiency of checkpoint activation in a panel of melanoma cell lines.

5.2 Mutational status of a panel of human malignant melanoma cell lines

In order to analyse the cell cycle checkpoint proficiency in melanoma cell lines, and to establish whether any variations may be attributed to specific oncogenic mutations, I examined a panel of eleven human melanoma cell lines. Cell lines were selected based on their oncogene status (B-Raf or N-Ras) and their tumour suppressor status (CDK2NA, PTEN and p53) (See Table 5.1). Melanoma is known to be a progressive condition whereby the cancer cells typically go through several phases of growth: radial, followed by vertical and finally metastatic growth to both local and distant sites; therefore I also selected one radial growth phase (WM35) and one vertical growth phase (WM793) cell line in order to have a comparison with the other metastatic cell lines. Finally I also included

one cell line which has recently been shown to be haplo-insufficient for Chk1, MRI-H-221 (Papp et al, 2007), in order to analyse whether one copy of Chk1 is sufficient for checkpoint proficiency.

Cell Line	Oncogene (B-Raf/N-Ras)	CDKN2A status	PTEN status	Other known mutations
A375MM	B-Raf V600E	WT	-	-
WM35	B-Raf V600E	Mutant	-	-
WM793	B-Raf V600E	-	-	Cdk4 mutation
Sk-Mel-5	B-Raf V600E	WT	Mutant	-
Sk-Mel-28	B-Raf V600E	WT	Mutant	p53 (L145R) Cdk4 (R24C)
Sk-Mel-37	B-Raf V600E	WT	Mutant (loss of exon2)	p53 (R175H), Cdk4 (R24H)
Sk-Mel-39	B-Raf V600E	WT	Mutant (1352InsA)	p53, Cdk4 (K22Q)
Sk-Mel-2	N-Ras Q61R	-	-	-
Sk-Mel-103	N-Ras Q61R	Null	-	-
Sk-Mel-147	N-Ras Q61R	Mutant	-	-
MRI-H-221	-	-	-	Chk1 haplo-insufficient

Table 5.1: Panel of Melanoma cell lines with oncogene and tumour suppressor status.

5.3 Analysis of G2/M checkpoint proficiency and Chk1 activation following irradiation-induced DNA damage

The G2/M checkpoint is activated when dividing cells have acquired DNA damage during S or G2 phase of the cell cycle in order to prevent them from entering mitosis. The cells subsequently block in the G2 phase of the cell cycle until the damage is either repaired or they are targeted for cell death (apoptosis). The checkpoint is assayed using a flow cytometry technique whereby the DNA

content is measured via propidium iodide (PI) staining. This gives a cell cycle profile as seen in Figure 5.1Ai whereby the G1 (2N DNA content) and the G2/M phases (4N DNA content) can be visualised as two distinct peaks with S-phase cells in-between. Phosphorylated histone H3 (pH3) is used as a marker of mitotic cells. Checkpoint proficient cells will display an accumulation in the G2/M peak but with negativity for pH3 after irradiation treatment (IR) which generates DNA DSBs. The cells are also treated with Nocodozole (Noc), a spindle poison, which blocks the cells in mitosis and acts as a positive control for the accumulation of pH3-positive mitotic cells in undamaged cultures.

In the B-Raf oncogene containing cell lines we can see that WM35, Sk-Mel-5 and Sk-Mel-39 (Figure 5.1B, D and G respectively) all display a functional G2/M checkpoint. This is demonstrated by their accumulation in the G2/M peak as assayed by PI accompanied by diminished pH3 staining (Figure 5.1Biii, Diii and Giii respectively), indicating the cells are blocked in G2 and not progressing to mitosis as seen in the Noc only treated (Figure 5.1Bii, Dii and Gii respectively). However in the B-Raf oncogene containing cell lines A375MM, WM793, Sk-Mel-28 and Sk-Mel-37 (Figure 5.1A, C, E and F respectively) we can see that there is variation in G2/M checkpoint proficiency with the cells not fully blocking in G2 after IR. This can be seen by the positive pH3 staining observed (Figure 5.1Aiii, Ciii, Eiii and Fiii respectively) after IR treatment indicating cells are not blocking in G2 but are still able to progress into mitosis in the presence of DNA damage. When the pH3 accumulation in the IR samples are compared as a percentage of the Noc only treated samples (taken as 100%) for each cell line (Figure 5.1H) we can see that A375MM, WM793 and Sk-Mel-37 have a decreased ability to block in G2 after IR with 40-60% of cells positive for pH3 staining (indicated by the black stars in Figure 5.1H). This shows that in the presence of DNA damage a significant proportion of cells can still progress into mitosis. However Sk-Mel-28 has a completely defective G2/M checkpoint (indicated by the red star in Figure 5.1H) showing that the pH3 positivity and thus mitotic progression is not inhibited at all by the presence of DNA damage.

In the N-Ras oncogene containing cell lines we can see that Sk-Mel-2, Sk-Mel-103 and Sk-Mel-147 (Figure 5.2A, B and C respectively) all display a functional G2/M checkpoint. This is demonstrated by their accumulation in the G2/M peak as

assayed by PI accompanied by diminished pH3 staining (Figure 5.2Aiii, Biii and Ciii respectively), indicating the cells are blocked in G2 and not progressing to mitosis as seen in the Noc only treated (Figure 5.2Aii, Bii and Cii respectively). This can be further seen when the pH3 accumulation in the IR samples are compared as a percentage of the Noc only treated samples (taken as 100%) for each cell line (Figure 5.2E) we can see that there is a small amount of pH3 staining (as indicated by the white stars in Figure 5.2E) which is less than that seen in the untreated samples for each cell line. This represents an effective block to progression into mitosis in the presence of DNA damage.

H.
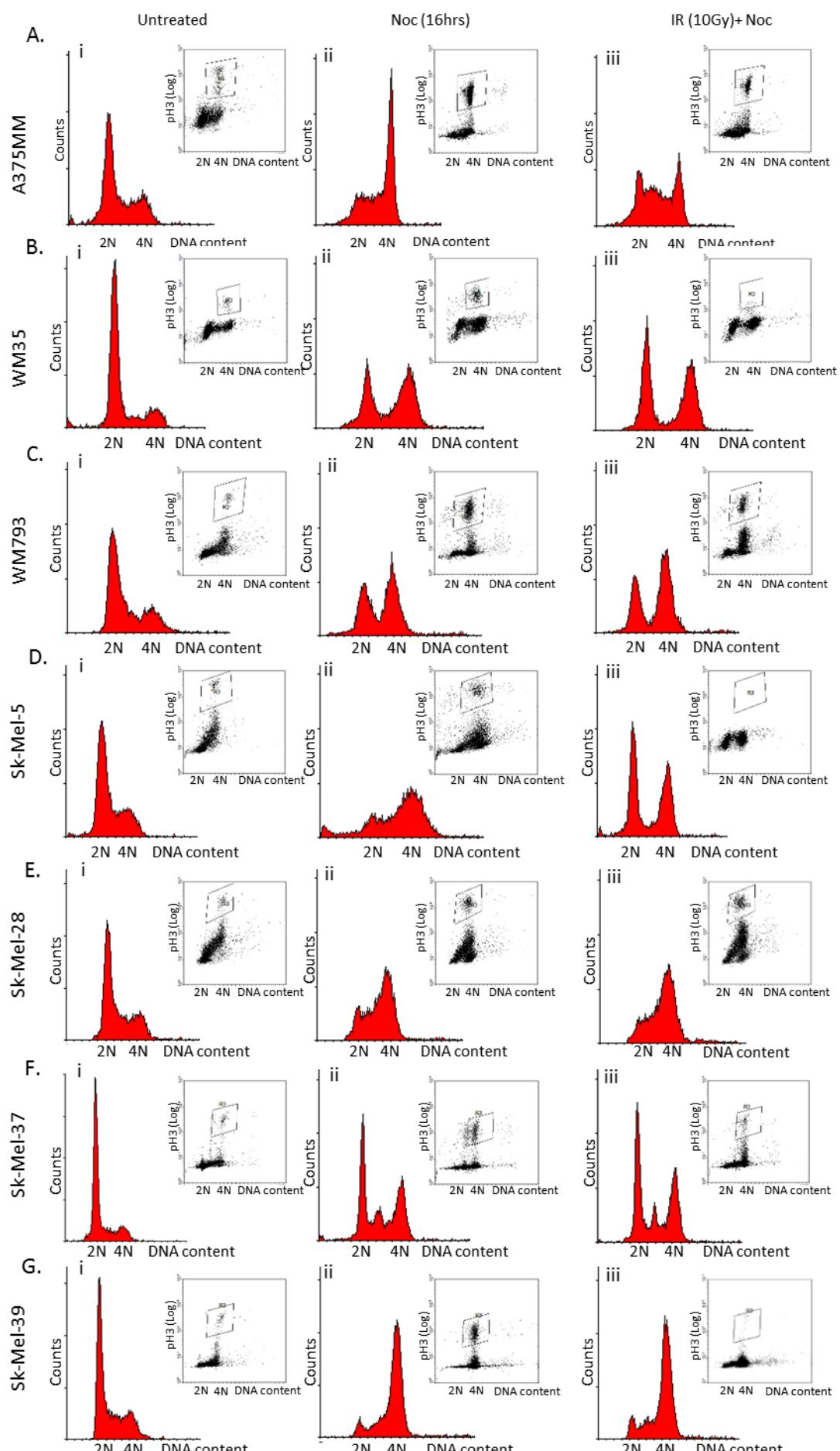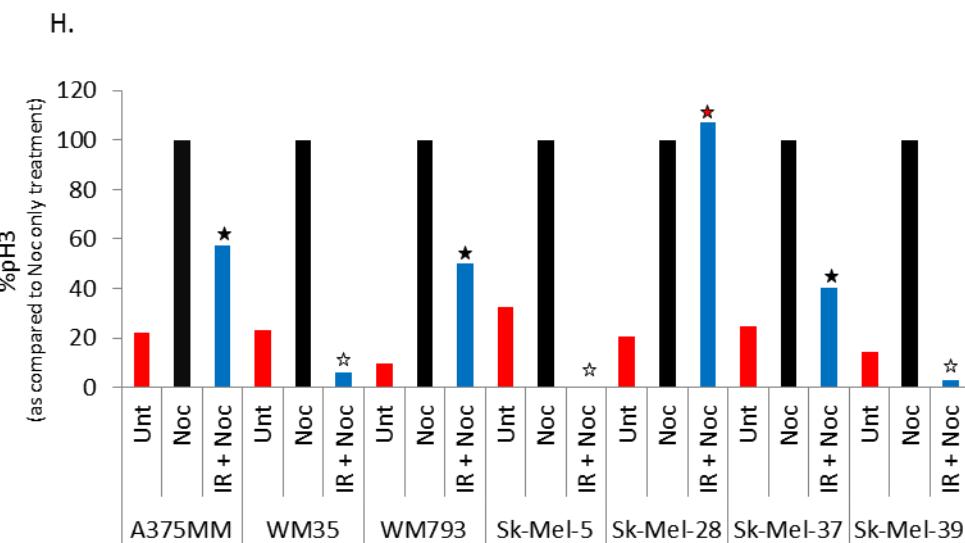
Figure5.1: Characterisation of G2/M checkpoint proficiency in B-Raf mutant melanoma cell lines. (A-G) G$_2$/M Checkpoint Assay. Cells were treated for 16hrs with Nocodazole (Noc) with or without 10Gy γIR. The number of mitotic cells (pH3 positive) after 16hrs was assessed by flow cytometry. Dot plots and DNA histograms are shown. (H) Quantification of the number of mitotic cells taken as a percentage of Noc only treated for each cell line. White stars represent G$_2$/M checkpoint proficient cell lines, red star represents a G$_2$/M defective cell line and black stars represent cell lines with intermediate G$_2$/M checkpoint proficiency.

Collectively this data demonstrates that there is a significant variation in the G2/M checkpoint proficiency in melanoma cell lines (4 out of 11 have a weak or defective G2 arrest). Based on this small analysis we can see that the loss of this checkpoint only occurs in B-Raf mutant cell lines and not in N-Ras mutant cell lines however this is only a small collection of cell lines and may not be representative of melanoma as a whole. We can also note that the checkpoint is functional in the early radial growth phase cell line (WM35, Figure 5.1B) but is partially defective in the more advanced vertical growth phase cell line (WM793, Figure 5.1C). This may represent a possible mechanism for increased genetic instability and subsequently transition to more aggressive forms of melanoma. Loss of checkpoint function as a mechanism for malignant transition is already well documented (Kaufmann et al, 2001; Mukherjee et al, 2010; Nuciforo et al, 2007). Loss or mutation of p53 is a common marker of cancer cells and is thought to be present in up to 50% of all cancers, although this is a less common occurrence in melanoma. One consequence of the mutation or loss of p53 signalling is the loss of the G1/S checkpoint (Bartek & Lucas, 2001; Ryan et al, 2001). The G1/S checkpoint is activated when dividing cells have acquired DNA damage during G1 or M phase of the cell cycle in order to prevent them from entering the DNA replication phase of the cell cycle. It is interesting to note that

only four of the melanoma cell lines appear to have a functional G1/S checkpoint after IR treatment as assessed by the substantial G1 peak seen in these cell lines; WM35, WM793, Sk-Mel-5, Sk-Mel-37 and Sk-Mel-147 (Figure 5.1Biii, Ciii, Diii, Fiii and 5.2Ciii respectively).
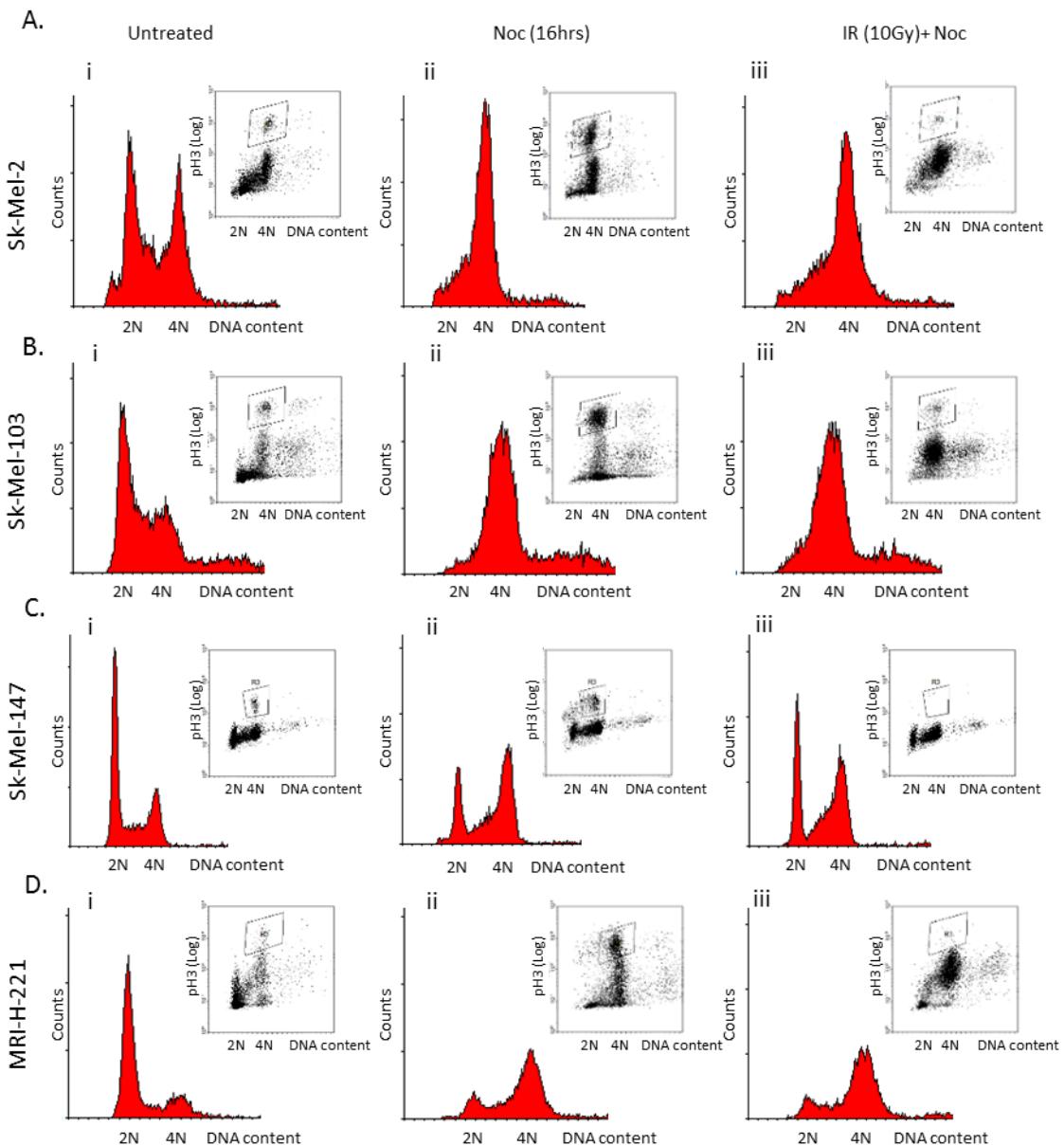
E.
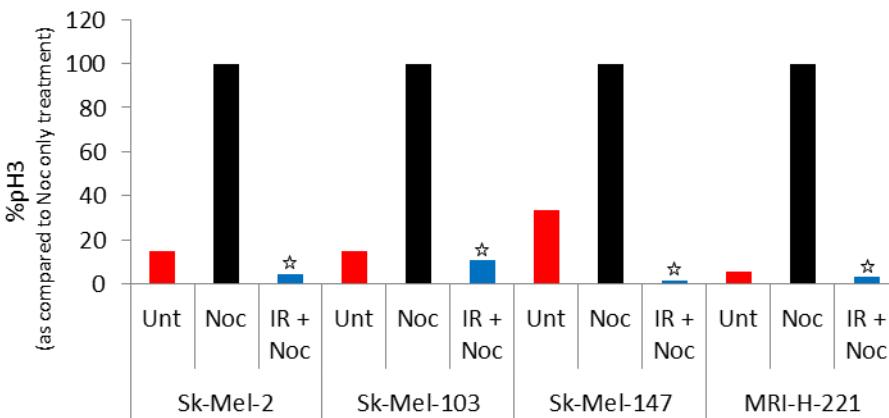
Figure 5.2: Characterisation of G2/M checkpoint proficiency in N-Ras mutant melanoma cell lines. (A-D) G_2/M Checkpoint Assay. Cells were treated for 16hrs with Nocodazole (Noc) with or without 10Gy γIR. The number of mitotic cells (pH3 positive) after 16hrs was assessed by flow cytometry. Dot plots and DNA histograms are shown. (E) Quantification of the number of mitotic cells taken as a percentage of Noc only treated for each cell line. White stars represent G_2/M checkpoint proficient cell lines.

In the Chk1 haplo-insufficient melanoma cell line we can see that there is a functional G2/M checkpoint (Figure 5.2D). The cells accumulate in G2/M as assayed by PI accompanied by a lack of pH3 staining (Figure 5.2Diii), indicating the cells are blocked in G2 and not progressing to mitosis in the presence of DNA damage. This is further quantified by the pH3 accumulation in the IR samples as compared as a percentage of the Noc only treated samples (taken as 100%) (Figure 5.2E). We can see that there is a small amount of pH3 staining (as indicated by the white star in Figure 5.2E) which is less than that seen in the untreated sample. This represents a lack of progression into mitosis in the presence of DNA damage. This data demonstrates that one functional allele for Chk1 is sufficient for Chk1 activity in the G2/M checkpoint, at least in this particular cell line.

Analysis of Chk1 activation in the G2/M checkpoint proficient cell lines by WB (Figure 5.3A-G) shows a consistent pattern of activating phosphorylation of Chk1 on S345 after IR treatment. Chk1 is phosphorylated on S345 within 10mins-1hr after treatment which is then maintained in all cells lines for 6hrs and up to 16hrs in some cells lines (Sk-Mel-39 and MRI-H-221). Chk2 activation in the G2/M proficient cell lines shows a more varied pattern. In cell lines WM35, Sk-Mel-5, Sk-Mel-2 and MRI-H-221 (Figure 5.3A, B, D and G respectively) there is a consistent pattern of activating phosphorylation on T68 after IR treatment. Chk2

is phosphorylated on T68 within 10mins treatment which is then maintained for 16hrs. However in cell lines Sk-Mel-39 (Figure 5.3C) and Sk-Mel-103 (Figure 5.3E) there is no detectable induction of pChk2 in either the untreated or IR treated samples at any time point. In cell line Sk-Mel-147 (Figure 5.3F) there are very low basal levels of pChk2 with a small increase seen 10mins after treatment but which is subsequently reduced by 1hr and lost by 6hrs after IR treatment.
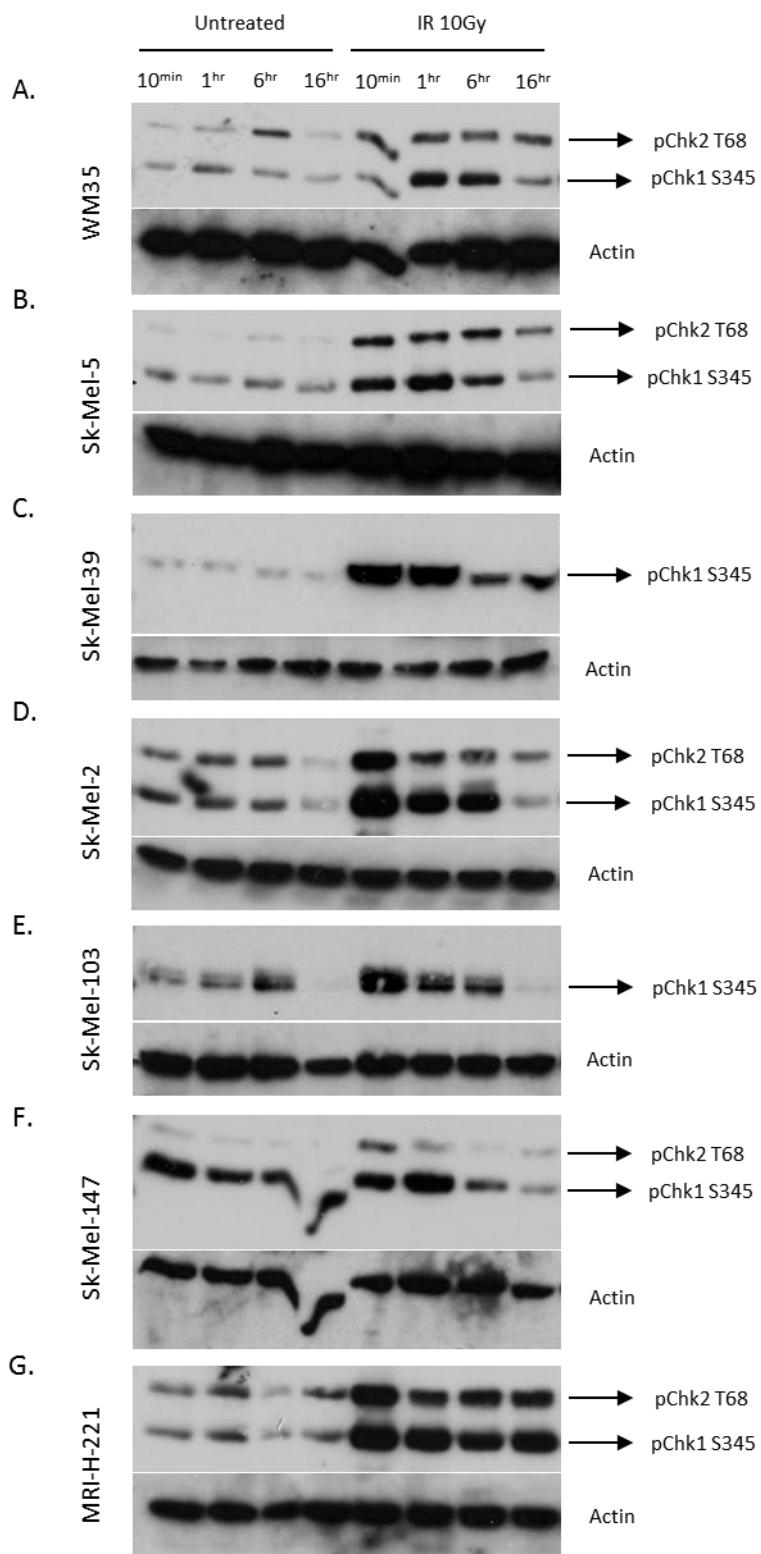
Figure 5.3: Activation of Chk1 and Chk2 signalling post γIR treatment in melanoma cell lines with efficient G2/M checkpoint activation. (A-G) Western blot analysis of activating phosphorylation on Chk1 and Chk2. Cells were harvested 10mins, 1hr, 6hr and 16hr post 10Gy γIR. Antibodies against pChk1 S345 and pChk2 T68 were used. An equal quantity of protein was loaded as determined by Bradford Assay and confirmed by antibody against actin.

Chk1 activation was analysed in the cell lines which demonstrated a variation in their G2/M checkpoint function by WB (Figure 5.4A-D). These cell lines show variations in their activation patterns of Chk1. A375MM cells (Figure 5.4A) show an increase in the pChk1 S345 levels 10mins after IR treatment, which is maintained for 6hrs post treatment. This pattern of activation is as expected and was seen in the G2/M proficient cell lines. This suggests there may be a problem with signalling downstream of Chk1 in this cell line. In cell lines WM793 (Figure 5.4B) and Sk-Mel-37 (Figure 5.4D) there is a sharp increase in pChk1 levels however this is only seen at one time point for each cell line, after 6hrs IR treatment in WM793 cells and after 1hr IR treatment in Sk-Mel-37 cells and is not maintained at any other times. This pattern suggests that Chk1 activation may be turned off rapidly (potentially by phosphatases) or that the upstream activating signal is short-lived. In cell line Sk-Mel-28 (Figure 5.4C) there is a small increase in pChk1 levels after 10mins treatment which is then maintained for 6hrs; this is the expected pattern of activation however the basal levels of activated Chk1 in the untreated samples are very high. This suggests that potentially the pathway is always on and perhaps the cells are no longer responsive to the DNA damage signal. Chk2 activation in these cell lines is also variable. In cell lines A375MM (Figure 5.4A) and Sk-Mel-28 (Figure 5.4C) which have the expected pattern of Chk1 activation also show increases in pChk2 levels that are similar to the G2/M proficient cell lines. Chk2 is phosphorylated on T68 after 10mins IR treatment and is maintained for 6hrs post treatment. This clearly shows that these cell lines have functional pathway signalling upstream of Chk1 and Chk2 however the signal maybe lost at some point downstream so that they have diminished G2/M checkpoint proficiency. WM793 cells (Figure 5.4B) show a sharp increase in pChk2 levels after 10mins however the signal is not maintained with loss of the signal by 1hr. This is consistent with the pChk1 levels in these cells which also showed a short sharp increase. This data suggests that WM793 cells may have problems with activation of upstream signalling of Chk1 and Chk2.
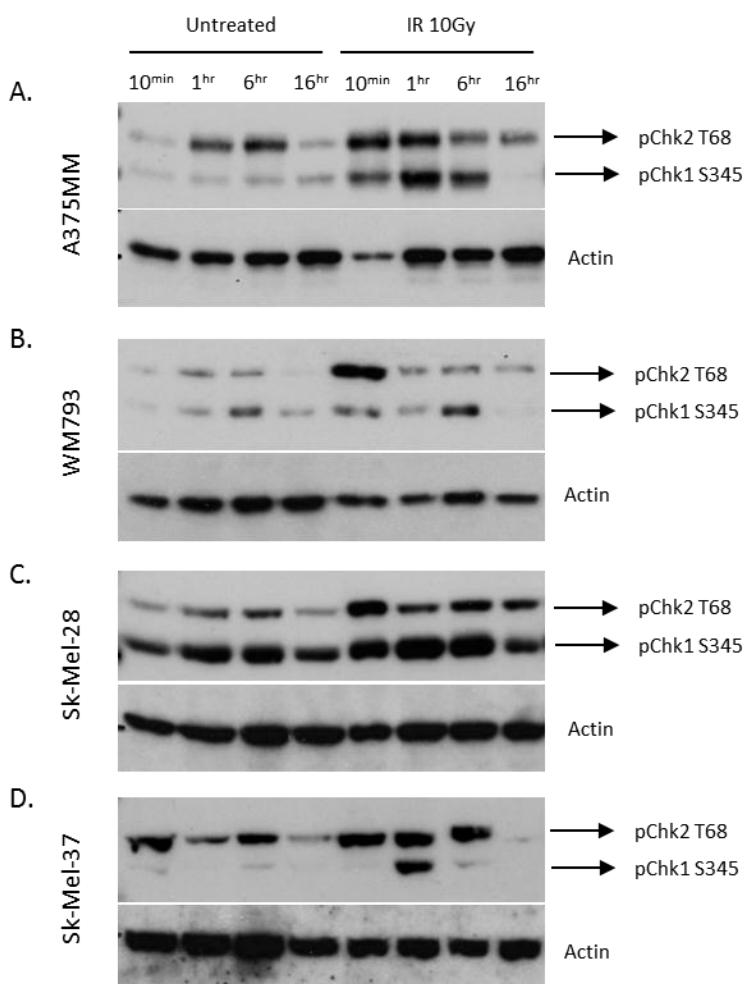
Figure 5.4: Activation of Chk1 and Chk2 signalling post γIR treatment in melanoma cell lines with deficient and intermediate G2/M checkpoint proficiency. (A-D) Western blot analysis of activating phosphorylation on Chk1 and Chk2. Cells were harvested 10mins, 1hr, 6hr and 16hr post 10Gy γIR. Antibodies against pChk1 S345 and pChk2 T68 were used. An equal quantity of protein was loaded as determined by Bradford Assay and confirmed by antibody against actin.

5.4 Analysis of S/M checkpoint proficiency and Chk1 activation following replication stress

The S/M checkpoint is activated when dividing cells encounter problems during DNA replication which cause stalling of replication forks. The checkpoint is activated in order to prevent collapse of these replication forks and ultimately prevent cells from entering mitosis in the presence of DNA which is not fully replicated. The cells will block in S phase of the cell cycle until the DNA is properly replicated or they are targeted for cell death (apoptosis). The checkpoint is assayed using a flow cytometry technique whereby the DNA content is analysed via PI staining giving a cell cycle profile where the G1 (2N DNA content) and the G2/M phases (4N DNA content) are visualised as two distinct peaks with a bridge in-between representing the S-phase cells. The DNA

content of these cells is gradually changing from 2N to 4N. Phosphorylated histone H3 (pH3) is used as a marker of mitotic cells. Checkpoint proficient cells will display a blockage at early S-phase with failure to progress to G/M and negativity for pH3 after aphidicolin treatment (Aph) which inhibits DNA polymerase causing stalling of active replication forks. The cells are also treated with Nocodozole (Noc), a spindle poison, which blocks the cells in mitosis and acts as a positive control for accumulation of pH3-positive mitotic cells in the absence of DNA synthesis inhibition.

All the melanoma cell lines tested (Figure 5.5A-G and Figure 5.6A-D) displayed a functional S/M checkpoint upon inhibition of DNA replication. Treatment with Aph caused all cells to block in early to late S-phase, as assayed by PI staining accompanied by severely diminished pH3 staining (Figure 5.5Aiii-Giii and Figure 5.6Aiii-Diii). When the pH3 accumulation in the Aph treated samples are compared as a percentage for each individual cell line to the Noc only treated samples (taken as 100%) (Figure 5.5H and Figure 5.6E) we can see that the pH3 positivity is equal to or below the level seen in the untreated samples for each cell line.

This data demonstrates that the S/M checkpoint is always functional in melanoma cell lines. Based on this small analysis we can suggest that although loss or impairment of checkpoint functions; both G1/S by p53 mutation, as seen in cell lines Sk-Mel-28 and Sk-Mel-39 which both harbour a known p53 mutation and have lost an apparent G1/S checkpoint after IR treatment, and G2/M as seen above, can contribute to malignant transformation, the S/M checkpoint is possibly essential for tumour cell growth and proliferation and as such is always retained. However this hypothesis is only based on a small number of cell lines and may not be true for a larger scale of melanoma cell lines. This data also demonstrates that one functional allele for Chk1 is sufficient for full S/M checkpoint proficiency.
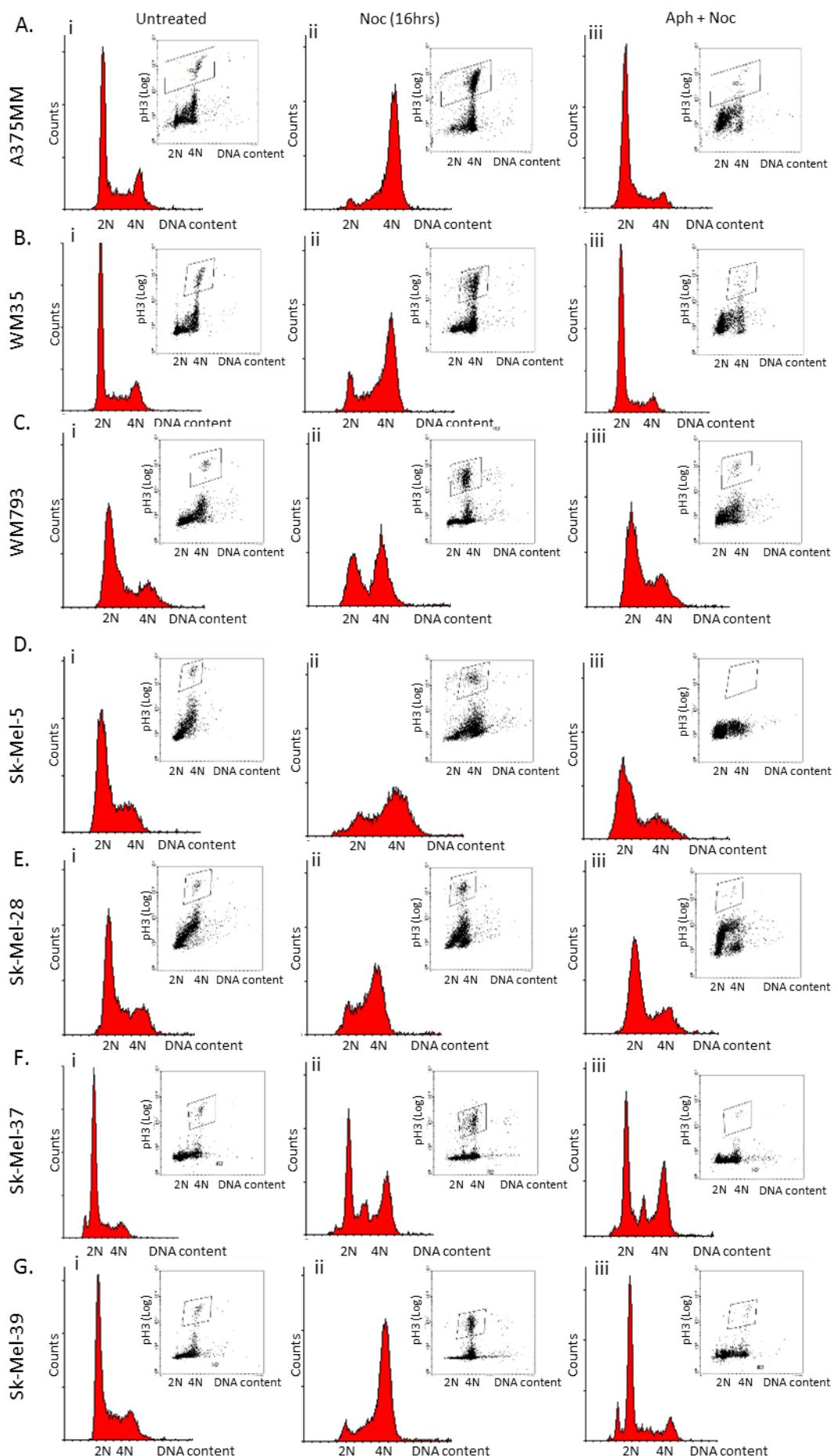
H.
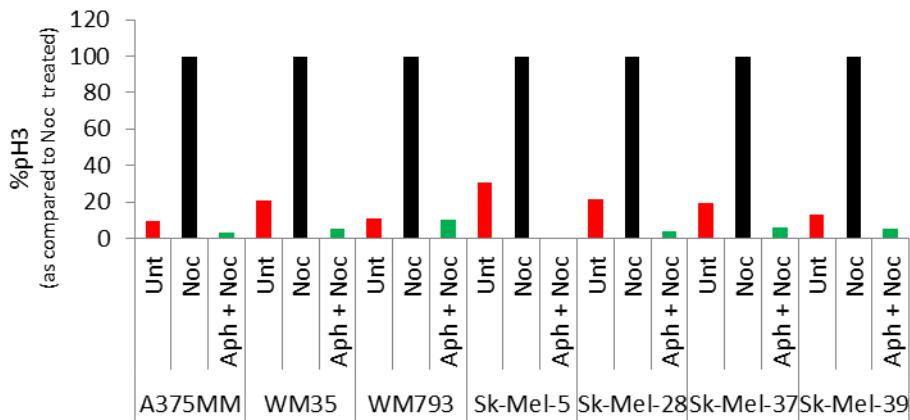
Figure 5.5: Characterisation of S/M checkpoint proficiency in B-Raf mutant melanoma cell lines. (A-G) S-M Checkpoint Assay. Cells were treated for 16hrs with Nocodazole (Noc) with or without [20µM] Aphidicolin. The number of mitotic cells (pH3 positive) after 16hrs was assessed by flow cytometry. Dot plots and DNA histograms are shown. (H) Quantification of the number of mitotic cells taken as a percentage of Noc only treated for each cell line.

E.
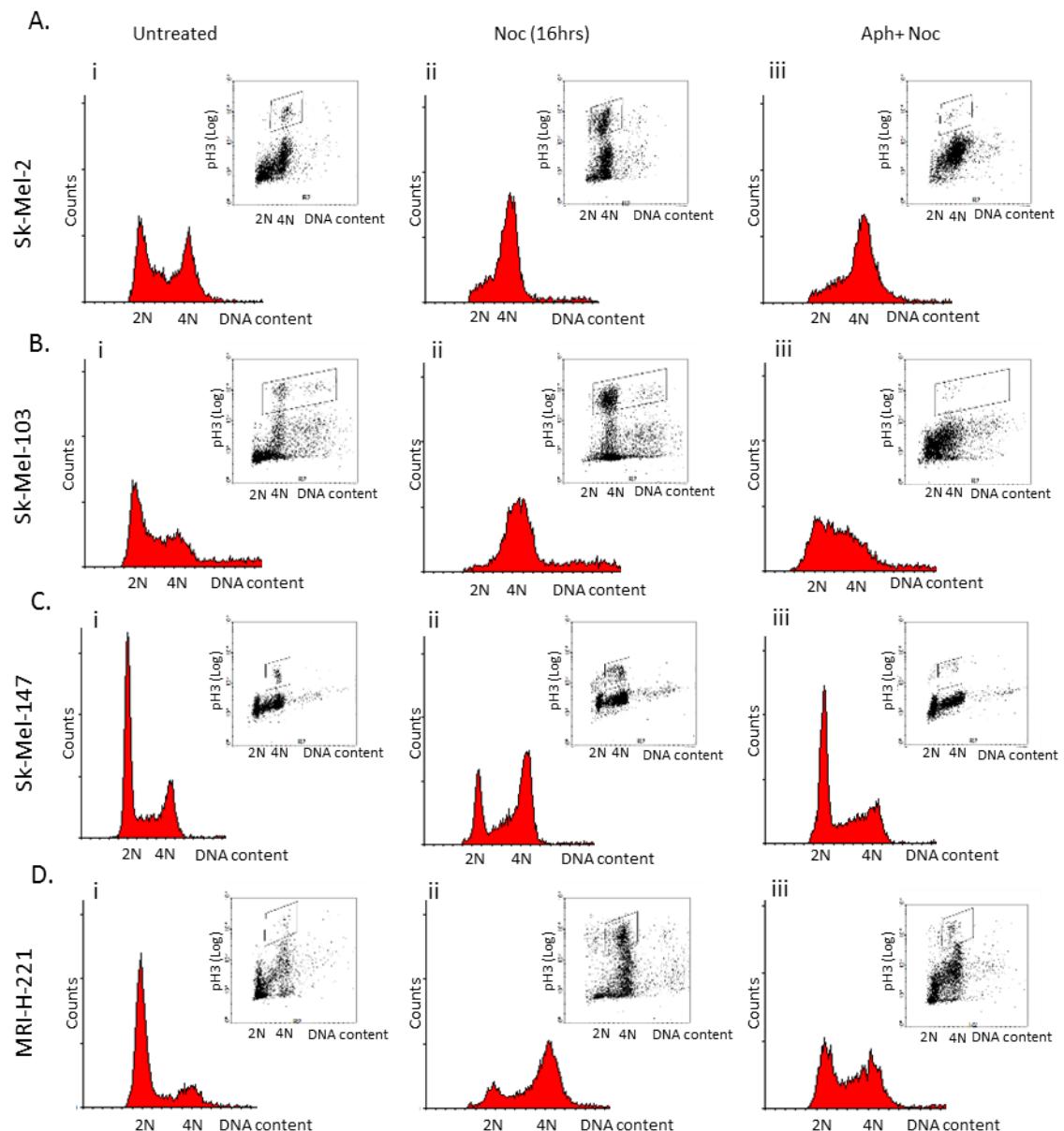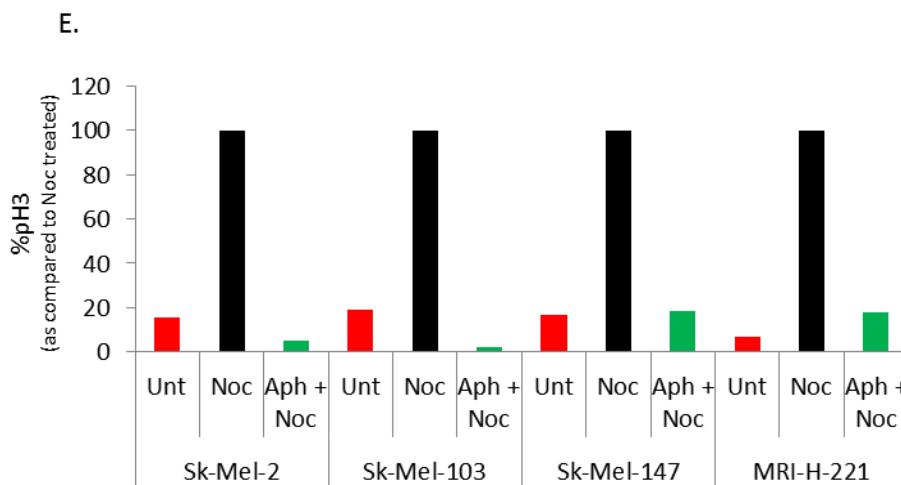
Figure 5.6: Characterisation of S/M checkpoint proficiency in N-Ras mutant melanoma cell lines. (A-D) S-M Checkpoint Assay. Cells were treated for 16hrs with Nocodazole (Noc) with or without [20μM] Aphidicolin. The number of mitotic cells (pH3 positive) after 16hrs was assessed by flow cytometry. Dot plots and DNA histograms are shown. (E) Quantification of the number of mitotic cells taken as a percentage of Noc only treated for each cell line.

Analysis of Chk1 activation by WB after Aph treatment shows a consistent pattern of activating phosphorylation on S345 (Figure 5.7A-K). Chk1 is phosphorylated on S345 within 10mins of treatment in most cell lines and at the latest by 1hr in cell lines WM793 and SK-Mel-147 (Figure 5.7C and J respectively). There is a peak of pChk1 S345 after 1hr to 6hr treatment with maintenance of this activating phosphorylation until 16hrs after Aph treatment in all cell lines except Sk-Mel-103 (Figure 5.7I) which is back to basal levels by this time point. Chk2 activation shows a more varied pattern of activating phosphorylation on T68. In cell lines Sk-Mel-39 and Sk-Mel-103 (Figure 5.7G and I respectively) there are no detectable levels of pChk2 T68 in either the untreated or treated samples at any time point. In cell lines A375MM, WM793 and MRI-H-221 (Figure 5.7A, C and K respectively) there is no significant increase in pChk2 levels beyond the basal levels of activation seen in the untreated samples. In cell lines WM35, Sk-Mel-5, Sk-Mel-28, Sk-Mel-2 and Sk-Mel-147 (Figure 5.7B, D, E, H and J respectively) there is activation of Chk2 at one or more time points for each cell line after Aph treatment, however these vary between cell line. Finally in cell line SK-Mel-37 (Figure 5.7F) there is activation of pChk2 above basal levels 16hrs after Aph treatment. These data demonstrate that Chk1 is activated after DNA replication stress in all cell lines whereas activation of Chk2 is cell line-dependent. This may reflect variations in the ability of each cell line

to repair damage caused by replication fork stalling. Cell lines which activate Chk2 as well as Chk1 may be less efficient at stabilising stalled forks and potentially DNA DSBs could be generated as well as ssDNA, through fork collapse or other mechanisms.
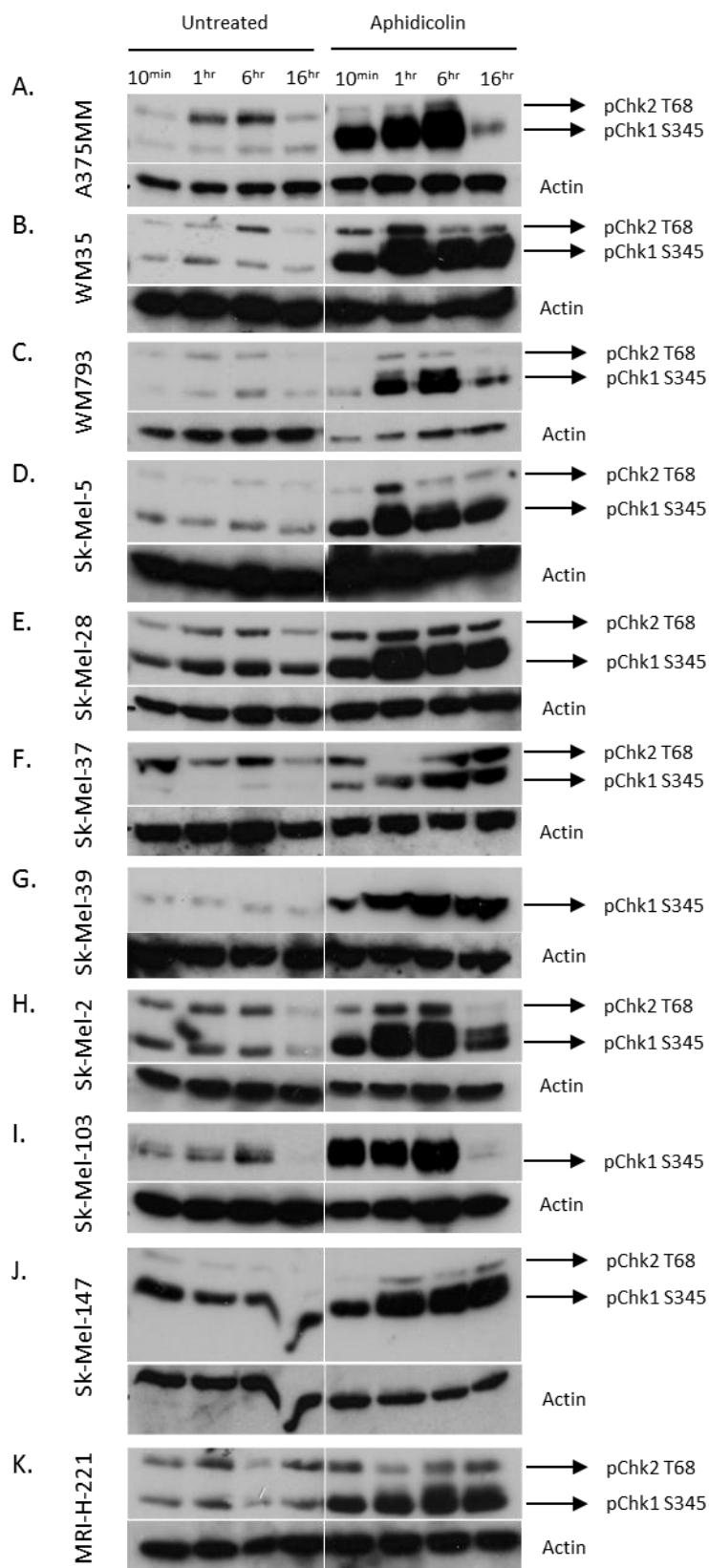
Figure 5.7: Activation of Chk1 and Chk2 signalling post Aphidicolin treatment in melanoma cell lines. (A-K) Western blot analysis of activating phosphorylation on Chk1 and Chk2. Cells were harvested 10mins, 1hr, 6hr and 16hr post [20µM] Aphidicolin treatment. Antibodies against pChk1 S345 and pChk2 T68 were used. An equal quantity of protein was loaded as determined by Bradford Assay and confirmed by antibody against actin.

5.5 Analysis of MRN complex in malignant melanoma cell lines

In order to assess whether the variations in G2/M and S/M checkpoint function and Chk1/Chk2 signalling patterns observed before could be due to differences in the protein expression levels of components of the DNA damage response pathways in each cell line, I analysed several important proteins involved in the processing and execution of this pathway. The core components of the DNA damage checkpoint response pathway can be classified into three main groups; sensors, signal transducers and effectors. Sensor proteins are the first class to be activated upon DNA damage and these proteins are involved in the initial sensing and processing of the DNA damage signal (D'Amours & Jackson, 2002). A key player in the initial sensing and processing of DNA DSBs is the MRN complex; consisting of three components Mre11, Rad50 and Nbs1.

Protein lysates of human melanoma cell lines were analysed by WB for their basal levels of the MRN complex members (Figure 5.8). Unexpectedly both Mre11 and Nbs1 were undetectable in two of the cell lines (Sk-Mel-39 and Sk-Mel-103) with a corresponding reduction in the Rad50 levels. The levels of Mre11, Nbs1 and Rad50 are also greatly reduced in cell line Sk-Mel-147. These data could suggest that these cell lines could potentially have a defective response to DNA DSBs. This would be consistent with their lack of active Chk2. Phosphorylated Chk2 on T68 is a direct read-out of active ATM which is activated in conjunction with the MRN complex. In cell lines Sk-Mel-39 and Sk-Mel-103 we have previously seen that these cell lines lack detectable levels of pChk2 T68 after irradiation (Figure 5.3C and E respectively). This could now be attributed to their lack of Mre11 and Nbs1 complex members and thus their inability to activate ATM. In cell lines Sk-Mel-147 we have seen previously that they have very low levels of basal pChk2 in untreated samples and are only able to activate pChk2 for a very short time after IR (Figure 5.3F). Again this could now be attributed to their apparent low levels of the MRN complex members with respect to other melanoma cell lines. However it should be noted that all these cell lines are still able to activate Chk1 after IR and possess a functional G2/M checkpoint. All other cell lines show presence of all three complex members to varying degrees however it should be noted that Nbs1 appears to exist in two isoforms with different apparent molecular mass. A lower molecular mass Nbs1

appears in cell lines A375MM, Sk-Mel-5 and Sk-Mel-37 and is also present in the human colon cancer cell line HCT-116. In the remaining cell lines there is a higher molecular mass Nbs1. This is possibly due to post-translational modifications of Nbs1or alternatively it could represent differences splicing. In fact Nbs1 is known to have several DNA damage inducible phosphorylation sites (Seno & Dynlacht, 2004).
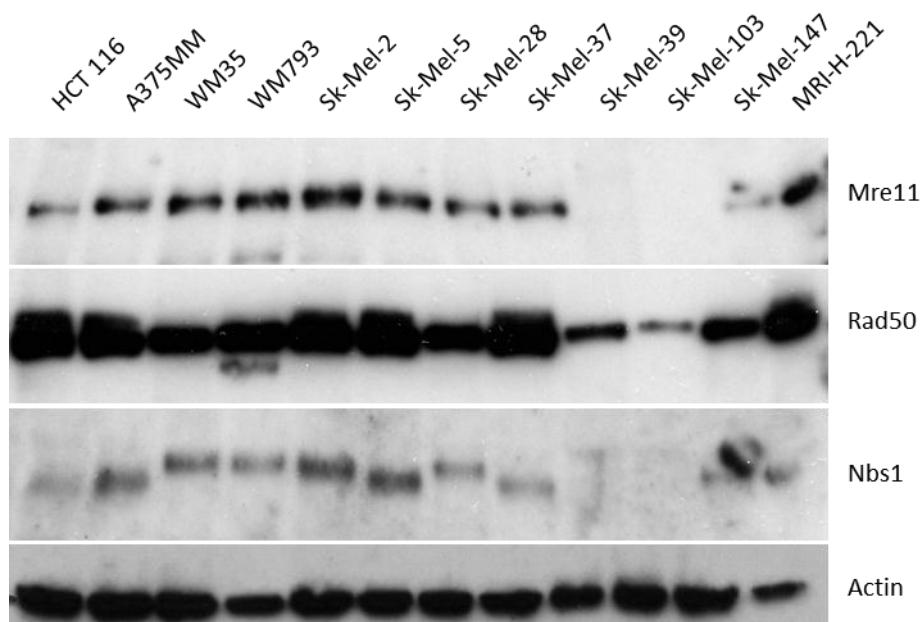
Figure 5.8: Levels of MRN complex components in melanoma cells. Western blot analysis of the components of the MRN complex which senses DNA DSBs. Antibodies against Mre11, Rad50 and Nbs1 were used. An equal quantity of protein was loaded as determined by Bradford Assay and confirmed by antibody against actin.

The second class of proteins in the DNA damage response checkpoint pathway are the signal transducers. These proteins are able to convert the signal from the sensor proteins and activate downstream effector kinases. Main players in this response are the ATM and ATR serine/threonine protein kinases which are activated in response to DNA DSBs and ssDNA respectively, and the ATR partner protein, ATRIP. Protein lysates of human melanoma cell lines were analysed by WB for their basal levels of ATM, ATR and ATRIP (Figure 5.9). The ATM kinase is present in most cell lines but appears to be absent or at reduced levels in cell lines Sk-Mel-39, Sk-Mel-103 and Sk-Mel-147 which have all been aforementioned to lack or have very low levels of MRN complex expression. The ATR kinase is present in all cell lines to varying degrees however at lower levels than in the

human colon cancer cell line HCT-116. The ATR binding protein ATRIP is present in all cell lines at similar levels.
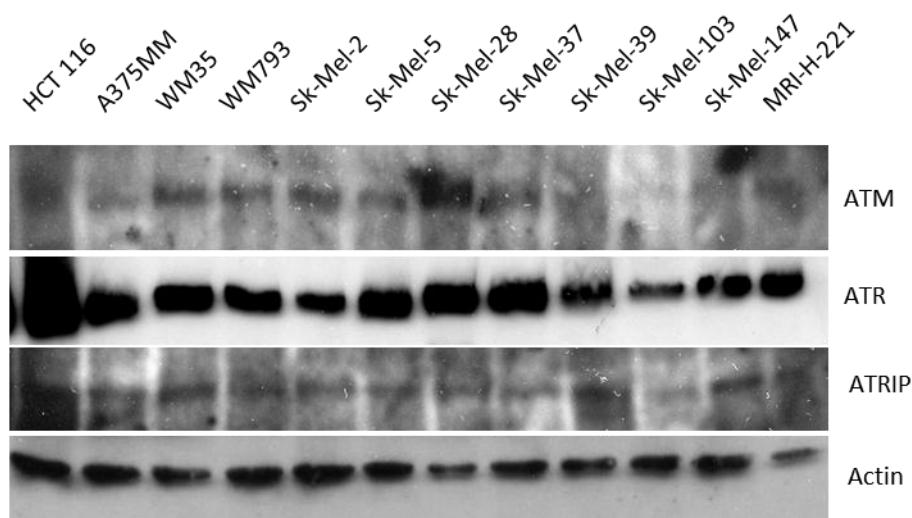
Figure 5.9: Ataxia telangiectasia mutated (ATM), Ataxia telangiectasia and Rad3 related (ATR) and ATR-interacting protein (ATRIP) expression in melanoma cells. Western blot analysis of the levels of expression of kinases ATM and ATR which are activated in response to DNA DSBs and ssDNA respectively, and the essential ATR adaptor protein ATRIP. Antibodies against ATM, ATR and ATRIP were used. An equal quantity of protein was loaded as determined by Bradford Assay and confirmed by antibody against actin.

The third class of proteins in the DNA damage response checkpoint pathway are the effector kinases that are directly responsible for checkpoint activation. The main effectors are the Chk1 and Chk2 protein kinases which are activated primarily by ATR and ATM respectively. Downstream targets of Chk1 include activation of the Wee1 kinase (which subsequently imposes inhibitory phosphorylation on CDK1) and inhibition of CDC25C phosphatases (O'Connell et al, 1997; Peng et al, 1997; Rhind et al, 1997; Sanchez et al, 1997). Downstream targets of Chk2 include activation of p53 and inhibition of CDC25A phosphatases (Mailand et al, 2000). The overall effect of Chk1/2 activation is to block progression from one phase of the cell cycle to the next by inhibiting CDK/Cyclin complexes.

Protein lysates of human melanoma cell lines were analysed by WB for their basal levels of Chk1, Chk2, Wee1, Cdk1 and CDC25A (Figure 5.10). The Chk1 protein kinase is present in all the cell lines however it is expressed substantially less in all the melanoma cell lines compared to human colon cancer HCT 116

cells. Chk1 protein levels are the lowest in cell line MRI-H-221 which is to be expected as this cell line only has one functional allele of Chk1. Wee1 kinase, a downstream target of Chk1, appears to be absent in Sk-Mel-103 cells, however these cells have both a functional S/M and G2/M checkpoint therefore this loss does not seem to affect signalling downstream of Chk1. This could be due to CDC25C, another target of Chk1, over-riding the loss of Wee1 signalling in these cells. In A375MM cells the Wee1 levels are very low. These cells have displayed a partially defective G2/M checkpoint in response to IR (Figure 5.1A) despite having increased pChk1 levels (Figure 5.4A). This phenotype could perhaps be accounted for by the low levels of Wee1. In all other cell lines there is a similar basal level of Wee1. The CDK1 kinase, a downstream target of Wee1, is expressed in all cell lines. The Chk2 protein kinase appears to be absent in cell line Sk-Mel-28 and Sk-Mel-39 and at low levels in cell lines WM35 and MRI-H-221. However the antibody is not very clear therefore it is hard to make any definitive conclusions. It should be noted that Chk2 is clearly present in cell line Sk-Mel-103 and Sk-Mel-147 all of which have displayed absent or very low basal levels of pChk2 T68 after IR treatment (Figure 5.3E and F respectively), therefore this absence is not due to the loss of Chk2 itself but the loss of signalling to Chk2. The CDC25A serine/threonine phosphatase, a downstream target of Chk2, is expressed in all the cell lines at very similar levels.
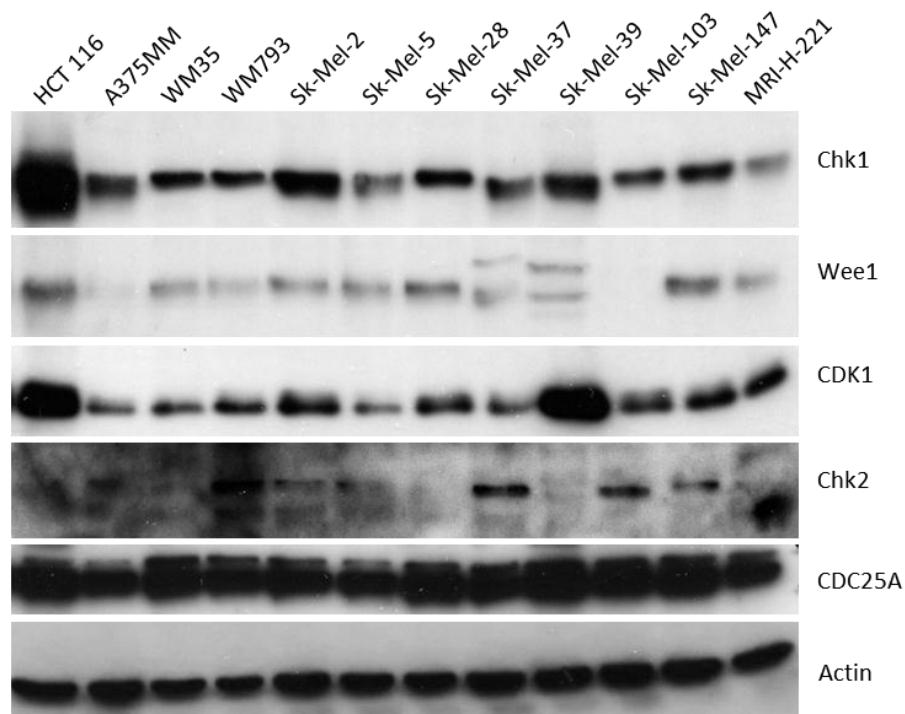
Figure 5.10: Levels of the essential effector kinase Chk1 and Chk2 in melanoma cells.
Western blot analysis of the expression of kinases Chk1 and Chk2, which are activated by ATR and ATM respectively, and downstream targets of checkpoint signalling. Antibodies against Chk1, Chk2, Wee1, Cdk1 and Cdc25A were used. An equal quantity of protein was loaded as determined by Bradford Assay and confirmed by antibody against actin.

These data demonstrate that there are variations in the levels of certain proteins involved in the DNA damage checkpoint response pathway in melanoma cells, however there does not appear to be any obvious consistent differences in the A375MM, WM793, Sk-Mel-37 and SK-Mel-28 cell lines compared to the others which would account for their lack of a fully functional G2/M checkpoint. This suggests that the mechanism responsible for the loss of function may be different in each affected cell line. However it is interesting to note that several proteins; ATR, Chk1 and CDK1 are lower in their basal expression levels in the melanoma cells compared to HCT 116 cells, this may be an example of cell type-specific difference.

5.6 The requirement of MRN complex for Chk1 activation after IR

The MRN complex is responsible for the initial sensing and processing of DNA DSBs, and also the recruitment and activation of Chk2 via ATM (Uziel et al, 2003). However due to its role in strand resection, a process initiated by the nuclease activity of Mre11 to generate tracks of ssDNA, it has also been implicated in activation of ATR and Chk1 after DNA DSBs (Chen et al, 2008; Lewis et al, 2004). In my previous data I have shown that indeed the MRN complex is required for activation of ATM and thus Chk2. Melanoma cell line Sk-Mel-103 lacks both the Mre11 and Nbs1 components with a corresponding reduction in the Rad50 levels (Figure 5.8). This cell line also lacks any detectable levels of pChk2 T68, a read out of active ATM, in both untreated and IR treated samples (Figure 5.3E) despite possessing Chk2 (Figure 5.10). In comparison all Mre11 proficient cell lines (A375MM, WM35, WM793, Sk-Mel-2, Sk-Mel-5, Sk-Mel-28, Sk-Mel-37, Sk-Mel-147 and MRI-H-221) (Figure 5.8) are able to phosphorylate Chk2 after IR induced DNA damage (Figure 5.3 and 5.4). There is even a suggestion of a linear reduction in the activation of the pathway whereby cell line Sk-Mel-147, which has very low levels of both Mre11 and Nbs1 compared to the other cell lines, also displays a concurrent reduction in the activation levels of pChk2 after IR (Figure 5.3F) However despite that fact Sk-Mel-103 cells are unable to activate Chk2 they do not appear to have any problems activating Chk1 after IR (Figure 5.3E).

In order to assess if the restriction of functional MRN complex in these cells would alter the activation of Chk1, I transiently transfected wild type human Mre11 into both Sk-Mel-103 and Sk-Mel-39 cells and analysed the phosphorylation of Chk1 on S345 after both IR and Aph treatment. Transfection efficiency in both cell lines was 20-25% after 24hrs. Protein lysates of Sk-Mel-39 and Sk-Mel-103 cells which had been transfected with either a control plasmid or a plasmid expressing wild type Mre11 (donated from Stephen Jackson's lab with permission granted from Yossi Shiloh) for 24hrs then treated with either IR or Aph and analysed by WB. In both Sk-Mel-39 and Sk-Mel-103 cells Mre11 protein was successfully expressed after transfection (Figure 5.11A and B respectively). In Sk-Mel-39 cells it could be observed that after IR treatment in the presence of

Mre11 the levels of active pChk1 S345 are increased at each time point
compared to controls. After quantification with compensation for differences in
loading (as assessed by the actin protein levels) we can see that there was a
significant increase in the activation of Chk1 after IR in the presence of Mre11
with the highest increase at 6hrs post IR treatment (>1 = increase in
experimental group, 1=no change between control and experimental group, <1=
decrease in experimental group). No significant difference was seen in the
activation of Chk1 after Aph compared to controls (Figure 5.12A). In Sk-Mel-103
cells a similar phenotype can also be observed in that after IR in the presence of
Mre11 the levels of active pChk1 S345 are increased compared to the control
cells (Figure 5.11B), however quantification shows that this increase is only
significant at the later time point of 6hrs post IR with no real increase compared
to controls observed at either 10mins or 1hr post IR (Figure 5.12B).
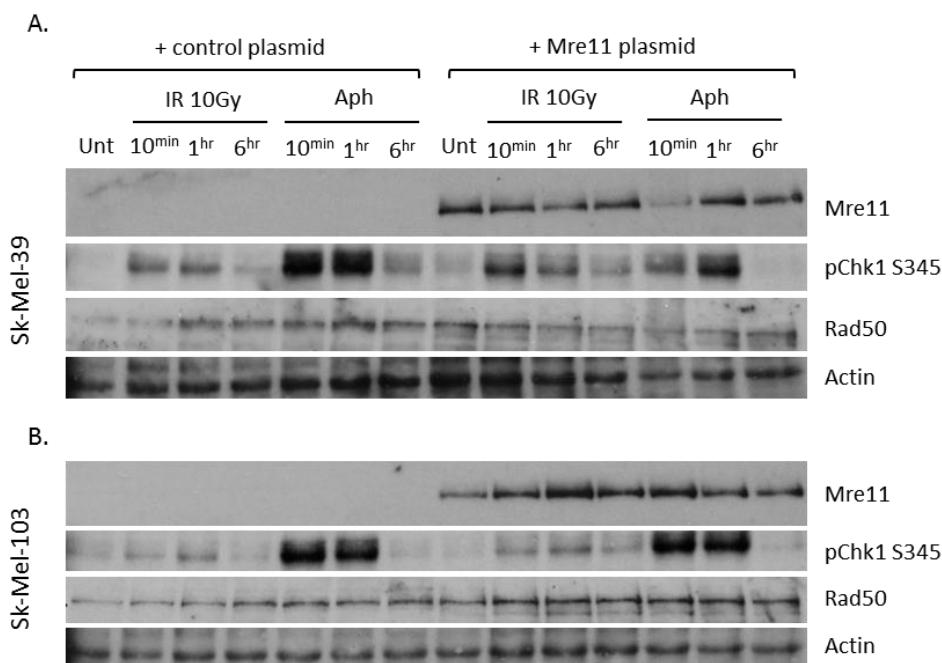
Figure 5.11: Chk1 and Chk2 phosphorylation after γIR or Aphidicolin following transient transfection of Mre11 into Mre11-deficient melanoma cell lines. (A-B) Western blot analysis of activating phosphorylation of Chk1 and Chk2 in Sk-Mel-39 and Sk-Mel-103 cell lines respectively. Cells were transiently transfected with either control plasmid or plasmid expressing Mre11 for 24hrs, then harvested 10mins, 1hr and 6hr post 10Gy γIR or [20μM] aphidicolin treatment. Antibodies against Mre11, pChk1 S345, pChk2 T68 and Rad50 were used. An equal quantity of protein was loaded as determined by Bradford Assay and confirmed by antibody against actin.

A.

B.
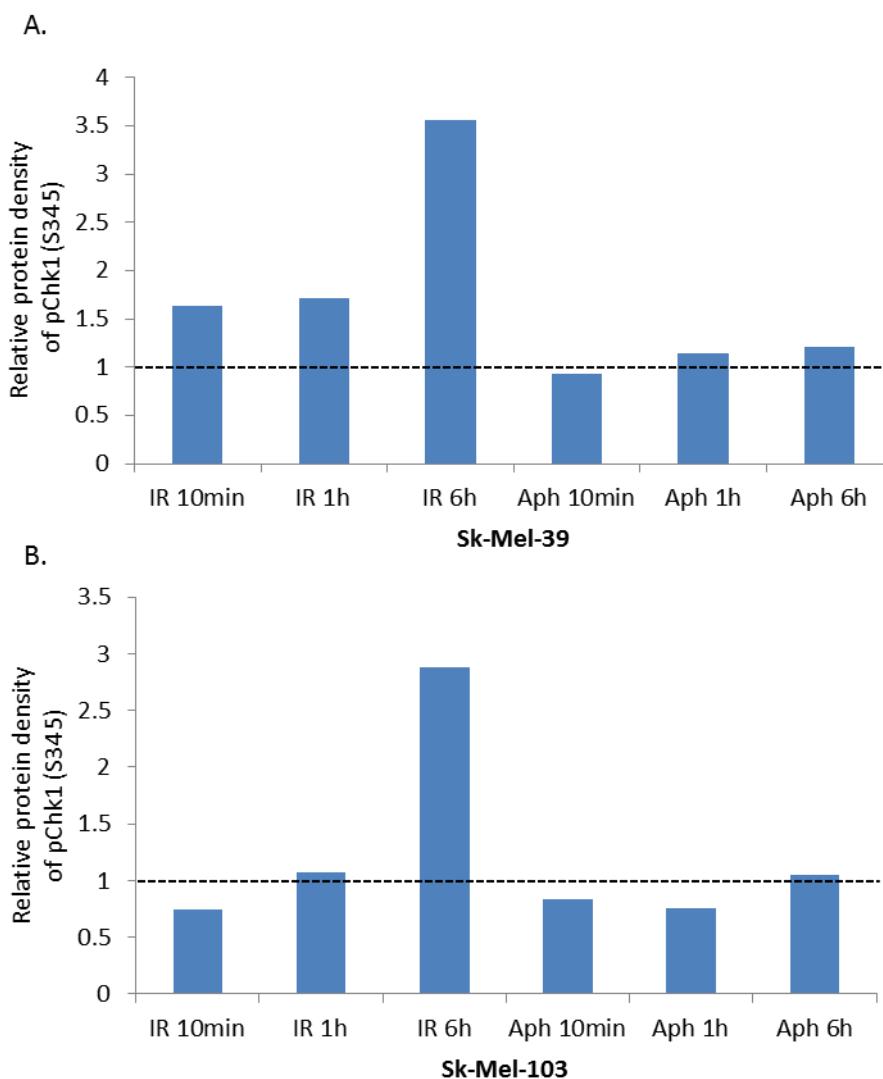

Figure 5.12: Western blot quantification of pChk1 (S345) levels. (A-B) Quantification of pChk1 (S345) levels in Mre11 transfected cells compared to control cells after 10Gy γIR and [20µM] aphidicolin treatment in Sk-Mel-39 and Sk-Mel-103 cell lines respectively. Protein levels were corrected for loading by actin. 1= no difference between pChk1 levels in Mre11 transfected cells compared to control cells. >1= increase in pChk1 levels in Mre11 transfected cells compared to control cells.

These data demonstrate that although in both cell lines Sk-Mel-39 and Sk-Mel-103 a functional MRN complex is required for activation of ATM/Chk2 it is not absolutely required for activation of ATR/Chk1 after irradiation. However the presence of functional Mre11 is sufficient to increase the activation of Chk1 after IR especially at later time points. This suggests that the initial activation of Chk1 after IR treatment does not require strand resection of the DSB but that at later time points strand resection is required in order to maintain the activation of Chk1. This demonstrates that there may be two distinct waves of activation of Chk1 after DNA DSBs with two distinct mechanisms; one of which is reliant on

processing of the DNA strand by the MRN complex. In fact a recent study has shown that CtIP, a key factor in DNA resection, was dispensable for the initial activation of Chk1 following DNA damage with both camptothecin and IR, with rapid activation of Chk1 seen before any detectable end resection. In contrast it was shown that DNA end resection was critically required for sustained ATR/Chk1 activity in both the intra-S and G2-phase checkpoints (Kousholt et al, 2012)

5.7 Discussion

The main aim of this chapter was to understand whether melanoma cells have any common phenotypic defects in their DNA damage responses and whether these can be attributed to specific oncogenic mutations. This could be important as studies have shown that melanomas display high levels of chromosomal instability (Bauer & Bastian, 2006) and display large numbers of nuclear foci positive for γH2AX (a marker of DNA damage) (Gorgoulis et al, 2005; Warters et al, 2005). Such defects could potentially account for their ability to proliferate in the presence of high levels of chromosomal instability and perhaps underlie a mechanism for the continued accrual of genetic alterations. DNA damage response pathways play key roles in maintaining genome integrity in cells during cellular division. In fact studies have shown that DNA damage response activation in early benign legions can act as a strong tumour suppression mechanism (Bartkova et al, 2005; Bartkova et al, 2006; Di Micco et al, 2006) preventing malignant transformation.

When examining the G2/M checkpoint after IR-induced DNA DSBs and the S/M checkpoint after blockage of DNA replication by Aph in a panel of melanoma cell lines, I was able to observe that while the S/M checkpoint function was maintained in all cell lines there is a significant variation in the G2/M checkpoint proficiency of melanoma cell lines (4 out of 11 display variations). This data suggests that while the G2/M checkpoint is dispensable for cell survival the S/M checkpoint may not be. In fact studies have shown that DNA damage induced checkpoint function can be disrupted in cells without affecting survival (Wilsker et al, 2008), whereas complete loss of Chk1 is not conducive with cell survival as shown by embryonic lethality in Chk1 null mice (Lam et al, 2004). In fact the

only cell line able to survive without Chk1 is the DT40 avian cell line (Zachos et al, 2003). The data also suggests that this variation in G2/M checkpoint proficiency may be associated with mutations in the B-Raf oncogene but not mutations in the N-Ras oncogene.

Recent studies have also shown that B-Raf oncogenic melanoma cell lines display significant attenuation of G2/M checkpoint function with an average of 38% of G2 cells evading the checkpoint in a panel of 16 cells lines, however they also showed that N-Ras oncogenic cell lines displayed a more mild but still significant attenuation of the G2/M checkpoint with an average of 21% of G2 cells evading the checkpoint (Kaufmann et al, 2008). Other studies have also shown that Ras oncogenes are able to attenuate G2/M checkpoint function (Agapova et al, 2004; Knauf et al, 2006), possibly by enhancing the expression of cyclin B1 and CDK1 the key CDK/cyclin complex involved in promoting the onset of mitosis (Santana et al, 2002). The G2/M and S/M checkpoints are regulated through the activity of the protein kinase Chk1 which acts by positively regulating Wee1, the inhibitor of CDK1. Wee1 functions by adding inhibitory phosphorylation to CDK1 (T14/ Y15) thereby preventing activation of the CDK1/cyclin B1 complex. Chk1 also acts by negatively regulating CDC25C, the activator of CDK1. CDC25C functions by removing the inhibitory phosphorylation from CDK1.

In order to elucidate how cells are able to maintain an efficient S/M checkpoint in the face of variable G2/M checkpoint proficiency when both act through a common effector, Chk1, I analysed the activation pattern of Chk1 after IR and Aph treatment. As expected after Aph treatment all cell lines activated Chk1 strongly (as assessed by phosphorylation on S345) with maintenance of the signal for up to 16hrs post treatment (Figure 5.7A-K). After IR treatment all the G2/M checkpoint proficient cell lines activated Chk1 strongly with maintenance of the signal for up to 16hrs post treatment (Figure 5.3A-G). Cell lines with variable G2/M checkpoint proficiency displayed variations in their Chk1 activation patterns. In cell lines WM793 and Sk-Mel-37 (Figure 5.4B and D respectively) it was observed that there is a sharp increase in pChk1 levels however this is only seen at one time point for each cell line, after 6hrs IR treatment in WM793 cells and after 1hr IR treatment in Sk-Mel-37 cells and is not maintained at any other times. This pattern suggests that the upstream signal for Chk1 activation after

DNA DSBs may be short lived or that Chk1 itself is 'turned off' rapidly. This could possibly be through the action of phosphatases, both PP1 and PP2A phosphatases have been shown to inactivate Chk1 following DNA damage (Elzen & O'Connell, 2004; Leung-Pineda et al, 2006). This suggests a potential mechanism for the loss of signalling after IR-induced damage compared to DNA replicative stress as, replicative stress directly activates ATR/Chk1 by generation of ssDNA tracts whereas DSBs require resection by the MRN complex before ATR/Chk1 can be activated. In cell lines A357MM and Sk-Mel-28 (Figure 5.4A and C) there is an increase in pChk1 S345 levels 10mins after IR treatment which is maintained for 6hrs post treatment. This pattern of activation is similar to that seen in the G2/M proficient cell lines. This pattern suggests that the upstream activation of Chk1 is efficient however the signal is not appropriately transmitted downstream of Chk1. The targets of Chk1 in the S/M and G2/M checkpoint are thought to be the same therefore how cells are able to distinguish between the two signals in order to maintain a functional S/M checkpoint with variable G2/M checkpoint proficiency is unclear. One possibility is that cells may be able to distinguish between the two signals due to the cell cycle phase at which the signal is initiated. In S-phase cells the levels of cyclin B are quite low whereas in G2-phase cells the levels of cyclin B are high. The key way in which Chk1 activity works to regulate mitotic entry is to regulate the CDK1/cyclin B1 complex. Therefore Chk1 activity may need to be higher in G2 phase cells in order to prevent mitotic entry than in S-phase cells. Together this data shows that partial or complete loss of G2/M checkpoint function but not S/M checkpoint function can be seen in a sub-set of melanoma cells and may present a functional mechanism in melanoma for the accumulation of genetic instability and malignant progression. A recent study of genome wide susceptibility loci in melanoma showed mutations in ATM as a common event (Barrett et al, 2011). Loss of checkpoint function as a contributory factor in malignant transition is an already well documented phenotype. Loss or mutation of p53 is a common event in cancer cells and is thought to occur in up to 50% of all cancers, although this is a less common occurrence in melanoma. One consequence of the mutation or loss of p53 signalling is the loss of the G1/S checkpoint.

When examining the importance of MRN complex signalling in activation of ATR/Chk1 after IR-induced DNA DSBs I was able to observe that cell lines which

possessed Mre11, Nbs1 and Rad50 were able to phosphorylate both Chk2 and Chk1 after IR. In contrast cell lines which lacked the Mre11 and Nbs1 components of the MRN complex were still able to phosphorylate Chk1 but had lost their ability to activate Chk2 (Sk-Mel-39 and Sk-Mel-103, Figure 5.3C and E respectively). This loss of Chk2 activation is consistent with studies which have shown that the MRN complex is essential for activation of ATM/Chk2 (Takemura et al, 2006). However the situation with Chk1 is less clear. In my experiments I have shown that Chk1 activation is still able to occur after IR despite that lack of the MRN complex, this is in direct opposition to studies which have shown that Mre11 nuclease activity is critical for efficient ATR/Chk1 signalling via generation of RPA-coated ssDNA that is needed for ATR recruitment and activation (Jazayeri et al, 2005; Limbo et al, 2011). However by adding back Mre11 by transient transfection into these cell lines (Sk-Mel-39 and Sk-Mel-103, Figure 5.11A and B respectively) I was able to show that the addition of Mre11 and presumed activation of the MRN complex was able to enhance the activation of Chk1 after IR, especially at later time points (6hrs). This is consistent with other recent studies that have shown that although the initial activation of Chk1 is not dependant on MRN complex signalling it does play a role in the maintenance of Chk1 activation after IR-induced DNA damage (Buis et al, 2008; Kousholt et al, 2012; Sartori et al, 2007). It is interesting to note that mutations in Mre11 are the hallmark of the radiosensitive ataxia-telangiectasia-like disorder (Delia et al, 2004) and are commonly associated with mismatch-repair deficient cancers such as colon, breast and haematological (Giannini et al, 2002). Mre11 mutant cancers show supressed responses to replicative stress coupled with disruption of replication forks (Wen et al, 2008), possibly demonstrating a connection between MRN complex signalling and Chk1 signalling, which has been shown to be important during S-phase of unperturbed cells and in the maintenance of stalled replication forks during perturbed S-phase. Furthermore recent studies have highlighted the importance of MRN complex signalling and Chk1. The Mre11 nuclease has been shown to be critical for the sensitivity of cells to Chk1 inhibition, with Mre11-deficient ATLD1 cells being highly resistant to Chk1 inhibition. It was shown that Mre11 is required for the appearance of both ssDNA and DNA DSBs following Chk1 inhibition, with inhibition or lack of Mre11 protein preventing the appearance of these DNA lesions following treatment with a Chk1 inhibitor (Thompson et al, 2012).

Chapter 6: Chk1 inhibition as a therapeutic strategy

6 Chk1 Inhibition as a therapeutic strategy

6.1 Introduction

The treatment of cancer is beginning to focus on more personalised therapies targeting specific genetic alterations present in tumours, for instance Vemurafenib and Dabrafenib, two B-Raf (V600E) inhibitors currently being trialled in the treatment of melanoma (Hauschild et al, 2012; Ravnan & Matalka, 2012). However the standard treatment strategy for most cancers still focuses on the use of genotoxic agents (which cause severe DNA damage) such as radiation therapy and chemotherapeutics which will activate cellular DNA damage responses. As a result, in recent years much interest has focused on whether manipulating these responses could be useful for therapy (Basu et al, 2012). In particular Chk1 has appeared as a potential target for drug development as it is known to be a key effector in multiple cell cycle checkpoint responses triggered by both DNA damage and replication stress. Initially Chk1 inhibitors were trialled in combination with standard genotoxic agents to determine whether there was a synergistic effect on cell killing (Dent et al, 2011; Hotte et al, 2006; Ma et al, 2012; Xu et al, 2011; Zhang et al, 2009) and more recently in combination with other inhibitors which target important cell cycle proteins such as Wee1 (Aarts et al, 2012; Carrassa et al, 2012). However more recent studies have also shown that Chk1 inhibitors may have potential as single agents in some cancer types (Brooks et al, 2012; Davies et al, 2011a; Ferrao et al, 2012). Therefore I examined the effect of a specific allosteric inhibitor of Chk1 (CHIR-124) on a sub-set of metastatic melanoma cell lines from the previously mentioned panel (Table 6.1) to determine the potential benefit as a single agent treatment in melanoma.

6.2 The Chk1 inhibitor CHIR-124

CHIR-124 is a quinolone-based small molecule that is structurally unrelated to other known inhibitors of Chk1. CHIR-124 was generated by the Chiron Corporation and has been shown to be a potent and selective inhibitor of Chk1 with an IC_{50} of 0.32nM compared to 697nM for Chk2 (Ni et al, 2006). It has also been shown to have 500-fold, 5000-fold and 1500-fold selectively of Chk1 over cdk2/cyclin A, cdk4/cyclin D and cdk1/cyclin B complexes respectively. Its basic

structure is a ABIQ (4-(aminoalkylamino)-3-benzimidazole-quinolin-one) scaffold (Figure 6.1A) which binds to the hinge region of the ATP binding pocket of Chk1 forming hydrogen bonds with the Glu85 and Cys87 residues. Its specificity over other related kinases is determined by the charge-charge interactions between the tertiary amine of the inhibitor and residues Glu91 and Glu134 (Figure 6.1B). In studies CHIR-124 has been shown to synergise with a number of known cytotoxic agents including with topoisomerase inhibitors in MDA-MB-435 breast cancer cells (Tse et al, 2007) and increasing radio-sensitivity in HCT 116 cells especially in a p53 null background (Tao et al, 2009). In more recent studies CHIR-124 has been shown to increase the sensitivity to cell death induced by histone deacetylase inhibitors, which is associated with extensive mitotic disruption (Lee J et al, 2011), and to enhance the sensitivity to gemcitabine in a multicellular tumour spheroid model of pancreatic cancer (Dufau et al, 2012).
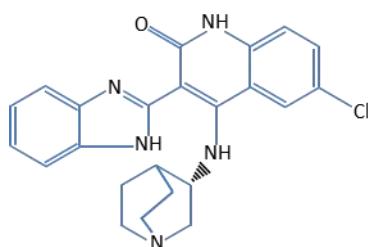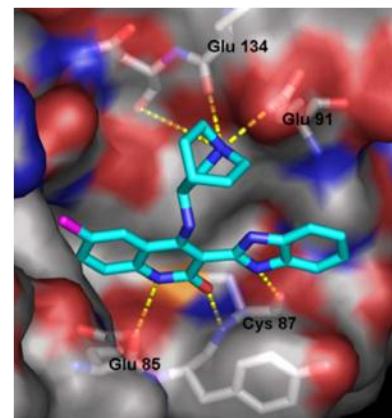
Figure 6.1: CHIR-124 structural interactions. (A) Chemical structure of CHIR-124. (B) X-ray co-crystal structure of CHIR-124 bound to Chk1.

6.3 CHIR-124 inhibits the G2/M checkpoint function of Chk1 in melanoma cells

The G2/M checkpoint is assayed using a flow cytometry techniques described previously in Chapter 3.3. Checkpoint proficient cells will display an accumulation in the G2/M peak but with diminished pH3 staining after irradiation treatment (IR). The cells are also treated with Nocodozole (Noc), a spindle poison, which blocks the cells in mitosis and acts as a positive control for the accumulation of pH3-positive mitotic cells in undamaged cultures.

In the Sk-Mel-2 melanoma cell line we can see that after treatment with CHIR-124 [500nM] for 8hrs prior to IR the cells were subsequently unable to arrest in

G2-phase, compared to the IR + Noc treated alone, and progressed into mitosis as assessed by pH3 staining. This indicates that inhibition of Chk1 by CHIR-124 is able to over-ride the DNA damage-induced G2/M checkpoint (Figure 6.2A). Quantification of the pH3 accumulation in the CHIR-124+ IR+ Noc and IR+ Noc samples are compared as a percentage of the Noc only treated (taken as 100%) (Figure 6.2B) also demonstrates that in the presence of CHIR-124 the cells are no longer able to block in G2 efficiently and continue cycling into mitosis (as indicated by black star in Figure 6.2B). It should be noted that treatment with CHIR-124 itself does not decrease the accumulation of the cells into mitosis as seen in the control whereby cells are treated with CHIR-124 [500nM] 8hrs prior to Noc only treatment.

Downstream targets of Chk1 include activation of the Wee1 kinase, which imposes inhibitory phosphorylation on CDK1, and inhibition of CDC25C phosphatases, which reverse this modification (O'Connell et al, 1997; Peng et al, 1997; Rhind et al, 1997; Sanchez et al, 1997). Analysis of signalling downstream of Chk1 by WB (Figure 6.2C) shows that treatment with CHIR-124 supresses both the inhibitory phosphorylation of CDK1 and the activating phosphorylation of CDC25C (S216) both alone and after IR treatment. It is interesting to note that CHIR-124 treatment leads to induction of Chk1 phosphorylation at S345 to a greater extent even than IR treatment. This data shows that CHIR-124 effectively inhibits Chk1 signalling in melanoma cell lines.
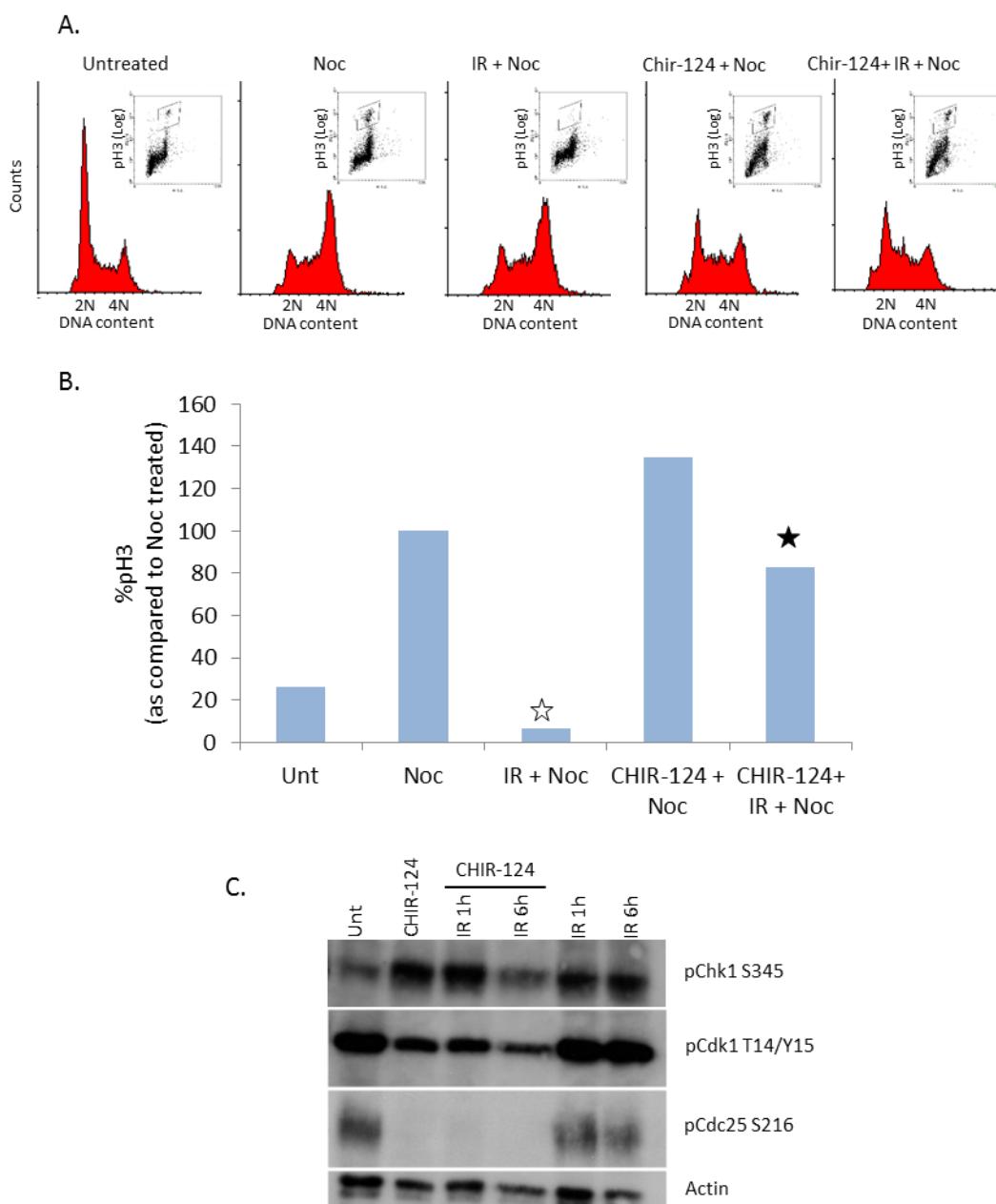
Figure 6.2: CHIR-124 inhibition of G2/M checkpoint function in Sk-Mel-2 melanoma cell line.
(A) G2/M checkpoint assay. Cells were treated for 8hrs with [1μM] CHIR-124, and then treated with Noc with or without 10Gy γIR. The number of mitotic cells (pH3 positive) after 24hrs was assessed by flow cytometry. Dot plots and DNA histograms are shown. (B) Quantification of the number of mitotic cells taken as a percentage of Noc only treated, n=1. White star represents G2/M checkpoint activation. Black star represents inhibition of checkpoint in the presence of CHIR-124. (C) Western blot analysis of Chk1 activation and downstream signalling. Antibodies against pChk1 S345, pCdk1 T14/Y15 and pCdc25C S216 were used. An equal quantity of protein was loaded as determined by Bradford Assay and confirmed by antibody against actin.

6.4 Chk1 Inhibition causes apoptotic cell death

Cellular death by apoptosis is assayed using a flow cytometry technique whereby living cells are double labelled for Annexin V and PI. Annexin V is used as a probe to detect expression of phosphatidylserine (PS) on the surface of cells, an event which occurs during programmed cell death. PI stains DNA; in live cells with an

intact membrane PI is unable to enter and bind to the DNA, however in apoptotic cells where the cell membrane integrity is compromised PI can bind to exposed DNA. Cells are analysed for staining with both markers, whereby staining with Annexin V represents early apoptosis and double Annexin V: PI staining represents late apoptosis.

In a set of metastatic melanoma cell lines we can see that after continual treatment with 1µM CHIR-124 cells become firstly Annexin V positive (24hrs) and then progress to Annexin V: PI positive (48hrs) in a time dependent manner (Figure 6.3A, B, C, D, F and G respectively) This phenotype is exacerbated with 10µM CHIR-124 treatment. In the Sk-Mel-39 cell line there is no detectable level of Annexin V positivity with the cells becoming single PI positive after both 24hrs and 48hrs with both 1µM and 10µM CHIR-124 treatment. This phenotype is also seen in the staurosporine (Sts) treated Sk-Mel-5, Sk-Mel-28 and Sk-Mel-39 cells (Figure 6.3C, D and E respectively) and may represent a cell type-specific variation in the mechanism of cell death. When we quantify the percentage of double positive cells (Figure 6.3H) we can see that in most cells lines there is a small increase of 5-20% after 24hrs of treatment which increases further to 25%-60% after 48hrs with 1µM CHIR-124 treatment. This is exacerbated by 10µM CHIR-124 treatment, with the percentage of double positive cells ranging from 25-90% after 24hrs of treatment which increases further to 80%-100% after 48hrs. The phenotype is slightly different in the Sk-Mel-5 cell line where with both 1µM and 10µM treatment there is no increase in double positive cells between 24hrs and 48hrs.
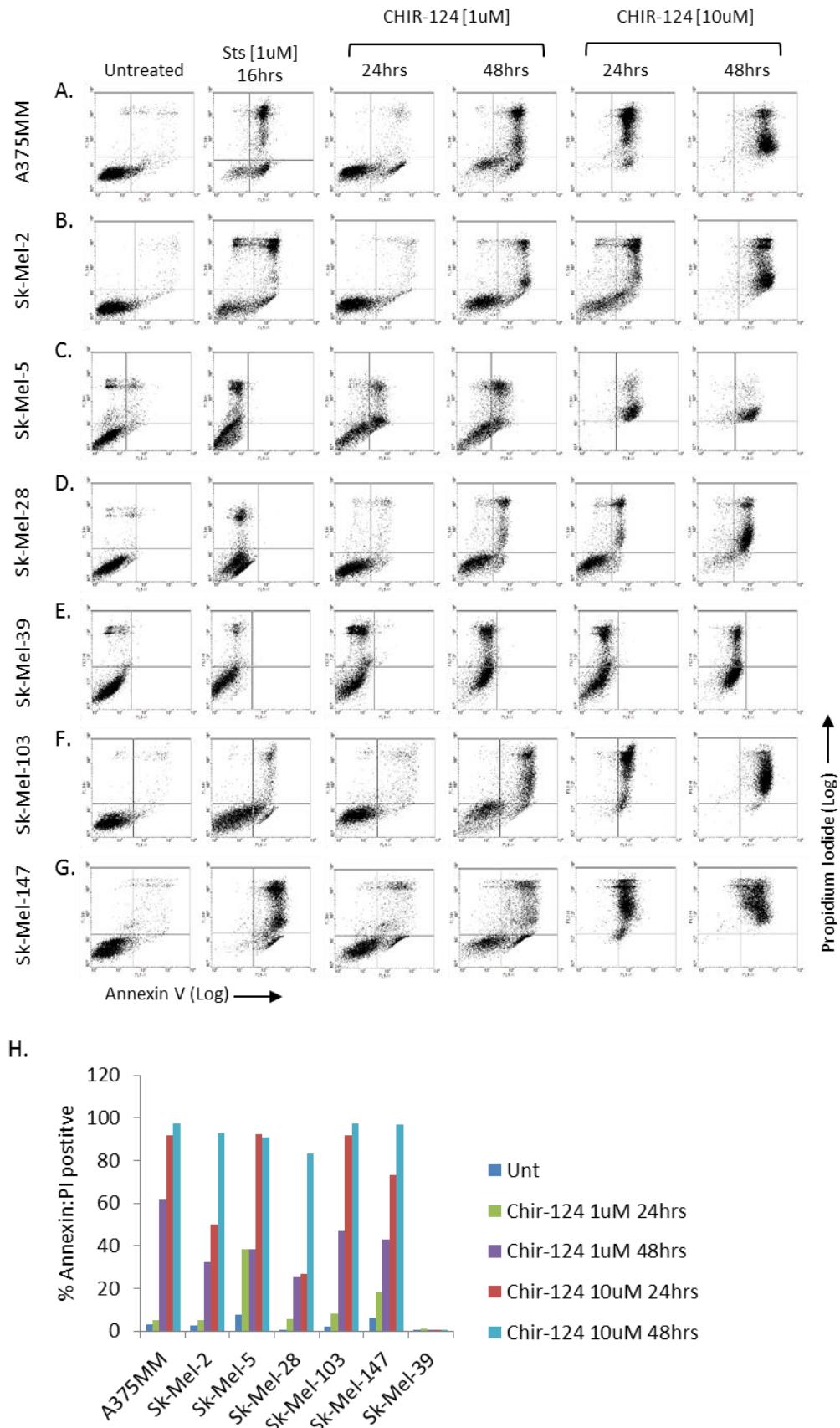
Figure 6.3: Characterisation of Annexin-V and PI staining in CHIR-124 treated metastatic melanoma cells. (A-G) Melanoma cells lines A375MM, Sk-Mel-2, Sk-Mel-5, Sk-Mel-28, Sk-Mel-39, Sk-Mel-103 and Sk-Mel-147 respectively were treated with [1µM] and [10µM] CHIR-124. Cells were harvested after 24hrs and 48hrs and analysed for Annexin-V and PI labelling. Cells were treated with [1µM] staurosporine (Sts) for 16hrs as a positive control. Dot plots are shown, n=1. (H) Quantification of the number of double positive Annexin-V: PI labelled cells after CHIR-124 treatment in each cell line.

This data shows that metastatic melanoma cell lines are highly sensitive to inhibition of Chk1 with CHIR-124 resulting in a high percentage of cell death after 48hrs treatment. Cell death is attributable to apoptosis as indicated by positive staining for Annexin V, except in cell line Sk-Mel-39 where cells become single PI positive therefore losing their membrane integrity without translocation of PS to the outer membrane.

To further confirm that cell death upon Chk1 inhibition occurs by apoptosis, protein extracts of cell lines were analysed by WB for cleavage of PARP. PARP is a nuclear protein that participates in DNA damage detection and repair, however during apoptosis the protein is cleaved by caspase-3 and caspase-7 (Duriez et al, 1997; Germain et al, 1999). This cleavage efficiently stops the ability of PARP to participate in DNA repair and contributes to the cell fate of apoptosis. Analysis of PARP cleavage shows that in cell lines A375MM and Sk-Mel-2 there is clear cleavage of PARP after treatment with 1µM CHIR-124 (Figure 6.4A and B respectively). In A375MM cells the cleavage is detectable at 6hrs post-treatment whereas in Sk-Mel-2 cells the cleavage is already detectable at 3hrs post-treatment with a further increase seen at 6hrs. In cell lines Sk-Mel-5 and Sk-Mel-28 there may be a small detectable level of PARP cleavage at 6hrs post treatment with 1µM CHIR-124 (Figure 6.4C and D respectively). In all other cells lines which became Annexin V: PI positive within 48hrs of treatment with 1µM CHIR-124 there is no detectable cleavage of PARP with 1µM CHIR-124 at either 3hrs or 6hrs post treatment. This may be a cell type specific response with cleavage of PARP happening at later time points in these cells. However if a higher concentration of CHIR-124 is used, 10µM we can see that all cell lines which become Annexin V: PI positive have cleavage of PARP at both 3hrs and 6hrs post- treatment with a time dependant increase (Figure 6.4A-D, F and G). In cell line SK-Mel-39 which does not become Annexin V positive after either Sts or CHIR-124 treatment we can see that there is also no cleavage of PARP seen with either drug at any concentration. This suggests that the cell line SK-Mel-39 does not undergo apoptosis but instead may die by necrosis. Collectively this data shows that most metastatic melanoma cell lines are highly sensitive to Chk1 inhibition alone and undergo apoptotic cell death as seen by cleavage of PARP at early time points (3-6hrs) followed by Annexin V and PI positivity at later time

points (24-48hrs), however the data also shows that there are variations in the response with some cell lines showing cleavage of PARP sooner than others and a range of 25%-60% double Annexin V: PI positivity after 48hrs treatment.
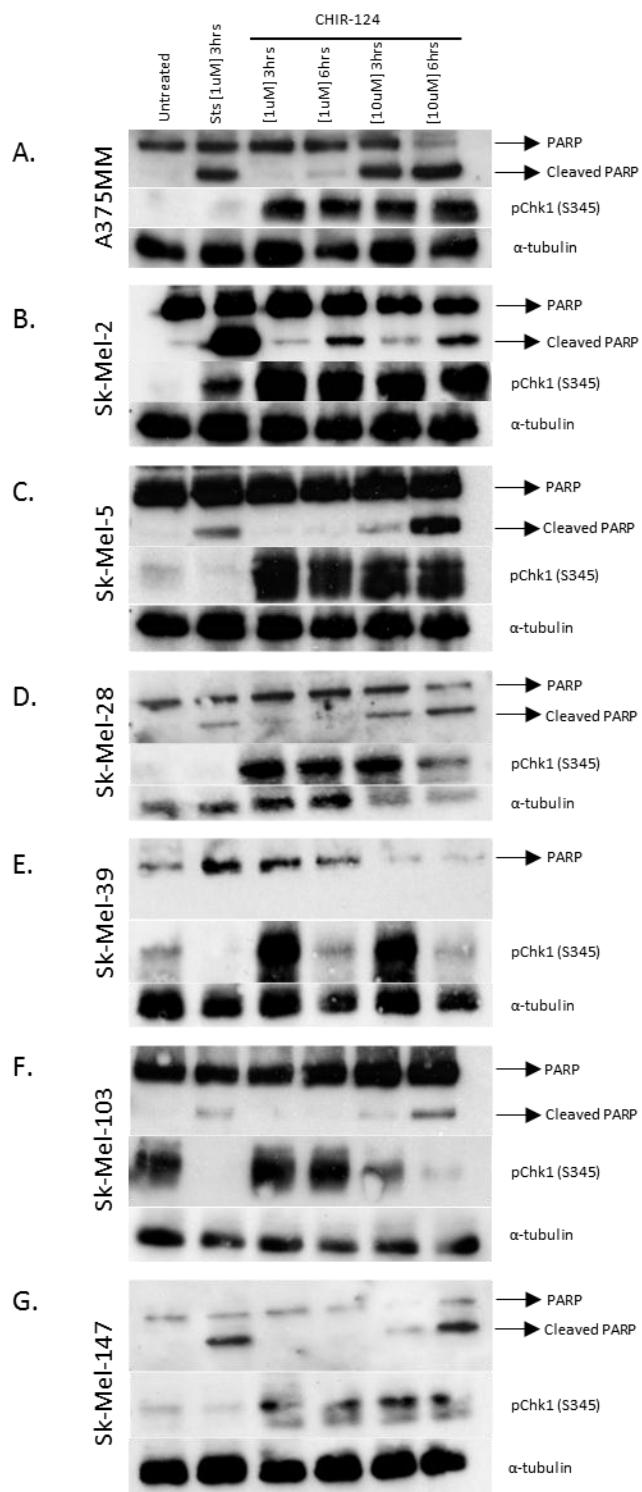
Figure 6.4: Western blot analysis of PARP cleavage and Chk1 activation in CHIR-124 treated metastatic melanoma cells. (A-G) Melanoma cells lines A375MM, Sk-Mel-2, Sk-Mel-5, Sk-Mel-28, Sk-Mel-39, Sk-Mel-103 and Sk-Mel-147 respectively were treated with [1µM] and [10µM] CHIR-124 for 3hrs and 6hrs. Cells were treated with [1µM] staurosporine (Sts) for 3hrs as a positive control. Antibodies against PARP (full length and cleaved forms) and pChk1 (S345) were used. An equal quantity of protein was loaded as determined by Bradford Assay and confirmed by antibody against actin.

6.5 Chk1 inhibition causes generation of DNA damage specifically in S-phase cells with blockage of cells in S-phase

During S-phase of the cell cycle DNA replication occurs thus allowing the specific labelling of S-phase cells using nucleoside analogs which become incorporated into the DNA. Examples include 5-bromo-2'-deoxyuridine (BrdU) and 5-ethynyl-2'-deoxyuridine (EdU) which are both synthetic analogs of thymidine. BrdU can be visualised using anti-BrdU antibodies whereas EdU can be visualised using a click-reaction (Figure 6.5), whereby a copper (I) catalysed reaction occurs between an azide and an alkyne. The alkyne is contained within the EdU molecule which reacts with an azide conjugated to a detection reagent to form a stable triazole ring.
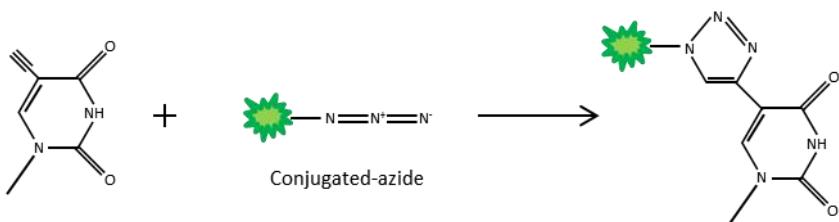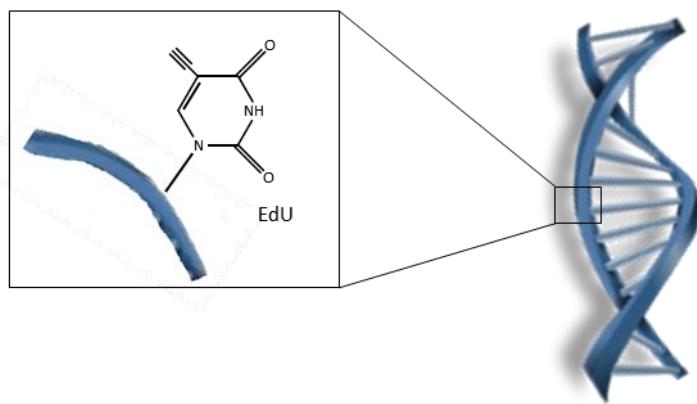
Figure 6.5: Incorporation and detection of EdU. (EdU) is incorporated into the DNA as a thymidine analog. EdU is visualised using a copper (I) catalysed click-reaction which occurs between a fluorescently conjugated azide and incorporated EdU.

In order to analyse if treatment with CHIR-124 causes the generation of DNA damage before inducing apoptosis I treated cell lines A375MM and Sk-Mel-2, which were the most sensitive to CHIR-124 in terms of their cleavage of PARP, with EdU in combination with 1µM CHIR-124 for 1hr and analysed cells by IF. The appearance of DNA damage, as marked by γH2AX following treatment with 1µM CHIR-124 was only seen in EdU+ (S-phase) cells in both A375MM (Figure 6.6A) and

Sk-Mel-2 (Figure 6.7A) cells, whereas treatment with etoposide, an anti-cancer DNA damaging agent, induced DNA damage in all cells regardless of their EdU status. When the intensity of the γH2AX signal was quantified in both EdU+ and EdU- cell populations we can see that the intensity of the γH2AX signal is not only specific to EdU+ cells after CHIR-124 treatment but also that the intensity is half of that seen in the etoposide treated cells (which show no selectivity for EdU+/ EdU-) in both A375MM (Figure 6.6B) and Sk-Mel-2 (Figure 6.7B) cells. This suggests that less DNA damage is generated with CHIR-124 treatment than with etoposide, at least with this relatively short time frame. In the EdU- cells treated with CHIR-124 the γH2AX signal is equivalent to that of untreated cells (both EdU+ and EdU- cell populations).
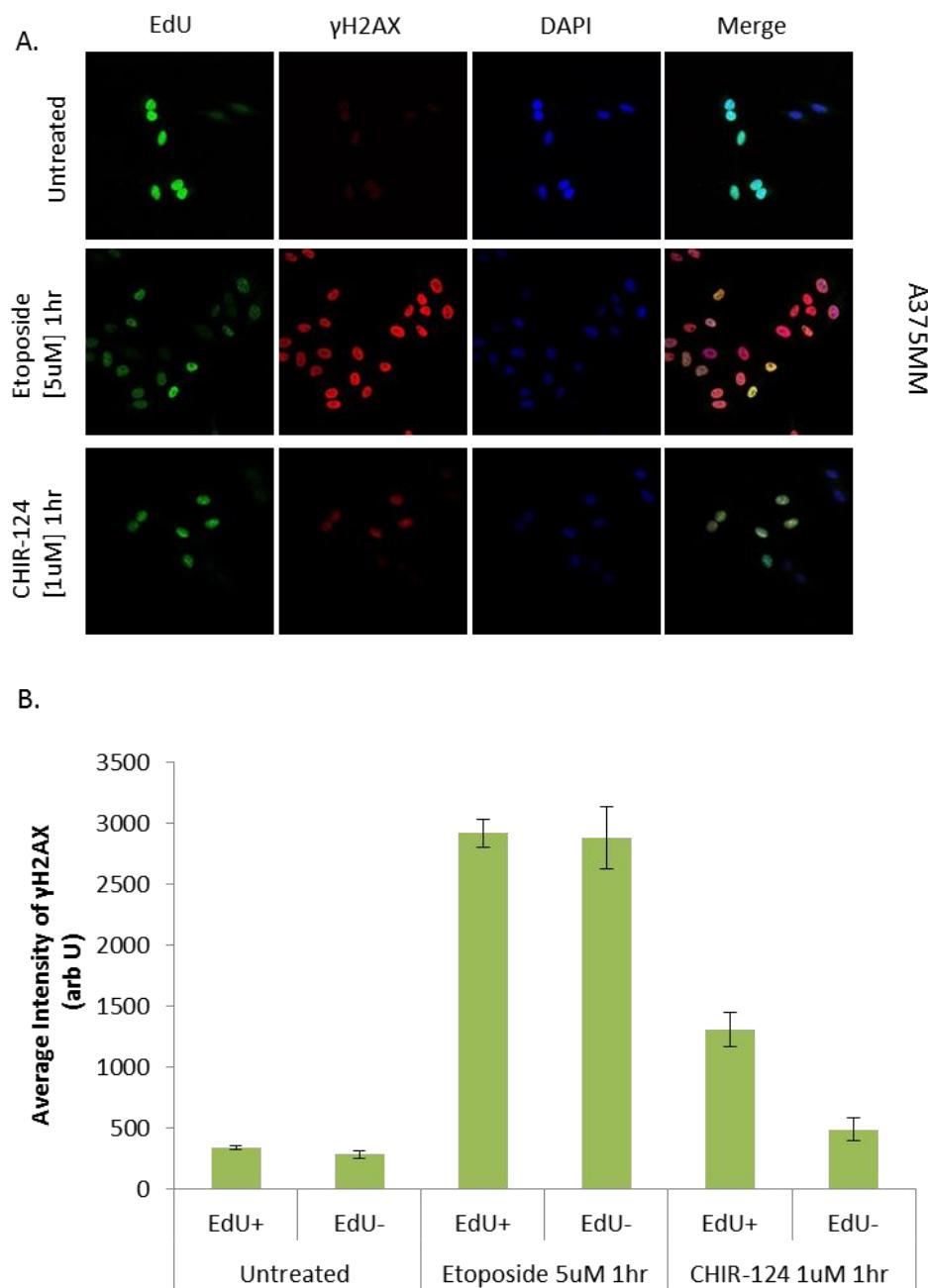
Figure 6.6: Characterisation of DNA damage induction with CHIR-124. (A) Immunofluorescence (IF) microscopy of A375MM cells. Cells were grown on glass coverslips then treated simultaneously with EdU to label proliferating cells and [1μM] CHIR-124 for 1hr. Cells were treated with [5μM] etoposide as a positive control. Cells were labelled for EdU and γH2AX and mounted in vectashield containing dapi. Cells were examined by confocal fluorescence microscopy. (B) Quantification of the intensity of γH2AX labelling in both EdU positive (S-phase cells) and EdU negative cells. IF images were quantified using arbitrary units for fluorescence intensity.
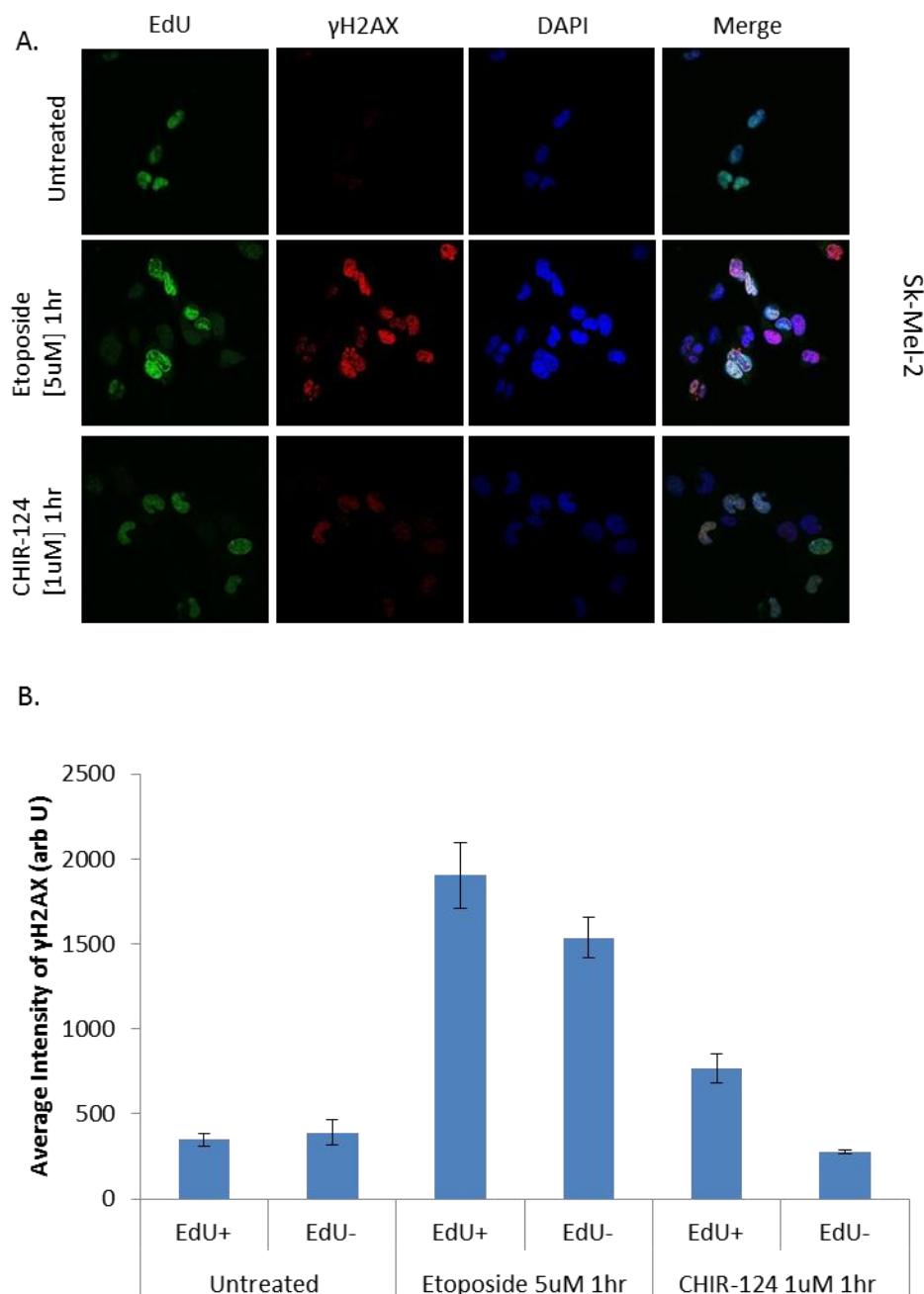
Figure 6.7: Characterisation of DNA damage induction with CHIR-124. (A) Immunofluorescence (IF) microscopy of Sk-Mel-2 cells. Cells were grown on glass coverslips then treated simultaneously with EdU to label proliferating cells and [1μM] CHIR-124 for 1hr. Cells were treated with [5μM] etoposide as a positive control. Cells were labelled for EdU and γH2AX and mounted in vectashield containing dapi. Cells were examined by confocal fluorescence microscopy. (B) Quantification of the intensity of γH2AX labelling in both EdU positive (S-phase cells) and EdU negative cells. IF images were quantified using arbitrary units for fluorescence intensity.

Due to the observation that CHIR-124 specifically generated DNA damage in S-phase cells we analysed the cell cycle profile of these cells using flow cytometry. BrdU incorporation after a 1hr pulse is used as a marker of S-phase cells giving an arc of positive cells ranging between the negative G1 and G2/M populations. To assess how Chk1 inhibition is affecting the cell cycle distribution, BrdU positive cells were gated into early S-phase and late S-phase populations.

At low concentrations of CHIR-124 (100nM) treated for 24hrs there is an initial increase in the percentage of cells in late S-phase (6%) with no change in the early S-phase population. This is possibly due to the slowing of cells through S-phase in the presence of Chk1 inhibition, causing a small number of cells to persist in S-phase for longer than normal. However with increasing concentrations of CHIR-124 (200nM to 1µM) we can observe that there is a dose-dependent increase in the percentage of cells in early S-phase with a concurrent decrease in late S-phase cells. This suggests that in the presence of CHIR-124 the cells are still able to initiate DNA replication however inhibition of Chk1 prevents them from progressing normally resulting in a build of cells in early S-phase (Figure 6.8).
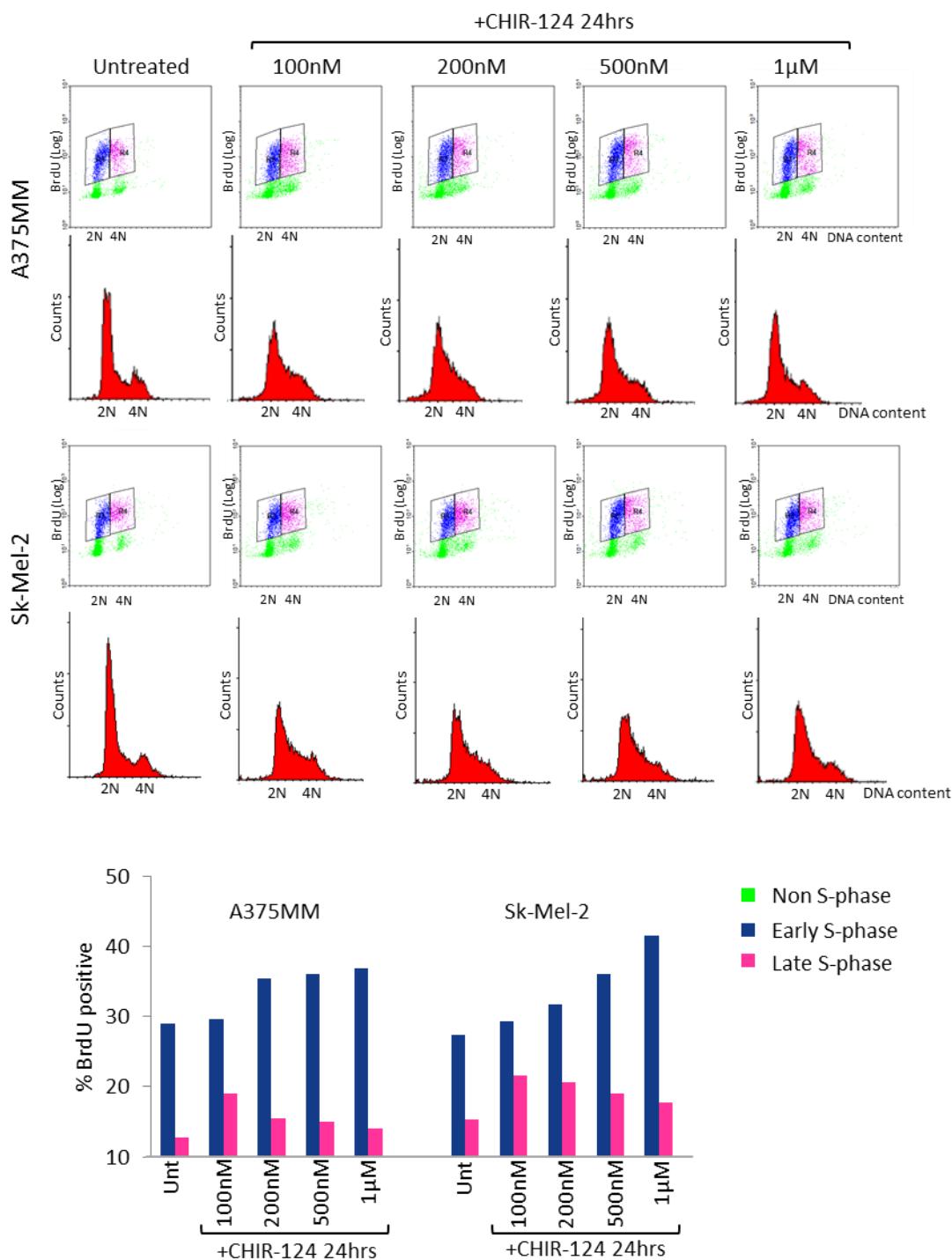
Figure 6.8: Analysis of S-phase progression during CHIR-124 treatment. (A-B) Assessment of BrdU incorporation as a marker of S-phase cells in A375MM and Sk-Mel-2 cell lines respectively. Cells were treated with a range of concentrations of CHIR-124 from 100nM to 1μM for 24hrs. During the last hour of treatment cells were treated with BrdU to label S-phase cells. Early and late S-phase populations are marked as dark blue and pink respectively. Dot plots and DNA histograms are shown. (C) Quantification of the percentage of total cells which incorporated BrdU.

This observation is suggestive of the distinct role that Chk1 plays during an unperturbed cell cycle in comparison to its role during a perturbed cell cycle. This data suggests that upon Chk1 inhibition in unperturbed cells there is a blockage of cells in early S-phase. Studies have shown that Chk1 is important in

replication initiation and replication fork stability during an unperturbed cell cycle (Feijoo et al, 2001; Paulsen & Cimprich, 2007; Petermann & Caldecott, 2006; Petermann et al, 2006; Petermann et al, 2010). Thus inhibition of Chk1 in this situation may cause collapse of replication forks resulting in the S-phase blockage seen. During a perturbed cell cycle where DNA replication is inhibited with Aphidicolin which causes acute stalling of replication forks directly, there is activation of the S/M checkpoint. The S/M checkpoint is mediated via activation of Chk1 in order to prevent collapse of these replication forks and ultimately prevent cells from entering mitosis in the presence of DNA which is not fully replicated. The cells will block in S phase of the cell cycle until the DNA is properly replicated or they are targeted for cell death (apoptosis). This S-phase blockage is phenotypically similar but functionally distinct to that seen with Chk1 inhibition.

6.6 Chk1 inhibition causes replication fork collapse

Replication forks are dynamic structures which are formed during DNA replication whereby the DNA double helix is unwound by helicases to form two single strands of DNA which act as templates for DNA synthesis (Chagin et al, 2010). Chk1 has been shown be important during S-phase of unperturbed cell cycles, where it has functions in both the initiation of replication and stability of replication forks (Feijoo et al, 2001; Paulsen & Cimprich, 2007; Petermann & Caldecott, 2006; Petermann et al, 2006; Petermann et al, 2010). Therefore I assessed replication fork stability in the presence of CHIR-124 in cell lines A375MM and Sk-Mel-2 to determine if the inhibition of Chk1 in these cells is affecting DNA synthesis, and whether this could be the source of DNA damage in Chk1 inhibited cells. Replication fork stability was assessed using a double EdU/BrdU pulse assay and flow cytometry. In control cells (Figure 6.9A-B) we can see that incubation with EdU for 1hr or BrdU for 1hr can be selectively detected using different fluorophores. In double EdU/BrdU incubated cells, were cells were incubated with EdU for 1hr and then BrdU for a subsequent 1hr, we can detect four distinct populations of cells. Double negative cells in green represent cells which were not in S-phase during the total incubation time. Single EdU positive cells in dark blue represent cells which were in S-phase with active replication forks during the first incubation but had finished or collapsed before the second incubation. Single BrdU positive cells in pink represent cells which

had entered S-phase during the second incubation. Double EdU/BrdU positive cells in light blue represents cells which were in S-phase with active replication forks during both incubation periods.
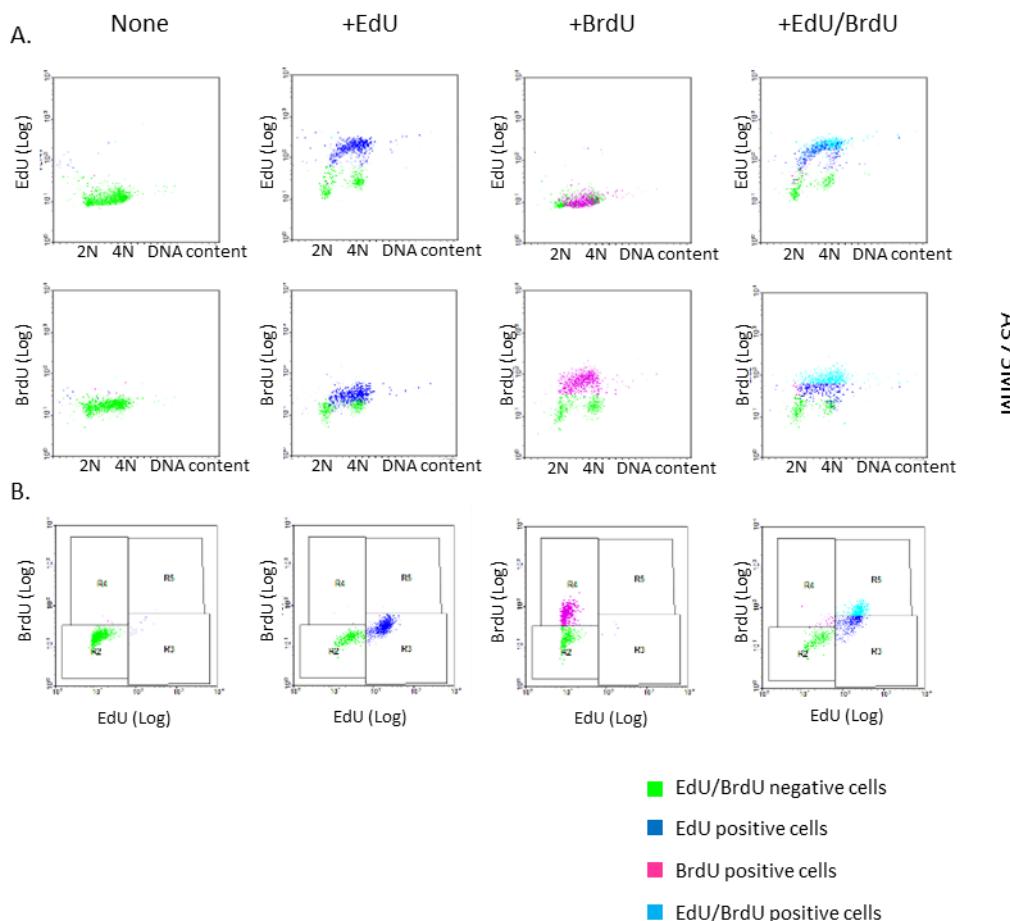
Figure 6.9: Dual pulse-labelling of proliferating melanoma cells. A375MM cells were treated with either EdU or BrdU for 1hr, or sequentially with EdU for 1hr followed by BrdU for 1hr to label proliferating S-phase cells. EdU labelled cells are visualised using a click-it reaction. BrdU labelled cells are visualised using an antibody which does not cross react with EdU. EdU and BrdU incorporation was assessed by flow cytometry. Dark blue represents EdU positive cells, pink represent BrdU positive cells and light blue represents double EdU and BrdU positive cells. Dot plots are shown; single dot plots (A) show EdU and BrdU labelling on separate plots, double dot plots (B) show EdU and BrdU labelling on the same plot.

In order to analyse the effect of Chk1 inhibition on the stability of replication forks cells were pre-labelled with EdU for 1hr in order to label active replication forks, EdU was then removed and the cells were incubated with 20µM aphidicolin alone or in combination with 1µM CHIR-124 for 1-4hrs. Cells were then subsequently released from aphidicolin arrest and pulse-labelled with BrdU for 1hr (Figure 6.10A). Aphidicolin is a reversible inhibitor of DNA polymerase which

stalls active replication forks. In this assay double labelling identifies replication forks which were active prior to the addition of aphidicolin and which remained capable of resuming replication after the period of arrest. Single EdU and BrdU labelling identifies replication forks which were active prior to the addition of aphidicolin but that subsequently collapsed during the period of arrest and replication forks which became active during the period of arrest with aphidicolin respectively.

In both A375MM and Sk-Mel-2 cell lines there is a relative increase in the EdU+ population in the presence of CHIR-124 compared to aphidicolin treated alone for 4hrs (Figure 6.10B). In A375MM cells this increase in the EdU+ population is evident at all time-points treated with CHIR-124 (1-4hrs) however in cell line Sk-Mel-2 it is not visible until later time-points (3-4hrs). There is a concurrent decrease in the double EdU+/BrdU+ populations and BrdU+ populations. Quantification of the percentages of each population shows that in A375MM cells there is a time-dependant increase/ decrease in the respective populations; the EdU+ population increases from 28% to 65% (2.3-fold increase), the EdU+/BrdU+ population decreases from 40% to 17% (2.4-fold decrease) and the BrdU+ population decreases from 3% to 1.9% (1.6-fold decrease)(Figure 6.10Ci). Quantification of the percentages of each population in Sk-Mel-2 cells also show there is a time-dependant increase/ decrease in respective populations; the EdU+ population increases from 18% to 35% (1.9-fold increase), the EdU+/BrdU+ population decreases from 40% to 23% (1.7-fold decrease) and the BrdU+ population decreases from 4% to 1% (4-fold decrease) (Figure 6.10Cii).
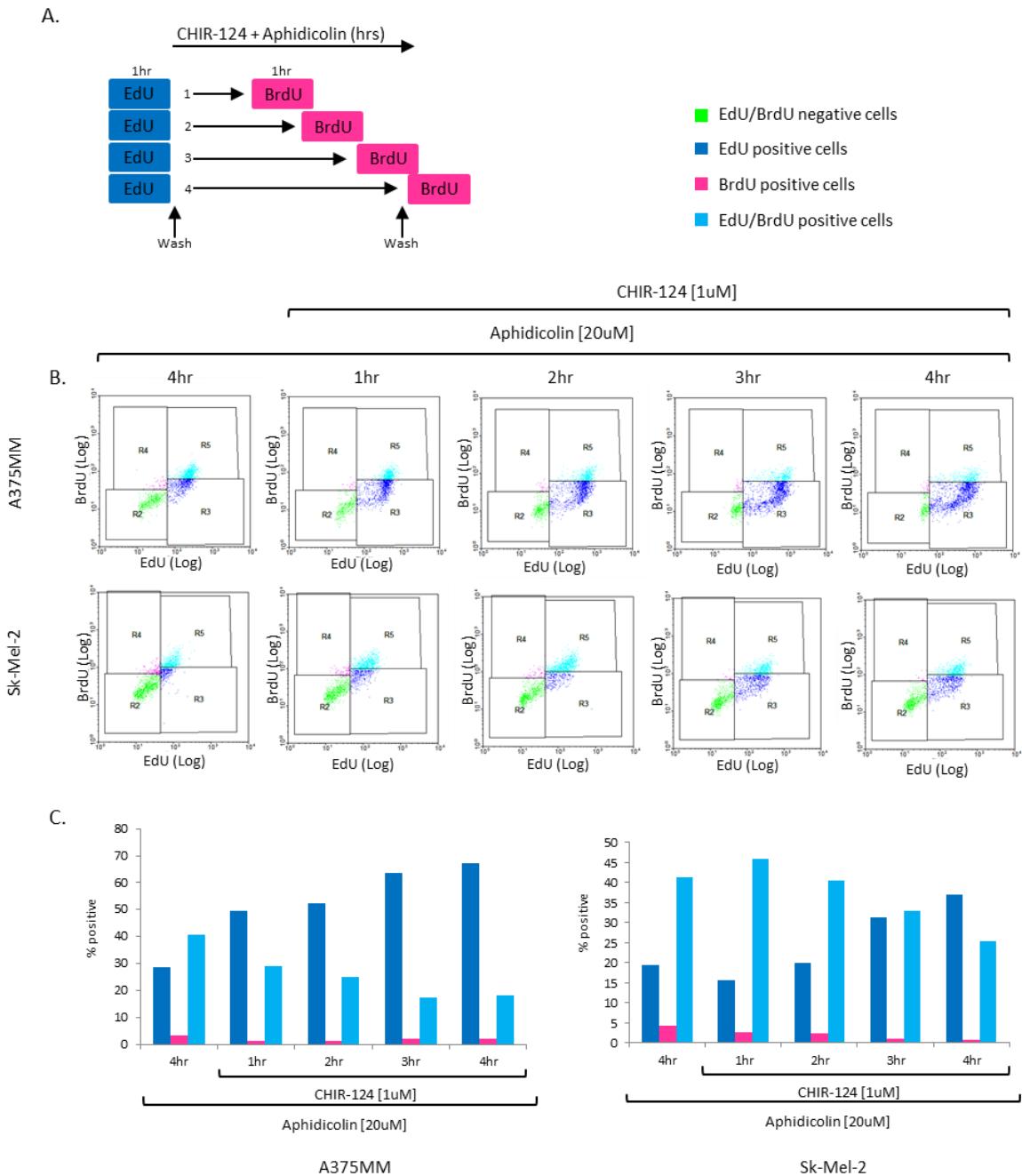
Figure 6.10: Loss of replication fork viability in CHIR-124 treated cells during replication arrest. (A) Experimental protocol (see text for details). Cells were pre-labelled with EdU, then pulse-labelled with BrdU following 1-4hrs treatment with Aphidicolin with or without CHIR-124. (B) Double pulse labelling. A375MM and Sk-Mel-2 treated cells were assessed for EdU and BrdU incorporation by flow cytometry after treatment with aphidicolin to arrest replication with or without CHIR-124. Dot plots are shown where green represents no incorporation; dark blue represents EdU positive cells, pink represent BrdU positive cells and light blue represents double EdU and BrdU positive cells. (C) Quantification of the number of EdU+, BrdU+ and EdU/BrdU+ cells in the presence of aphidicolin plus CHIR-124 over 1-4hrs.

This data shows that the effect of Chk1 inhibition on EdU+/BrdU+ labelling, which represents replication forks which were active prior to the addition of aphidicolin and which resumed replication after the period of arrest, is decreased compared to aphidicolin arrested cells. In contrast EdU+ labelling,

which represents replication forks that were previously active but became incapable of resuming replication, is increased. These observations suggest that active Chk1 is required to maintain the viability of stalled replication forks in these melanoma cell lines. Replication fork collapse may represent a mechanism by which DNA damage is generated as a consequence of Chk1 inhibition. This is consistent with recent studies which have revealed that the activities of Chk1 are required during normal S-phase to avoid deleterious DNA breakage (Beck et al, 2010; Lam et al, 2004; Syljuasen et al, 2005), and that inhibition of Chk1 or siRNA knockdown of Chk1 causes rapid destabilisation of the genome associated with massive amounts of DNA DSBs (Syljuasen et al, 2005). It has also recently been shown that loss of Chk1 leads to increased CDK activity resulting in loss of control of replication co-ordination (Beck et al, 2010).

.

6.7 Chk1 inhibition exhibits single agent toxicity against melanoma cell lines *in vitro* and xenografts *in vivo*

In recent years the treatment of advanced melanoma has begun to focus on targeted therapies, for instance Vemurafenib and Dabrafenib are two B-Raf (V600E) inhibitors currently being trialled in the treatment of melanoma (Hauschild et al, 2012; Ravnan & Matalka, 2012). However the standard single agent chemotherapeutic treatment of advanced melanoma is still focused on the use of dacarbazine (DTIC), a DNA alkylating agent. DTIC was the first FDA approved chemotherapeutic agent for the treatment of metastatic melanoma in 1975. DTIC has an overall response rate of 15-25% with median response durations of 5–6 months, but less than 5% of complete response (Comis et al, 1976; Hill et al, 1979). The related agent, temozolomide (TMZ), an orally available analog of DTIC, has also demonstrated efficacy in the treatment of advanced melanoma with overall response rate of 14% (Bleehen et al, 1995; Middleton et al, 2000; Newlands et al, 1992). However advanced melanoma still remains one of the most treatment-refractory cancers.

Owing to my previous observations in which Chk1 inhibition in human melanoma cell lines lead to DNA damage, replication fork collapse and apoptosis, I tested the *in vitro* efficacy of CHIR-124 as a single agent treatment for killing metastatic melanoma cell lines. In order to evaluate the cytotoxic effect, cells were seeded in a 96-well plate format. After 24hrs cells were treated with CHIR-

124, DTIC or TMZ for 72hrs; CHIR-124 treatment 0 -100μM, DTIC/TMZ treatment 0-1mM in a 12-step 1:3 dilution range in triplicate. After 72hrs incubation alamar blue was added to the cells for 1-4hrs. Alamar blue is a cell viability indicator which contains resazurin, a non-fluorescent compound. Within metabolically active cells resazurin is reduced to resorufin, a red-fluorescent compound which can be quantified by absorbance at 570nm and 600nm (Figure 6.11). The amount of fluorescence produced is proportional to the number of living cells in each well. Dose-response curves were generated to calculate the half maximal effective concentration (EC_{50}) of each agent which gives a measure of drug potency. Cells treated with vehicle alone were used as a positive control (red colour) whereas empty wells were used as a negative control (blue colour), as can be seen in the bottom two rows respectively of the example plate shown in figure 6.11.
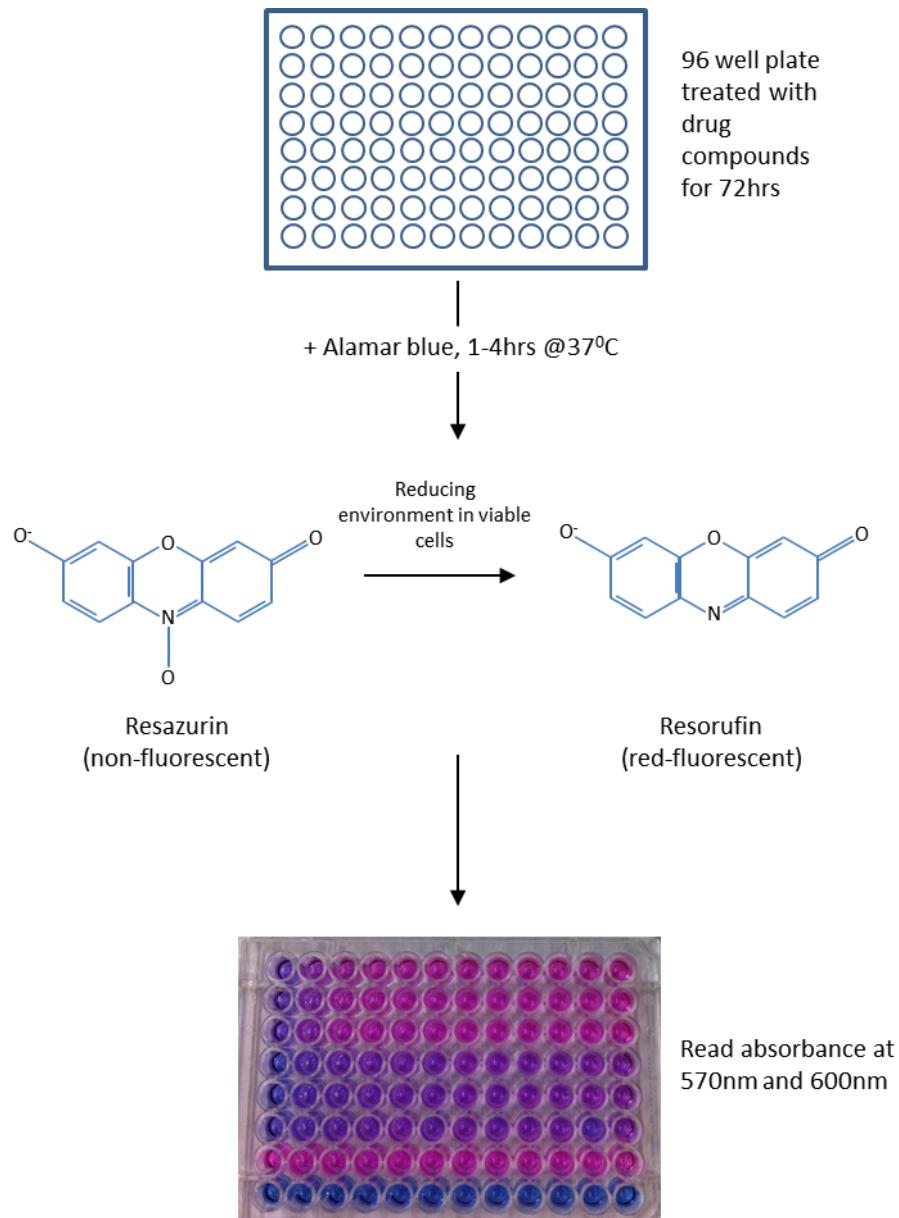
Figure 6.11: Analysis of cell viability by Alamar Blue. Experimental protocol. Cells were cultivated in 96 well plates (2000 cells/well) and treated with drug compounds for 72hrs. Addition of alamar blue (1:10 dilution) assessed the number of metabolically active cells by a reduction reaction which produces the red fluorescent compound resorufin. Pink= reducing environment, Blue= non-reducing environment, where amount of reduction is proportional to the number of viable cells in each well.

Dose-response curves for each individual cell line show that in all metastatic melanoma cell lines tested A375MM, Sk-Mel-2, SK-Mel-5, Sk-Mel-28, Sk-Mel-39, Sk-Mel-103 and Sk-Mel-147 (Figure 6.12A-G respectively) CHIR-124 is more toxic as a single agent than either DTIC or TMZ alone, as can be seen by the red curve in each graph which is shifted to the left in respect of both the blue (TMZ) and green (DTIC) curves. In addition the dose-response curves for DTIC and TMZ are similar to each other in each respective cell lines showing that the potency of DTIC and TMZ in each cell line is similar. However they differ from one cell line

to the other showing cell line specific variations in sensitivity. Although CHIR-124 is more potent as a single agent than either DTIC or TMZ when dose-response curves for CHIR-124 treatment were plotted on the same axis it was observed that there was a large range of sensitivity to CHIR-124. Two distinct groups of cell lines are apparent with CHIR-124 showing less potency in cell lines Sk-Mel-5, Sk-Mel-28 and Sk-Mel-39 (Figure 6.13 green, blue and purple lines respectively) than cell lines A375MM, Sk-Mel-2, Sk-Mel-103 and Sk-Mel-147 (Figure 6.13 red, orange, pink and grey lines respectively) which appeared more sensitive to the cytotoxic effects of CHIR-124. Interestingly the most sensitive cell lines are all N-Ras mutant (except A375MM) whereas the less sensitive cell lines are all B-Raf mutant. EC_{50} values were calculated using a non-linear regression dose response curve with variable slope analysis in graph-pad prism software. Melanoma cell lines have a large variation in their calculated EC_{50} values ranging from the low nano-molar range (71.6 ± 11.9 nM) in Sk-Mel-147 cells to micro-molar range (19.186 ±3.326 µM) in Sk-Mel-28 cells (Table 6.1).
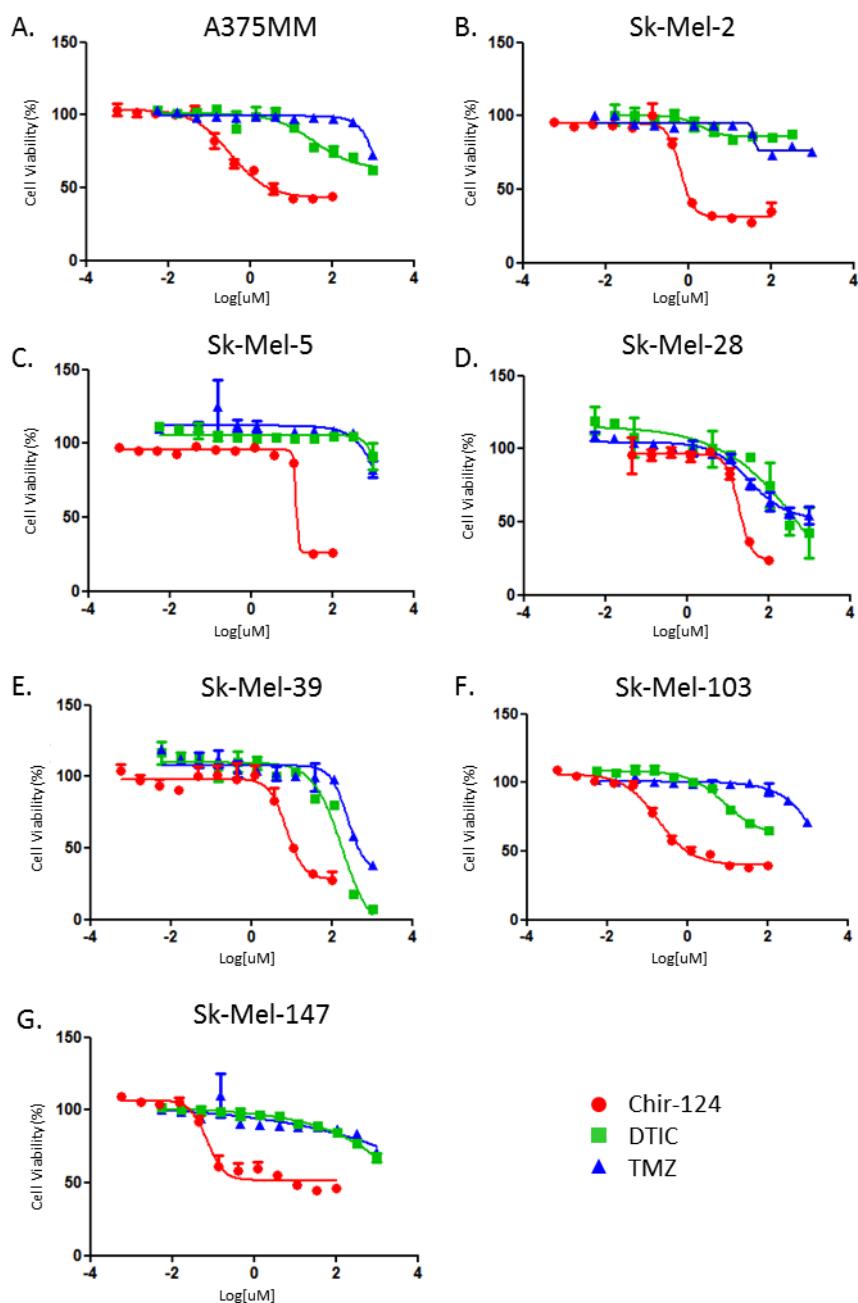
Figure 6.12: Drug-dose response curves for Dacarbazine, Temozolomide and CHIR-124 in metastatic melanoma cell lines. (A-G) Cell viability for cell lines A375MM, Sk-Mel-2, Sk-Mel-5, Sk-Mel-28, Sk-Mel-39, Sk-Mel-103 and Sk-Mel-147 respectively were assessed over a range of drug concentrations for DTIC (max 1mM), TMZ (max 1mM) and CHIR-124 (max 100μM). Dose-response curves were generated using absorbance measurements taken at 570nm and 600nm. Graphpad prism software was used to plot survival curves on a logarithmic scale.
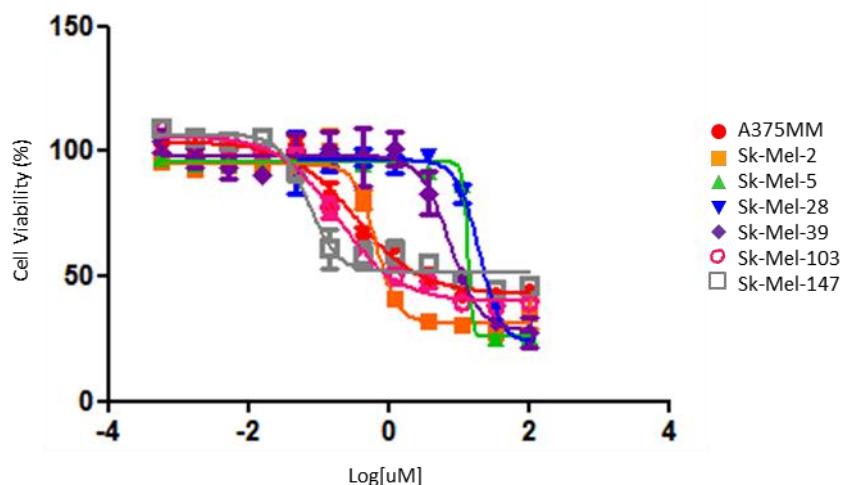
Figure 6.13: Drug-dose response curves for CHIR-124 treatment in metastatic melanoma cell lines. Cell viability for cell lines A375MM, Sk-Mel-2, Sk-Mel-5, Sk-Mel-28, Sk-Mel-39, Sk-Mel-103 and Sk-Mel-147 respectively were assessed over a range of concentrations for CHIR-124 (max 100µM). Dose-response curves were generated using absorbance measurements taken at 570nm and 600nm. Graphpad prism software was used to plot survival curves on a logarithmic scale and to calculate EC_{50} values.

	CHIR-124 EC_{50} (nM)
A375MM	341 ± 71.8
Sk-Mel-2	653 ± 71.5
Sk-Mel-5	12971 ± ?
Sk-Mel-28	19186 ± 3326
Sk-Mel-39	7406 ± 1495
Sk-Mel-103	189 ± 27.7
Sk-Mel-147	71.6 ± 11.9

Table 6.1: Table 6.1: EC50 values for CHIR-124 in metastatic melanoma cell line

The previous data demonstrates that Chk1 inhibition by CHIR-124 has anti-proliferative activity *in vitro* in a number of metastatic melanoma cell lines, associated with an apoptotic cell death. To evaluate if CHIR-124 has potential as a single agent treatment in advanced melanoma, with toxicity greater than that of standard chemotherapeutic approaches I utilised a tumour xenograft model of

melanoma. In order to assess *in vivo* potential melanoma cells (A375MM) were grown in culture until they were in a logarithmic phase of growth (70-80% confluent). Cells were then harvested and injected subcutaneously to the lower right flank of 6 week old female CD1 nudes at a concentration of 1×10^6 cells per mouse. Five days after injection 32 mice were randomised into the following treatment groups: vehicle alone (14 mice), twice daily dosing of CHIR-124 at 20mg/kg for 6 consecutive days (9 mice) or twice daily dosing of DTIC at 20mg/kg for 3 consecutive days (9 mice). The vehicle group was further divided into oral gavage (6 mice) and IP (8 mice) which were the control groups for CHIR-124 and DTIC treatment respectively.

The rate of increase in tumour growth was analysed over time for each cohort with correction for the initial tumour size. Analysis of tumour growth in the treated cohorts (DTIC and CHIR-124) showed that both treatments slowed the rate of growth of the subcutaneous tumours as compared to their respective vehicle treated controls (Figure 6.14A and B). However this slowing of the growth rate was not statistically significant in either case; p=0.510128 and p=0.13249 for CHIR-124 vs. vehicle and DTIC vs. vehicle respectively. The trend in the reduction of tumour growth is quite convincing therefore the lack of statistical significance as calculated by the Mann-Whitney test is possibly due to the small sample size. Only 32 mice in total were used during the experiment with a significant number failing to establish a tumour at all (9/32). Furthermore analysis of tumour growth rate of the DTIC treated cohort compared to the CHIR-124 treated cohort (Figure 6.15) showed that CHIR-124 slowed the rate of tumour growth compared to DTIC treatment which is a conventional chemotherapeutic treatment for melanoma, however again this was also not statistically significant, p=0.133632.
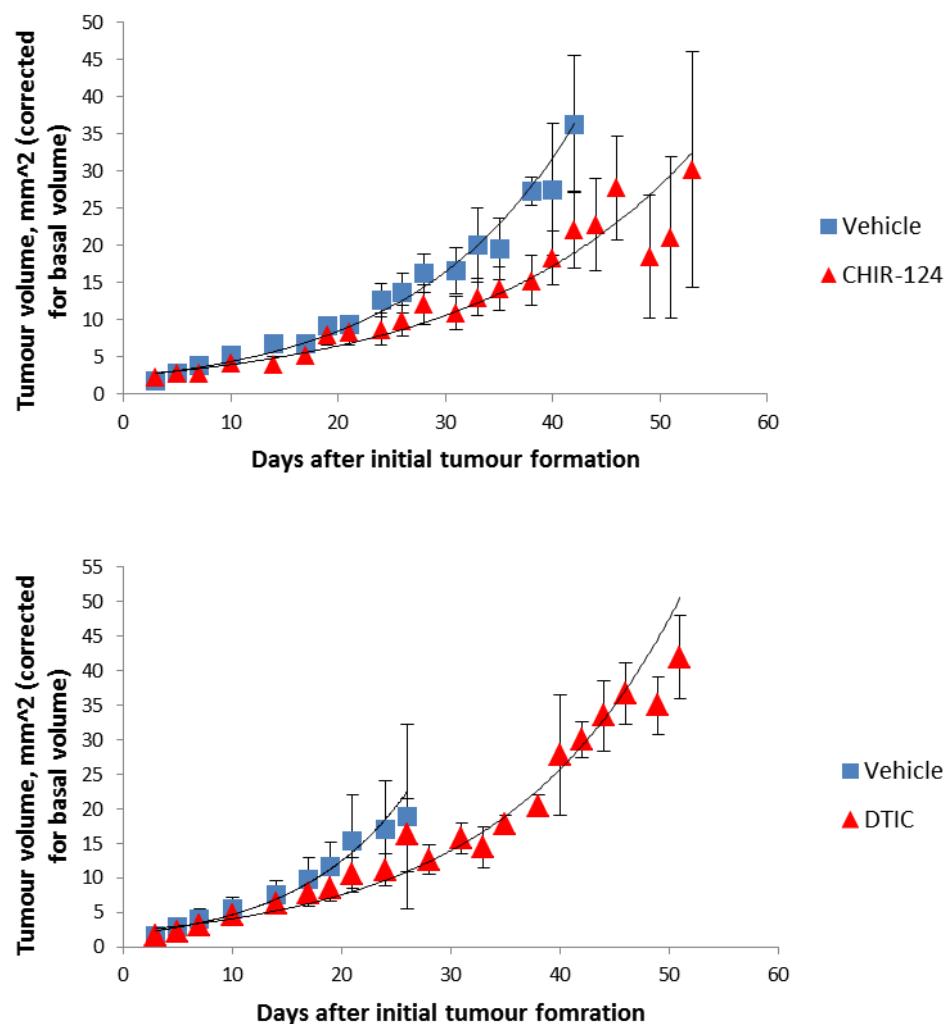
Figure 6.14: Chk1 inhibition and Dacarbazine treatment on tumour formation in A375MM cells *in vivo*. (A) Analysis of the rate of tumour growth, as assessed by the increase in tumour volume over time as compared to the initial tumour volume in vehicle and CHIR-124 treated cohorts; n=4 vehicle cohort, n=7 CHIR-124 cohort. (B) Analysis of the rate of tumour growth, as assessed by the increase in tumour volume over time as compared to the initial tumour volume in vehicle and DTIC treated cohorts; n=5 vehicle cohort, n=7 DTIC cohort.
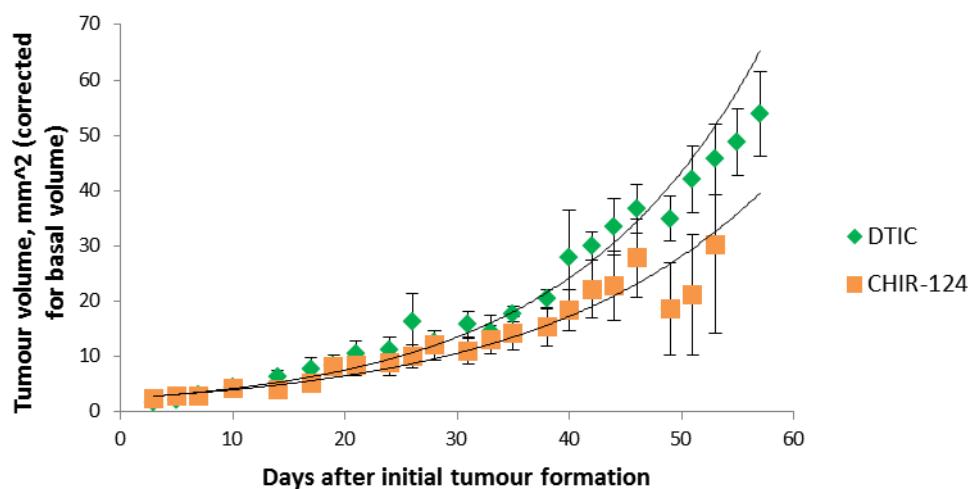
Figure 6.15: Chk1 inhibition and Dacarbazine treatment on tumour formation in A375MM cells *in vivo*. Analysis of the rate of tumour growth, as assessed by the increase in tumour volume over time as compared to the initial tumour volume in CHIR-124 and DTIC treated cohorts; n=7 for both cohorts.

This data shows that Chk1 inhibition by the specific allosteric inhibitor CHIR-124 may exhibit potential as a single agent treatment in advanced melanoma, in particular in N-Ras mutant melanoma where it appears to be more toxic. This is of interest as most new current targeted therapies for melanoma are targeted to B-Raf mutant melanoma, for instance Vemurafenib and Dabrafenib with only one N-Ras inhibitor (R115777) in Phase II trials (Eggermont & Robert, 2011). However CHIR-124 still showed efficacy in B-Raf mutant cell lines. This is consistent with recent papers which have shown other Chk1 inhibitors to have efficacy as single agents in cancer cells (Brooks et al, 2012; Davies et al, 2011a; Ferrao et al, 2012). In Myc-driven lymphomas Chk1 inhibition showed single agent efficacy associated with high levels of endogenous replicative stress (Ferrao et al, 2012) with collapse of DNA replication followed by apoptosis (Davies et al, 2011a). In melanoma two novel inhibitors of Chk1 have been shown to display single agent potency, whereby they saw premature entry of late S-phase cells into an aberrant mitosis (Brooks et al, 2012).

6.8 Discussion

The main aim of this chapter was to discover if Chk1 inhibition by the specific allosteric inhibitor CHIR-124 exhibits any potential as a therapeutic agent for the treatment of advanced metastatic melanoma. This could be of particular

importance as advanced metastatic melanoma has a very low survival rate, with a median survival of stage IV melanoma being 6-9 months with only a 15% 5-year survival rate (Siegel et al, 2012). Overall improvements in survival in the last 20 years have been minimal (Pollack et al, 2011) with advanced melanoma remaining one of the most treatment refractory malignancies. Despite recent advancements with selective B-Raf inhibitors which showed an overall survival increase after 6 months treatment compared to DTIC, 84% vs. 64%, (Chapman et al, 2011) advanced melanoma is still considered incurable.

Due to the well-established role of Chk1 in the DDR pathway in both the S/M and G2/M checkpoints, as well as the vital role shown during maintenance of S-phase in unperturbed cell cycling, many Chk1 inhibitors have been developed for cancer therapy. In preclinical trials inhibitors of Chk1 showed efficacy in combination trials, whereby they enhanced the anti-tumour activity of a number of anti-cancer agents including gemcitabine, irinotecan, topotecan, cisplatin, IR and docetaxel with several progressing to clinical phase I and II trials. Although initial trials focused on Chk1 inhibitors in combination therapy more recently Chk1 inhibitors have been shown to have single agent efficacy in some cancers, including PF-477736 in lymphoma (Ferrao et al, 2012), Chk1-A in leukaemia (Davies et al, 2011a) and most interestingly AR323 and AR678 in melanoma (Brooks et al, 2012).

Evaluation of the functional ability of CHIR-124 showed that CHIR-124 was indeed able to over-ride the G2-M checkpoint (Figure 6.2A and B) which would normally be induced by Chk1 after IR treatment, and that downstream targets of Chk1 associated with induction of the checkpoint such as CDC25C and CDK1 are successfully supressed in the presence of CHIR-124 both alone and after IR treatment (Figure 6.2C). Thus as CHIR-124 was successfully shown to inhibit phenotypes associated with active Chk1, evaluation of the anti-survival effects of CHIR-124 on a panel of metastatic melanoma cell lines was undertaken. Analysis showed that CHIR-124 was able to induce cell death in all melanoma cell lines tested, with between 25-60% of cells double Annexin: PI positive within 48hrs of treatment (Figure 6.3H). In most, although not all, cases cell death induced was characterised by an apoptotic phenotype, including cleavage of PARP (Figure 6.4) and Annexin V staining (Figure 6.3A-G). This data suggests that cell death induced by Chk1 inhibition is apoptotic, which is concurrent with other studies which looked at Chk1 inhibition as a single agent (Brooks et al,

2012; Davies et al, 2011a; Ferrao et al, 2012). These studies also saw that Chk1 inhibition caused cell death by caspase-dependant apoptosis in their respective systems. Genetic analysis shows that cell line Sk-Mel-28 carries a mutant p53 (L145R) and cell lines Sk-Mel-103 and Sk-Mel-147 are null/mutant for the CDK2NA locus respectively (Table 5.1). The CDK2NA locus is a common site for mutations in melanoma (Ibrahim & Haluska, 2009) and encodes both the p16 and ARF proteins. ARF is a negative inhibitor of the p53 inhibitor MDM2 (Sherr, 2006) therefore cell lines Sk-Mel-103 and Sk-Mel-147 have a deregulated p53 pathway. This suggests that the apoptotic cell death induced by Chk1 inhibition in these cell lines is independent of the p53 pathway. Although p53 is well known to be a key initiator of apoptosis recent studies have shown that in p53 deficient cell lines, HCT 116 (p53-/-) and Hep3B, apoptotic cell death can be induced in a TRAIL/DR5 –dependant manner (Cheng et al, 2012; Yeh et al, 2012). In HCT 116 (p53-/-) cells this was shown to be dependent on the up regulation of TRIAL/DR5 by JNK signalling (Cheng et al, 2012). However Sk-Mel-39 which also carries a mutant p53 fails to initiate cell death by apoptosis upon Chk1 inhibition with no cleavage of PARP or Annexin V staining after treatment (Figure 6.4E and Figure 6.3E respectively). This may be a result of the p53 status of this cell line however it could also represent a cell line specific phenotype as Sk-Mel-39 cells also fail to induce apoptosis after staurosporine treatment despite staurosporine being shown to induce both caspase -dependant and –independent apoptosis in melanoma cell lines (Zhang et al, 2004).

Inhibition of Chk1 by CHIR-124 during an unperturbed cell cycle caused the generation of DNA damage specifically in S-phase cells (Figure 6.6 and 6.7), with a concurrent blockage of cells in early S-phase (Figure 6.8). This data suggests that Chk1 inhibition does not affect entry to S-phase, but once there normal DNA replication is inhibited and DNA damage is generated. Studies have shown that Chk1 is important during unperturbed S-phase where active Chk1 is required to avoid deleterious DNA breakage in the absence of exogenous DNA damaging agents (Lam et al, 2004; Maya-Mendoza et al, 2007; Petermann & Caldecott, 2006). A possible mechanism for this indicates that DNA damage occurs as a consequence of the deregulation of the ATR-CHK1-CDC25-CDK pathway with uncontrolled CDK activity being implicated (Beck et al, 2010; Sorenson et al, 2004; Toledo et al, 2011). This has been demonstrated by studies whereby the

deleterious effects of Chk1 inhibition or siRNA knockdown, such as accumulation of ssDNA and DNA DSBs, can be blocked by depleting CDC25C (Beck et al, 2010). Other studies have shown that siRNA knockdown of Wee1 also rapidly induces DNA damage in S-phase cells, similar to Chk1 inhibition (Beck et al, 2010). As the target of Chk1, Wee1 and CDC25C is the CDK1, it has been postulated that uncontrolled CDK1 activity is responsible for the generation of DNA damage. Furthermore depletion of ATR leads to DNA damage and deregulation of CDC25 in the absence of exogenous DNA damaging agents (Sorenson et al, 2004), with the damage occurring in this instance blocked by depletion of CDC25 (Toledo et al, 2011).

In a perturbed cell cycle whereby DNA replication is block by aphidicolin the inhibition of Chk1 leads to destabilisation and collapse of stalled replication forks (Figure 6.9) which were generated by the inhibition of DNA polymerase by aphidicolin. Studies have shown that Chk1 is also important during perturbed S-phase cycling where it acts to stabilise replication forks and supress the firing of late origins (Conti et al, 2007; Seiler et al, 2007; Zachos et al 2003; Zachos et al 2005). Although CHIR-124 did cause destabilisation of stalled replication forks there was no evidence in this instance for the generation of new replication origins of firing during Chk1 inhibition as seen in previous studies. Calculation of EC_{50} values generated from dose-response curves showed that CHIR-124 had significant toxicity in all metastatic melanoma cell lines, with the calculated EC_{50} being less than that of DTIC or TMZ for all cell lines (Figure 6.12). There was a broad variation in the relative toxicity of CHIR-124 (Figure 6.13) with cell lines A375MM, Sk-Mel-2, Sk-Mel-103 and Sk-Mel-147 showing the greatest sensitivity after 72hrs treatment. *In vivo* analysis of the tumour growth rate of subcutaneously injected A375MM melanoma cells in CD1 nudes showed that CHIR-124 treatment caused a clear reduction in the tumour growth rate as compared to vehicle (Figure 6.14). This reduction was also greater than that seen in DTIC treated animals (Figure 6.15).

This data suggests that CHIR-124 could have potential as a single agent in the treatment of advanced melanoma, especially in N-Ras mutant cell lines which were most sensitive. This could be of clinical importance as most new targeted therapies for melanoma are for the treatment of B-Raf mutated melanomas with

only one inhibitor of N-Ras currently in clinical trials (R115777) (Eggermont &
Robert, 2011). CHIR-124 could also have potential in combination therapy with
both known anti-cancer therapies and novel inhibitors of cell cycle proteins.
Although not tested here it has been shown to increase the efficacy of known
cytotoxic agents such as topoisomerase inhibitors in MDA-MB-435 breast cancer
cells (Tse et al, 2007), IR in HCT 116 cells (Tao et al, 2009) and gemcitabine in a
multicellular tumour spheroid model of pancreatic cancer (Dufau et al, 2012). In
more recent studies CHIR-124 has been shown to increase the sensitivity to cell
death induced by histone deacetylase inhibitors (Lee J et al, 2011) and Wee1
(Carassa et al, 2012; Davies et al, 2011b). Furthermore recent studies have
shown that chemo-resistance in melanoma cells could be, at least in part,
through a MAPK-dependant alteration of Chk1 signalling. It has been shown that
the p90 ribosomal S6 kinase, a direct downstream target of MAPK signalling from
both N-Ras and B-Raf mutant melanomas, phosphorylates Chk1 on an inhibitory
site, S280, both *in vitro* and *in vivo* (Ray-David et al, 2012). In addition inhibition
of p90 ribosomal S6 kinase increased Chk1 activity in response to DNA damaging
agents, and concurrently increased the sensitivity of melanoma cells to these
agents (Ray-David et al, 2012).

Chapter 7: Summary & Future Directions

7 Summary & Future Directions

7.1 Summary

One of the key aims of this thesis was to investigate the requirement of Chk1 in melanocyte cell survival and melanoma initiation, maintenance, and progression *in vivo*, which is described in Chapters 3 and 4 respectively.

In order to address the first question I utilised a conditional knockout mouse model of Chk1 in combination with a melanocyte-specific Cre-recombinase. This allowed for the specific deletion of Chk1 in the melanocyte lineage during embryogenesis. Melanocytes were visualised using a reporter gene, LacZ, which was driven from a melanocyte-specific promoter.

Using this model I showed that Chk1 expression is essential for the survival of melanocyte precursor cells, melanoblasts, during embryonic development. Homozygous deletion of Chk1 caused a complete loss of melanoblasts during development resulting in a non-pigmented adult mouse. IHC analysis showed that there were high levels of DNA damage, as marked by γH2AX, in these Chk1 deleted melanoblasts. In addition I also showed that while homozygous deletion of Chk1 is severely detrimental to the survival of melanoblasts, hemizygous deletion has no effect on the phenotype of adult mice, with only a small but nevertheless significant decrease in melanoblast numbers during development. These data show that while complete Chk1 loss is not consistent with cell survival, loss of one copy of Chk1 is well tolerated demonstrating that one copy of Chk1 is mostly capable of performing the essential functions of Chk1 in melanocytes.

While I have been able to show that Chk1 is essential for the survival of melanocyte precursor cells during development, which are the cells of origin for melanoma, in order to further determine the role of Chk1 in melanocytes during melanoma development I utilised another mouse model. In order to address the second question I used the aforementioned conditional knockout mouse model of Chk1 in combination with an inducible melanocyte-specific Cre-recombinase. This allows for spatially and temporally controlled deletion of Chk1 from melanocytes. These mice were crossed onto a mouse model of melanoma whereby an oncogenic N-Ras (Q61K) is expressed specifically in melanocytes on a

p16^{Ink4a}-deficient background. From these mice cell lines were generated which were subsequently used for allograft experiments in CD1 nude mice.

Using this model I showed that complete loss of Chk1 during tumour development caused a profound reduction in the proliferation potential of melanoma tumour formation with a concurrent significant increase in survival time in these mice. In addition I also showed that hemizygous deletion of Chk1 during tumour development exerts a more modest but nevertheless measurable effect on melanoma tumour formation, however with no demonstrable effect on survival time. Furthermore in metastatic models (tail-vein injected CD1 nudes) hemizygous deletion of Chk1 had a significant but transient effect on the metastatic growth rate, as demonstrated by the increase in survival time, but with the same metastatic burden at time of death. This data shows that reduction in Chk1 levels modestly effects both the primary tumour formation of melanoma *in vivo*, and the proliferation/survival of metastatic growths. In addition while hemizygous deletion has a slight effect, the complete loss of Chk1 is severely detrimental for primary tumour formation of melanoma *in vivo*. Collectively these data show that Chk1 is essential for the maintenance and progression of melanoma *in vivo*.

Another aim of this thesis was to examine the function of ATR/Chk1 signalling in melanoma cells, which is described in Chapter 5.

The ATR/Chk1 pathway is activated by RPA-coated tracts of ssDNA which are generated in response to replicative stress, DNA damaging agents that directly cause single-stranded breaks and after resection of DNA DSBs, and is therefore important in the response to a wide variety of cellular stresses. Two of the cell cycle checkpoints that ATR/Chk1 are required for are the G2/M and S/M checkpoints; however they also play key roles in the intra-S checkpoint and the mitotic spindle checkpoint.

In order to determine the functions of ATR/Chk1 signalling in melanoma cells I first assessed G2/M and S/M checkpoint proficiency in response to IR and replicative stress respectively. Interestingly, I demonstrate that in response to replicative stress, induced by inhibition of DNA polymerase upon aphidicolin

treatment, all melanoma cell lines tested were able to activate Chk1 and induce a cell cycle arrest such that no cells entered mitosis in the presence of DNA which was not fully replicated. However in response to DNA DSBs induced by IR, most but not all melanoma cell lines were able to activate Chk1 and induce a G2-phase blockage. In the cell lines which displayed a weaker G2/M checkpoint response the mechanism by which Chk1 function is altered in unclear. Several cell lines showed that activation of Chk1 was impaired, suggesting that the upstream signal is short-lived or that Chk1 itself is 'turned off' rapidly. However several other melanoma cell lines with as weak checkpoint responses showed strong activation of Chk1 as expected in response to IR, suggesting that the upstream signalling is intact but that the signal is somehow not transmitted appropriately downstream of Chk1.

This data suggests that while the G2/M checkpoint is apparently dispensable for cell survival, the S/M checkpoint may not be. Other studies have also shown that DNA damage-induced checkpoint function of Chk1 can be disrupted in cells without affecting cell survival (Wilsker et al, 2008). In addition, although not fully understood mechanistically, this data also shows that despite functioning through presumably the same downstream cyclin/CDK targets the G2/M and S/M checkpoints can be distinguished from each other, with loss of G2/M checkpoint but maintenance of S/M checkpoint function in some melanoma cell lines.

In addition I also analysed the importance of MRN complex signalling in Chk1 activation following IR-induced DNA DSBs. The MRN complex is a key sensor of DNA DSBs and is important in activating the ATM/Chk2 pathway and for DNA strand resection, facilitating DNA repair and ATR/Chk1 activation. In melanoma cell lines that lacked expression of Mre11, with concurrent reductions in both Nbs1 and Rad50, I showed that the MRN complex is essential for activation of Chk2 following IR treatment but not for activation of Chk1. Although after transient transfection of Mre11 into these cell lines, I was able to show that the addition of Mre11, and presumed activation of the MRN complex, was able to enhance the activation of Chk1 following IR treatment, especially at later time points post-treatment. This is consistent with other recent studies that have shown that although the initial activation of Chk1 is not dependant on MRN complex signalling it does play a role in the maintenance of Chk1 activation

after IR-induced DNA damage (Buis et al, 2008; Kousholt et al, 2012, Sartori et al, 2007).

The final aim of this thesis was to determine if inhibition of Chk1 is a viable therapeutic strategy in the treatment of advanced metastatic melanoma, a cancer that is largely refractory to current standard treatments, which is described in Chapter 6.

Due to the well-established role of Chk1 in the DDR pathway and during unperturbed cell cycling many Chk1 inhibitors have been developed for cancer therapy. In order to assess the potential of Chk1 inhibition for melanoma therapy I used a specific allosteric inhibitor of Chk1, CHIR-124, which has been shown to have high selectivity for Chk1 over other related kinases.

Firstly I showed that inhibition of Chk1 with CHIR-124 was effective at causing apoptotic cell death in a dose- and time-dependent manner in most metastatic melanoma cell lines, as demonstrated by cleavage of PARP and subsequent Annexin V staining. However there was one single cell line that did not induce apoptotic cell death in the presence of CHIR-124, with no cleavage of PARP or Annexin V staining, but rather becoming only PI positive after treatment suggesting another mechanism of cell death. This could be due to the mutant p53 status of this cell line; however it could also represent a cell line-specific phenotype as another p53 mutant cell line was also able to initiate apoptotic cell death.

In order to elucidate mechanistically why Chk1 inhibition causes cell death I analysed the generation of DNA damage upon CHIR-124 treatment in otherwise unperturbed cycling cells. I was able to show that DNA damage, as marked by γH2AX, was generated specifically in S-phase cells, labelled by EdU incorporation, upon Chk1 inhibition which is in contrast to other DNA damaging agents that generate DNA damage non-selectively of cell cycle. I also showed, by pulse-labelling of S-phase cells with BrdU, that in the presence of CHIR-124 melanoma cells could enter S-phase normally but once there normal DNA replication was inhibited resulting in DNA damage. In addition during a perturbed cell cycle, whereby S-phase is blocked by aphidicolin which causes

active replication forks to stall, Chk1 inhibition resulted in collapse of these stalled replication forks. This is consistent with studies which have shown that Chk1 is important during unperturbed S-phase where active Chk1 is required to avoid deleterious DNA breakage even in the absence of exogenous DNA damaging agents (Lam et al, 2004, Petermann & Caldecott, 2006; Maya-Mendoza et al, 2007), and also during perturbed S-phase cycling where it acts to stabilise replication forks and supress the firing of late origins (Conti et al, 2007; Seiler et al, 2007; Zachos et al, 2003; Zachos et al, 2005).

I also showed via analysis of cell viability in response to a range of drug doses that CHIR-124 has significant toxicity *in vitro* in all metastatic melanoma cell lines, with the calculated EC_{50} being less than that of dacarbazine and temozolomide in each cell line; two chemotherapeutic alkylating agents used in the treatment of advanced melanoma. However there was a broad range of relative toxicities to Chk1 inhibition between cell lines. Further *in vivo* analysis also showed that CHIR-124 treatment caused a measurable reduction in the tumour growth rate of subcutaneously injected metastatic melanoma cells in CD1 nude mice. This data suggests that Ch1 inhibition could have potential as a single agent treatment for advanced melanoma, especially in N-Ras mutant cell lines which were most sensitive to CHIR-124 treatment. Recent studies have also demonstrated that Chk1 inhibition may have potential as a single agent treatment in some cancer types; including lymphoma, leukaemia and melanoma (Brooks et al, 2012; Davies et al, 2011a; Ferrao et al, 2012), with Chk1 activity recently being implicated in the chemo-resistant phenotype of melanoma cells to DNA damaging agents (Ray-David et al, 2012).

7.2 Future Directions

The work presented here demonstrates that Chk1 is essential for the survival of normal melanocytes during development *in vivo*. In addition, complete loss of Chk1 is severely detrimental for melanoma tumour growth in allograft nude mouse models, whilst Chk1 hemizygousity is also detrimental although to a lesser degree. However it is still unclear what role Chk1 may play in melanoma formation in a more physiologically relevant *in vivo* model. Furthermore owing to the relatively rapid growth of implanted tumour cells in nude mouse studies it

is difficult to determine the role that Chk1 may play at different stages of tumour development. For instance would Chk1 deletion have a more or less profound effect on tumour initiation if deleted before the onset of a tumour, compared to its effect on tumour maintenance and progression if deleted at later stages of tumour development? If Chk1 was deleted once a tumour has formed, would this prevent further tumour progression, slow but not stop tumour progression, or cause regression of the primary tumour? In addition there is data to suggest that Chk1 may act as a dose-dependent tumour suppressor with Chk1 haplo- insufficiency promoting tumour development in some instances, whilst inhibiting tumour development in others. As such, how does hemizygousity for Chk1 at different stages of growth specifically affect melanoma tumour development?

In addition other work presented in this thesis demonstrates that Chk1 inhibition alone can have cytotoxic effects in melanoma tumour cells both *in vitro* and *in vivo*, with cell death being associated with high levels of DNA damage induced in S-phase cells accompanied by collapse of replication forks. However I observed a broad range of sensitivity to the cytotoxic effects of Chk1 inhibition, with EC_{50} values ranging from the nano-molar to micro-molar range. Although this data suggest that targeting Chk1 may have therapeutic potential it is still unclear how Chk1 inhibition mechanistically affects both tumour and normal cells, and how this initiates cell death. In addition it is also unclear what mechanisms may underlie any apparent selectivity and sensitivity to Chk1 inhibition, and how these could be manipulated for therapy. Collectively this could be of importance for the clinical application of Chk1 inhibitors; both in terms of understanding any potential side effects and to which tumour types Chk1 therapy should be targeted.

As with data presented here whereby Chk1 loss severely inhibited melanoma tumour growth other studies have also shown that Chk1 deficiency inhibits tumour formation in other systems. In both mammary tumour formation and skin carcinogenesis studies (Fishler et al, 2010; Tho et al, 2012) Chk1 deficiency inhibited tumour formation, however these studies primarily examined tumour initiation. In this thesis Chk1 loss was induced one week after tumour cell implantation, in the mammary study Chk1 was constitutively deleted using a

mammary-specific Cre-recombinase (Fishler et al, 2010), and in the skin carcinogenesis study Chk1 was deleted prior to initiation with chemical carcinogens (Tho et al, 2012). In fact, if treatment with chemical carcinogens was delayed for some time after Chk1 deletion, which allowed for repopulation of the skin with Chk1 proficient cells, normal sensitivity was restored, highlighting the importance of Chk1 expression for tumour initiation (Tho et al, 2012).

While complete Chk1 loss therefore inhibits tumour growth, hemizygous deletion has more varied effects. In data presented here Chk1 hemizygousity had a detrimental effect on melanoma tumour formation although to a lesser degree than complete loss. However in contrast to this Chk1 hemizygousity in mammary tissue enhanced tumour formation on both a p53 null background (Fishler et al, 2010) and a WNT-1 transgenic model (Liu et al, 2000). Whilst in skin carcinogenesis Chk1 hemizygousity had no effect on benign papilloma formation but did increase the propensity for conversion to carcinoma (Tho et al, 2012). It is interesting to note that while Chk1 hemizygousity in mice can affect tumour formation in combination with other oncogenic changes or chemical carcinogens, in the absence of such initiating stimuli it does not increase spontaneous development of cancer, but rather has modest effects on normal tissue homeostasis. For instance in the mammary gland Chk1 hemizygousity causes abnormal development of the tissue associated with cell cycle defects (Fishler et al, 2010; Liu et al, 2000), while in the haematopoietic system it causes cellular defects resulting in anaemia (Boles et al, 2010). This is consistent with data presented here whereby hemizygous loss of Chk1 from melanocytes during embryogenesis caused a slight but significant decrease in cell number but with no observable alteration to the coat phenotype of adult mice. This apparent difference in sensitivity to Chk1 loss between normal unperturbed cells and tumour cells could be explained by the increase in genomic instability seen in tumour cells during malignant progression. As a consequence of this tumour cells may be more sensitive to alterations in Chk1 levels, thereby affecting cell maintenance, and promoting malignant transformation. In addition this apparent selectivity could also be due to the high replicative rate of tumour cells versus normal cells, as Chk1 has seen shown to be important during S-phase of cycling cells. This could account for the more dramatic effect seen in the

haematopoietic system, as this is a normal cell type which is rapidly proliferating in humans.

In data presented here Chk1 appears to be rate-limiting to melanoma tumour growth. If this was true in other systems it could be expected that Chk1 expression and activation may alter during malignant progression. Studies have shown that, at least in some cell types, Chk1 expression does alter during cancer development in humans. In colorectal cancer Chk1 protein expression is used as a marker of cancer, with 100% of tumours at various stages staining positive for Chk1 (Madoz-Gurpide et al, 2007). In colorectal cancer it has been shown that there is a strong accumulation of Chk1, with an intense nuclear and cytoplasmic staining compared to normal tissue, with total Chk1 expression being up-regulated in late stages (Madoz-Gurpide et al, 2007). In myc-amplified neuroblastoma cells and high-risk primary tumour samples both Chk1 mRNA levels and phosphorylated protein (S345) levels were constitutively increased compared to normal cell lines and low-risk primary tumours (Cole et al, 2011). This suggests that Chk1 is probably important during maintenance and progression of late stage tumours as well as for initiation, with Chk1 potentially being more important at later stages, as demonstrated by its increased expression and activity. Late stage tumours have high levels of genetic instability; Chk1 plays an important role in maintaining genomic stability. Therefore Chk1 could potentially be important to maintain the levels of genetic instability at levels which are compatible with tumour cell survival. However this increase in Chk1 expression and activity could also be a consequence of the increased DNA damage associated with advanced tumours. Therefore are changes in Chk1 levels causative or consequential to tumour development? It is interesting to note that Chk1 protein levels in the melanoma cells examined in this thesis are much lower than in HCT-116 cells, a colon-carcinoma cell line (Figure 5.9).

Chk1 inhibition has been developed as a potential therapeutic target for cancer both in combination with standard chemotherapeutic agents and recently with more targeted selective partners such as Wee1 inhibitors (Carrassa et al, 2012; Davies et al, 2011b). In addition use as a single agent in some cancer types has been studied (Davies et al, 2011a; Ferrao et al, 2012). Chk1 inhibition as a

clinical modality initially came about as a targeted synthetic lethal approach in combination with standard chemotherapeutics. The rationale behind this approach was that most standard chemotherapeutics induce large amounts of DNA damage, which will subsequently activate Chk1. In this instance Chk1 activation is thought to be protective triggering cell cycle arrest while the DNA damage is repaired. This is similar to the initial concept for PARP inhibition which was thought to protect cells following DNA damaging agents by activating DNA repair pathways, although the mechanism for PARP selectivity has recently shown to be more complex with PARP inhibition playing a role in increasing spontaneous DNA damage as well as blocking DNA repair (Murai et al, 2012). The philosophy behind those approaches is in contrast to other recent drug development strategies which have focused on targeting specific molecular alterations within cancer cells that are essential for their survival, such as Gleevec which targets the oncogenic bcr-abl kinase in CML.

In data presented here it was demonstrated that Chk1 inhibition alone can have cytotoxic effects in melanoma cell lines both *in vitro* and *in vivo*, however with a wide range in sensitivity. One potential mechanism for the variations in sensitivity seen to Chk1 inhibition could be inherent differences in proficiency of DDR pathway signalling within melanoma cells. Chk1 is an important effector kinase in cell cycle checkpoints of the DDR pathway, and as such Chk1 inhibition has been shown to be more potent in tumours where other aspects of this pathway are deficient. For example, tumour cells deficient in Fanconi anaemia (FA) genes, which are responsible for the repair of cross-linked DNA lesions, are hyper-sensitive to Chk1 inhibition and siRNA knockdown in comparison to FA-proficient cells (Chen et al, 2009). Silencing of FA genes resulted in hyper-activation of Chk1, which when inhibited was associated with increased DNA and chromosomal breaks (Chen et al, 2009). The MRN complex is a key sensor of DNA DSBs, and is important in initiating cell cycle checkpoints and processing of the lesions to allow DNA repair. Recently it has been shown that the Mre11 protein, a component of the MRN complex, is critical for sensitivity to Chk1 inhibition with loss of Mre11 leading to resistance associated with decreased levels of ssDNA and DNA DSBs following Chk1 inhibition (Thompson et al, 2012). Although not completely consistent I did observe that one of the melanoma cell lines which was deficient for both Mre11 and Nbs1 expression, Sk-Mel-39, was also

more resistant to Chk1 inhibition as compared to other cell lines (Figure 6.13). However cell lines Sk-Mel-103 and Sk-Mel-147, which lack Mre11 expression or have low levels of Mre11 expression respectively, did not show this resistance. Another important component of the DDR pathway is p53. p53 is a potent inducer of cell death under conditions of DNA damage and a key regulator of the G1/S checkpoint. p53 is mutated or lost in many cancers which as a result lose G1/S checkpoint function which theoretically makes them more reliant of other checkpoints controlled by Chk1. Studies have shown that p53-deficient triple negative breast cancer cells are sensitive to Chk1 inhibition resulting in cell death (Ma et al, 2012). Other studies have shown that Chk1 inhibition potentiates the cytotoxic effects of DNA damaging agents in p53-deficient cells but not in p53-proficient cells of various tissue origins (Chen et al, 2006). However other findings show that p53 status does not necessary predict the efficacy of Chk1 inhibition (Zenvirt et al, 2010). Thus in experiments where Chk1 inhibition was shown to abrogate cell cycle arrest following DNA damage, p53-deficient cells were no more sensitive to Chk1 inhibition than p53-proficient cells (Zenvirt et al, 2010). In contrast, in myc-driven lymphoma cells *in vitro* and *in vivo*, p53 wild-type: Arf null cells were more sensitive to Chk1 inhibition than there p53 null: Arf wild-type counterparts (Ferrao et al, 2012). This is consistent with data presented here, whereby melanoma cell lines which were null or mutant for the CDKN2A locus, Sk-Mel-103 and Sk-Mel-147, were more sensitive to Chk1 inhibition than those with a wildtype CDKN2A locus, Sk-Mel-5, Sk-Mel-28 and Sk-Mel-39 (Figure 6.13). This apparent discrepancy could be explained by recent data which suggests that sensitivity to Chk1 inhibition is due to loss of p21 expression, a downstream target of p53, rather than p53 itself (Origanti et al, 2012). In this study loss of p21 sensitised cells to Chk1 inhibition in combination with DNA damaging agents much more than p53 loss. In addition basal pools of p21, which are p53-independent, provided protection to 53 null cells following treatment (Origanti et al, 2012).

Other potential mechanisms associated with sensitivity to Chk1 inhibition are high levels of endogenous DNA damage and replicative stress. In melanoma cell lines sensitivity to Chk1 inhibition correlated with the levels of endogenous DNA damage, an indicator of replicative stress, while normal melanocytes were only sensitive at much higher concentrations of drug (Brooks et al, 2012). In these

cells Chk1 inhibition promoted premature mitotic entry of aberrant S-phase cells resulting in a dysfunctional mitosis and cell death (Brooks et al, 2012). Similarly, in both myc-driven lymphoma and neuroblastoma cells, which exhibit high levels of DNA damage due to myc-induced replicative stress, Chk1 inhibition induced cytotoxic effects resulting in accumulation of DNA damage and cell death that was not seen in either normal B-cells or normal NC-cells respectively (Cole et al, 2011; Ferrao et al, 2012). In myc-amplified neuroblastoma cells apoptosis was shown to be specifically induced during replication (Cole et al, 2011). Consistent with this, data presented in this thesis has also pointed to the idea that there is a replication associated mechanism for the cytotoxic effects of Chk1 inhibition, as DNA damage following Chk1 inhibition was specifically generated in S-phase cells. In addition Chk1 inhibition seemed to alter progression through S-phase with an increase in replication fork collapse. Studies have suggested that this may be due to uncontrolled CDK activity; however a mechanism is still unclear. It would be interesting to elucidate if sensitivity to Chk1 inhibition in melanoma cells, at least in part, is attributable to the proliferation rate of these cells; for instance are senescent melanocyte cells resistant to Chk1 inhibition? Data would suggest that while Chk1 loss causes acute cell death in a subset of cells within normal tissues there is no dramatic effect to the overall homeostasis of the tissue (Greenow et al, 2009; Tho et al, 2012). For instance in the small intestine Chk1 loss resulted in crypt cell death while in skin Chk1 loss resulted in cell death mainly within the hair follicle, however in both incidences there was no overt defect to the tissue structure (Greenow et al, 2009; Tho et al, 2012) suggesting that most cells in a tissue which are differentiated are not affected by Chk1 loss. Furthermore deletion of ATR in adult mice leads to the rapid appearance of age-related phenotypes including hair greying. These phenotypes were associated with a dramatic reduction in tissue-specific stem and progenitor cells, resulting in exhaustion of tissue renewal and homeostatic capacity (Ruzankina et al, 2007). This could be important for understanding the clinical application of Chk1 inhibitors, especially in terms of side effects. Collectively these data might suggest that Chk1 inhibition in cancer cells may act, either in combination with other drugs or due to genetic alterations already present, by increasing the genomic instability to such an extent that cell survival is no longer viable.

This concept has similar parallels to that of standard chemotherapeutics which have been proposed to exploit the mutator phenotype of cancer cells, however perhaps with a slightly more targeted rational. The mutator phenotype of cancer cells refers to the high levels of genetic instability seen in cancers which may facilitate cellular plasticity and adaptation allowing for the continued growth of cancer cells in otherwise detrimental conditions (Fox & Loeb, 2010). However a major consequence of this genetic instability is that many cancer cells may exist at a threshold of mutational load, beyond which cell survival is no longer possible. Most standard cancer therapies induce DNA damage which may in some situations at least push the cancer cells above this threshold resulting in cell death through lethal mutagenesis. Evidence that Chk1 may protect against such effects comes from recent data which shows that overexpression of Chk1, by addition of an extra allele, is protective and promotes transformation (Lopez-Contreras et al, 2012). *In vitro* mouse embryonic fibroblasts (MEFs) expressing an extra allele of Chk1 were protected against agents that induce replicative stress, and furthermore against oncogene-induced replicative stress. This suppression of replicative stress was associated with increased efficiency of transformation (Lopez-Contreras et al, 2012). This suggests that targeting genomic instability and the inherent increased mutation rate of cancer cells could be a viable therapeutic strategy. Evidence for this comes from the observation that PARP inhibitors are more lethal in cancer cells which lack HR repair, than those that are proficient. Cancer cells which lack HR repair have a high rate of mutagenesis and genomic instability. In this instance inhibition of PARP, which is responsible for base excision repair, will presumably increase the mutation rate and thus genomic instability of these cells resulting in cell death (Audeh et al, 2010; McCabe et al, 2006).

In addition to the work presented here I also carried out a limited *in vitro* analysis of Chk1 inhibition in combination with 5-flurouracil (5-FU) and with a selective PARP inhibitor (AZD2281). In this limited analysis, carried out on three metastatic melanoma cell lines, I did not see any synergy between the Chk1 inhibitor CHIR-124 and 5-FU. In fact, in most cases the addition of 5-FU decreased the apparent sensitivity to CHIR-124. This is in contrast to a study which has shown that siRNA of Chk1 in HCT-116 cells is able to sensitize them to 5-FU treatment (Ganzinelli et al, 2008). Analysis with PARP inhibition was less

clear with synergy seen in some but not all cell lines. Recent studies have shown that both Chk1 inhibitors and dual Chk1/2 inhibitors increase endogenous PARP activity, which is blocked by PARP1 inhibition resulting in increased cell death in a breast cancer cell lines (Mitchell et al, 2010; Tang et al, 2012). In addition there is other published data demonstrating that Chk1 inhibition increases the cytotoxic effects of other known genotoxins including IR, cisplatin, gemcitabine and topoisomerase inhibitors. It would be interesting to examine which combinations do show, if any, synergy with the Chk1 inhibitor CHIR-124 both *in vitro* and *in vivo*, in the context of melanoma? Interestingly a recent synergistic relation between Chk1 and its downstream target Wee1 has been discovered, with Wee1 inhibitors markedly increasing the cytotoxic effects of Chk1 inhibition in ovarian and neuroblastoma cells (Carrassa et al, 2012; Russell et al, 2012).

In conclusion the work presented here suggests that Chk1 is important for the development of malignant melanoma, and that targeted Chk1 inhibitors may be a viable therapeutic application for the treatment of melanoma. However whether this is in combination with other drugs or in context with the specific genetic background of cancer types remains to be seen.

List of References

Aarts, M., R. Sharpe, et al. (2012). "Forced mitotic entry of S-phase cells as a therapeutic strategy induced by inhibition of WEE1." Cancer discovery **2**(6): 524-539.

Abdel-Malek, Z. A., A. L. Kadekaro, et al. (2010). "Stepping up melanocytes to the challenge of UV exposure." Pigment Cell Melanoma Res **23**(2): 171-186.

Abraham, R. T. (2001). "Cell cycle checkpoint signaling through the ATM and ATR kinases." Genes Dev **15**(17): 2177-2196.

Ackermann, J., M. Frutschi, et al. (2005). "Metastasizing melanoma formation caused by expression of activated N-RasQ61K on an INK4a-deficient background." Cancer Res **65**(10): 4005-4011.

Acloque, H., M. S. Adams, et al. (2009). "Epithelial-mesenchymal transitions: the importance of changing cell state in development and disease." J Clin Invest **119**(6): 1438-1449.

Agapova, L. S., J. L. Volodina, et al. (2004). "Activation of Ras-Ral pathway attenuates p53-independent DNA damage G2 checkpoint." The Journal of Biological Chemistry **279**(35): 36382-36389.

Ahn, J. Y., X. Li, et al. (2002). "Phosphorylation of threonine 68 promotes oligomerization and autophosphorylation of the Chk2 protein kinase via the forkhead-associated domain." The Journal of Biological Chemistry **277**(22): 19389-19395.

Ahn, J. Y., J. K. Schwarz, et al. (2000). "Threonine 68 phosphorylation by ataxia telangiectasia mutated is required for efficient activation of Chk2 in response to ionizing radiation." Cancer Res **60**(21): 5934-5936.

Antoni, L., N. Sodha, et al. (2007). "CHK2 kinase: cancer susceptibility and cancer therapy - two sides of the same coin?" Nat Rev Cancer **7**(12): 925-936.

Aoki, H. and O. Moro (2002). "Involvement of microphthalmia-associated transcription factor (MITF) in expression of human melanocortin-1 receptor (MC1R)." Life Sci **71**(18): 2171-2179.

Ashwell, S., J. W. Janetka, et al. (2008). "Keeping checkpoint kinases in line: new selective inhibitors in clinical trials." Expert Opin Investig Drugs **17**(9): 1331-1340.

Astuti, P., T. Pike, et al. (2009). "MAPK pathway activation delays G2/M progression by destabilizing Cdc25B." The Journal of Biological Chemistry **284**(49): 33781-33788.

Audeh, M. W., J. Carmichael, et al. (2010). "Oral poly(ADP-ribose) polymerase inhibitor olaparib in patients with BRCA1 or BRCA2 mutations and recurrent ovarian cancer: a proof-of-concept trial." Lancet **376**(9737): 245-251.

Aylaj, B., F. Luciani, et al. (2011). "Melanoblast proliferation dynamics during mouse embryonic development. Modeling and validation." J Theor Biol **276**(1): 86-98.

Bahassi, E. M., J. L. Ovesen, et al. (2008). "The checkpoint kinases Chk1 and Chk2 regulate the functional associations between hBRCA2 and Rad51 in response to DNA damage." Oncogene **27**(28): 3977-3985.

Bailis, J. M., D. D. Luche, et al. (2008). "Minichromosome maintenance proteins interact with checkpoint and recombination proteins to promote s-phase genome stability." Mol Cell Biol **28**(5): 1724-1738.

Bakkenist, C. J. and M. B. Kastan (2003). "DNA damage activates ATM through intermolecular autophosphorylation and dimer dissociation." Nature **421**(6922): 499-506.

Barrett, J. H., M. M. Iles, et al. (2011). "Genome-wide association study identifies three new melanoma susceptibility loci." Nature Genetics **43**(11): 1108-1113.

Bartek, J., J. Bartkova, et al. (2007). "DNA damage signalling guards against activated oncogenes and tumour progression." Oncogene **26**(56): 7773-7779.

Bartek, J. and J. Lukas (2001). "Pathways governing G1/S transition and their response to DNA damage." FEBS Lett **490**(3): 117-122.

Bartek, J. and J. Lukas (2003). "Chk1 and Chk2 kinases in checkpoint control and cancer." Cancer Cell **3**(5): 421-429.

Bartkova, J., Z. Horejsi, et al. (2005). "DNA damage response as a candidate anti-cancer barrier in early human tumorigenesis." Nature **434**(7035): 864-870.

Bartkova, J., N. Rezaei, et al. (2006). "Oncogene-induced senescence is part of the tumorigenesis barrier imposed by DNA damage checkpoints." Nature **444**(7119): 633-637.

Basu, B., T. A. Yap, et al. (2012). "Targeting the DNA damage response in oncology: past, present and future perspectives." Current Opinion in Oncology **24**(3): 316-324.

Bauer, J. and B. C. Bastian (2006). "Distinguishing melanocytic nevi from melanoma by DNA copy number changes: comparative genomic hybridization as a research and diagnostic tool." Dermatol Ther **19**(1): 40-49.

Bauer, J., J. A. Curtin, et al. (2007). "Congenital melanocytic nevi frequently harbor NRAS mutations but no BRAF mutations." J Invest Dermatol **127**(1): 179-182.

Baynash, A. G., K. Hosoda, et al. (1994). "Interaction of endothelin-3 with endothelin-B receptor is essential for development of epidermal melanocytes and enteric neurons." Cell **79**(7): 1277-1285.

Beausejour, C. M., A. Krtolica, et al. (2003). "Reversal of human cellular senescence: roles of the p53 and p16 pathways." EMBO J **22**(16): 4212-4222.

Beck, H., V. Nahse, et al. (2010). "Regulators of cyclin-dependent kinases are crucial for maintaining genome integrity in S phase." The Journal of Cell Biology **188**(5): 629-638.

Bender, C. F., M. L. Sikes, et al. (2002). "Cancer predisposition and hematopoietic failure in Rad50(S/S) mice." Genes Dev **16**(17): 2237-2251.

Berson, J. F., A. C. Theos, et al. (2003). "Proprotein convertase cleavage liberates a fibrillogenic fragment of a resident glycoprotein to initiate melanosome biogenesis." The Journal of Cell Biology **161**(3): 521-533.

Bertoni, F., A. M. Codegoni, et al. (1999). "CHK1 frameshift mutations in genetically unstable colorectal and endometrial cancers." Genes Chromosomes Cancer **26**(2): 176-180.

Bevona, C., W. Goggins, et al. (2003). "Cutaneous melanomas associated with nevi." Arch Dermatol **139**(12): 1620-1624; discussion 1624.

Birch, J. M. (1994). "Li-Fraumeni syndrome." European Journal of Cancer **30A**(13): 1935-1941.

Blasina, A., I. V. de Weyer, et al. (1999). "A human homologue of the checkpoint kinase Cds1 directly inhibits Cdc25 phosphatase." Curr Biol **9**(1): 1-10.

Bleehen, N. M., E. S. Newlands, et al. (1995). "Cancer Research Campaign phase II trial of temozolomide in metastatic melanoma." J Clin Oncol **13**(4): 910-913.

Blomen, V. A. and J. Boonstra (2007). "Cell fate determination during G1 phase progression." Cell Mol Life Sci **64**(23): 3084-3104.

Blow, J. J. and P. J. Gillespie (2008). "Replication licensing and cancer--a fatal entanglement?" Nat Rev Cancer **8**(10): 799-806.

Blow, J. J. and B. Hodgson (2002). "Replication licensing--defining the proliferative state?" Trends Cell Biol **12**(2): 72-78.

Bohm, M., G. Moellmann, et al. (1995). "Identification of p90RSK as the probable CREB-Ser133 kinase in human melanocytes." Cell Growth Differ **6**(3): 291-302.

Boles, N. C., S. Peddibhotla, et al. (2010). "Chk1 haploinsufficiency results in anemia and defective erythropoiesis." PloS One **5**(1): e8581.

Bondurand, N., F. Dastot-Le Moal, et al. (2007). "Deletions at the SOX10 gene locus cause Waardenburg syndrome types 2 and 4." Am J Hum Genet **81**(6): 1169-1185.

Brannan, C. I., S. D. Lyman, et al. (1991). "Steel-Dickie mutation encodes a c-kit ligand lacking transmembrane and cytoplasmic domains." Proceedings of the National Academy of Sciences of the United States of America **88**(11): 4671-4674.

Branzei, D. and M. Foiani (2005). "The DNA damage response during DNA replication." Curr Opin Cell Biol **17**(6): 568-575.

Briani, C., M. Schlotter, et al. (2006). "Development of a mantle cell lymphoma in an ATM heterozygous woman after occupational exposure to ionising radiation and somatic mutation of the second allele." Leuk Res **30**(9): 1193-1196.

Broderick, R. and H. P. Nasheuer (2009). "Regulation of Cdc45 in the cell cycle and after DNA damage." Biochem Soc Trans **37**(Pt 4): 926-930.

Brooks, K., V. Oakes, et al. (2012). "A potent Chk1 inhibitor is selectively cytotoxic in melanomas with high levels of replicative stress." Oncogene **32**(6): 788-796.

Buis, J., Y. Wu, et al. (2008). "Mre11 nuclease activity has essential roles in DNA repair and genomic stability distinct from ATM activation." Cell **135**(1): 85-96.

Byun, T. S., M. Pacek, et al. (2005). "Functional uncoupling of MCM helicase and DNA polymerase activities activates the ATR-dependent checkpoint." Genes Dev **19**(9): 1040-1052.

Cai, Z., N. H. Chehab, et al. (2009). "Structure and activation mechanism of the CHK2 DNA damage checkpoint kinase." Molecular Cell **35**(6): 818-829.

Camacho-Hubner, A. and F. Beermann (2001). "Increased transgene expression by the mouse tyrosinase enhancer is restricted to neural crest-derived pigment cells." Genesis **29**(4): 180-187.

Campaner, S. and B. Amati (2012). "Two sides of the Myc-induced DNA damage response: from tumor suppression to tumor maintenance." Cell Div **7**(1): 6.

Cancer Research, UK. (2012). "Cancer Stats: Skin Cancer."

Cano, A., M. A. Perez-Moreno, et al. (2000). "The transcription factor snail controls epithelial-mesenchymal transitions by repressing E-cadherin expression." Nature Cell Biology **2**(2): 76-83.

Caporali, S., E. Alvino, et al. (2012). "Down-regulation of the PTTG1 proto-oncogene contributes to the melanoma suppressive effects of the cyclin-dependent kinase inhibitor PHA-848125." Biochem Pharmacol **84**(5): 598-611.

Carl, T. F., C. Dufton, et al. (1999). "Inhibition of neural crest migration in Xenopus using antisense slug RNA." Dev Biol **213**(1): 101-115.

Carrassa, L., M. Broggini, et al. (2004). "Chk1, but not Chk2, is involved in the cellular response to DNA damaging agents: differential activity in cells expressing or not p53." Cell Cycle **3**(9): 1177-1181.

Carrassa, L., R. Chila, et al. (2012). "Combined inhibition of Chk1 and Wee1: In vitro synergistic effect translates to tumor growth inhibition in vivo." Cell Cycle **11**(13): 2507-2517.

Chagin, V. O., J. H. Stear, et al. (2010). "Organization of DNA replication." Cold Spring Harb Perspect Biol **2**(4): a000737.

Chapman, P. B., A. Hauschild, et al. (2011). "Improved survival with vemurafenib in melanoma with BRAF V600E mutation." N Engl J Med **364**(26): 2507-2516.

Chaturvedi, P., W. K. Eng, et al. (1999). "Mammalian Chk2 is a downstream effector of the ATM-dependent DNA damage checkpoint pathway." Oncogene **18**(28): 4047-4054.

Chehab, N. H., A. Malikzay, et al. (2000). "Chk2/hCds1 functions as a DNA damage checkpoint in G(1) by stabilizing p53." Genes Dev **14**(3): 278-288.

Chen, C. C., R. D. Kennedy, et al. (2009). "CHK1 inhibition as a strategy for targeting Fanconi Anemia (FA) DNA repair pathway deficient tumors." Mol Cancer **8**: 24.

Chen, L., D. M. Gilkes, et al. (2005). "ATM and Chk2-dependent phosphorylation of MDMX contribute to p53 activation after DNA damage." EMBO J **24**(19): 3411-3422.

Chen, L., C. J. Nievera, et al. (2008). "Cell cycle-dependent complex formation of BRCA1.CtIP.MRN is important for DNA double-strand break repair." The Journal of Biological Chemistry **283**(12): 7713-7720.

Chen, P., C. Luo, et al. (2000). "The 1.7 A crystal structure of human cell cycle checkpoint kinase Chk1: implications for Chk1 regulation." Cell **100**(6): 681-692.

Chen, Z., L. C. Trotman, et al. (2005). "Crucial role of p53-dependent cellular senescence in suppression of Pten-deficient tumorigenesis." Nature **436**(7051): 725-730.

Chen, Z., Z. Xiao, et al. (2006). "Selective Chk1 inhibitors differentially sensitize p53-deficient cancer cells to cancer therapeutics." Int J Cancer **119**(12): 2784-2794.

Cheng, H., B. Hong, et al. (2012). "Mitomycin C potentiates TRAIL-induced apoptosis through p53-independent upregulation of death receptors: Evidence for the role of c-Jun N-terminal kinase activation." Cell Cycle **11**(17).

Chhajlani, V. and J. E. Wikberg (1992). "Molecular cloning and expression of the human melanocyte stimulating hormone receptor cDNA." FEBS Lett **309**(3): 417-420.

Chin, L. (2003). "The genetics of malignant melanoma: lessons from mouse and man." Nat Rev Cancer **3**(8): 559-570.

Chin, L., A. Tam, et al. (1999). "Essential role for oncogenic Ras in tumour maintenance." Nature **400**(6743): 468-472.

Cho, S. H., C. D. Toouli, et al. (2005). "Chk1 is essential for tumor cell viability following activation of the replication checkpoint." Cell Cycle **4**(1): 131-139.

Choi, J. H., L. A. Lindsey-Boltz, et al. (2010). "Reconstitution of RPA-covered single-stranded DNA-activated ATR-Chk1 signaling." Proceedings of the National Academy of Sciences of the United States of America **107**(31): 13660-13665.

Christmann, M., M. T. Tomicic, et al. (2003). "Mechanisms of human DNA repair: an update." Toxicology **193**(1-2): 3-34.

Chudnovsky, Y., A. E. Adams, et al. (2005). "Use of human tissue to assess the oncogenic activity of melanoma-associated mutations." Nat Genet **37**(7): 745-749.

Cimprich, K. A. and D. Cortez (2008). "ATR: an essential regulator of genome integrity." Nat Rev Mol Cell Biol **9**(8): 616-627.

Clark, W. H., Jr., D. E. Elder, et al. (1984). "A study of tumor progression: the precursor lesions of superficial spreading and nodular melanoma." Hum Pathol **15**(12): 1147-1165.

Cohen, C., A. Zavala-Pompa, et al. (2002). "Mitogen-actived protein kinase activation is an early event in melanoma progression." Clinical Cancer Research : an official Journal of the American Association for Cancer Research **8**(12): 3728-3733.

Cole, K. A., J. Huggins, et al. (2011). "RNAi screen of the protein kinome identifies checkpoint kinase 1 (CHK1) as a therapeutic target in neuroblastoma." Proceedings of the National Academy of Sciences of the United States of America 108(8): 3336-3341.

Collins, C. J. and J. M. Sedivy (2003). "Involvement of the INK4a/Arf gene locus in senescence." Aging Cell 2(3): 145-150.

Collins, N., R. McManus, et al. (1995). "Consistent loss of the wild type allele in breast cancers from a family linked to the BRCA2 gene on chromosome 13q12-13." Oncogene 10(8): 1673-1675.

Colombo, S., V. Petit, et al. (2007). "Flanking genomic region of Tyr::Cre mice, rapid genotyping for homozygous mice." Pigment Cell Res 20(4): 305-306.

Comis, R. L. (1976). "DTIC (NSC-45388) in malignant melanoma: a perspective." Cancer Treatment Reports 60(2): 165-176.

Cone, R. D., K. G. Mountjoy, et al. (1993). "Cloning and functional characterization of a family of receptors for the melanotropic peptides." Ann N Y Acad Sci 680: 342-363.

Conti, C., J. A. Seiler, et al. (2007). "The mammalian DNA replication elongation checkpoint: implication of Chk1 and relationship with origin firing as determined by single DNA molecule and single cell analyses." Cell Cycle 6(22): 2760-2767.

Cui, R., H. R. Widlund, et al. (2007). "Central role of p53 in the suntan response and pathologic hyperpigmentation." Cell 128(5): 853-864.

Cummins, D. L., J. M. Cummins, et al. (2006). "Cutaneous malignant melanoma." Mayo Clin Proc 81(4): 500-507.

Dai, Y. and S. Grant (2010). "New insights into checkpoint kinase 1 in the DNA damage response signaling network." Clinical Cancer Research : an official Journal of the American Association for Cancer Research 16(2): 376-383.

D'Amours, D. and S. P. Jackson (2002). "The Mre11 complex: at the crossroads of dna repair and checkpoint signalling." Nat Rev Mol Cell Biol 3(5): 317-327.

Damsky, W. E., Jr. and M. Bosenberg (2010). "Mouse melanoma models and cell lines." Pigment Cell Melanoma Res 23(6): 853-859.

Dankort, D., D. P. Curley, et al. (2009). "Braf(V600E) cooperates with Pten loss to induce metastatic melanoma." Nat Genet 41(5): 544-552.

Davies, H., G. R. Bignell, et al. (2002). "Mutations of the BRAF gene in human cancer." Nature 417(6892): 949-954.

Davies, K. D., P. L. Cable, et al. (2011). "Chk1 inhibition and Wee1 inhibition combine synergistically to impede cellular proliferation." Cancer Biol Ther **12**(9): 788-796.

Davies, K. D., M. J. Humphries, et al. (2011). "Single-agent inhibition of Chk1 is antiproliferative in human cancer cell lines in vitro and inhibits tumor xenograft growth in vivo." Oncol Res **19**(7): 349-363.

Davies, M. A., P. S. Fox, et al. (2012). "Phase I study of the combination of sorafenib and temsirolimus in patients with metastatic melanoma." Clinical Cancer Research : an official Journal of the American Association for Cancer Research **18**(4): 1120-1128.

Delacroix, S., J. M. Wagner, et al. (2007). "The Rad9-Hus1-Rad1 (9-1-1) clamp activates checkpoint signaling via TopBP1." Genes Dev **21**(12): 1472-1477.

Delia, D., M. Piane, et al. (2004). "MRE11 mutations and impaired ATM-dependent responses in an Italian family with ataxia-telangiectasia-like disorder." Hum Mol Genet **13**(18): 2155-2163.

Delmas, V., F. Beermann, et al. (2007). "Beta-catenin induces immortalization of melanocytes by suppressing p16INK4a expression and cooperates with N-Ras in melanoma development." Genes Dev **21**(22): 2923-2935.

Delmas, V., S. Martinozzi, et al. (2003). "Cre-mediated recombination in the skin melanocyte lineage." Genesis **36**(2): 73-80.

Demunter, A., M. Stas, et al. (2001). "Analysis of N- and K-ras mutations in the distinctive tumor progression phases of melanoma." J Invest Dermatol **117**(6): 1483-1489.

den Elzen, N., A. Kosoy, et al. (2004). "Resisting arrest: recovery from checkpoint arrest through dephosphorylation of Chk1 by PP1." Cell Cycle **3**(5): 529-533.

den Elzen, N. R. and M. J. O'Connell (2004). "Recovery from DNA damage checkpoint arrest by PP1-mediated inhibition of Chk1." EMBO J **23**(4): 908-918.

Den Haese, G. J., N. Walworth, et al. (1995). "The Wee1 protein kinase regulates T14 phosphorylation of fission yeast Cdc2." Molecular Biology of the Cell **6**(4): 371-385.

Dent, P., Y. Tang, et al. (2011). "CHK1 inhibitors in combination chemotherapy: thinking beyond the cell cycle." Mol Interv **11**(2): 133-140.

Dhomen, N., J. S. Reis-Filho, et al. (2009). "Oncogenic Braf induces melanocyte senescence and melanoma in mice." Cancer Cell **15**(4): 294-303.

Di Micco, R., M. Fumagalli, et al. (2006). "Oncogene-induced senescence is a DNA damage response triggered by DNA hyper-replication." Nature **444**(7119): 638-642.

Ding, L., G. Getz, et al. (2008). "Somatic mutations affect key pathways in lung adenocarcinoma." Nature **455**(7216): 1069-1075.

DiTullio, R. A., Jr., T. A. Mochan, et al. (2002). "53BP1 functions in an ATM-dependent checkpoint pathway that is constitutively activated in human cancer." Nature Cell Biology **4**(12): 998-1002.

Donehower, L. A., M. Harvey, et al. (1992). "Mice deficient for p53 are developmentally normal but susceptible to spontaneous tumours." Nature **356**(6366): 215-221.

Dorsky, R. I., R. T. Moon, et al. (1998). "Control of neural crest cell fate by the Wnt signalling pathway." Nature **396**(6709): 370-373.

Du, J. and D. E. Fisher (2002). "Identification of Aim-1 as the underwhite mouse mutant and its transcriptional regulation by MITF." The Journal of Biological Chemistry **277**(1): 402-406.

Dufau, I., C. Frongia, et al. (2012). "Multicellular tumor spheroid model to evaluate spatio-temporal dynamics effect of chemotherapeutics: application to the gemcitabine/CHK1 inhibitor combination in pancreatic cancer." BMC Cancer **12**: 15.

Dunn, K. J., M. Brady, et al. (2005). "WNT1 and WNT3a promote expansion of melanocytes through distinct modes of action." Pigment Cell Res **18**(3): 167-180.

Dunn, K. J., B. O. Williams, et al. (2000). "Neural crest-directed gene transfer demonstrates Wnt1 role in melanocyte expansion and differentiation during mouse development." Proceedings of the National Academy of Sciences of the United States of America **97**(18): 10050-10055.

Dupin, E., C. Glavieux, et al. (2000). "Endothelin 3 induces the reversion of melanocytes to glia through a neural crest-derived glial-melanocytic progenitor." Proceedings of the National Academy of Sciences of the United States of America **97**(14): 7882-7887.

Duriez, P. J., S. Desnoyers, et al. (1997). "Characterization of anti-peptide antibodies directed towards the automodification domain and apoptotic fragment of poly (ADP-ribose) polymerase." Biochimica et Biophysica Acta **1334**(1): 65-72.

Eggermont, A. M. and C. Robert (2011). "New drugs in melanoma: it's a whole new world." European Journal of Cancer **47**(14): 2150-2157.

Elledge, S. J. (1996). "Cell cycle checkpoints: preventing an identity crisis." Science **274**(5293): 1664-1672.

Eller, M. S., M. Yaar, et al. (1994). "DNA damage and melanogenesis." Nature **372**(6505): 413-414.

End, D. W., G. Smets, et al. (2001). "Characterization of the antitumor effects of the selective farnesyl protein transferase inhibitor R115777 in vivo and in vitro." Cancer Res **61**(1): 131-137.

Erickson, C. A. and M. V. Reedy (1998). "Neural crest development: the interplay between morphogenesis and cell differentiation." Curr Top Dev Biol **40**: 177-209.

Errico, A., V. Costanzo, et al. (2007). "Tipin is required for stalled replication forks to resume DNA replication after removal of aphidicolin in Xenopus egg extracts." Proceedings of the National Academy of Sciences of the United States of America **104**(38): 14929-14934.

Eskandarpour, M., J. Hashemi, et al. (2003). "Frequency of UV-inducible NRAS mutations in melanomas of patients with germline CDKN2A mutations." J Natl Cancer Inst **95**(11): 790-798.

Eskandarpour, M., S. Kiaii, et al. (2005). "Suppression of oncogenic NRAS by RNA interference induces apoptosis of human melanoma cells." Int J Cancer **115**(1): 65-73.

Falck, J., J. H. Petrini, et al. (2002). "The DNA damage-dependent intra-S phase checkpoint is regulated by parallel pathways." Nat Genet **30**(3): 290-294.

Fang, D., T. K. Nguyen, et al. (2005). "A tumorigenic subpopulation with stem cell properties in melanomas." Cancer Res **65**(20): 9328-9337.

Feijoo, C., C. Hall-Jackson, et al. (2001). "Activation of mammalian Chk1 during DNA replication arrest: a role for Chk1 in the intra-S phase checkpoint monitoring replication origin firing." The Journal of Cell Biology **154**(5): 913-923.

Ferguson, B., H. Konrad Muller, et al. (2010). "Differential roles of the pRb and Arf/p53 pathways in murine naevus and melanoma genesis." Pigment Cell Melanoma Res **23**(6): 771-780.

Ferguson, C. A. and S. H. Kidson (1997). "The regulation of tyrosinase gene transcription." Pigment Cell Res **10**(3): 127-138.

Ferlay, J., H. R. Shin, et al. (2010). "Estimates of worldwide burden of cancer in 2008: GLOBOCAN 2008." Int J Cancer **127**(12): 2893-2917.

Fernandez-Capetillo, O., A. Lee, et al. (2004). "H2AX: the histone guardian of the genome." DNA Repair **3**(8-9): 959-967.

Ferrao, P. T., E. P. Bukczynska, et al. (2012). "Efficacy of CHK inhibitors as single agents in MYC-driven lymphoma cells." Oncogene **31**(13): 1661-1672.

Fishler, T., Y. Y. Li, et al. (2010). "Genetic instability and mammary tumor formation in mice carrying mammary-specific disruption of Chk1 and p53." Oncogene **29**(28): 4007-4017.

Fitzpatrick, T. B. (1988). "The validity and practicality of sun-reactive skin types I through VI." Arch Dermatol **124**(6): 869-871.

Flaherty, K. T., J. R. Infante, et al. (2012). "Combined BRAF and MEK inhibition in melanoma with BRAF V600 mutations." N Engl J Med **367**(18): 1694-1703.

Fox, E. J. and L. A. Loeb (2010). "Lethal mutagenesis: targeting the mutator phenotype in cancer." Semin Cancer Biol **20**(5): 353-359.

Frank, N. Y., A. Margaryan, et al. (2005). "ABCB5-mediated doxorubicin transport and chemoresistance in human malignant melanoma." Cancer Res **65**(10): 4320-4333.

Fujimoto, A., R. Morita, et al. (1999). "p16INK4a inactivation is not frequent in uncultured sporadic primary cutaneous melanoma." Oncogene **18**(15): 2527-2532.

Furumura, M., C. Sakai, et al. (1996). "The interaction of agouti signal protein and melanocyte stimulating hormone to regulate melanin formation in mammals." Pigment Cell Res **9**(4): 191-203.

Ganzinelli, M., L. Carrassa, et al. (2008). "Checkpoint kinase 1 down-regulation by an inducible small interfering RNA expression system sensitized in vivo tumors to treatment with 5-fluorouracil." Clinical Cancer Research : an official Journal of the American Association for Cancer Research **14**(16): 5131-5141.

Garcia-Borron, J. C., B. L. Sanchez-Laorden, et al. (2005). "Melanocortin-1 receptor structure and functional regulation." Pigment Cell Res **18**(6): 393-410.

Garraway, L. A., H. R. Widlund, et al. (2005). "Integrative genomic analyses identify MITF as a lineage survival oncogene amplified in malignant melanoma." Nature **436**(7047): 117-122.

Geissler, E. N., M. A. Ryan, et al. (1988). "The dominant-white spotting (W) locus of the mouse encodes the c-kit proto-oncogene." Cell **55**(1): 185-192.

Germain, M., E. B. Affar, et al. (1999). "Cleavage of automodified poly(ADP-ribose) polymerase during apoptosis. Evidence for involvement of caspase-7." The Journal of Biological Chemistry **274**(40): 28379-28384.

Giannini, G., E. Ristori, et al. (2002). "Human MRE11 is inactivated in mismatch repair-deficient cancers." EMBO Rep **3**(3): 248-254.

Giebel, L. B. and R. A. Spritz (1991). "Mutation of the KIT (mast/stem cell growth factor receptor) protooncogene in human piebaldism." Proceedings of the National Academy of Sciences of the United States of America **88**(19): 8696-8699.

Gilad, O., B. Y. Nabet, et al. (2010). "Combining ATR suppression with oncogenic Ras synergistically increases genomic instability, causing synthetic lethality or tumorigenesis in a dosage-dependent manner." Cancer Res **70**(23): 9693-9702.

Goding, C. R. (2000). "Mitf from neural crest to melanoma: signal transduction and transcription in the melanocyte lineage." Genes Dev **14**(14): 1712-1728.

Goel, V. K., N. Ibrahim, et al. (2009). "Melanocytic nevus-like hyperplasia and melanoma in transgenic BRAFV600E mice." Oncogene **28**(23): 2289-2298.

Gorgoulis, V. G., L. V. Vassiliou, et al. (2005). "Activation of the DNA damage checkpoint and genomic instability in human precancerous lesions." Nature **434**(7035): 907-913.

Gray-Schopfer, V. C., S. da Rocha Dias, et al. (2005). "The role of B-RAF in melanoma." Cancer Metastasis Rev **24**(1): 165-183.

Greenow, K. R., A. R. Clarke, et al. (2009). "Chk1 deficiency in the mouse small intestine results in p53-independent crypt death and subsequent intestinal compensation." Oncogene **28**(11): 1443-1453.

Grichnik, J. M., J. A. Burch, et al. (2006). "Melanoma, a tumor based on a mutant stem cell?" J Invest Dermatol **126**(1): 142-153.

Guldberg, P., P. thor Straten, et al. (1997). "Disruption of the MMAC1/PTEN gene by deletion or mutation is a frequent event in malignant melanoma." Cancer Res **57**(17): 3660-3663.

Gumy-Pause, F., P. Wacker, et al. (2004). "ATM gene and lymphoid malignancies." Leukemia **18**(2): 238-242.

Guyonneau, L., F. Murisier, et al. (2004). "Melanocytes and pigmentation are affected in dopachrome tautomerase knockout mice." Mol Cell Biol **24**(8): 3396-3403.

Halazonetis, T. D., V. G. Gorgoulis, et al. (2008). "An oncogene-induced DNA damage model for cancer development." Science **319**(5868): 1352-1355.

Hangaishi, A., S. Ogawa, et al. (2002). "Mutations of Chk2 in primary hematopoietic neoplasms." Blood **99**(8): 3075-3077.

Hardy, C. F. (1997). "Identification of Cdc45p, an essential factor required for DNA replication." Gene **187**(2): 239-246.

Hari, L., V. Brault, et al. (2002). "Lineage-specific requirements of beta-catenin in neural crest development." The Journal of Cell Biology **159**(5): 867-880.

Hari, L., I. Miescher, et al. (2012). "Temporal control of neural crest lineage generation by Wnt/beta-catenin signaling." Development **139**(12): 2107-2117.

Harris, M. L., L. L. Baxter, et al. (2010). "Sox proteins in melanocyte development and melanoma." Pigment Cell Melanoma Res **23**(4): 496-513.

Hartwell, L. H. and T. A. Weinert (1989). "Checkpoints: controls that ensure the order of cell cycle events." Science **246**(4930): 629-634.

Hatzivassiliou, G., K. Song, et al. (2010). "RAF inhibitors prime wild-type RAF to activate the MAPK pathway and enhance growth." Nature **464**(7287): 431-435.

Hauschild, A., J. J. Grob, et al. (2012). "Dabrafenib in BRAF-mutated metastatic melanoma: a multicentre, open-label, phase 3 randomised controlled trial." Lancet **380**(9839): 358-365.

Healy, E., S. A. Jordan, et al. (2001). "Functional variation of MC1R alleles from red-haired individuals." Hum Mol Genet **10**(21): 2397-2402.

Heidorn, S. J., C. Milagre, et al. (2010). "Kinase-dead BRAF and oncogenic RAS cooperate to drive tumor progression through CRAF." Cell **140**(2): 209-221.

Heikkinen, K., V. Mansikka, et al. (2005). "Mutation analysis of the ATR gene in breast and ovarian cancer families." Breast Cancer Res **7**(4): R495-501.

Hemesath, T. J., E. R. Price, et al. (1998). "MAP kinase links the transcription factor Microphthalmia to c-Kit signalling in melanocytes." Nature **391**(6664): 298-301.

Herbarth, B., V. Pingault, et al. (1998). "Mutation of the Sry-related Sox10 gene in Dominant megacolon, a mouse model for human Hirschsprung disease." Proceedings of the National Academy of Sciences of the United States of America **95**(9): 5161-5165.

Hill, G. J., 2nd, G. E. Metter, et al. (1979). "DTIC and combination therapy for melanoma. II. Escalating schedules of DTIC with BCNU, CCNU, and vincristine." Cancer Treatment Reports **63**(11-12): 1989-1992.

Hirao, A., A. Cheung, et al. (2002). "Chk2 is a tumor suppressor that regulates apoptosis in both an ataxia telangiectasia mutated (ATM)-dependent and an ATM-independent manner." Mol Cell Biol **22**(18): 6521-6532.

Hirose, Y., M. S. Berger, et al. (2001). "Abrogation of the Chk1-mediated G(2) checkpoint pathway potentiates temozolomide-induced toxicity in a p53-independent manner in human glioblastoma cells." Cancer Res **61**(15): 5843-5849.

Hodgkinson, C. A., K. J. Moore, et al. (1993). "Mutations at the mouse microphthalmia locus are associated with defects in a gene encoding a novel basic-helix-loop-helix-zipper protein." Cell **74**(2): 395-404.

Hodi, F. S., S. J. O'Day, et al. (2010). "Improved survival with ipilimumab in patients with metastatic melanoma." N Engl J Med **363**(8): 711-723.

Hoglund, A., L. M. Nilsson, et al. (2011). "Therapeutic implications for the induced levels of Chk1 in Myc-expressing cancer cells." Clinical Cancer Research :an official Journal of the American Association for Cancer Research **17**(22): 7067-7079.

Hornyak, T. J., D. J. Hayes, et al. (2001). "Transcription factors in melanocyte development: distinct roles for Pax-3 and Mitf." Mech Dev **101**(1-2): 47-59.

Hosoda, K., R. E. Hammer, et al. (1994). "Targeted and natural (piebald-lethal) mutations of endothelin-B receptor gene produce megacolon associated with spotted coat color in mice." Cell **79**(7): 1267-1276.

Hotte, S. J., A. Oza, et al. (2006). "Phase I trial of UCN-01 in combination with topotecan in patients with advanced solid cancers: a Princess Margaret Hospital Phase II Consortium study." Ann Oncol **17**(2): 334-340.

Hou, L., H. Arnheiter, et al. (2006). "Interspecies difference in the regulation of melanocyte development by SOX10 and MITF." Proceedings of the National Academy of Sciences of the United States of America **103**(24): 9081-9085.

Howlader N, N. A., Krapcho M, Neyman N, Aminou R, Waldron W, Alterkruse SF, Kpsary CL, Ruhl J, Tatalovich Z, Cho H, Mariotto A, Eisner MP, Lewis DR, Chen HS, Feuer EJ, Cronon KA. (2012). "SEER Cancer Statistics Review, 1975-2009 (Vintage 2009 Populations)."

Hussussian, C. J., J. P. Struewing, et al. (1994). "Germline p16 mutations in familial melanoma." Nat Genet **8**(1): 15-21.

Ibrahim, N. and F. G. Haluska (2009). "Molecular pathogenesis of cutaneous melanocytic neoplasms." Annu Rev Pathol **4**: 551-579.

Ikenoue, T., Y. Hikiba, et al. (2004). "Different effects of point mutations within the B-Raf glycine-rich loop in colorectal tumors on mitogen-activated protein/extracellular signal-regulated kinase kinase/extracellular signal-regulated kinase and nuclear factor kappaB pathway and cellular transformation." Cancer Res **64**(10): 3428-3435.

Ikeya, M., S. M. Lee, et al. (1997). "Wnt signalling required for expansion of neural crest and CNS progenitors." Nature **389**(6654): 966-970.

Imokawa, G., T. Kobayashi, et al. (1997). "The role of endothelin-1 in epidermal hyperpigmentation and signaling mechanisms of mitogenesis and melanogenesis." Pigment Cell Res **10**(4): 218-228.

Imokawa, G., Y. Yada, et al. (1996). "Signalling mechanisms of endothelin-induced mitogenesis and melanogenesis in human melanocytes." Biochem J **314** (Pt 1): 305-312.

Ingvarsson, S., B. I. Sigbjornsdottir, et al. (2002). "Mutation analysis of the CHK2 gene in breast carcinoma and other cancers." Breast Cancer Res **4**(3): R4.

Jalili, A., C. Wagner, et al. (2012). "Dual Suppression of the Cyclin-Dependent Kinase Inhibitors CDKN2C and CDKN1A in Human Melanoma." J Natl Cancer Inst **104**(21): 1673-1679.

Jazayeri, A., J. Falck, et al. (2006). "ATM- and cell cycle-dependent regulation of ATR in response to DNA double-strand breaks." Nature Cell Biology **8**(1): 37-45.

Jemal, A., R. Siegel, et al. (2010). "Cancer statistics, 2010." CA Cancer J Clin **60**(5): 277-300.

Jeong, S. Y., A. Kumagai, et al. (2003). "Phosphorylated claspin interacts with a phosphate-binding site in the kinase domain of Chk1 during ATR-mediated activation." The Journal of Biological Chemistry **278**(47): 46782-46788.

Jiao, Z., R. Mollaaghababa, et al. (2004). "Direct interaction of Sox10 with the promoter of murine Dopachrome Tautomerase (Dct) and synergistic activation of Dct expression with Mitf." Pigment Cell Res **17**(4): 352-362.

Johannessen, C. M., J. S. Boehm, et al. (2010). "COT drives resistance to RAF inhibition through MAP kinase pathway reactivation." Nature **468**(7326): 968-972.

Johnson, D. G. and C. L. Walker (1999). "Cyclins and cell cycle checkpoints." Annu Rev Pharmacol Toxicol **39**: 295-312.

Jordan, S. A. and I. J. Jackson (2000). "MGF (KIT ligand) is a chemokinetic factor for melanoblast migration into hair follicles." Dev Biol **225**(2): 424-436.

Kalluri, R. and R. A. Weinberg (2009). "The basics of epithelial-mesenchymal transition." J Clin Invest **119**(6): 1420-1428.

Kamijo, T., F. Zindy, et al. (1997). "Tumor suppression at the mouse INK4a locus mediated by the alternative reading frame product p19ARF." Cell **91**(5): 649-659.

Kanetsky, P. A., J. Swoyer, et al. (2002). "A polymorphism in the agouti signaling protein gene is associated with human pigmentation." Am J Hum Genet **70**(3): 770-775.

Kang, J., R. T. Bronson, et al. (2002). "Targeted disruption of NBS1 reveals its roles in mouse development and DNA repair." EMBO J **21**(6): 1447-1455.

Karnitz, L. M., K. S. Flatten, et al. (2005). "Gemcitabine-induced activation of checkpoint signaling pathways that affect tumor cell survival." Mol Pharmacol **68**(6): 1636-1644.

Kastan, M. B. and D. S. Lim (2000). "The many substrates and functions of ATM." Nat Rev Mol Cell Biol **1**(3): 179-186.

Kaufmann, W. K., C. I. Behe, et al. (2001). "Aberrant cell cycle checkpoint function in transformed hepatocytes and WB-F344 hepatic epithelial stem-like cells." Carcinogenesis **22**(8): 1257-1269.

Kaufmann, W. K., K. R. Nevis, et al. (2008). "Defective cell cycle checkpoint functions in melanoma are associated with altered patterns of gene expression." J Invest Dermatol **128**(1): 175-187.

Kelly, T. J. and G. W. Brown (2000). "Regulation of chromosome replication." Annu Rev Biochem **69**: 829-880.

Kelsall, S. R. and B. Mintz (1998). "Metastatic cutaneous melanoma promoted by ultraviolet radiation in mice with transgene-initiated low melanoma susceptibility." Cancer Res **58**(18): 4061-4065.

Kemp, M. G., Z. Akan, et al. (2010). "Tipin-replication protein A interaction mediates Chk1 phosphorylation by ATR in response to genotoxic stress." The Journal of Biological Chemistry **285**(22): 16562-16571.

Kerzendorfer, C. and M. O'Driscoll (2009). "Human DNA damage response and repair deficiency syndromes: linking genomic instability and cell cycle checkpoint proficiency." DNA Repair **8**(9): 1139-1152.

Kitagawa, R., C. J. Bakkenist, et al. (2004). "Phosphorylation of SMC1 is a critical downstream event in the ATM-NBS1-BRCA1 pathway." Genes Dev **18**(12): 1423-1438.

Klein, W. M., B. P. Wu, et al. (2007). "Increased expression of stem cell markers in malignant melanoma." Mod Pathol **20**(1): 102-107.

Knauf, J. A., B. Ouyang, et al. (2006). "Oncogenic RAS induces accelerated transition through G2/M and promotes defects in the G2 DNA damage and mitotic spindle checkpoints." The Journal of Biological Chemistry **281**(7): 3800-3809.

Kneissl, M., V. Putter, et al. (2003). "Interaction and assembly of murine pre-replicative complex proteins in yeast and mouse cells." J Mol Biol **327**(1): 111-128.

Kondratov, R. V. and M. P. Antoch (2007). "Circadian proteins in the regulation of cell cycle and genotoxic stress responses." Trends Cell Biol **17**(7): 311-317.

Koniaras, K., A. R. Cuddihy, et al. (2001). "Inhibition of Chk1-dependent G2 DNA damage checkpoint radiosensitizes p53 mutant human cells." Oncogene **20**(51): 7453-7463.

Kousholt, A. N., K. Fugger, et al. (2012). "CtIP-dependent DNA resection is required for DNA damage checkpoint maintenance but not initiation." The Journal of Cell Biology **197**(7): 869-876.

Kramer, A., N. Mailand, et al. (2004). "Centrosome-associated Chk1 prevents premature activation of cyclin-B-Cdk1 kinase." Nature Cell Biology **6**(9): 884-891.

Krimpenfort, P., K. C. Quon, et al. (2001). "Loss of p16Ink4a confers susceptibility to metastatic melanoma in mice." Nature **413**(6851): 83-86.

Kumagai, A. and W. G. Dunphy (2003). "Repeated phosphopeptide motifs in Claspin mediate the regulated binding of Chk1." Nature Cell Biology **5**(2): 161-165.

Kumagai, A., S. M. Kim, et al. (2004). "Claspin and the activated form of ATR-ATRIP collaborate in the activation of Chk1." The Journal of Biological Chemistry **279**(48): 49599-49608.

Kumagai, A., J. Lee, et al. (2006). "TopBP1 activates the ATR-ATRIP complex." Cell **124**(5): 943-955.

LaBonne, C. and M. Bronner-Fraser (1999). "Molecular mechanisms of neural crest formation." Annu Rev Cell Dev Biol **15**: 81-112.

LaBonne, C. and M. Bronner-Fraser (2000). "Snail-related transcriptional repressors are required in Xenopus for both the induction of the neural crest and its subsequent migration." Dev Biol **221**(1): 195-205.

Lam, M. H., Q. Liu, et al. (2004). "Chk1 is haploinsufficient for multiple functions critical to tumor suppression." Cancer Cell **6**(1): 45-59.

Lamason, R. L., M. A. Mohideen, et al. (2005). "SLC24A5, a putative cation exchanger, affects pigmentation in zebrafish and humans." Science **310**(5755): 1782-1786.

Lang, D. and J. A. Epstein (2003). "Sox10 and Pax3 physically interact to mediate activation of a conserved c-RET enhancer." Hum Mol Genet **12**(8): 937-945.

Lapouge, G., K. K. Youssef, et al. (2011). "Identifying the cellular origin of squamous skin tumors." Proceedings of the National Academy of Sciences of the United States of America **108**(18): 7431-7436.

Lavin, M. F. (2008). "Ataxia-telangiectasia: from a rare disorder to a paradigm for cell signalling and cancer." Nat Rev Mol Cell Biol **9**(10): 759-769.

Lavin, M. F. and S. Kozlov (2007). "ATM activation and DNA damage response." Cell Cycle **6**(8): 931-942.

Le Douarin, N. M., S. Creuzet, et al. (2004). "Neural crest cell plasticity and its limits." Development **131**(19): 4637-4650.

Lee, H. O., J. M. Levorse, et al. (2003). "The endothelin receptor-B is required for the migration of neural crest-derived melanocyte and enteric neuron precursors." Dev Biol **259**(1): 162-175.

Lee, J., A. Kumagai, et al. (2001). "Positive regulation of Wee1 by Chk1 and 14-3-3 proteins." Molecular Biology of the Cell **12**(3): 551-563.

Lee, J., A. Kumagai, et al. (2003). "Claspin, a Chk1-regulatory protein, monitors DNA replication on chromatin independently of RPA, ATR, and Rad17." Molecular Cell **11**(2): 329-340.

Lee, J. H., M. L. Choy, et al. (2011). "Role of checkpoint kinase 1 (Chk1) in the mechanisms of resistance to histone deacetylase inhibitors." Proceedings of the National Academy of Sciences of the United States of America **108**(49): 19629-19634.

Lee, J. H. and T. T. Paull (2005). "ATM activation by DNA double-strand breaks through the Mre11-Rad50-Nbs1 complex." Science **308**(5721): 551-554.

Lee, J. H. and T. T. Paull (2007). "Activation and regulation of ATM kinase activity in response to DNA double-strand breaks." Oncogene **26**(56): 7741-7748.

Lee, J. S., K. M. Collins, et al. (2000). "hCds1-mediated phosphorylation of BRCA1 regulates the DNA damage response." Nature **404**(6774): 201-204.

Lee, M., J. Goodall, et al. (2000). "Direct regulation of the Microphthalmia promoter by Sox10 links Waardenburg-Shah syndrome (WS4)-associated hypopigmentation and deafness to WS2." The Journal of Biological Chemistry **275**(48): 37978-37983.

Lee, M. H. and H. Y. Yang (2001). "Negative regulators of cyclin-dependent kinases and their roles in cancers." Cell Mol Life Sci **58**(12-13): 1907-1922.

Leung-Pineda, V., J. Huh, et al. (2009). "DDB1 targets Chk1 to the Cul4 E3 ligase complex in normal cycling cells and in cells experiencing replication stress." Cancer Res **69**(6): 2630-2637.

Leung-Pineda, V., C. E. Ryan, et al. (2006). "Phosphorylation of Chk1 by ATR is antagonized by a Chk1-regulated protein phosphatase 2A circuit." Mol Cell Biol **26**(20): 7529-7538.

Levy, C., M. Khaled, et al. (2006). "MITF: master regulator of melanocyte development and melanoma oncogene." Trends Mol Med **12**(9): 406-414.

Lewis, L. K., F. Storici, et al. (2004). "Role of the nuclease activity of Saccharomyces cerevisiae Mre11 in repair of DNA double-strand breaks in mitotic cells." Genetics **166**(4): 1701-1713.

Limbo, O., M. E. Porter-Goff, et al. (2011). "Mre11 nuclease activity and Ctp1 regulate Chk1 activation by Rad3ATR and Tel1ATM checkpoint kinases at double-strand breaks." Mol Cell Biol **31**(3): 573-583.

Lister, J. A., C. P. Robertson, et al. (1999). "nacre encodes a zebrafish microphthalmia-related protein that regulates neural-crest-derived pigment cell fate." Development **126**(17): 3757-3767.

Liu, J. J. and D. E. Fisher (2010). "Lighting a path to pigmentation: mechanisms of MITF induction by UV." Pigment Cell Melanoma Res **23**(6): 741-745.

Liu, P., L. R. Barkley, et al. (2006). "The Chk1-mediated S-phase checkpoint targets initiation factor Cdc45 via a Cdc25A/Cdk2-independent mechanism." The Journal of Biological Chemistry **281**(41): 30631-30644.

Liu, Q., S. Guntuku, et al. (2000). "Chk1 is an essential kinase that is regulated by Atr and required for the G(2)/M DNA damage checkpoint." Genes Dev **14**(12): 1448-1459.

Liu, S., B. Shiotani, et al. (2011). "ATR autophosphorylation as a molecular switch for checkpoint activation." Molecular Cell **43**(2): 192-202.

Ljungman, M. (2009). "Targeting the DNA damage response in cancer." Chem Rev **109**(7): 2929-2950.

Lopez-Contreras, A. J., P. Gutierrez-Martinez, et al. (2012). "An extra allele of Chk1 limits oncogene-induced replicative stress and promotes transformation." J Exp Med **209**(3): 455-461.

Lopez-Fauqued, M., R. Gil, et al. (2010). "The dual PI3K/mTOR inhibitor PI-103 promotes immunosuppression, in vivo tumor growth and increases survival of sorafenib-treated melanoma cells." Int J Cancer **126**(7): 1549-1561.

Lukas, C., J. Falck, et al. (2003). "Distinct spatiotemporal dynamics of mammalian checkpoint regulators induced by DNA damage." Nature Cell Biology **5**(3): 255-260.

Ma, C. X., S. Cai, et al. (2012). "Targeting Chk1 in p53-deficient triple-negative breast cancer is therapeutically beneficial in human-in-mouse tumor models." J Clin Invest **122**(4): 1541-1552.

Mackenzie, M. A., S. A. Jordan, et al. (1997). "Activation of the receptor tyrosine kinase Kit is required for the proliferation of melanoblasts in the mouse embryo." Dev Biol **192**(1): 99-107.

Maclaine, N. J. and T. R. Hupp (2009). "The regulation of p53 by phosphorylation: a model for how distinct signals integrate into the p53 pathway." Aging (Albany NY) **1**(5): 490-502.

Madoz-Gurpide, J., M. Canamero, et al. (2007). "A proteomics analysis of cell signaling alterations in colorectal cancer." Mol Cell Proteomics **6**(12): 2150-2164.

Mailand, N., J. Falck, et al. (2000). "Rapid destruction of human Cdc25A in response to DNA damage." Science **288**(5470): 1425-1429.

Maki, R. G., D. R. D'Adamo, et al. (2009). "Phase II study of sorafenib in patients with metastatic or recurrent sarcomas." J Clin Oncol **27**(19): 3133-3140.

Mallette, F. A. and G. Ferbeyre (2007). "The DNA damage signaling pathway connects oncogenic stress to cellular senescence." Cell Cycle **6**(15): 1831-1836.

Mallette, F. A., M. F. Gaumont-Leclerc, et al. (2007). "The DNA damage signaling pathway is a critical mediator of oncogene-induced senescence." Genes Dev **21**(1): 43-48.

Margolin, K. A., J. Moon, et al. (2012). "Randomized phase II trial of sorafenib with temsirolimus or tipifarnib in untreated metastatic melanoma (S0438)." Clinical Cancer Research : an official Journal of the American Association for Cancer Research **18**(4): 1129-1137.

Marks, M. S. and M. C. Seabra (2001). "The melanosome: membrane dynamics in black and white." Nat Rev Mol Cell Biol **2**(10): 738-748.

Matsuoka, S., M. Huang, et al. (1998). "Linkage of ATM to cell cycle regulation by the Chk2 protein kinase." Science **282**(5395): 1893-1897.

Matsuoka, S., G. Rotman, et al. (2000). "Ataxia telangiectasia-mutated phosphorylates Chk2 in vivo and in vitro." Proceedings of the National Academy of Sciences of the United States of America **97**(19): 10389-10394.

Maya-Mendoza, A., E. Petermann, et al. (2007). "Chk1 regulates the density of active replication origins during the vertebrate S phase." EMBO J **26**(11): 2719-2731.

McCabe, N., N. C. Turner, et al. (2006). "Deficiency in the repair of DNA damage by homologous recombination and sensitivity to poly(ADP-ribose) polymerase inhibition." Cancer Res **66**(16): 8109-8115.

McGill, G. G., M. Horstmann, et al. (2002). "Bcl2 regulation by the melanocyte master regulator Mitf modulates lineage survival and melanoma cell viability." Cell **109**(6): 707-718.

Menoyo, A., H. Alazzouzi, et al. (2001). "Somatic mutations in the DNA damage-response genes ATR and CHK1 in sporadic stomach tumors with microsatellite instability." Cancer Res **61**(21): 7727-7730.

Meredith, P. and T. Sarna (2006). "The physical and chemical properties of eumelanin." Pigment Cell Res **19**(6): 572-594.

Meulemans, D. and M. Bronner-Fraser (2004). "Gene-regulatory interactions in neural crest evolution and development." Dev Cell **7**(3): 291-299.

Middleton, M. R., J. J. Grob, et al. (2000). "Randomized phase III study of temozolomide versus dacarbazine in the treatment of patients with advanced metastatic malignant melanoma." J Clin Oncol **18**(1): 158-166.

Miller, A. J. and M. C. Mihm, Jr. (2006). "Melanoma." N Engl J Med **355**(1): 51-65.

Mimura, S. and H. Takisawa (1998). "Xenopus Cdc45-dependent loading of DNA polymerase alpha onto chromatin under the control of S-phase Cdk." EMBO J **17**(19): 5699-5707.

Mirza, A., Q. Wu, et al. (2003). "Global transcriptional program of p53 target genes during the process of apoptosis and cell cycle progression." Oncogene **22**(23): 3645-3654.

Mitchell, C., M. Park, et al. (2010). "Poly(ADP-ribose) polymerase 1 modulates the lethality of CHK1 inhibitors in carcinoma cells." Mol Pharmacol **78**(5): 909-917.

Montoliu, L., T. Umland, et al. (1996). "A locus control region at -12 kb of the tyrosinase gene." EMBO J **15**(22): 6026-6034.

Monzani, E., F. Facchetti, et al. (2007). "Melanoma contains CD133 and ABCG2 positive cells with enhanced tumourigenic potential." European Journal of Cancer **43**(5): 935-946.

Moore, K. A. and I. R. Lemischka (2006). "Stem cells and their niches." Science **311**(5769): 1880-1885.

Moore, K. J. (1995). "Insight into the microphthalmia gene." Trends Genet **11**(11): 442-448.

Mordes, D. A., G. G. Glick, et al. (2008). "TopBP1 activates ATR through ATRIP and a PIKK regulatory domain." Genes Dev **22**(11): 1478-1489.

Morgan, D. O. (1997). "Cyclin-dependent kinases: engines, clocks, and microprocessors." Annu Rev Cell Dev Biol **13**: 261-291.

Morita, R., S. Nakane, et al. (2010). "Molecular mechanisms of the whole DNA repair system: a comparison of bacterial and eukaryotic systems." J Nucleic Acids **2010**: 179594.

Mukherjee, S., S. Manna, et al. (2010). "Sequential loss of cell cycle checkpoint control contributes to malignant transformation of murine embryonic fibroblasts induced by 20-methylcholanthrene." Journal of Cellular Physiology **224**(1): 49-58.

Murai, J., S. Y. Huang, et al. (2012). "Trapping of PARP1 and PARP2 by Clinical PARP Inhibitors." Cancer Res **72**(21): 5588-5599.

Murga, M., S. Bunting, et al. (2009). "A mouse model of ATR-Seckel shows embryonic replicative stress and accelerated aging." Nat Genet **41**(8): 891-898.

Murga, M., S. Campaner, et al. (2011). "Exploiting oncogene-induced replicative stress for the selective killing of Myc-driven tumors." Nat Struct Mol Biol **18**(12): 1331-1335.

Murisier, F., S. Guichard, et al. (2007). "The tyrosinase enhancer is activated by Sox10 and Mitf in mouse melanocytes." Pigment Cell Res **20**(3): 173-184.

Nazarian, R., H. Shi, et al. (2010). "Melanomas acquire resistance to B-RAF(V600E) inhibition by RTK or N-RAS upregulation." Nature **468**(7326): 973-977.

Neuhausen, S. L. and C. J. Marshall (1994). "Loss of heterozygosity in familial tumors from three BRCA1-linked kindreds." Cancer Res **54**(23): 6069-6072.

Newlands, E. S., G. R. Blackledge, et al. (1992). "Phase I trial of temozolomide (CCRG 81045: M&B 39831: NSC 362856)." Br J Cancer **65**(2): 287-291.

Newton, J. M., O. Cohen-Barak, et al. (2001). "Mutations in the human orthologue of the mouse underwhite gene (uw) underlie a new form of oculocutaneous albinism, OCA4." American Journal of Human Genetics **69**(5): 981-988.

Ni, Z. J., P. Barsanti, et al. (2006). "4-(Aminoalkylamino)-3-benzimidazole-quinolinones as potent CHK-1 inhibitors." Bioorganic & Medicinal Chemistry Letters **16**(12): 3121-3124.

Nigg, E. A. (2001). "Mitotic kinases as regulators of cell division and its checkpoints." Nat Rev Mol Cell Biol **2**(1): 21-32.

Niida, H., Y. Katsuno, et al. (2007). "Specific role of Chk1 phosphorylations in cell survival and checkpoint activation." Mol Cell Biol **27**(7): 2572-2581.

Nishimura, E. K., S. R. Granter, et al. (2005). "Mechanisms of hair graying: incomplete melanocyte stem cell maintenance in the niche." Science **307**(5710): 720-724.

Nishimura, E. K., S. A. Jordan, et al. (2002). "Dominant role of the niche in melanocyte stem-cell fate determination." Nature **416**(6883): 854-860.

Nishitani, H. and Z. Lygerou (2002). "Control of DNA replication licensing in a cell cycle." Genes Cells **7**(6): 523-534.

Nogueira, C., K. H. Kim, et al. (2010). "Cooperative interactions of PTEN deficiency and RAS activation in melanoma metastasis." Oncogene **29**(47): 6222-6232.

Norbury, C. J. and B. Zhivotovsky (2004). "DNA damage-induced apoptosis." Oncogene **23**(16): 2797-2808.

Nuciforo, P. G., C. Luise, et al. (2007). "Complex engagement of DNA damage response pathways in human cancer and in lung tumor progression." Carcinogenesis **28**(10): 2082-2088.

Nurse, P. (2000). "A long twentieth century of the cell cycle and beyond." Cell **100**(1): 71-78.

Nyberg, K. A., R. J. Michelson, et al. (2002). "Toward maintaining the genome: DNA damage and replication checkpoints." Annu Rev Genet **36**: 617-656.

O'Connell, M. J., J. M. Raleigh, et al. (1997). "Chk1 is a wee1 kinase in the G2 DNA damage checkpoint inhibiting cdc2 by Y15 phosphorylation." EMBO J **16**(3): 545-554.

O'Donovan, P. J. and D. M. Livingston (2010). "BRCA1 and BRCA2: breast/ovarian cancer susceptibility gene products and participants in DNA double-strand break repair." Carcinogenesis **31**(6): 961-967.

Oe, T., N. Nakajo, et al. (2001). "Cytoplasmic occurrence of the Chk1/Cdc25 pathway and regulation of Chk1 in Xenopus oocytes." Dev Biol **229**(1): 250-261.

Okamoto, I., A. P. Otte, et al. (2004). "Epigenetic dynamics of imprinted X inactivation during early mouse development." Science **303**(5658): 644-649.

Oliver, A. W., A. Paul, et al. (2006). "Trans-activation of the DNA-damage signalling protein kinase Chk2 by T-loop exchange." EMBO J **25**(13): 3179-3190.

Omholt, K., D. Krockel, et al. (2006). "Mutations of PIK3CA are rare in cutaneous melanoma." Melanoma Res **16**(2): 197-200.

Origanti, S., S. R. Cai, et al. (2012). "Synthetic lethality of Chk1 inhibition combined with p53 and/or p21 loss during a DNA damage response in normal and tumor cells." Oncogene.

Osawa, M., G. Egawa, et al. (2005). "Molecular characterization of melanocyte stem cells in their niche." Development **132**(24): 5589-5599.

Panka, D. J., W. Wang, et al. (2006). "The Raf inhibitor BAY 43-9006 (Sorafenib) induces caspase-independent apoptosis in melanoma cells." Cancer Res **66**(3): 1611-1619.

Papp, T., A. Niemetz, et al. (2007). "Mutational analysis of Chk1, Chk2, Apaf1 and Rb1 in human malignant melanoma cell lines." Oncol Rep **17**(1): 135-140.

Papp, T., H. Pemsel, et al. (2003). "Mutational analysis of N-ras, p53, CDKN2A (p16(INK4a)), p14(ARF), CDK4, and MC1R genes in human dysplastic melanocytic naevi." Journal of Medical Genetics **40**(2): E14.

Parichy, D. M., J. F. Rawls, et al. (1999). "Zebrafish sparse corresponds to an orthologue of c-kit and is required for the morphogenesis of a subpopulation of melanocytes, but is not essential for hematopoiesis or primordial germ cell development." Development **126**(15): 3425-3436.

Paulsen, R. D. and K. A. Cimprich (2007). "The ATR pathway: fine-tuning the fork." DNA Repair **6**(7): 953-966.

Pellegrini, M., A. Celeste, et al. (2006). "Autophosphorylation at serine 1987 is dispensable for murine Atm activation in vivo." Nature **443**(7108): 222-225.

Peng, C. Y., P. R. Graves, et al. (1997). "Mitotic and G2 checkpoint control: regulation of 14-3-3 protein binding by phosphorylation of Cdc25C on serine-216." Science **277**(5331): 1501-1505.

Perez-Losada, J., M. Sanchez-Martin, et al. (2002). "Zinc-finger transcription factor Slug contributes to the function of the stem cell factor c-kit signaling pathway." Blood **100**(4): 1274-1286.

Petermann, E. and K. W. Caldecott (2006). "Evidence that the ATR/Chk1 pathway maintains normal replication fork progression during unperturbed S phase." Cell Cycle **5**(19): 2203-2209.

Petermann, E., A. Maya-Mendoza, et al. (2006). "Chk1 requirement for high global rates of replication fork progression during normal vertebrate S phase." Molecular and Cellular Biology **26**(8): 3319-3326.

Petermann, E., M. Woodcock, et al. (2010). "Chk1 promotes replication fork progression by controlling replication initiation." Proceedings of the National Academy of Sciences of the United States of America **107**(37): 16090-16095.

Petrella, T., I. Quirt, et al. (2007). "Single-agent interleukin-2 in the treatment of metastatic melanoma: a systematic review." Cancer Treat Rev **33**(5): 484-496.

Pollack, L. A., J. Li, et al. (2011). "Melanoma survival in the United States, 1992 to 2005." J Am Acad Dermatol **65**(5 Suppl 1): S78-86.

Pollock, P. M., U. L. Harper, et al. (2003). "High frequency of BRAF mutations in nevi." Nat Genet **33**(1): 19-20.

Potterf, S. B., M. Furumura, et al. (2000). "Transcription factor hierarchy in Waardenburg syndrome: regulation of MITF expression by SOX10 and PAX3." Hum Genet **107**(1): 1-6.

Potterf, S. B., R. Mollaaghababa, et al. (2001). "Analysis of SOX10 function in neural crest-derived melanocyte development: SOX10-dependent transcriptional control of dopachrome tautomerase." Dev Biol **237**(2): 245-257.

Poynter, J. N., J. T. Elder, et al. (2006). "BRAF and NRAS mutations in melanoma and melanocytic nevi." Melanoma Res **16**(4): 267-273.

Primot, A., A. Mogha, et al. (2010). "ERK-regulated differential expression of the Mitf 6a/b splicing isoforms in melanoma." Pigment Cell Melanoma Res **23**(1): 93-102.

Pritchard, C. A., L. Hayes, et al. (2004). "B-Raf acts via the ROCKII/LIMK/cofilin pathway to maintain actin stress fibers in fibroblasts." Mol Cell Biol **24**(13): 5937-5952.

Rai, R., G. Peng, et al. (2007). "DNA damage response: the players, the network and the role in tumor suppression." Cancer Genomics Proteomics **4**(2): 99-106.

Rana, B. K., D. Hewett-Emmett, et al. (1999). "High polymorphism at the human melanocortin 1 receptor locus." Genetics **151**(4): 1547-1557.

Ravnan, M. C. and M. S. Matalka (2012). "Vemurafenib in Patients With BRAF V600E Mutation-Positive Advanced Melanoma." Clinical Therapeutics **34**(7): 1474-1486.

Ray-David, H., Y. Romeo, et al. (2012). "RSK promotes G2 DNA damage checkpoint silencing and participates in melanoma chemoresistance." Oncogene.

Rees, J. L. (2003). "Genetics of hair and skin color." Annu Rev Genet **37**: 67-90.

Reinhardt, H. C. and M. B. Yaffe (2009). "Kinases that control the cell cycle in response to DNA damage: Chk1, Chk2, and MK2." Curr Opin Cell Biol **21**(2): 245-255.

Rhind, N., B. Furnari, et al. (1997). "Cdc2 tyrosine phosphorylation is required for the DNA damage checkpoint in fission yeast." Genes Dev **11**(4): 504-511.

Ringholm, A., J. Klovins, et al. (2004). "Pharmacological characterization of loss of function mutations of the human melanocortin 1 receptor that are associated with red hair." J Invest Dermatol **123**(5): 917-923.

Robert, C., L. Thomas, et al. (2011). "Ipilimumab plus dacarbazine for previously untreated metastatic melanoma." N Engl J Med **364**(26): 2517-2526.

Rohren, E. M., T. G. Turkington, et al. (2004). "Clinical applications of PET in oncology." Radiology **231**(2): 305-332.

Rowley, R., J. Hudson, et al. (1992). "The wee1 protein kinase is required for radiation-induced mitotic delay." Nature **356**(6367): 353-355.

Russell, M., K. Levin, et al. (2012). "Combination therapy targeting the Chk1 and Wee1 kinases demonstrates therapeutic efficacy in neuroblastoma." Cancer Res.

Ruzankina, Y., C. Pinzon-Guzman, et al. (2007). "Deletion of the developmentally essential gene ATR in adult mice leads to age-related phenotypes and stem cell loss." Cell Stem Cell **1**(1): 113-126.

Ryan, K. M., A. C. Phillips, et al. (2001). "Regulation and function of the p53 tumor suppressor protein." Curr Opin Cell Biol **13**(3): 332-337.

Saldana-Caboverde, A. and L. Kos (2010). "Roles of endothelin signaling in melanocyte development and melanoma." Pigment Cell Melanoma Res **23**(2): 160-170.

Sancar, A., L. A. Lindsey-Boltz, et al. (2004). "Molecular mechanisms of mammalian DNA repair and the DNA damage checkpoints." Annu Rev Biochem **73**: 39-85.

Sanchez, Y., C. Wong, et al. (1997). "Conservation of the Chk1 checkpoint pathway in mammals: linkage of DNA damage to Cdk regulation through Cdc25." Science **277**(5331): 1497-1501.

Sanchez-Martin, M., J. Perez-Losada, et al. (2003). "Deletion of the SLUG (SNAI2) gene results in human piebaldism." Am J Med Genet A **122A**(2): 125-132.

Santana, C., E. Ortega, et al. (2002). "Oncogenic H-ras induces cyclin B1 expression in a p53-independent manner." Mutat Res **508**(1-2): 49-58.

Sartori, A. A., C. Lukas, et al. (2007). "Human CtIP promotes DNA end resection." Nature **450**(7169): 509-514.

Sato-Jin, K., E. K. Nishimura, et al. (2008). "Epistatic connections between microphthalmia-associated transcription factor and endothelin signaling in Waardenburg syndrome and other pigmentary disorders." FASEB J **22**(4): 1155-1168.

Schafer, K. A. (1998). "The cell cycle: a review." Vet Pathol **35**(6): 461-478.

Schepsky, A., K. Bruser, et al. (2006). "The microphthalmia-associated transcription factor Mitf interacts with beta-catenin to determine target gene expression." Mol Cell Biol **26**(23): 8914-8927.

Schiaffino, M. V. (2010). "Signaling pathways in melanosome biogenesis and pathology." Int J Biochem Cell Biol **42**(7): 1094-1104.

Schoppy, D. W., R. L. Ragland, et al. (2012). "Oncogenic stress sensitizes murine cancers to hypomorphic suppression of ATR." J Clin Invest **122**(1): 241-252.

Seiler, J. A., C. Conti, et al. (2007). "The intra-S-phase checkpoint affects both DNA replication initiation and elongation: single-cell and -DNA fiber analyses." Mol Cell Biol **27**(16): 5806-5818.

Seno, J. D. and J. R. Dynlacht (2004). "Intracellular redistribution and modification of proteins of the Mre11/Rad50/Nbs1 DNA repair complex following irradiation and heat-shock." Journal of Cellular Physiology **199**(2): 157-170.

Serrano, M., H. Lee, et al. (1996). "Role of the INK4a locus in tumor suppression and cell mortality." Cell **85**(1): 27-37.

Serrano, M., A. W. Lin, et al. (1997). "Oncogenic ras provokes premature cell senescence associated with accumulation of p53 and p16INK4a." Cell **88**(5): 593-602.

Sharma, A., N. R. Trivedi, et al. (2005). "Mutant V599EB-Raf regulates growth and vascular development of malignant melanoma tumors." Cancer Res **65**(6): 2412-2421.

Sharpless, E. and L. Chin (2003). "The INK4a/ARF locus and melanoma." Oncogene **22**(20): 3092-3098.

Sharpless, N. E., N. Bardeesy, et al. (2001). "Loss of p16Ink4a with retention of p19Arf predisposes mice to tumorigenesis." Nature **413**(6851): 86-91.

Shaw, R. J. and L. C. Cantley (2006). "Ras, PI(3)K and mTOR signalling controls tumour cell growth." Nature **441**(7092): 424-430.

Shay, J. W., O. M. Pereira-Smith, et al. (1991). "A role for both RB and p53 in the regulation of human cellular senescence." Exp Cell Res **196**(1): 33-39.

Sherr, C. J. (1996). "Cancer cell cycles." Science **274**(5293): 1672-1677.

Sherr, C. J. (2006). "Divorcing ARF and p53: an unsettled case." Nat Rev Cancer **6**(9): 663-673.

Shieh, S. Y., J. Ahn, et al. (2000). "The human homologs of checkpoint kinases Chk1 and Cds1 (Chk2) phosphorylate p53 at multiple DNA damage-inducible sites." Genes Dev **14**(3): 289-300.

Shiloh, Y. and M. B. Kastan (2001). "ATM: genome stability, neuronal development, and cancer cross paths." Adv Cancer Res **83**: 209-254.

Shimada, M., H. Niida, et al. (2008). "Chk1 is a histone H3 threonine 11 kinase that regulates DNA damage-induced transcriptional repression." Cell **132**(2): 221-232.

Shin, M. K., J. M. Levorse, et al. (1999). "The temporal requirement for endothelin receptor-B signalling during neural crest development." Nature **402**(6761): 496-501.

Siegel, R., C. Desantis, et al. (2012). "Cancer treatment and survivorship statistics, 2012." CA Cancer J Clin **62**(4): 220-241.

Smalley, K. S., N. K. Haass, et al. (2006). "Multiple signaling pathways must be targeted to overcome drug resistance in cell lines derived from melanoma metastases." Mol Cancer Ther **5**(5): 1136-1144.

Smith, J., L. M. Tho, et al. (2010). "The ATM-Chk2 and ATR-Chk1 pathways in DNA damage signaling and cancer." Adv Cancer Res **108**: 73-112.

Smith, J., L. M. Tho, et al. (2010). "The ATM-Chk2 and ATR-Chk1 pathways in DNA damage signaling and cancer." Adv Cancer Res **108**: 73-112.

Smits, V. A., P. M. Reaper, et al. (2006). "Rapid PIKK-dependent release of Chk1 from chromatin promotes the DNA-damage checkpoint response." Curr Biol **16**(2): 150-159.

Society, A. C. (2012). "Cancer Facts & Figures 2012."

Soengas, M. S. and S. W. Lowe (2003). "Apoptosis and melanoma chemoresistance." Oncogene **22**(20): 3138-3151.

Song, X., N. Mosby, et al. (2009). "alpha-MSH activates immediate defense responses to UV-induced oxidative stress in human melanocytes." Pigment Cell Melanoma Res **22**(6): 809-818.

Sorensen, C. S., L. T. Hansen, et al. (2005). "The cell-cycle checkpoint kinase Chk1 is required for mammalian homologous recombination repair." Nature Cell Biology **7**(2): 195-201.

Sorensen, C. S. and R. G. Syljuasen (2012). "Safeguarding genome integrity: the checkpoint kinases ATR, CHK1 and WEE1 restrain CDK activity during normal DNA replication." Nucleic Acids Res **40**(2): 477-486.

Sorensen, C. S., R. G. Syljuasen, et al. (2003). "Chk1 regulates the S phase checkpoint by coupling the physiological turnover and ionizing radiation-induced accelerated proteolysis of Cdc25A." Cancer Cell **3**(3): 247-258.

Sorensen, C. S., R. G. Syljuasen, et al. (2004). "ATR, Claspin and the Rad9-Rad1-Hus1 complex regulate Chk1 and Cdc25A in the absence of DNA damage." Cell Cycle **3**(7): 941-945.

Soriano, P. (1999). "Generalized lacZ expression with the ROSA26 Cre reporter strain." Nat Genet **21**(1): 70-71.

Southard-Smith, E. M., L. Kos, et al. (1998). "Sox10 mutation disrupts neural crest development in Dom Hirschsprung mouse model." Nat Genet **18**(1): 60-64.

Spritz, R. A. (1994). "Molecular basis of human piebaldism." J Invest Dermatol **103**(5 Suppl): 137S-140S.

Stahl, J. M., A. Sharma, et al. (2004). "Deregulated Akt3 activity promotes development of malignant melanoma." Cancer Res **64**(19): 7002-7010.

Steingrimsson, E., N. G. Copeland, et al. (2004). "Melanocytes and the microphthalmia transcription factor network." Annu Rev Genet **38**: 365-411.

Stevens, C., L. Smith, et al. (2003). "Chk2 activates E2F-1 in response to DNA damage." Nature Cell Biology **5**(5): 401-409.

Stewart, G. S., R. S. Maser, et al. (1999). "The DNA double-strand break repair gene hMRE11 is mutated in individuals with an ataxia-telangiectasia-like disorder." Cell **99**(6): 577-587.

Sturm, R. A., D. L. Duffy, et al. (2003). "Genetic association and cellular function of MC1R variant alleles in human pigmentation." Annals of the New York Academy of Sciences **994**: 348-358.

Su, Y., A. E. Vilgelm, et al. (2012). "RAF265 inhibits the growth of advanced human melanoma tumors." Clinical Cancer Research : an official Journal of the American Association for Cancer Research **18**(8): 2184-2198.

Sumimoto, H., M. Miyagishi, et al. (2004). "Inhibition of growth and invasive ability of melanoma by inactivation of mutated BRAF with lentivirus-mediated RNA interference." Oncogene **23**(36): 6031-6039.

Suzuki, K., S. Kodama, et al. (1999). "Recruitment of ATM protein to double strand DNA irradiated with ionizing radiation." The Journal of Biological Chemistry **274**(36): 25571-25575.

Swift, M., D. Morrell, et al. (1991). "Incidence of cancer in 161 families affected by ataxia-telangiectasia." N Engl J Med **325**(26): 1831-1836.

Syljuasen, R. G., C. S. Sorensen, et al. (2005). "Inhibition of human Chk1 causes increased initiation of DNA replication, phosphorylation of ATR targets, and DNA breakage." Mol Cell Biol **25**(9): 3553-3562.

Tachibana, M., Y. Kobayashi, et al. (2003). "Mouse models for four types of Waardenburg syndrome." Pigment Cell Res **16**(5): 448-454.

Takai, H., K. Naka, et al. (2002). "Chk2-deficient mice exhibit radioresistance and defective p53-mediated transcription." EMBO J **21**(19): 5195-5205.

Takeda, K., K. Yasumoto, et al. (2000). "Induction of melanocyte-specific microphthalmia-associated transcription factor by Wnt-3a." The Journal of Biological Chemistry **275**(19): 14013-14016.

Takemura, H., V. A. Rao, et al. (2006). "Defective Mre11-dependent activation of Chk2 by ataxia telangiectasia mutated in colorectal carcinoma cells in response to replication-dependent DNA double strand breaks." The Journal of Biological Chemistry **281**(41): 30814-30823.

Taketo, M., A. C. Schroeder, et al. (1991). "FVB/N: an inbred mouse strain preferable for transgenic analyses." Proceedings of the National Academy of Sciences of the United States of America **88**(6): 2065-2069.

Takuwa, N. and Y. Takuwa (2001). "Regulation of cell cycle molecules by the Ras effector system." Mol Cell Endocrinol **177**(1-2): 25-33.

Tan, Y., P. Raychaudhuri, et al. (2007). "Chk2 mediates stabilization of the FoxM1 transcription factor to stimulate expression of DNA repair genes." Mol Cell Biol **27**(3): 1007-1016.

Tang, Y., H. A. Hamed, et al. (2012). "Poly(ADP-ribose) polymerase 1 modulates the lethality of CHK1 inhibitors in mammary tumors." Mol Pharmacol **82**(2): 322-332.

Tao, Y., C. Leteur, et al. (2009). "Radiosensitization by Chir-124, a selective CHK1 inhibitor: effects of p53 and cell cycle checkpoints." Cell Cycle **8**(8): 1196-1205.

Tarhini, A. A., H. Gogas, et al. (2012). "IFN-alpha in the Treatment of Melanoma." J Immunol **189**(8): 3789-3793.

Teng, D. H., R. Hu, et al. (1997). "MMAC1/PTEN mutations in primary tumor specimens and tumor cell lines." Cancer Res **57**(23): 5221-5225.

Tessema, M., U. Lehmann, et al. (2004). "Cell cycle and no end." Virchows Arch **444**(4): 313-323.

Tho, L. M., S. Libertini, et al. (2012). "Chk1 is essential for chemical carcinogen-induced mouse skin tumorigenesis." Oncogene **31**(11): 1366-1375.

Thompson, R., R. Montano, et al. (2012). "The Mre11 nuclease is critical for the sensitivity of cells to Chk1 inhibition." PloS One **7**(8): e44021.

Thornton, T. M. and M. Rincon (2009). "Non-classical p38 map kinase functions: cell cycle checkpoints and survival." International Journal of Biological Sciences **5**(1): 44-51.

Toledo, L. I., M. Murga, et al. (2011). "A cell-based screen identifies ATR inhibitors with synthetic lethal properties for cancer-associated mutations." Nat Struct Mol Biol **18**(6): 721-727.

Tse, A. N., K. G. Rendahl, et al. (2007). "CHIR-124, a novel potent inhibitor of Chk1, potentiates the cytotoxicity of topoisomerase I poisons in vitro and in vivo." Clinical Cancer Research : an official Journal of the American Association for Cancer Research **13**(2 Pt 1): 591-602.

Tsujimura, T., E. Morii, et al. (1996). "Involvement of transcription factor encoded by the mi locus in the expression of c-kit receptor tyrosine kinase in cultured mast cells of mice." Blood **88**(4): 1225-1233.

Turner, N., A. Tutt, et al. (2005). "Targeting the DNA repair defect of BRCA tumours." Curr Opin Pharmacol **5**(4): 388-393.

Uziel, T., Y. Lerenthal, et al. (2003). "Requirement of the MRN complex for ATM activation by DNA damage." EMBO J **22**(20): 5612-5621.

VanBrocklin, M. W., J. P. Robinson, et al. (2010). "Targeted delivery of NRASQ61R and Cre-recombinase to post-natal melanocytes induces melanoma in Ink4a/Arflox/lox mice." Pigment Cell Melanoma Res **23**(4): 531-541.

Varon, R., C. Vissinga, et al. (1998). "Nibrin, a novel DNA double-strand break repair protein, is mutated in Nijmegen breakage syndrome." Cell **93**(3): 467-476.

Vassileva, V., A. Millar, et al. (2002). "Genes involved in DNA repair are mutational targets in endometrial cancers with microsatellite instability." Cancer Res **62**(14): 4095-4099.

Veis, D. J., C. M. Sorenson, et al. (1993). "Bcl-2-deficient mice demonstrate fulminant lymphoid apoptosis, polycystic kidneys, and hypopigmented hair." Cell **75**(2): 229-240.

Verastegui, C., K. Bille, et al. (2000). "Regulation of the microphthalmia-associated transcription factor gene by the Waardenburg syndrome type 4 gene, SOX10." The Journal of Biological Chemistry **275**(40): 30757-30760.

Vermeulen, K., D. R. Van Bockstaele, et al. (2003). "The cell cycle: a review of regulation, deregulation and therapeutic targets in cancer." Cell Prolif **36**(3): 131-149.

Walker, G. J., J. F. Flores, et al. (1998). "Virtually 100% of melanoma cell lines harbor alterations at the DNA level within CDKN2A, CDKN2B, or one of their downstream targets." Genes Chromosomes Cancer **22**(2): 157-163.

Walker, M., E. J. Black, et al. (2009). "Chk1 C-terminal regulatory phosphorylation mediates checkpoint activation by de-repression of Chk1 catalytic activity." Oncogene **28**(24): 2314-2323.

Wan, P. T., M. J. Garnett, et al. (2004). "Mechanism of activation of the RAF-ERK signaling pathway by oncogenic mutations of B-RAF." Cell **116**(6): 855-867.

Wang, H. T., B. Choi, et al. (2010). "Melanocytes are deficient in repair of oxidative DNA damage and UV-induced photoproducts." Proceedings of the National Academy of Sciences of the United States of America **107**(27): 12180-12185.

Wang, J., X. Han, et al. (2012). "Coupling cellular localization and function of checkpoint kinase 1 (Chk1) in checkpoints and cell viability." The Journal of Biological Chemistry **287**(30): 25501-25509.

Wang, J., X. Han, et al. (2012). "Autoregulatory mechanisms of phosphorylation of checkpoint kinase 1." Cancer Res **72**(15): 3786-3794.

Wang, Q., S. Fan, et al. (1996). "UCN-01: a potent abrogator of G2 checkpoint function in cancer cells with disrupted p53." J Natl Cancer Inst **88**(14): 956-965.

Warters, R. L., P. J. Adamson, et al. (2005). "Melanoma cells express elevated levels of phosphorylated histone H2AX foci." J Invest Dermatol **124**(4): 807-817.

Wehrle-Haller, B. (2003). "The role of Kit-ligand in melanocyte development and epidermal homeostasis." Pigment Cell Res **16**(3): 287-296.

Wehrle-Haller, B. and J. A. Weston (1995). "Soluble and cell-bound forms of steel factor activity play distinct roles in melanocyte precursor dispersal and survival on the lateral neural crest migration pathway." Development **121**(3): 731-742.

Wellbrock, C., M. Karasarides, et al. (2004). "The RAF proteins take centre stage." Nat Rev Mol Cell Biol **5**(11): 875-885.

Wellbrock, C. and R. Marais (2005). "Elevated expression of MITF counteracts B-RAF-stimulated melanocyte and melanoma cell proliferation." The Journal of Cell Biology **170**(5): 703-708.

Wellbrock, C., S. Rana, et al. (2008). "Oncogenic BRAF regulates melanoma proliferation through the lineage specific factor MITF." PloS One **3**(7): e2734.

Wen, Q., J. Scorah, et al. (2008). "A mutant allele of MRE11 found in mismatch repair-deficient tumor cells suppresses the cellular response to DNA replication fork stress in a dominant negative manner." Molecular Biology of the Cell **19**(4): 1693-1705.

Westerhof, W., S. Pavel, et al. (1987). "Melanin-related metabolites as markers of the skin pigmentary system." J Invest Dermatol **89**(1): 78-81.

White, A. C., K. Tran, et al. (2011). "Defining the origins of Ras/p53-mediated squamous cell carcinoma." Proceedings of the National Academy of Sciences of the United States of America **108**(18): 7425-7430.

Williams, B. R., O. K. Mirzoeva, et al. (2002). "A murine model of Nijmegen breakage syndrome." Curr Biol **12**(8): 648-653.

Wilsker, D., E. Petermann, et al. (2008). "Essential function of Chk1 can be uncoupled from DNA damage checkpoint and replication control." Proceedings of the National Academy of Sciences of the United States of America **105**(52): 20752-20757.

Winston, J. T. and W. J. Pledger (1993). "Growth factor regulation of cyclin D1 mRNA expression through protein synthesis-dependent and -independent mechanisms." Molecular Biology of the Cell **4**(11): 1133-1144.

Wong, A. K. and L. Chin (2000). "An inducible melanoma model implicates a role for RAS in tumor maintenance and angiogenesis." Cancer Metastasis Rev **19**(1-2): 121-129.

Wu, H., V. Goel, et al. (2003). "PTEN signaling pathways in melanoma." Oncogene **22**(20): 3113-3122.

Wu, M., T. J. Hemesath, et al. (2000). "c-Kit triggers dual phosphorylations, which couple activation and degradation of the essential melanocyte factor Mi." Genes Dev **14**(3): 301-312.

Wu, X., S. R. Webster, et al. (2001). "Characterization of tumor-associated Chk2 mutations." The Journal of Biological Chemistry **276**(4): 2971-2974.

Xu, H., I. Y. Cheung, et al. (2011). "Checkpoint kinase inhibitor synergizes with DNA-damaging agents in G1 checkpoint-defective neuroblastoma." Int J Cancer **129**(8): 1953-1962.

Xu, Y., T. Ashley, et al. (1996). "Targeted disruption of ATM leads to growth retardation, chromosomal fragmentation during meiosis, immune defects, and thymic lymphoma." Genes Dev **10**(19): 2411-2422.

Yajima, I., E. Belloir, et al. (2006). "Spatiotemporal gene control by the Cre-ERT2 system in melanocytes." Genesis **44**(1): 34-43.

Yasumoto, K., K. Takeda, et al. (2002). "Microphthalmia-associated transcription factor interacts with LEF-1, a mediator of Wnt signaling." EMBO J **21**(11): 2703-2714.

Yasumoto, K., K. Yokoyama, et al. (1995). "Microphthalmia-associated transcription factor as a regulator for melanocyte-specific transcription of the human tyrosinase gene." Mol Cell Biol **15**(3): 1833.

Yeh, C. H., Y. Y. Yang, et al. (2012). "Induction of apoptosis in human Hep3B hepatoma cells by norcantharidin through a p53 independent pathway via TRAIL/DR5 signal transduction." Chin J Integr Med **18**(9): 676-682.

Yu, Q., J. La Rose, et al. (2002). "UCN-01 inhibits p53 up-regulation and abrogates gamma-radiation-induced G(2)-M checkpoint independently of p53 by targeting both of the checkpoint kinases, Chk2 and Chk1." Cancer Res **62**(20): 5743-5748.

Zachos, G., M. D. Rainey, et al. (2003). "Chk1-deficient tumour cells are viable but exhibit multiple checkpoint and survival defects." EMBO J **22**(3): 713-723.

Zachos, G., M. D. Rainey, et al. (2005). "Chk1-dependent S-M checkpoint delay in vertebrate cells is linked to maintenance of viable replication structures." Mol Cell Biol **25**(2): 563-574.

Zaidi, M. R., C. P. Day, et al. (2008). "From UVs to metastases: modeling melanoma initiation and progression in the mouse." J Invest Dermatol **128**(10): 2381-2391.

Zaugg, K., Y. W. Su, et al. (2007). "Cross-talk between Chk1 and Chk2 in double-mutant thymocytes." Proceedings of the National Academy of Sciences of the United States of America **104**(10): 3805-3810.

Zenvirt, S., N. Kravchenko-Balasha, et al. (2010). "Status of p53 in human cancer cells does not predict efficacy of CHK1 kinase inhibitors combined with chemotherapeutic agents." Oncogene **29**(46): 6149-6159.

Zhang, C., Z. Yan, et al. (2009). "PF-00477736 mediates checkpoint kinase 1 signaling pathway and potentiates docetaxel-induced efficacy in xenografts." Clinical Cancer Research : an official Journal of the American Association for Cancer Research **15**(14): 4630-4640.

Zhang, X. D., S. K. Gillespie, et al. (2004). "Staurosporine induces apoptosis of melanoma by both caspase-dependent and -independent apoptotic pathways." Mol Cancer Ther **3**(2): 187-197.

Zhang, Y. W., D. M. Otterness, et al. (2005). "Genotoxic stress targets human Chk1 for degradation by the ubiquitin-proteasome pathway." Molecular Cell **19**(5): 607-618.

Zhao, H., J. L. Watkins, et al. (2002). "Disruption of the checkpoint kinase 1/cell division cycle 25A pathway abrogates ionizing radiation-induced S and G2 checkpoints." Proceedings of the National Academy of Sciences of the United States of America **99**(23): 14795-14800.

Zhao, S., L. J. Rizzolo, et al. (1997). "Differentiation and transdifferentiation of the retinal pigment epithelium." Int Rev Cytol **171**: 225-266.

Zhou, B. B. and J. Bartek (2004). "Targeting the checkpoint kinases: chemosensitization versus chemoprotection." Nat Rev Cancer **4**(3): 216-225.

Zighelboim, I., A. P. Schmidt, et al. (2009). "ATR mutation in endometrioid endometrial cancer is associated with poor clinical outcomes." J Clin Oncol **27**(19): 3091-3096.

Zou, L. and S. J. Elledge (2003). "Sensing DNA damage through ATRIP recognition of RPA-ssDNA complexes." Science **300**(5625): 1542-1548.

Zuo, L., J. Weger, et al. (1996). "Germline mutations in the p16INK4a binding domain of CDK4 in familial melanoma." Nat Genet **12**(1): 97-99.